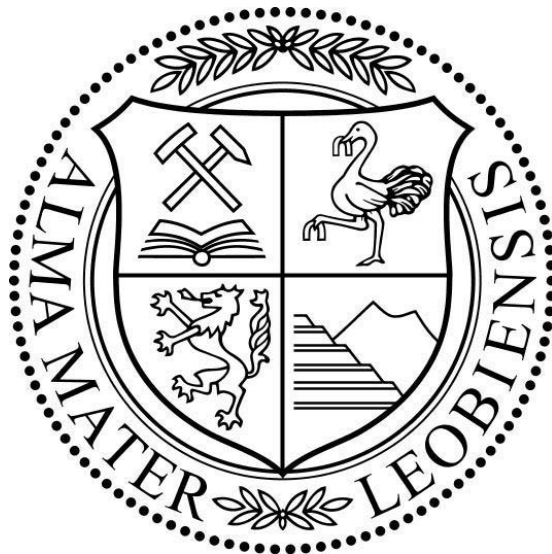**<u>DIPLOMA THESIS:</u>**

DEFINITION OF TOP-CRYSTALLINE BASEMENT
IN THE UPPER AUSTRIAN MOLASSE BASIN

- Leoben, 2010 -

<u>Author:</u>

Gloria Thürschmid, BSc

<u>Advisor of the Chair of Petroleum Geology:</u>

Univ.-Prof. Mag.rer.nat. Dr.mont. Reinhard Sachsenhofer

I declare in lieu of oath, that I wrote this thesis and performed the associated research myself, using only literature cited in this volume.

Leoben, May 2010

ACKNOWLEDGEMENTS

TABLE OF CONTENTS

ABSTRACT

In cooperation with Rohöl-AufsuchungsAG (RAG) a new log-based method is developed to identify precisely the depth of the top of the crystalline basement (Top-XX) within the Austrian Molasse basin.

Currently, different geophysical logs are used within the company with different emphasis. This results in varying depth estimates for Top-XX. Among the logs available (gamma ray, spontaneous potential, photoelectric effect, caliper, sonic, porosity, resistivity, density and formation micro imaging logs), resistivity logs are predominantely used to define the boundary.

Within the frame of this diploma thesis, six representative wells have been analyzed, whereof two wells provide each a crystalline basement overlain by sandstone horizons of Eocene (HIER-002A, MLRT-003C), Cenomanian (BH-N-001, BH-N-002) or Jurassic age (KH-003, V-037).
Based on detailed core inspections, Top-XX as well as the lithology above and below that boundary have been determined. Additionally, thin sections of representative core samples have been interpreted for petrographical composition. To determine log depths of the top of the crystalline basement, (total and spectral) core gamma ray (Core-GR) measurements were performed.

The result of this study indicates, that the well logging signal is influenced by several factors. These are, among others, the lithology, as well as heavy mineral contents at the base of the overlying sedimentary succession, but also the lithology and the degree of weathering of the crystalline basement (magmatic versus metamorphic). Therefore, a general log pattern across the Top-XX in the investigated wells cannot be observed.

However, close inspections show that all wells including Mesozoic sandstones overlying plutonic rocks exhibit high values of total GR at the base of the sandstones and significantly lower values of total GR within the uppermost part of the crystalline basement. Spectral Core-GR measurements indicate that high GR values are caused by heavy minerals (high contents of Th, U), whereas low GR contents result from weathering of the crystalline basement (removal of K). The content of potassium increases downwards, which suggests unweathered crystalline rocks including potassium feldspars.

In contrast to Mesozoic sandstones, Eocene sandstones provide a positive correlation of total GR values and the content of potassium. In this case, heavy minerals are not dominating GR values. According to the lithology of the crystalline basement, GR values are either increasing (metamorphic basement) or do not show significant changes (plutonitic rocks). Further investigations of different wells are necessary to determine if this is a general trend.

In summary, significant changes at the top of the crystalline basement are primarily visible in the GR log.

KURZFASSUNG

In Kooperation mit Rohöl-AufsuchungsAG (RAG) ist eine Methode entwickelt worden, mit welcher man die Oberkante des kristallinen Untergrunds in der Molassezone aus charakteristischen Logmustern eindeutig bestimmen kann.

Derzeit verwendet die RAG verschiedene Ansätze mit unterschiedlicher Gewichtung von geophysikalischen Logs. Dies führt zu unterschiedlichen Tiefenangaben für die Oberkante des Kristallins. Von den verfügbaren Logs (z.B. Gamma Ray, Eigenpotential, Photoelektrischer Effekt, Kaliber-, Sonic-, Porositäts-, Widerstands-, Dichte- und Formation Micro Imaging-Logs) kommen bisher vorwiegend Widerstandslogs zum Einsatz, um die Grenze zu bestimmen.

Im Rahmen der Diplomarbeit wurden sechs repräsentative Bohrungen bearbeitet, wovon das Kristallin in je zwei Bohrungen von Sandsteinhorizonten des Eozän (HIER-002A, MLRT-003C), des Cenoman (BH-N-001, BH-N-002), sowie des Jura (KH-003, V-037) überlagert wird.
Mithilfe detaillierter Bohrkernaufnahmen wurde die Oberkante des Kristallins, sowie die Lithologie ober- und unterhalb dieser Grenze identifiziert. Zusätzlich wurden für die petrographische Analyse Dünnschliffe von repräsentativen Bohrkernproben ausgewertet. Um die Logteufe dieser Grenze exakt festzulegen, wurden (totale und spektrale) Gamma-Messungen an den Bohrkernen durchgeführt.

Das Ergebnis der Studie zeigt, dass das Bohrlochmesssignal von verschiedenen Faktoren beeinflusst wird. Dazu zählen u.a. die Lithologie der überlagernden Formation, Schwermineralführung an deren Basis, Verwitterungsgrad und Lithologie des kristallinen Grundgebirges (magmatisch versus metamorph). Es kann daher kein generelles Logmuster im Bereich der Oberkante des Kristallins der untersuchten Bohrungen beobachtet werden.

Bei detaillierter Betrachtung zeigt sich allerdings, dass bei allen Bohrungen in denen mesozoische Sandsteine plutonische Gesteine überlagern, die totalen Gammawerte an der Basis der Sandsteine erhöht und in den obersten Metern des Kristallins stark erniedrigt sind. Spektrale Gammamessungen an Kernen indizieren, dass die erhöhten Gammawerte auf Schwerminerale (hohe Th, U Gehalte) und die geringen Werte auf Verwitterung des Kristallins (Abfuhr von K) zurückzuführen sind. Mit zunehmender Tiefe nimmt der Anteil an Kalium wieder zu, was auf unverwittertes Kristallin mit Kalifeldspat schließen lässt.

Im Gegensatz zu mesozoischen Sandsteinen, zeigen die totalen Gammawerte eozäner Sandsteine eine positive Korrelation mit dem Kaliumgehalt. Eine Kontrolle durch Schwerminerale ist daher unwahrscheinlich. Je nach Lithologie des Kristallins wird die Kristallinoberkante durch eine Zunahme des Gammawertes (Metamorphes Grundgebirge) oder keine signifikante Änderung (Plutonit) charakterisiert. Untersuchungen an weiteren Bohrungen sind nötig zu zeigen, ob es sich dabei um einen generellen Trend handelt.

Zusammenfassend zeigt sich, dass Änderungen an der kristallinen Oberkante hauptsächlich im Gamma-Log abzulesen sind.

1.1 Reason   for investigation

In the Molasse Basin the definition of the top of the crystalline basement (Top-XX) based on drilling evidence and well logs alone is often very difficult. Several approaches are used with different emphasis on the logs, resulting in varying depth estimates with partly significant difference. This illustrates the need of the company for a unique method to define Top-XX. However, from the logs available (gamma ray, spontaneous potential, photoelectric effect, caliper, sonic, porosity, resistivity, density and formation micro imaging logs) resistivity logs are predominantly used at Rohöl-AufsuchungsAG to define the boundary.

The definition of Top-XX is essential, because it typically defines the lower boundary of the area, which is attractive for petroleum exploration. This is true, although some minor petroleum might be found in weathered and fractured crystalline rocks. Moreover, an erroneously shallow position of Top-XX might result in overlooking potential reservoirs units, which frequently overlie the crystalline basement.

1.2 Workflow

Fig. 1 displays the workflow of this diploma thesis. At the beginning, representative wells with Middle Jurassic, Cenomanian and Eocene sediments overlying the crystalline basement have been selected by RAG personnel. The following wells have been selected based mainly on the availability of core material and modern well logs.

Jurassic: KH-003 and V-037
Cenomanian: BH-N-001 and BH-N-002
Eocene: HIER-002A and MLRT-003C

Core analysis in the Pettenbach core store was the next step and core data sheets were prepared for each core (see attachments). Core samples for thin section analysis were taken to gather more information on the petrography of the cores.

Spectral core gamma ray (Core-GR) logs have been measured by OMV on some of the studied cores. In order to compare and complete these results, (total and spectral) GR measurements were performed for selected cores also within the frame of the present study. The aim of these measurements was to compare the new results with those obtained by OMV and with well log GR. Considering certain corrections, this procedure allowed the exact definition of the Top crystalline basement in the well logs and thus the evaluation of characteristic log patterns at this boundary.

This workflow was done to check the logs by core data and develop a technique to determine Top-XX based on well logs alone, which represents the final goal of this diploma thesis. If a definition of Top-XX is possible only by identifying characteristic log patterns, performing the whole workflow would not be necessary anymore.
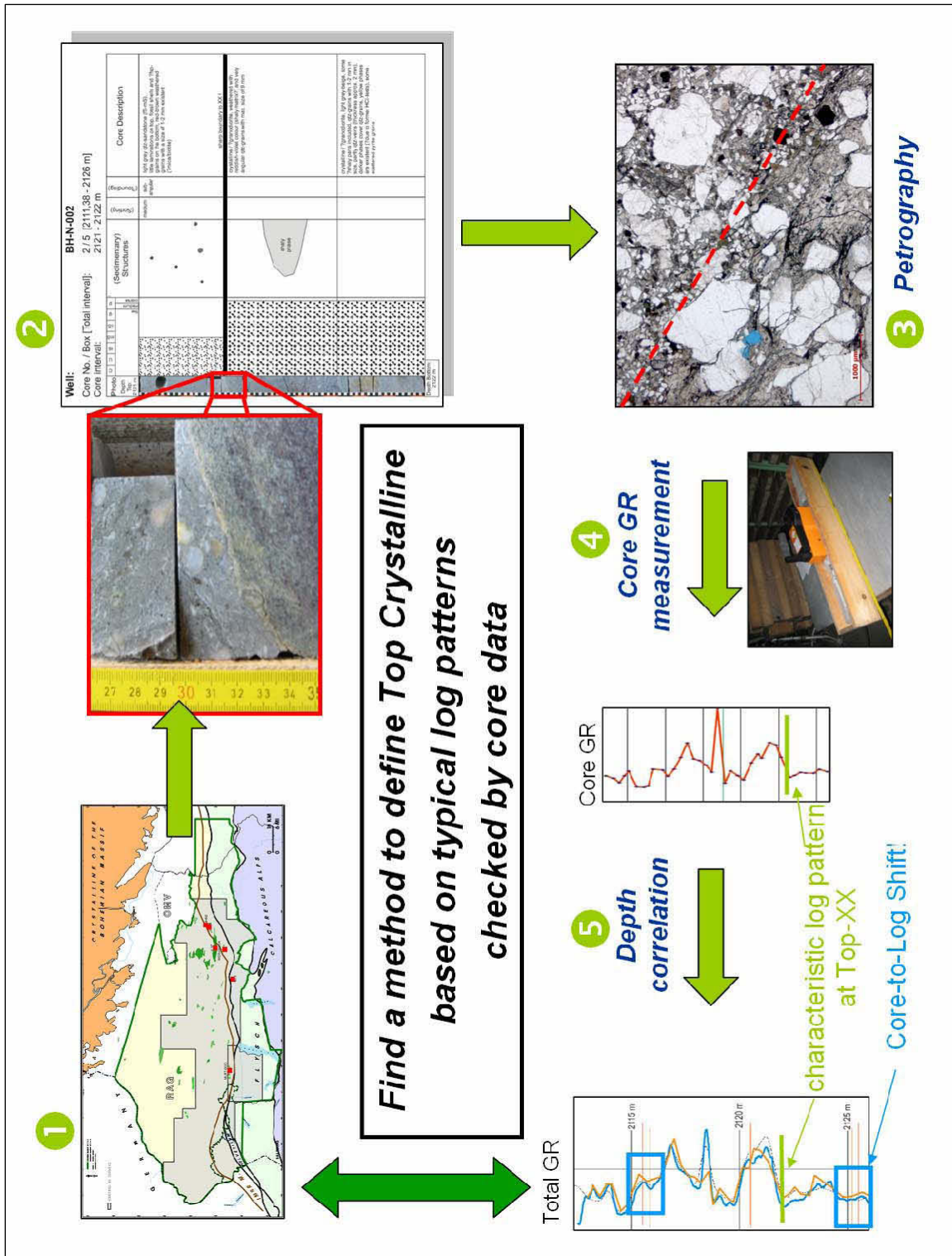
Fig. 1: Workflow to find a method to define top crystalline basement by well logs

1.3   Regional Geology of the Austrian Molasse Basin

The Austrian Molasse basin forms part of the North Alpine Foreland basin (NAFB). As illustrated in Fig. 2, it extends to the west into Bavaria and Switzerland and to the east into the Carpathian foredeep (Sissingh, 1997; Ziegler et al., 1995).
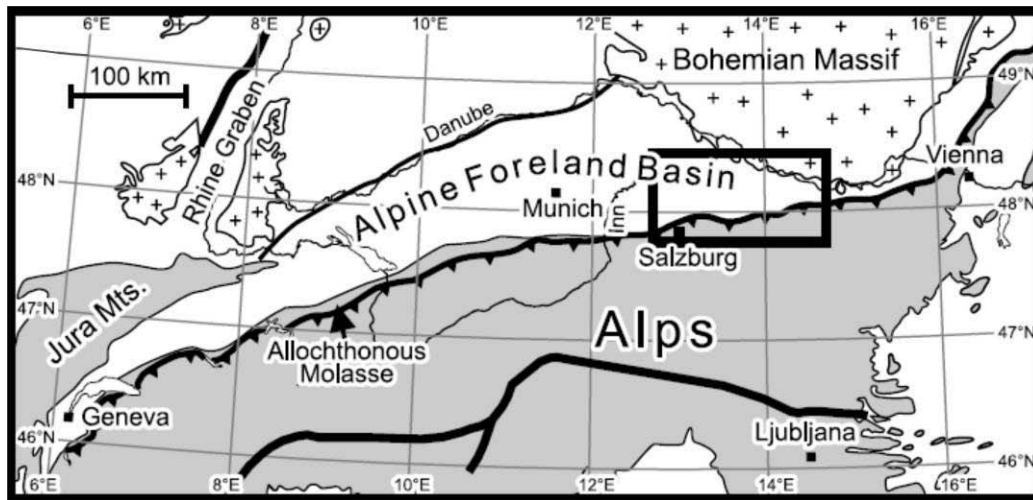

Fig. 2: Location of the Alpine Foreland Basin (fom Sachsenhofer and Schulz, 2006)

The asymmetric and south-dipping foredeep is bordered in the north by the Bohemian Massif and in the south by the main overthrust of the Alpine orogenic front (see Fig. 3), although autochthonous molasse is known to extend up to 40 km underneath the Alpine nappes. Underlying Eocene, Cretaceous or Jurassic rocks, equivalents of the Bohemian Massif represent the crystalline basement. The latter consists of (pre-)Paleozoic granites and metamorphic rocks (Wagner, 1996 and 1998).
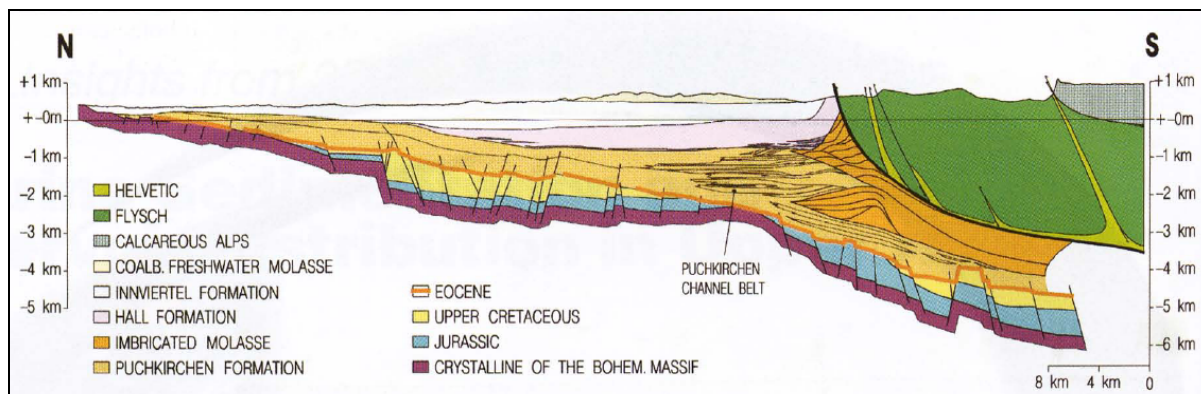

**Fig. 3: Regional geological cross-section of the Upper Austrian Molasse Basin
(modified from Kollmann et al., 1987)**

Strong lateral changes in shape with a decrease in width between the Alpine front and the northern basin margin from about 150 km in the German Molasse basin and less than 10 km at the spur of the Bohemian Massif can be detected (Wagner, 1996).

The infill of the basin consists predominantly of clastic "molasse" sediments of Tertiary age with a thickness of up to 4,500 m near the Alps. The term "molasse" derives from the Latin word "molare", which corresponds to the English verb "to crush" and characterizes a loosely deposited sandstone in French. Today, "molasse" characterizes rocks created by erosion of rapid uplifted orogens, independent from their depositional environment (Malzer et al., 1993).

Tectonic evolution:

The Upper Austrian Molasse basin developed from the late Eocene to the present in response to the loading of the southern margin of the European plate after the final continent-continent collision of the Apulian continental microplate and the North European craton (Wagner, 1998).

In general, the Alpine foreland was influenced by three major tectonic events. During Permo-Carboniferous time graben were created. A passive continental margin stadium developed within the Mesozoic, which was destroyed along fault systems and further affected by partial erosion. The third tectonic event was active within Tertiary time (Wagner, 1998).

The Bohemian Massif represents the basement of the Austrian Molasse basin and consists of crystalline rocks, which originate from the Variscian orogenesis. As a result of erosion, the surface appears as a bumpy, wavy surface. Crystalline rocks of the Bohemian Massif consist of medium- to high-grade metamorphic Precambrian to Paleozoic rocks (e.g. gneiss) and Variscan plutonic rocks (e.g. granite). Apart from granite, gneiss, granulite, migmatite and schists are the predominant lithologies (Wagner, 1998; Wieseneder et al., 1976).

Partially, the upper 80 m of crystalline basement are extremely affected by weathering, which complicates the definition of Top-XX based on seismic data. The most prominent alteration is weathering, which causes the transformation of feldspars to kaolinites (Wieseneder et al., 1976).

The crystalline complex subsides southward beneath the Alps to depths of 4,000 to 8,000 m and is separated by faults into structural highs ("Schwellen") and sub-basins. One of these structural highs is the Bavarian "Landshut-Neuöttinger Hoch", which continues into Upper Austria and represents the NW-SE trending "Central Swell Zone" (see Fig. 4).
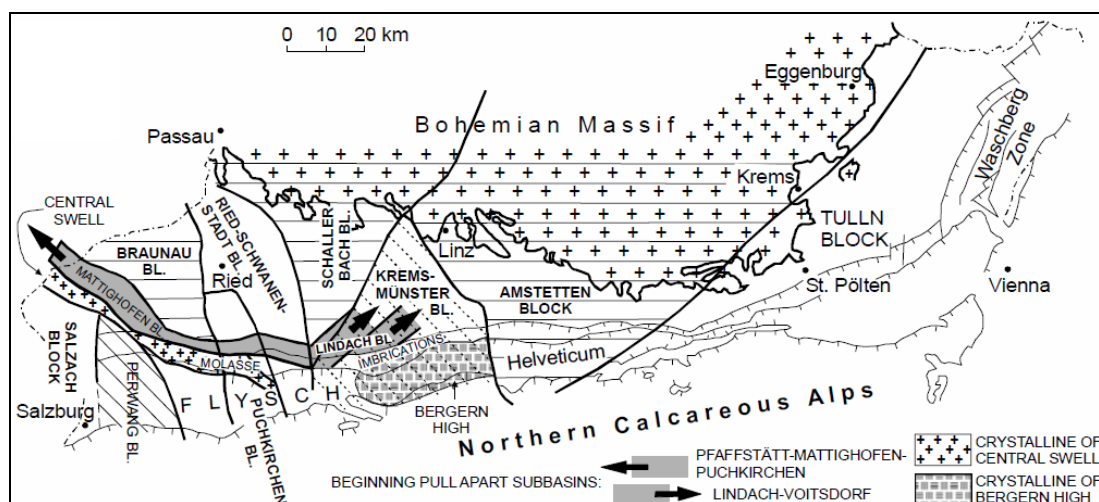

Fig. 4: Tectonic setting with fault blocks within the Alpine and Carpathian Foredeep (from Schulz, 2003; modified from Wagner, 1988)

Flexure of the foreland crust was accompanied by the development of a roughly W-E extensional fault network. Fracture zones appear to control the distribution of the Permo-Carboniferous continental series within the Bohemian Massif and along its margins. Other major fracture zones, which transect the Mesozioc series of Upper Austria and Salzburg may also have come into evidence during the Permo-Carboniferous phase of wrench faulting (Nachtmann and Wagner, 1986).

The reactivation of these fault systems (Wagner, 1998; Genser et al., 2007) is illustrated in Fig. 5. Today, the southern part of the Alpine Foredeep is strongly faulted and folded and generally deeply buried under the thrust-fold belt (Sissingh, 1997; Ziegler et al., 1995).
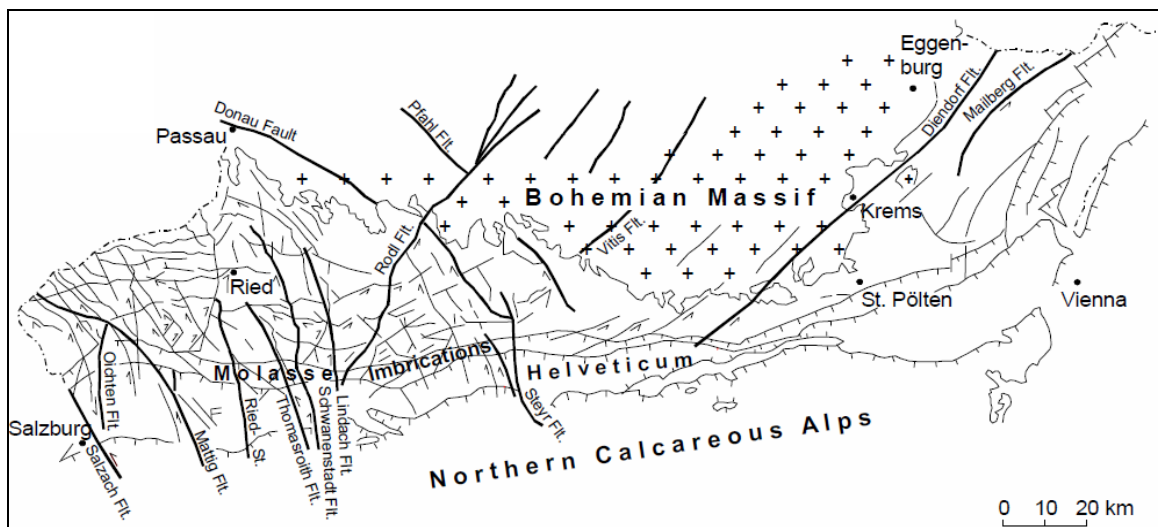

Fig. 5: **Tectonic setting with main faults within the Alpine and Carpathian Foredeep (from Schulz, 2003; modified from Wagner, 1998)**

The sediments of this asymmetric foreland basin are generally underlain by extensively truncated Mesozoic rocks. Truncation resulted from horizontal compressional stresses to which the Alpine foreland was subjected during the Senonian (representing time between Turonian and Maastrichtian, Upper Cretaceous) and especially in Paleocene time (Sissingh, 1997).
Locally, Tertiary foreland sediments unconformably overlie Cretaceous and Jurassic deposits, as well as crystalline basement to the north (Hubbard et al., 2005). The development of this regional unconformity was related to the uplift and erosion of the flexural forebulge in advance of the Alpine thrust belt. Locally, Molasse deposits cover also Paleozoic and basement rocks (Sissingh, 1997).

Cenozoic sediments are divided structurally into the Autochthonous Molasse and the Allochthonous Molasse. The Autochthonous Molasse rests relatively undisturbed on the European basement. The Allochthonous Molasse, including the Imbricated Molasse, is composed of Molasse sediments, which originate from the Alpine thrusts and were moved tectonically into and above the southern Autochthonous Molasse (Sachsenhofer and Schulz, 2006).
The overriding Alpine nappe complex comprises, going from bottom to top, units derived from the outer shelf to slope of the European continental margin (Helvetic nappe), followed by the Flysch nappes, and finally the Austro-Alpine complex in an upper plate position (Genser et al., 2007).

The continent-continent collision of the Apulian microplate and the North European craton resulted in rapid subsidence and an associated increase in water depth since Early Oligocene time. The evidence of this event is preserved in the condensed section of the Schöneck Formation, including dark fish shales and organic-rich marls (Wagner, 1998).

In contrast to Bavaria, the deep marine environment persisted in Upper Austria until Early Miocene time and formed a trough called "Puchkirchen Basin". The northern margin of the Puchkirchen Basin onlaps the crystalline basement (Bohemian Massif) and represents a stable, relatively gentle submarine slope that is almost entirely mud-prone. In comparison, the southern margin of the Puchkirchen Basin displays a steep, tectonically active slope, which is bounded in the south by the thrust complexes of the Helvetic Zone, the Rhenodanubian Flysch and the Northern Calcareous Alps (De Ruig, 2003; Genser et al., 2007).

As the basin was progressively overridden from the south by thrust sheets, sediment supply into the basin increased, whereas accommodation space decreased. This resulted in the deposition of a shallowing-upward, deep- to shallow- to non-marine clastic wedge (Hubbard et al., 2005). Partially, the Puchkirchen foreland deposits also have been incorporated in the Alpine thrust wedge and build an imbricated stack of thrust sheets along the southern basin margin, known as the "Imbricated Molasse" (Wagner, 1996).

Sedimentary history:

Within the Alpine foreland, the sedimentary history is characterized by three main stages separated by unconformities (Wagner, 1998):

- Permo-Carboniferous graben sedimentation
- Mesozoic mixed carbonate-siliciclastic shelf sedimentation (see Fig. 8)
- Cenozoic molasse sedimentation (see Fig. 9)

Paleozoic

Permo-Carboniferous

In the subsurface of the Upper Austrian Molasse Basin late Paleozoic sediments appear to be limited to graben structures on the southwestern margin of the Central Swell Zone. Sediments deposited during Permo-Carboniferous time consist of conglomerates and sandstones. The Permo-Carboniferous spores could have been reworked in situ before Upper Doggerian. Reworked Rotliegend spores were also found from upper Eocene sandstones in a few wells on top of the swell (Wagner, 1998).

Mesozoic

Jurassic:

During Middle Jurassic time (Bathonian-Bajocian) braided fluvial to shallow marine sandstones, partly containing coal layers, are the lowermost Mesozoic series. Between Callovian and early Cretaceous times, light grey to dark brown carbonates with numerous fossils were deposited on the tropical shelf of the Bohemian landmass. The Jurassic facies indicates a progressive shallowing from the SW below the thrust sheets to the margin of the Bohemian Massif (Wagner, 1996).

Fig. 6 displays the distribution of Jurassic sediments within the Upper Austrian Molasse Basin. As indicated by the grey zones, Jurassic sediments are missing on top of the Central Swell Zone and near the Bohemian Massif in the north.
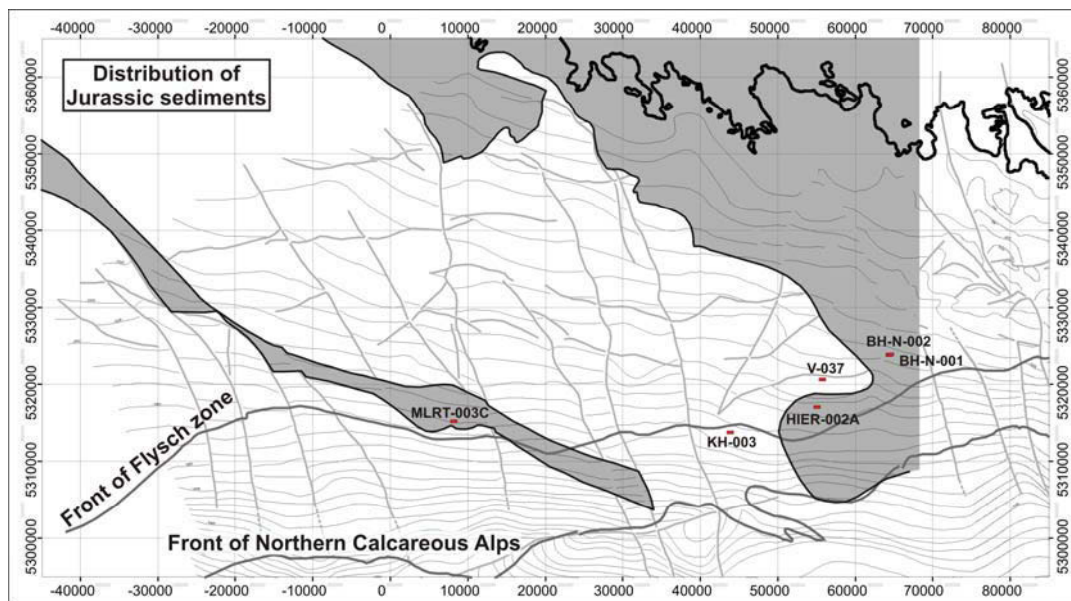

Fig. 6: Distribution of Jurassic sediments within the Molasse Basin
(modified from Goldbrunner, 2000)

Cretaceous:
At Early Cretaceous time, the Jurassic carbonate platform was uplifted, tectonically affected and subjected to erosion and karstification in Bavaria and Upper Austria (Malzer et al., 1993; Nachtmann et al, 1986).
During Cretaceous time the Bohemian Massif acted as a dividing, emergent land sill, which was affected by erosion (see Fig. 7). Deltas were created in positions, where river systems enter the sea (Fuchs et al., 1996).
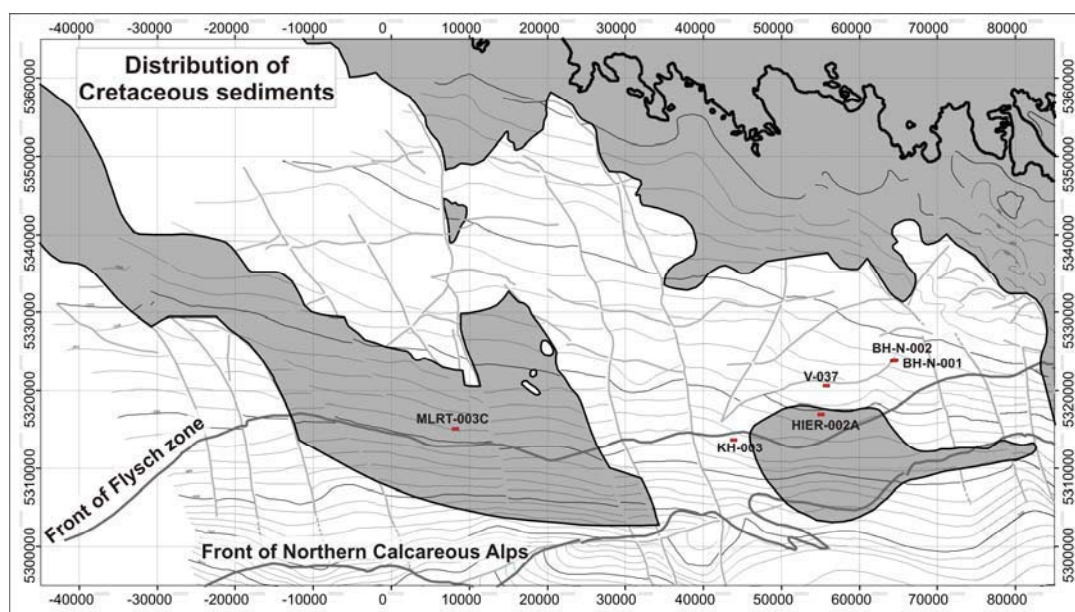
Fig. 7: Distribution of Cretaceous sediments within the Molasse Basin
(modified from Goldbrunner, 2000)

Between Aptian and Albian times, storms deposited Cenomanian glauconitic sands on the shelf. To the NE of the Central Swell Zone the oldest Cretaceous deposits are locally developed and consist of light-grey, white, red or green non-fossiliferous, coarse-grained fluvial sands. These so-called "Schutzfels Beds" (Schutzfels is a locality near Regensburg, Bavaria) infill the Jurassic karst to a depth of 100 m below the Jurassic surface and are overlain by Cenomanian coal-bearing marls which grade upwards into shallow-marine glauconitic sandstones (Wagner, 1998).
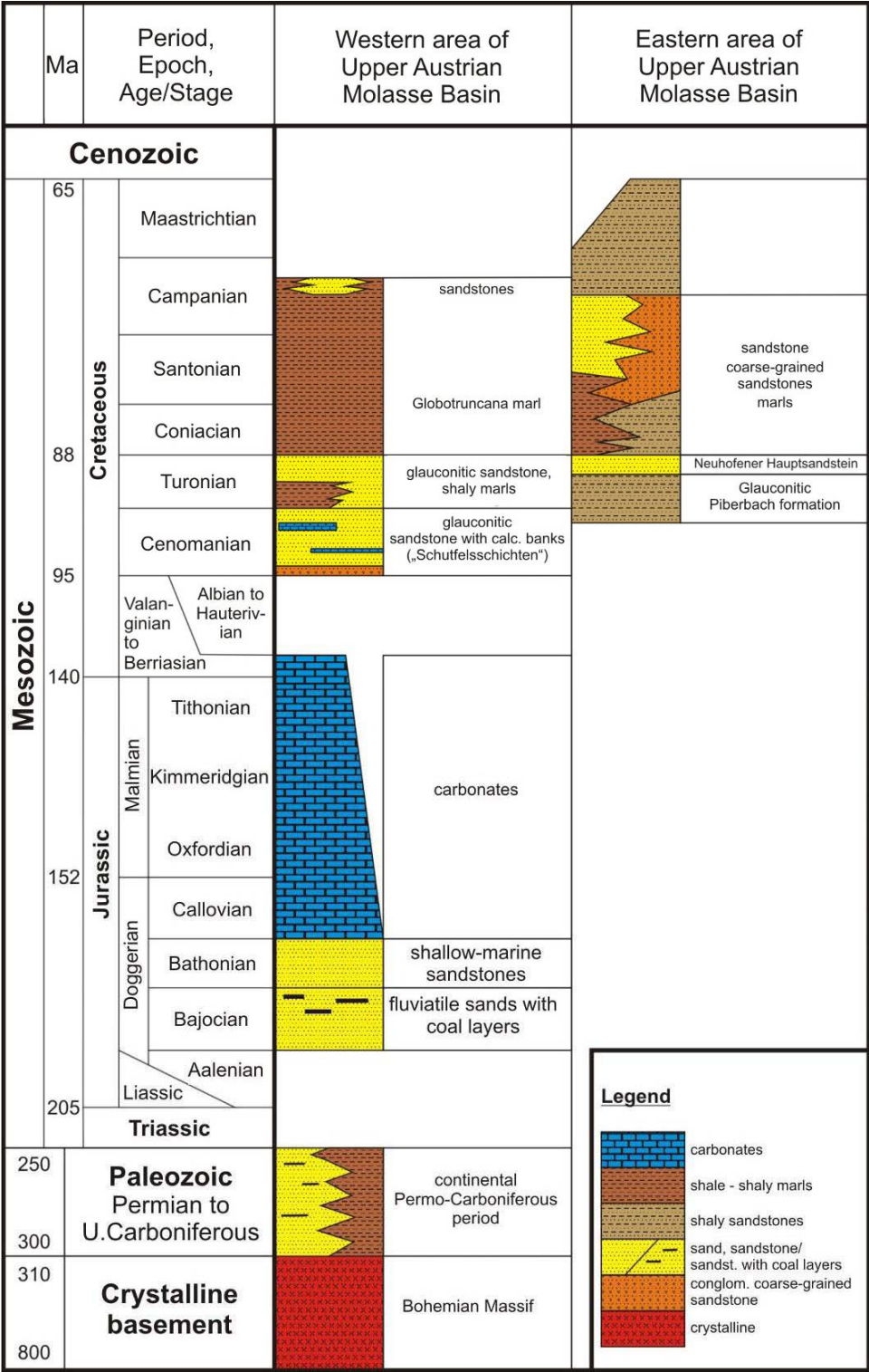
Fig. 8: Stratigraphy of the Upper Austrian Molasse Basin
(modified from Malzer et al., 1993)

In the Cenomanian, approximately 95 million years ago, a marine transgression coming from SW flooded the study area. The main part of Cenomanian sediments is 15 to 70 m thick and consists of storm-dominated, shallow-marine, glauconitic sandstones, which were deposited on a broad shelf. Lower Turonian clays containing glauconitic storm deposits in the upper part overlie Cenomanian clastics (Wagner, 1998).

Sediments of the Late Turonian to Late Campanian are intensively burrowed mudstones, which accumulated under outer-shelf conditions. During Late Campanian time, 300 m of sandstones were deposited NW of the Central Swell Zone and shale out across this tectonic element to the SW (Wagner, 1998).

Total sediment thickness of the Cretaceous can be up to 1,000 m (Malzer et al., 1993).

At the end of Cretaceous time (65 Ma) the Austrian Molasse Basin was uplifted, which resulted in partial erosion of the Mesozoic sediments (Malzer et al., 1993).

Cenozoic:

Sediments range from terrestrial to shallow marine clastics and limestones to marls of a deeper shelf (Genser et al., 2007).

Eocene:

The Molasse stage began in Late Eocene time with deposition of fluvial and shallow-marine sandstones, shales and carbonates. In Upper Eocene time the Molasse basin is flooded by the Helvetic Sea. From bottom to top, the Eocene deposits can be divided into the following sections (Nachtmann, 1989; Wagner, 1980):

· transgressive horizons directly overlying the pre-Tertiary basement
· infills of channels cut into limnic-brackish sediments
· littoral deposits, partly interfingering with Lithothamnium limestone
· fine-grained sandy marls and nummulitic sandstones within sublittoral to neritic sediments

The limnic-brackish series consist of marginal-marine depositions including marsh. Mudstones with various colours can be found at the base, whereas dark grey mudstones and clayey marls are present at the top. Remnants of plants and roots are included (Wagner, 1980).
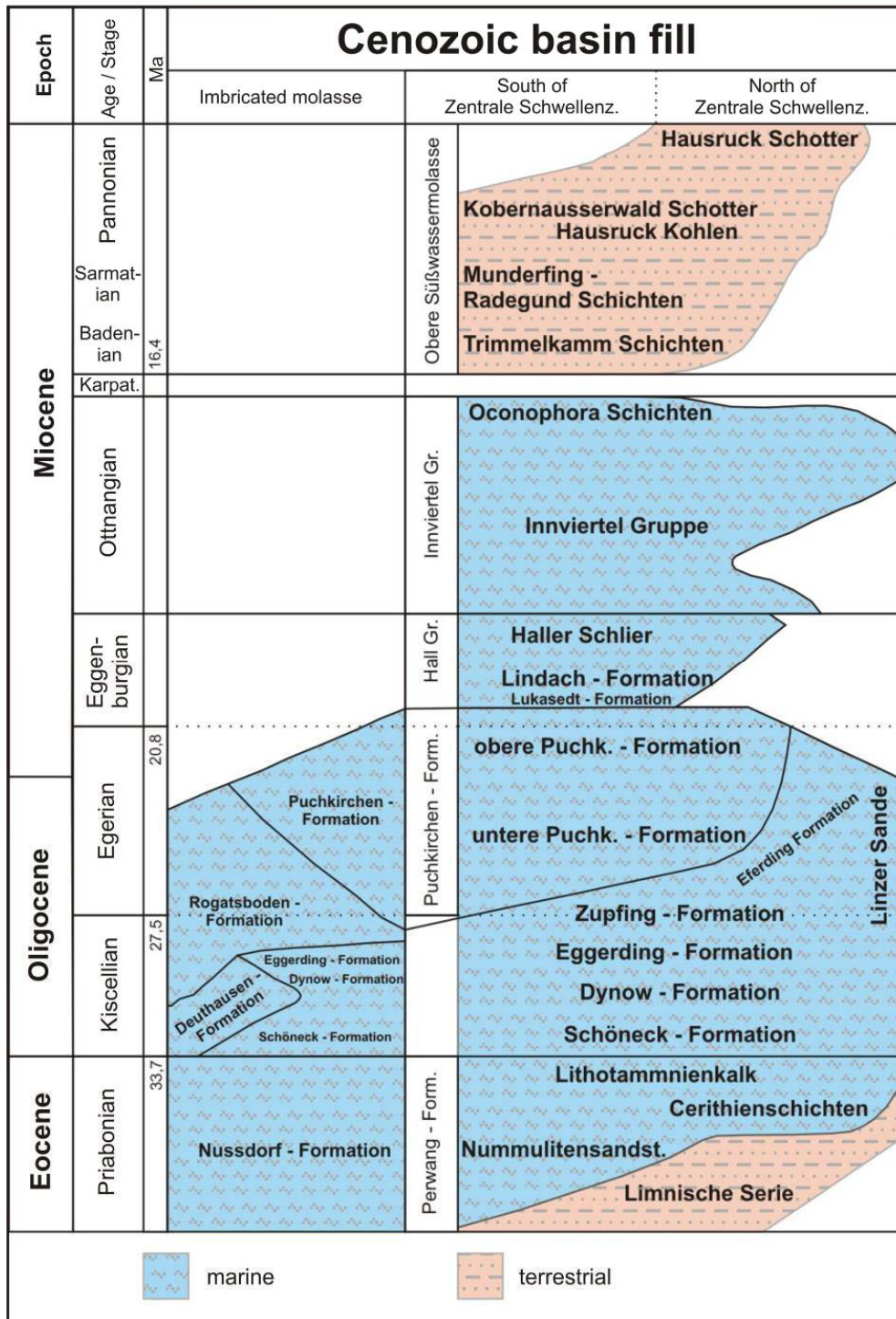
Fig. 9: Stratigraphy of Cenozoic basin fill of Molasse Basin
(modified from Wagner, 1998)

Siliciclastics dominate the basal development of the Late Eocene successions and consist of sandstones derived from erosion of the crystalline basement. Argillaceous sediments can be locally abundant. During Late Eocene times, a southern and a northern facies region can be separated. The northern one is dominated by coralline algae, whereas the southern one shows larger foraminifera and bryozoans. Rudstones composed of coralline algal branches are the most common algal limestones (Rasser and Piller, 2003).

Upper Eocene algal limestones of the Eastern Alpine Foreland in Austria contain three different types of crustose algal frameworks, which are the coralline-coral, the pure coralline algal and the Peyssonneliacean dominated frameworks. The coralline-coral frameworks develop from siliciclastic sediments and show succession from coverstones to bind- to cruststones, whereas the pure coralline algal frameworks are restricted to cruststones dominated by Lithothamnium and Neogoniolithon. Peyssonneliacean dominated frameworks occur with intercalations of coralline algal crusts and formed in muddy environments (Rasser and Piller, 2003).

The type of framework provides information on the crust-forming algal taxa, the sedimentary regime and the environmental setting. Crustose coralline algae are among the main carbonate producers in the Cenozoic and provide information on the palaeo-environmental situation (Rasser and Piller, 2003).

In general, Eocene sandstones are mainly medium to coarse-grained "subarcoses" with medium grade of sorting and angular components. Due to the low grade of rounding and mainly unweathered potassium feldspars, a very short-distance transport from a (gneiss)granitic source area, the Bohemian Massif, can be assumed. Shaly and marly sediments, several hundreds of metres thick, follow above the Eocene sediments (Nachtmann, 1989).

Oligocene:

After an initial stage of deep marine sediment-starved basin conditions, clastic detritus from the rising Alps started to fill the Molasse basin from mid Oligocene time onwards. During Early Kiscellian times the Schöneck Formation (or formerly "Lattorf Fischschiefer") has been deposited. It consists of dark grey or brown, shaly, thin-bedded marls and shales and include phosphorite nodules. The Schöneck Formation has a typical thickness of 10 to 20 m, abundant fish remnants and medium to deep-water calcareous and agglutinating foraminifera (Wagner, 1998).

The Schöneck Formation is overlain by the Dynow Formation, which represents a 5 to 15 m thick sequence of Rupelian light chalky marls dominated by cocco-lithophorides. On top of the Dynow Formation, the Eggerding Formation is deposited. It consists of banded marls with dark grey laminated pelites with thin white layers of nanoplankton, reaching a thickness of typically 35 to 50 m (Sachsenhofer and Schulz, 2006). The banded marl contains breccia of submarine reworked lithothamnium limestone and Schöneck formation (Wagner, 1998).

The Zupfing Formation can reach a thickness of up to 450 m including silty shales to marls of Rupelian time with fish remnants and increasingly dark brown, green and grey limestones with nanofossils. It is only present in the subsurface and was affected by intensive submarine erosion. Towards the south, these marls pass into sandstones and conglomerates that were derived from the rising Alps. Along the northern rim of the present basin and the spur of the Bohemian Massif terrestrial input dominated (Wagner, 1998).

The deep-marine Oligocene/Early Miocene trough in Upper Austria is known as the Puchkirchen Basin. It is characterized by a succession of gravity flow deposits with a total thickness of up to 2,000 m locally, forming part of the Rupelian sandstone, as well as the Upper Oligocene/Lower Miocene Puchkirchen Formation and the basal parts of the Miocene Hall Formation. The deposits of the Puchkirchen Basin contain a wide range of clastic lithologies, ranging from clast-supported sandy conglomerates, muddy matrix-supported conglomerates, massive and pebbly sandstones to fine-grained sandstones and siltstones (De Ruig, 2003).

The mainly deep-water Alpine foredeep was closed towards the end of the Eocene and succeeded by the generally shallow-water Molasse Basin, forming the western-most part of the Paratethys (Sissingh, 1997).
In the Egerian, the basin configuration remained essentially the same with terrestrial to shallow marine conditions along the northern margin. At the same time, the southernmost part of the basin was overridden by the advancing Alpine nappe complex, incorporating Molasse sediments. With Egerian time, the orogenic wedge reached essentially its present position and the basin axis shifted to the north. The basin also shows a transgression to the north and the spur of the Bohemian Massif indicates the first major phase of subsidence (Genser et al., 2007).

Miocene:
In the Ottnangian, the basin shallowed progressively and finally the sea regressed to the east of the Bohemian Massif at the end of this stage. From the Karpatian to the Pannonian stage, terrestrial sediments were deposited in the basin west of the Bohemian Massif. Only close to the Vienna basin, marine incursions into the Molasse basin occurred up to the Sarmatian stage. In the Pannonian stage, a change from mainly W- to E-directed transport occurred. After the Pontian stage, erosion of the sediments was induced by the uplift of the Molasse basin (Genser et al., 2007).

Petroleum System:

In 1891, the gas field Wels, which is situated approximately 37 km SW of Linz, was discovered by a well drilled for artesian water. This was the start of the hydrocarbon exploration era within the Upper Austrian Molasse Basin (Janoschek, 1961). The first economic oil well within the Upper Austrian Molasse Basin was Puchkirchen 1, which had been discovered in 1956 by RAG (Kollmann, 1977). The oil fields within the Austrian Molasse Basin and the position of the investigated wells are displayed in Fig. 10.

The Early Kiscellian Schöneck Formation (or formerly "Lattorf Fischschiefer") is the source rock for the Molasse oil (Wagner, 1998).

Two petroleum systems occur in the Alpine Foreland Basin east of Munich, which will be described below.

Mesozoic to Lower Oligocene thermally generated oil and gas system:

Most important reservoirs for oil and minor thermal gas are upper Eocene basal sandstones, typically on the upthrown side of W-E trending antithetic normal faults. Some hydrocarbons are trapped in Eocene carbonates (Sachsenhofer and Schulz, 2006). Additionally, oil and thermal gas is produced mainly from the Cenomanian sandstones (Nachtmann, 1989; Nachtmann, 1994).

Reservoirs are fluvial and shallow marine sandstones and, to a minor degree carbonates of Dogger, Cretaceous (Cenomanian, Turonian and Campanian), Upper Eocene and Oligocene (Rupelian) times. Combined stratigraphic and structural traps (mainly anticlinal structures) keep the oil in place (Wagner, 1996; Nachtmann, 1995). Correlations of the isotope and biomarker ratios of the oils with the rock extracts suggest that the thermogenic hydrocarbons are mainly sourced by the Lower Oligocene Schöneck Formation. The Dynow Marlstone and the Eggerding Formation show oil potential. The oil kitchen is approx. 4 to 7 km deep and lies beneath the Alpine nappes, indicating long-distance lateral migration. Hydrocarbon generation started during thrusting in Miocene time (Sachsenhofer and Schulz, 2006).

Oligocene-Miocene biogenic gas system:

Reservoirs for dry and isotopically light gas, considered biogenic in origin, are Oligocene (Egerian) and Miocene (Eggenburgian) sandstones and sandy conglomerates deposited within and in close vicinity of the Puchkirchen deep-sea channel belt. Significant accumulations of gas are stratigraphically and structurally trapped in channel thalweg and slope-fan sandstones, with more modest amounts in overbank lobe and tributary-channel deposits. Probably the biogenic gas was generated in Oligocene and Miocene shales (Sachsenhofer et al., 2006).
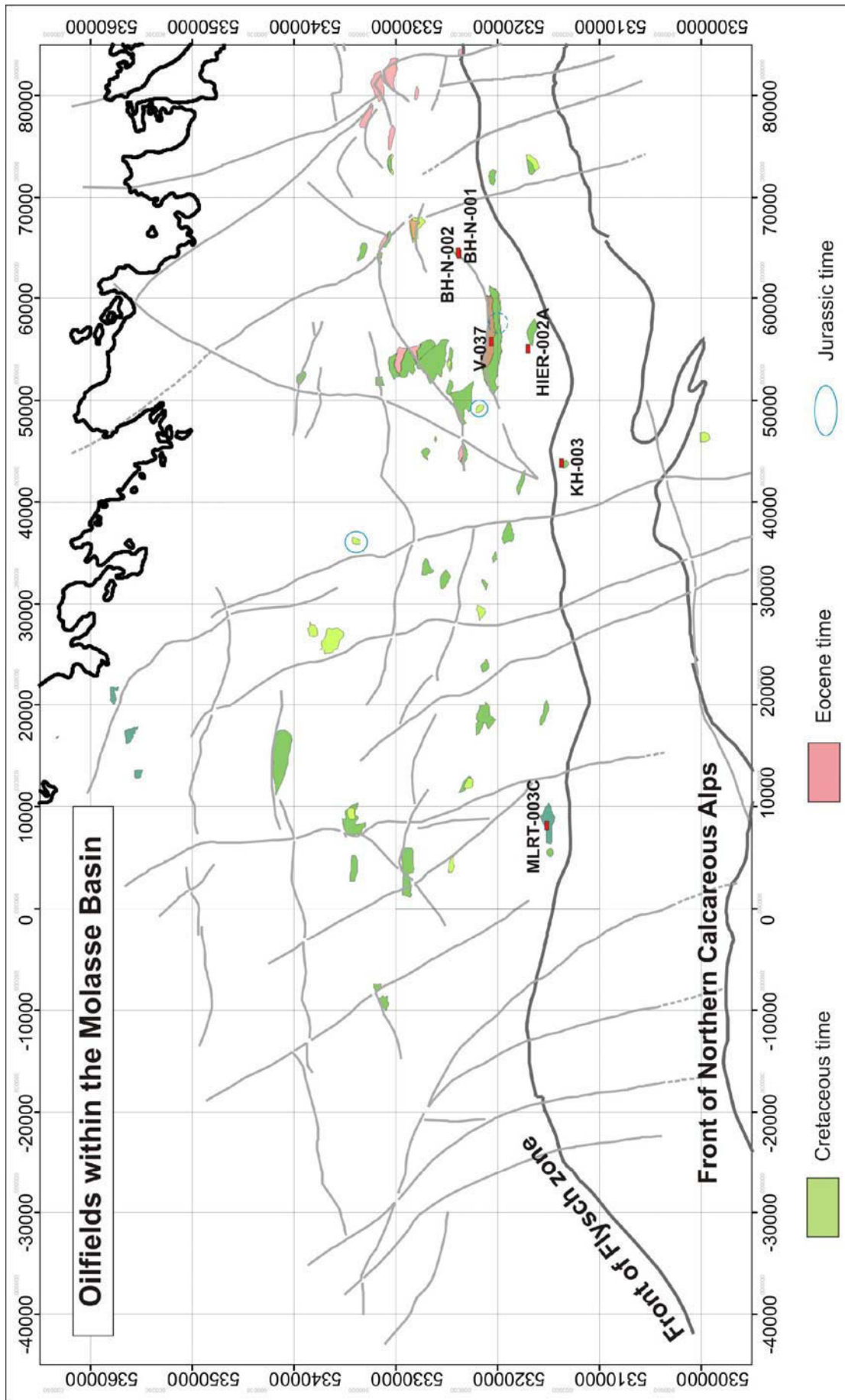
Fig. 10: Oil and thermal gas fields within the Molasse Basin hosted by formations with either Cretaceous, Eocene or Jurassic time (modified from Malzer et al., 1993)

2. DATA
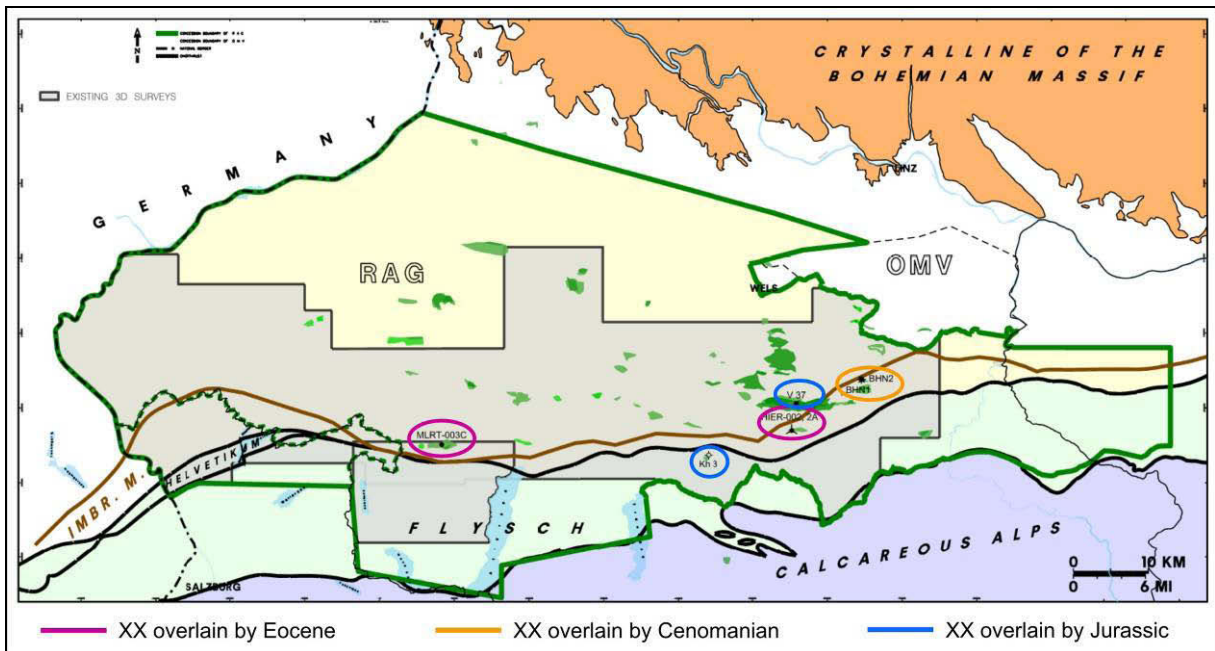
Fig. 11: Geographic position of studied wells. In wells MLRT-003C and HIER-002A (magenta) crystalline basement is overlain by Eocene rocks, in BH-N-001 and BH-N-002 (orange) by Cenomanian rocks and in KH-003 and V-037 (blue) by Jurassic rocks.

All six investigated wells are located within the Upper Austrian Molasse Basin (Fig. 11). The wellls have been selected based on the availbility of core material and the age of the sediments overlying the crystalline basement. In wells MLRT-003C and HIER-002A (magenta) crystalline basement is overlain by Eocene sandstone, whereas in BH-N-001 and BH-N-002 (orange) it is overlain by Cenomanian rocks. KH-003 and V-037 (blue) represent wells with Jurassic sediments overlying the crystalline basement.

Table 1 summarizes all data available and used for investigation of the wells selected.

Well name	Coordinates [m]		Ground level [m]	Sediments above Top-XX	Type of crystalline	Log data
	X	Y				
HIER-002A	55,238.35	5,316,965.97	515.52	Eocene	magmatic (granite)	Completion log, GR, SP, DT4P, ROP, HCAL, NPOR, NPHI, HLLS, HLLD, RXOZ, RHOZ, PEFZ
MLRT-003C	8,325.19	5,315,104.00	549.64		metamorphic (gneiss with migmatitic structures)	Completion log, GR, SP, HCAL, NPOR, HLLS, HLLD, RXOZ, RHOZ, PEFZ, FMI
BH-N-001	64,552.8	5,323,767.72	377.53	Cenomanian	magmatic (?granite)	Completion log, GR, SP, DT, HCAL, NPHI, NPOR, HLLD, HLLS, RXOZ, RHOZ, PEFZ
BH-N-002	64,595.38	5,323,831.22	374.30		magmatic (granodiorite-diorite)	Completion log, GR, SP, DT, HCAL, HLLS, HLLD, RXOZ, RHOZ, PEFZ
KH-003	44,031.49	5,313,700.51	452.20	Jurassic	magmatic (granite)	Completion log, GR, SP, CAL, DT, LLS, LLD, MSFL
V-037	55,838.23	5,320,598.20	461.35		metamorphic (?cordierit-bearing migmatite)	Completion log, GR, SP, CAL, DT, LLS, LLD, MSFL

Table 1: Summary of well data incl. coordinates, ground level, age of transgressive sediments and type of crystalline rocks, as well as log data available

Well BH-N-001 is situated near Bad Hall, approximately 40 km SSW of Linz. BH-N-001 was drilled in 2000 and produces oil out of Eocene and Cenomanian sandstones. According to core analysis, the crystalline basement (?granite) is overlain by Cenomanian sandstone. The top of the crystalline basement was identified in box no. 4 of core no. 3.

BH-N-002 was drilled in 2002 near BH-N-001. The crystalline basement of BH-N-002 consists of magmatic rocks (granodiorite-diorite) and is overlain by Cenomanian sandstone. Eocene sandstones within BH-N-002 are hydrocarbon bearing, but production is nearly impossible, because asphaltenes have plugged the pore space (Sachsenhofer and Schulz, 2006). Therefore, BH-N-002 only produces some gas out of this horizon. The top of the crystalline basement in well BH-N-002 is located in box no. 5 of core no. 2.

HIER-002A was drilled from December 2006 to February 2007 and is located in Hiersdorf near "Wartberg an der Krems", about 50 km SW of Linz. HIER-002A produces oil out of Eocene sandstones, which overlie crystalline basement (top within box no. 9 of core no. 3). Crystalline rocks are represented by coarse-grained granite.

Among the investigated wells, MLRT-003C has the westernmost geographic position, as illustrated in Fig. 11. It was drilled in 2008 and is situated in Mühlreith, approximately 15 km W of Vöcklabruck and 100 km SW of Linz.
As HIER-002A, also MLRT-003C represents Eocene sandstones above coarse gneiss with migmatitic structures, although these sandstones are tight. Oil has been found within Rupelian sediments, but currently there is no production. Top of crystalline basement can be identified within box no. 7 of core no. 4. In comparison to the other wells, an FMI log has only been measured in well MLRT-003C.

From October 1982 to January 1983 the well KH-003 was drilled in the region of Kirchham, approx. 50 km SW of Linz. KH-003 was an appraisal well drilled for oil, but encountered water-bearing Eocene and Cenomanian sandstones. According to RAG, especially logs of KH-003 could be affected by a log shift.
The top of the magmatic crystalline basement (granite) is located in box no. 1 of core no. 4 and is overlain by sandstones of Jurassic time.

The oil field Voitsdorf was discovered in 1962 and represented the largest oil field within the Molasse Basin. Within this oil field V-037 was a production well, drilled in 1981. Currently Eocene rocks are totally water bearing and Cenomanian sandstones shows more than 50 % water content. The well is located in Voitsdorf near "Ried im Traunkreis", approximately 35 km SW of Linz. The crystalline basement (?cordierit-bearing migmatite) of V-037 is overlain by Jurassic sandstones. According to the data investigated, it is questionable, if crystalline basement has been cored at all, although RAG has interpreted it.

3. GEOPHYSICAL WELL LOGGING

Geophysical well logging is performed to obtain detailed information concerning the composition of the subsurface and especially the target horizon.

As soon as a borehole is drilled into a formation, the rock-fluid system is altered in the near area of the borehole. The borehole and the rock surrounding are contaminated by drilling mud, which affects logging measurements. Fig. 12 illustrates the borehole environment for a better understanding.
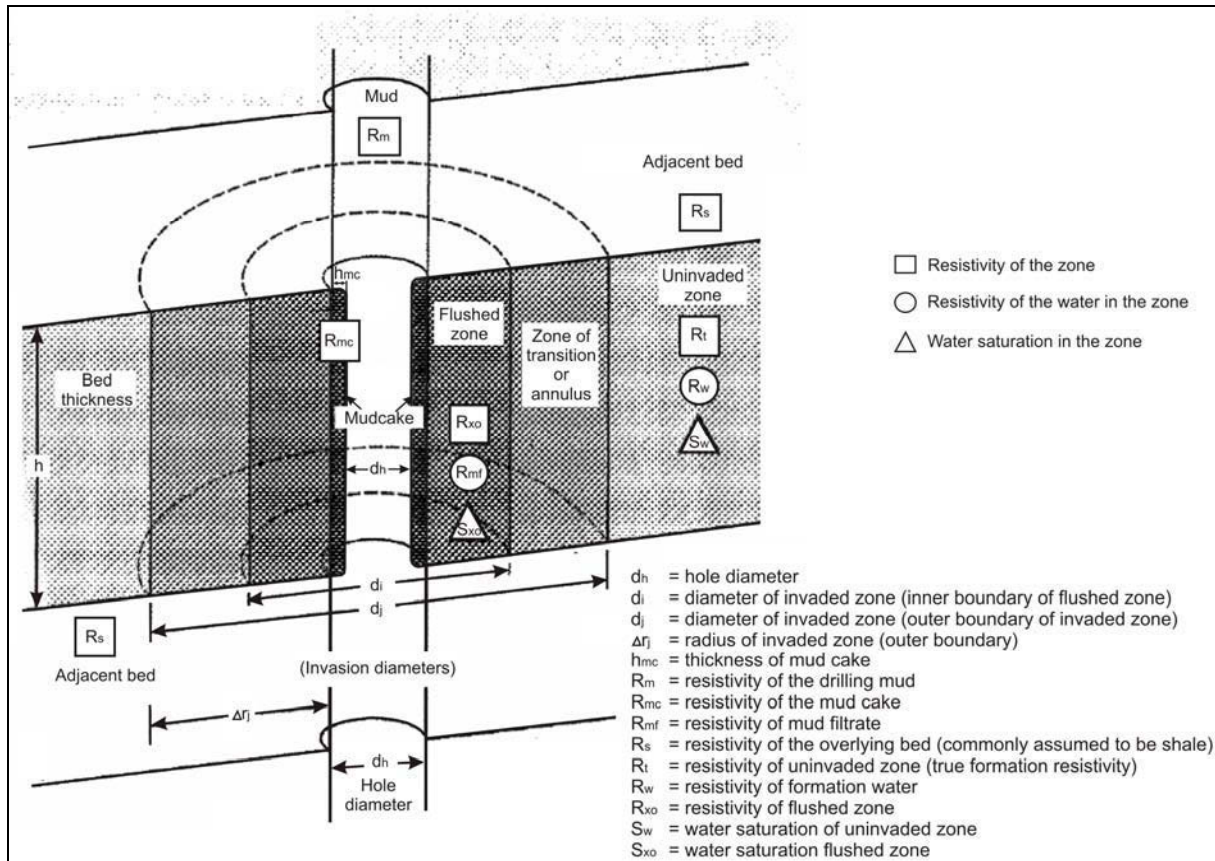
Fig. 12: Borehole environment (from Schlumberger, 1998)

The invaded zone is the area, in which the original fluid is replaced by mud filtrate. It consists of a flushed zone and a transition or annulus zone, where the formation fluids and mud filtrate are mixed. The flushed zone occurs close to the borehole where the mud filtrate has almost completely flushed out a formation's hydrocarbons and/or formation water, whereas the transition zone is located between flushed and uninvaded zone. The uninvaded zone is the area with true formation resistivity, which is not contaminated by mud filtrate. The amount of invasion present depends on permeability and not on porosity of the rock. Additionally, the mud cake acts as a barrier to further invasion (Asquith et al., 2004).

The following illustration (Fig. 13) gives an overview of the vertical resolution of the logging tools compared with the geological objects (volumes and surfaces).
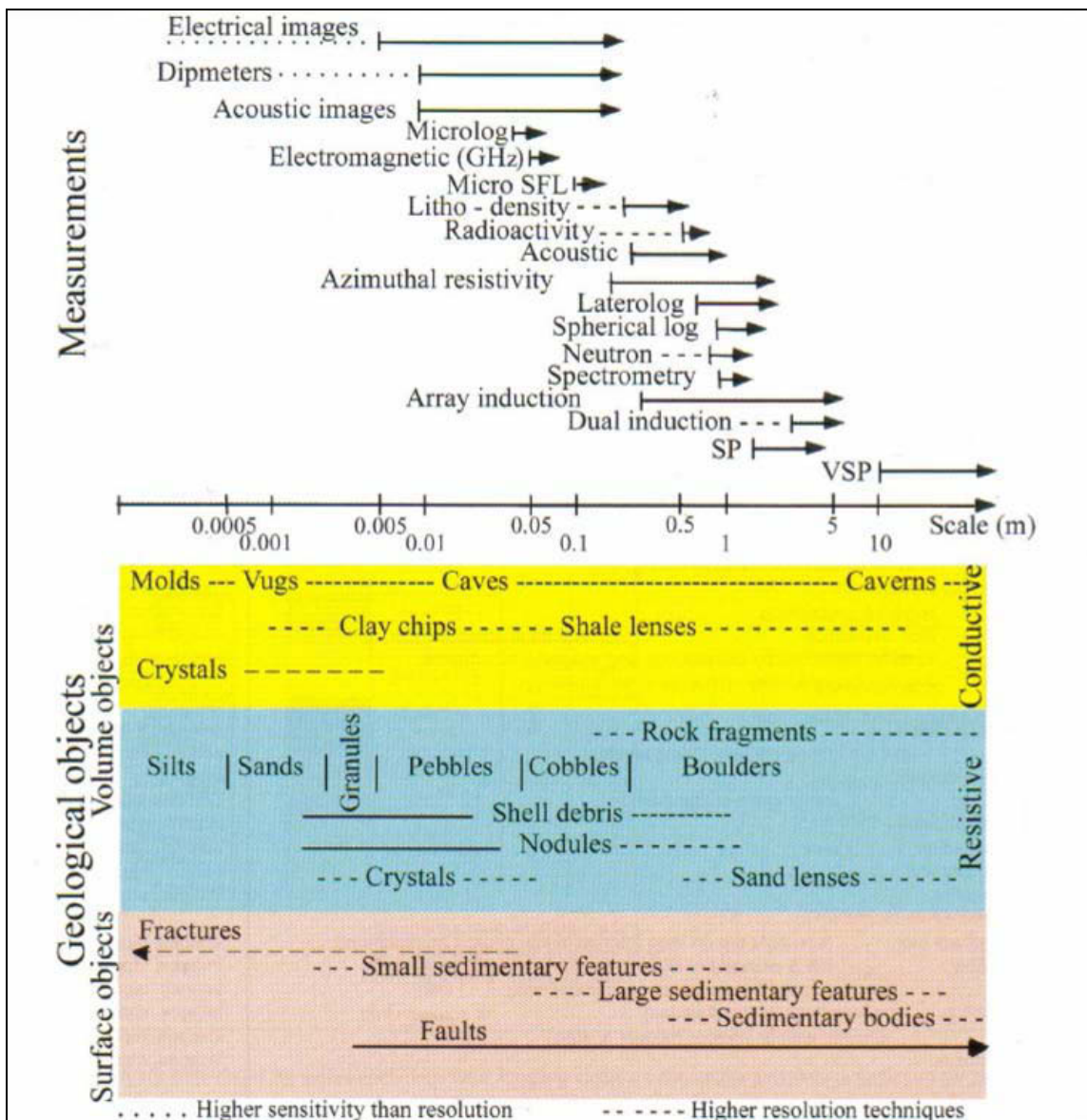
Fig. 13: Overview of vertical resolution of logging tools (from Serra, 2004)

3.1 Caliper   Log (CAL)

The caliper log records the maximum size of the borehole and, therefore, it is essential concerning corrections of other logs based on breakouts etc.

<u>Measuring principle:</u>
Caliper logging is an operation that is performed with multi-pad tools that are centered in the borehole. The sonde can include two to four arms (see Fig. 14, modified from "LIAG – Leibnitz-Institut für Angewandte Geophysik").
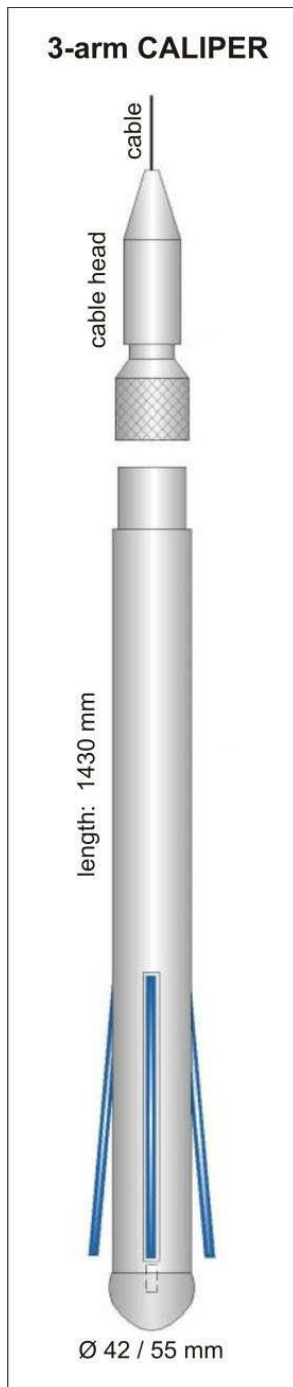
Usually, caliper log is measured mechanically, but sometimes it is measured also by using sonic log devices, like the ultrasonic caliper.

The determination of the borehole diameter is important for the calculation of the volume of cement required. Furthermore caliper provides qualitative indication of condition and stability of the wellbore and is used to determine the position of the packers used for openhole tests. As the mud cake can be easily identified and recorded by caliper log, it is also used to confirm the presence of porous and permeable layers (Desbrandes, 1985).

Fig. 14: Caliper sonde

3.2 Gamma Ray Log (GR)

Gamma ray (GR) logs measure the natural radioactivity in formations and can be used for identifying lithologies (e.g. shale/clay) and for correlation purposes. Shale-free sandstones and carbonates have low concentrations of radioactive material and give low GR readings. However, clean sandstone (i.e., with low shale content) might also produce a high gamma ray response if the sandstone contains potassium feldspars, micas, glauconite, heavy minerals or uranium-rich waters (Asquith et al., 2004).

The unit for radioactivity is API, which is the abbreviation for American Petroleum Institute. The definition for the API unit comes from an artificially radioactive formation constructed at the Houston University to simulate about twice the radioactivity of shale, which generates a standard value of 400 API units. This construction is used to calibrate measurement tools (Serra, 2004).
The GR log can be combined with any other tool, like neutron, resistivity, sonic tool etc. (Serra, 2004).

Radioactive source:
The main radioactive elements are uranium (^{238}U), thorium (^{232}Th) and potassium (^{40}K), which all have typical GR emission spectra (see Fig. 15).
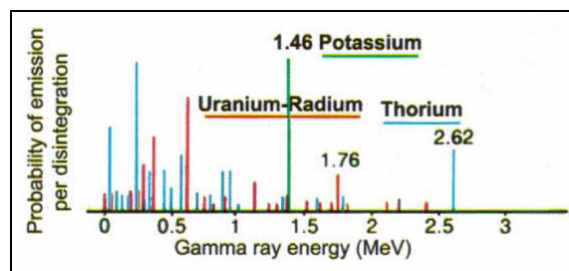
**Fig. 15: Theoretical GR emission spectra of K, Th, U
(from Serra, 2004)**

During alteration, some silicates, such as feldspars, are completely dissolved. At this stage, the *potassium* is thus liberated in ionic form and transported in solution. In contrast, mica may lose only part of its potassium during alteration, whereas the rest stays in the crystal lattice.
The source of *uranium* is often in magmatic rocks of acidic composition, like granite. Uranium has a lithophile character and represents different mobility in aqueous solutions concerning the type of environment. Under oxic conditions is it very soluble and can therefore be transported mainly in solution, rarely in suspension. It is dissolved during alteration or leaching of source minerals. Uranium may be absorbed on the surfaces of clay particles or accumulated in phosphates, very resistant minerals (zircon, monazite etc.) and organic matter.
Thorium originates also from igneous rocks like granites, pegmatites, syenites or nepheline syenites. During the alteration and leaching of rocks, up to 90 % of the thorium present can be removed. However, thorium is hardly soluble and thorium-bearing minerals are stable.

Consequently, almost all thorium is transported in suspension and is a common constituent of the heavy mineral fraction of sediments or can be found in certain beach-sands and placers. The small amount of dissolved thorium is absorbed onto clay minerals.

Unlike uranium, thorium is immobile during diagenesis. Table 2 gives detailed information concerning concentrations of the elements uranium, thorium and potassium, as well as the gamma ray-activity in API-units (Serra, 2004).

Mineral	Amount of Uranium [ppm]	Amount of Thorium [ppm]	Amount of Potassium [%]	GR-activity [API]
Montmorillonite	2-5	14-24	0-4.9	150-200
Chlorite	-	3-5	0-0.35	180-250
Kaolinite	1.5-9	6-42	0-0-6	80-130
Illite	1.5	10-25	3.5-8.3	250-300
Glauconite	-	< 10	3.2-5.8	-
Bentonite	10-36	4-55	-	-
Biotite	1-40	0.5-50	6.2-10.1	approx. 270
Muscovite	2-8	10-25	7.9-9.8	
Microcline	-	< 0.01	10.9	approx. 220
Orthoclase	-	< 0.01	11.8-14	
Plagioclase	0.2-5	0.5-3	-	0
Sylvinite	0	0	52.4	500
Monazite	500-3,000	25,000-200,000	-	-
Zircon	300-3,000	100-2,500	-	-

Table 2: Amount of Uranium, Thorium, Potassium and GR-activity of certain minerals

There are also trends concerning the natural radioactivity of rocks. For example, the larger the amount of SiO_2 in crystalline rocks, the higher the natural radioactivity. In contrast, the radioactivity of sedimentary rocks increases due to an increasing amount of clay minerals (Schön et al., 1999).

Table 3 shows thorium, uranium and potassium contents of igneous rocks (Serra, 2004).

Igneous rocks	Th [ppm]	U [ppm]	K [%]
Granite	19-20	3.6-4.7	2.75-4.26
Granodiorite	9.3-11.0	2.6	2-2.5
Diorite	8.5	2.0	1.1

Table 3: Contents of Th, U and K of igneous rocks (from Serra, 2004)

Gamma rays are absorbed or attenuated by the medium through which they travel, particularly when their energy is low or the medium dense. Therefore, a natural GR tool only detects radiation originating from a relatively small volume surrounding the detector. Furthermore, gamma radiation is attenuated to different degrees by the presence of drilling mud, tubing, casing, cement, as well as by the position of the tool, logging speed, hole condition etc., which can be corrected by use of correction charts. Unlike the SP log, the gamma ray response is not affected by formation water resistivity (Serra, 2004).

<u>Measuring principle:</u>

→ **TOTAL GR Spectroscopy**

The GR spectroscopy of total natural radioactivity is the technique of measuring the spectrum, or number and energy, of gamma rays emitted as natural radioactivity by the formation. Source of radioactivity are the isotopes of ^{40}K, ^{232}Th and ^{238}U.

Natural gamma ray spectroscopy logs were introduced in the early 1970s, although they had been studied from the 1950s (Oilfield glossary, SLB).

Generally, the GR tool contains one detector of scintillation-counter type. This type of counter is more efficient and rapid than the Geiger-Mueller counters previously used. Its dimension is shorter allowing a better vertical resolution. The detector records all the gamma rays emitted by the formation above some practical lower energy limit (on the order of 100 keV) (Serra, 2004).

→ **SPECTRAL GR Spectroscopy**

Spectral GR tools (see Fig. 16, modified from LIAG – Leibnitz-Institut für Angewandte Geophysik) provide insight into the mineral composition of formations. A log of spectral gamma ray usually presents the weight fraction of potassium (%), thorium (ppm) and uranium (ppm).

A scintillation detector records the number of gamma rays emitted by the formation. Furthermore, it records also the characteristic energy of each of the three main types of source elements thorium (^{232}Th), potassium (^{40}K) and uranium (^{238}U), as well as their decay products (Asquith et al., 2004).

To obtain a quantitative evaluation of thorium, uranium and potassium from an analysis of the total energy distribution, it is helpful to divide the spectrum into a high- and a low-energy region. The logging tools available differentiate each other, for example, through the type of sensors or the number of windows, which will have responses corresponding to the amounts of Th, U and K. Potassium (^{40}K) has a single energy of 1.46 MeV, whereas thorium and uranium emit radiation at various energies. However, they have typical energies at 2.614 MeV (^{232}Th) and 1.764 MeV (^{238}U) (Asquith et al., 2004).

Small peaks of thorium, uranium or potassium are only clearly visible on the low-energy windows. On the high-energy windows these peaks are difficult to separate from the statistical noise (Serra, 2004).

The Natural GR Spectroscopy (NGS) tool uses five-window spectroscopy to resolve the total gamma ray spectra into K, Th, and U curves. The standard gamma ray and the gamma ray minus the uranium component are also presented (SLB Oilfield glossary).

The most frequent type of detector is a sodium iodide (NaI) crystal. Another crystal type is the BGO (Bismuth germinate $Bi_4Ge_3O_{12}$), which is denser, more efficient especially for high energy GR and produces twice the count number for the same GR flux. Its size can be smaller than the NaI crystal for a similar precision and the uncertainties are lower. However, the resolution of the BGO crystal is lower and varies with temperature (Serra, 2004).
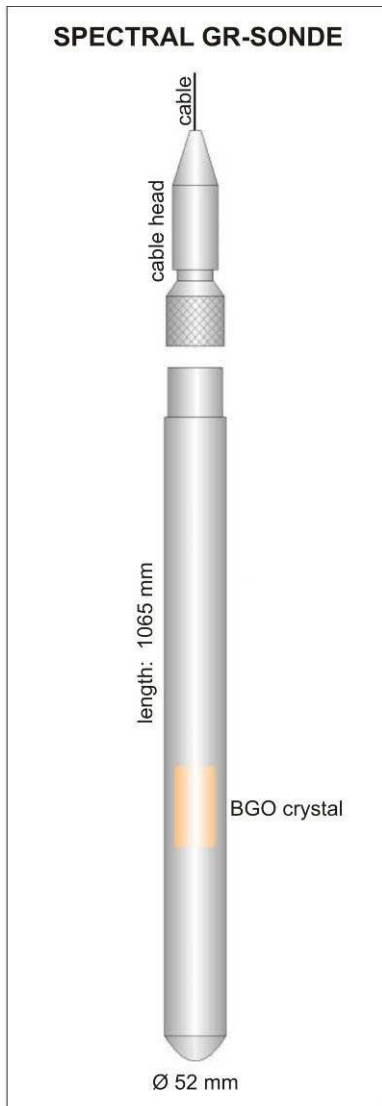
Fig. 16: Spectral GR-sonde

Application:
Among other things, the GR measurement is used to determine lithology and sedimentology. It is possible to detect shale beds and evaporates, as well as estimate grain size evolutions with depth (fining or coarsening upward sequences) (Serra, 2004). Additionally, the spectral GR log can be used to detect fractures and to define rock type in crystalline basement (Asquith et al., 2004).

Due to the fact that GR measurement is practically not affected by change in porosity or fluid content correlations between wells are possible. Furthermore, a sudden important change in the GR value may indicate an unconformity or a transgression (maximum flooding surface with highest GR). It is also possible to evaluate injection profiles due to radioactive tracer operations. An additional advantage of using GR spectroscopy is the possibility of depth control of sampling, perforating and testing equipment (Serra, 2004).

3.3 Spontaneous Potential Log (SP)

An electrical potential difference exists, spontaneously, between an electrode in the borehole and a remote reference electrode on the surface. The SP was first recognized by C. Schlumberger, M. Schlumberger and E.G. Leonardon in 1931 and the first published examples were from Russian oil fields (Oilfield glossary, SLB; Serra, 2004).

Measuring principle and source:
The quite simple measurement principle of the SP corresponds to recording versus depth of the difference between the electrical potential of a movable electrode in the borehole and the electrical potential of a fixed surface (Fig. 17). However, SP cannot be used in non-conductive mud (Serra, 2004).
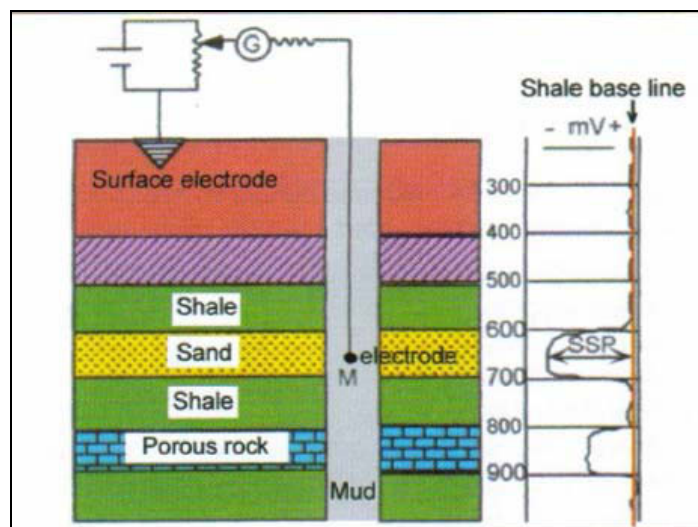
Fig. 17: Measurement principle of the SP Log (from Serra, 2004)

Usually the SP is caused by charge separation in clay or other minerals, by the presence of a semipermeable interface impeding the diffusion of ions through the pore space of rocks, or by natural flow of a conducting fluid (salty water) through the rocks. This potential varies from formation to formation, usually within the range of a few tens or hundreds of millivolts (mV) and can be measured relative to the level in shales (Serra, 2004).

The spontaneous potential opposite a formation can be attributed to two processes involving the movement of ions. On one side, there are electrokinetic (electrofiltration or streaming) potentials (E_k), which develop while an electrolyte penetrates a porous, non-metallic medium. On the other side, the electrochemical potential (E_c) is created when two fluids of different salinities are either in direct contact or separated by a semi-permeable membrane (such as a shale), see Fig. 18. The electrochemical SP "E_C" is the sum of "E_M" and "E_J".

The movement of ions is possible only in formations having a certain minimum permeability (fraction of millidarcy), although there is no direct relationship between the value of permeability or porosity and the magnitude of the SP deflection. It is essential that the drilling fluid is conductive, because this provides electrical continuity between the measuring electrode and the formation.
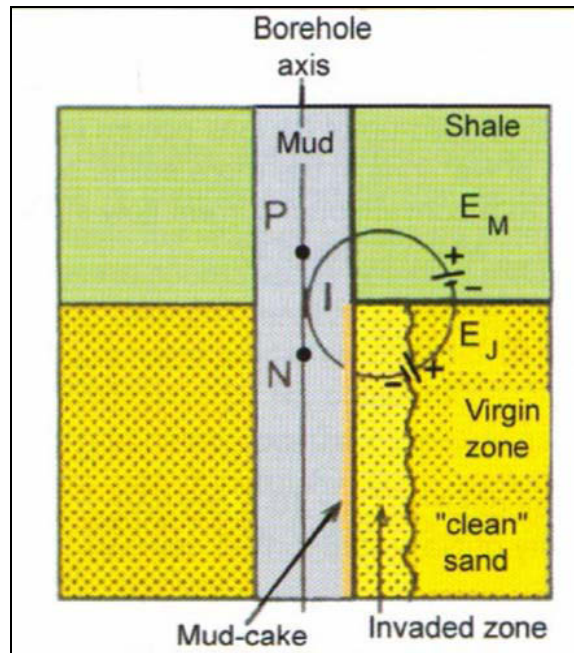
**Fig. 18: The principle of the electrochemical SP
(from Serra, 2004)**

The SP is constant across the permeable bed, dropping sharply to zero in the shales. That is the definition of the SSP (static spontaneous potential), where all deflections are measured relative to the shale baseline (Serra, 2004), see Fig. 19.
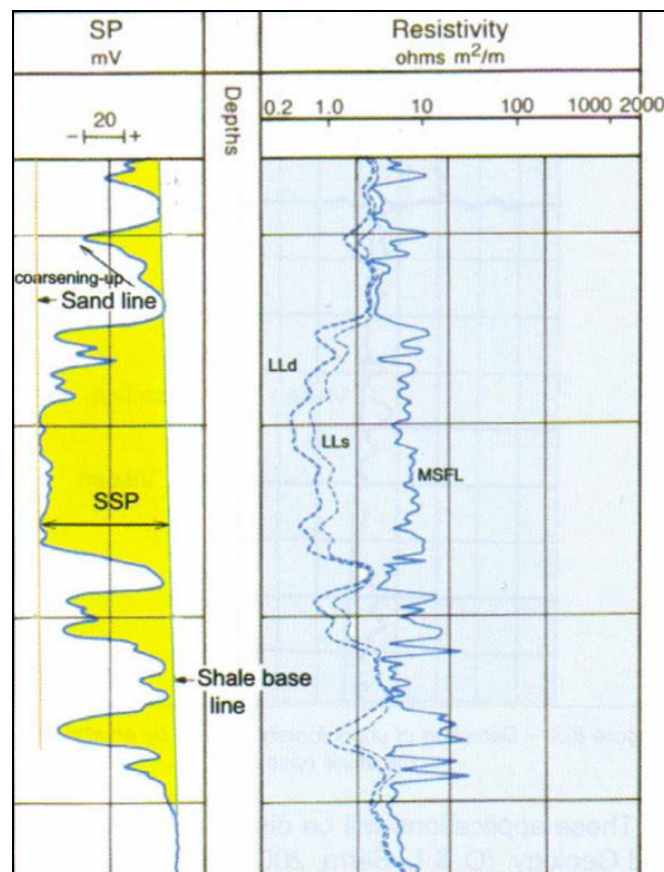
**Fig. 19: Example of SP log in a succession of sand and shale
(from Serra, 2004)**

SP is negative, if the interstitiel water is saltier than the filtrate, whereas positive SP values are thus mainly observed in fresh-water sands near the surface (Desbrandes, 1985).

Several factors can affect the SP, which make interpretation difficult. First, there are other possible sources of electrical potential not related to the electrochemical effect, for example, the electrokinetic potential and bimetallism. Bimetallism induces stray potentials due to the presence of two different metals in the mud near the SP electrode. Second, the SP can measure only the potential drop in the borehole and not the full electrochemical potential.

The ideal SP of a clean bed is known as the static spontaneous potential (SSP), whereas a shaly bed causes pseudostatic spontaneous potential (PSP). The SP is always less than the SSP or the PSP and more rounded at the boundaries between shales and permeable beds.

In the presence of hard impermeable layers, the shape of the SP may be condsiderably altered (Desbrandes, 1985).

As mentioned before, several parameters can affect amplitude and shape of the SP-curve. There may be a reduction of the SP by an increase in borehole size or a deepening invasion. A decreasing bed thickness can also reduce the SP, because it is a measurement of the rise and fall of electrical potential produced by current flow in the mud. Its amplitude approaches the SSP value only when the resistance to current flow offered by the formation and adjacent beds is negligible compared with that of the mud. Therefore, this condition is only met when the bed is thick (Serra, 2004).

Furthermore, the uninvaded zone and the bed boundaries are less sharply defined. The presence of hydrocarbons therefore attenuates the SP. There are several correction charts available, which should improve log interpretation.

Because of high resistivity, the SP current tends to flow deeply into a tight formation. The shale bed provides the only conductive path back to the mud and to the permeable strata. Within the impermeable section, the current flowing in the mud is constant, so the potential gradient is uniform.

A Spontaneous Potential baseline shift is not common, but it can occur where two zones of different connate water salinities are separated by shale that is not a "perfect" cationic membrane or where the salinity changes within a single bed.

A reduction of the spontaneous potential can be used for identification of the reservoir fluid, because gas- or oil-bearing reservoirs are very resistive (Serra, 2004).

Applications:

The SP log can be used to determine the resistivity of the formation water as soon as the resistivity of the mud filtrate and temperature are known. It can also help to identify reservoirs, shales and coal-seams. Furthermore, it provides qualitative estimation of the shale fraction, facies recognition, grain size, vertical evolution, correlation, indication of possible HC saturation and detection of unconformities marked by abrupt shift of the shale baseline (Serra, 2004).

In the following, sonic, density and neutron logs representing the group of porosity logs are discussed.

3.4 Sonic log (DT)

The sonic log (or acoustic log) is a porosity log that measures interval transit time (Δt or DT) of a compressional (p) sound wave travelling through the formation along the axis of the borehole. Usually, the sonic log device (see Fig. 20) consists of one or more ultrasonic transmitters and two or more receivers (Asquith et al., 2004).
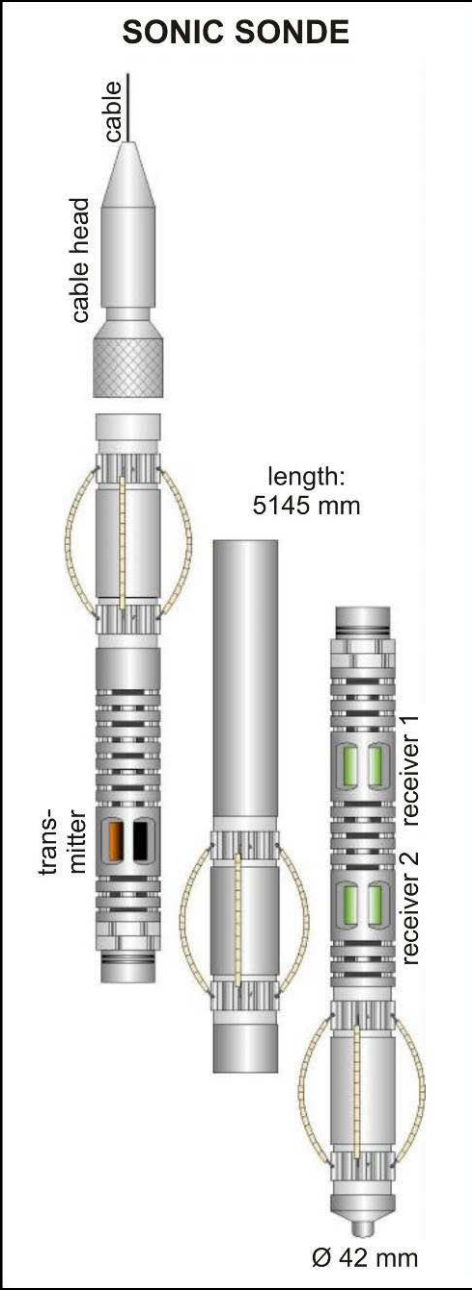
Fig. 20: Sonic sonde (modified from LIAG)

The interval transit time is measured in microseconds per metre (µs/m), which is the reciprocal of the velocity of a p-wave measured in metre per second (m/s). Both lithology and porosity affect the interval transit time, which requires a known formation's matrix interval transit time to derive sonic porosity (see Table 4).

The derivation of sonic porosity can be done by either the Wyllie time-average equation or the equation of Raymer, Hunt and Gardner (RHG). The formula of Wyllie et al. (1985) should be used for consolidated sandstones and carbonates with intergranular porosity (grainstones) or intercrystalline porosity (dolomites).

Medium	Matrix velocity [ft/s]	Δt_{matrix} (Wyllie) [µs/ft]	Δt_{matrix} (RHG) [µs/ft]
Sandstone	18,000-19,500	55.5-51.0	56
Limestone	21,000-23,000	47.6	49
Salt	15,000	66.7	-
Casing (iron)	17,500	57.0	-
Freshwater mud filtrate	5,280	189	-
Saltwater mud filtrate	5,980	185	-

Table 4: Sonic velocities and interval transit times for different media (from Asquith et al., 2004)

Measuring principle:

A magnetostrictive transducer, excited from the surface by a signal, emits a sound wave whose average frequency is of the order of 20 to 40 kHz. The duration of the emission is less than 1 ms but it is repeated 10 to 60 times per second, depending on the tool (Serra, 2004).

The wave spreads in all directions from the transmitter and produces spherical wavefronts. The wavefront passing through the mud is incident upon the borehole wall with increasing time and increasing angle of incidence as the distance from the transmitter increases (see Fig. 21). The reflected longitudinal waves travelling in the mud are slower than the refracted p-waves propagated in the formation, since the speed of sound in the rock is greater than that in mud (Serra, 2004).
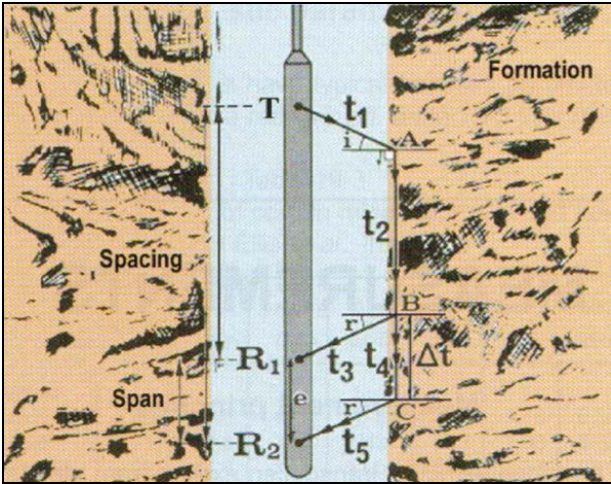
Fig. 21: Schematic of the principle for measuring DT (from Serra, 2004)

The first arrival or p-wave travelled from the transmitter to the formation at the compressional wave velocity of a fluid pressure wave. At the borehole wall it has been refracted under the critical incident angle, which induced travelling back to the receiver. Those waves refracted at the critical angle are of special interest as they are the fastest and propagate along the borehole wall.

Shear (s) waves generally have higher energy and cannot travel through fluid media, which makes it easy to separate them from compressional (p) waves (Serra, 2004).

Borehole-compensated (BHC) sondes:
Conventional sonic logs are borehole-compensated (BHC) devices, which greatly reduce the effects of borehole size variations as well as errors due to tilt of the tool with respect to the borehole axis. In general, this can be realized by averaging signals from different transmitter-receiver combinations over the same length of the borehole (Asquith et al., 2004).
The BHC tool (see Fig. 22) has two transmitters, one at the top and the other at the bottom, with four receivers in between. Transmitters are pulsed alternately and DT values are recorded on alternate pairs of receivers (R1 R2 and R'1 R'2). The frequency used is 20 or 40 kHz and the DT values from the two sets of receivers are averaged automatically by a computer at the surface for borehole compensation, which also integrates DT values to obtain total travel times (Serra, 2004).
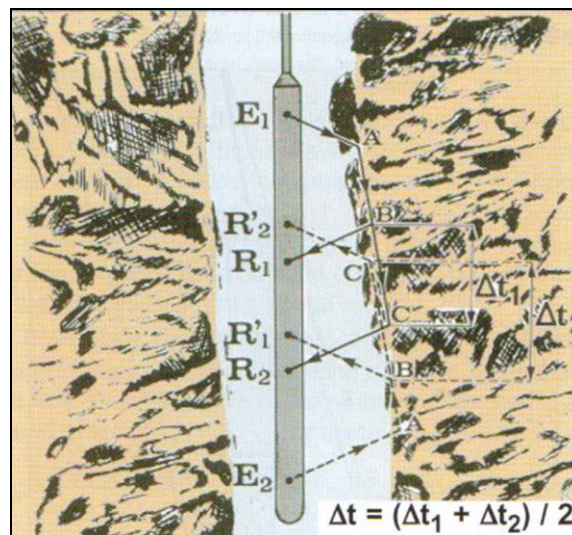
Fig. 22: Principle of the BHC sonic tool
(from Serra, 2004)

Long spacing sonic (LSS) sondes:
The LSS tool has two transmitters located at the bottom of the tool and two receivers. The transmitter-receiver spacings are longer than at standard sonic tools with 8 ft and 10 ft (~2.5 and 3 m), or 10 ft and 12 ft (~3 and 3.7 m) (Serra, 2004).
The rock near the borehole is sometimes altered by drilling fluids, stress relief or both, causing a thin zone whose velocity is lower than that of the true formation. With standard spacings, the wave traveling through the altered zone may arrive first at the receiver, since this zone is closer to both transmitter and receiver. The increased spacing permits the wave traveling through the true formation to arrive first and be measured. The depth of investigation varies with slowness and transmitter-receiver spacing but is of the order of 2 to 3 ft (approximately 70-90 cm). An increased transmitter-to-receiver spacing also allows better separation of waveforms relating to different acoustic waves, such as compressional (p), shear (s) and Stoneley arrivals (Oilfield glossary, SLB). Further advantages are lower frequency used with 11 kHz instead of 20 kHz and a lower attenuation of the signal (Serra, 2004).
However, in porous and permeable intervals, the long-spaced sonde shows the same results as the BHC sonde (Asquith et al., 2004).

3.5 Neutron Log (NL)

Neutrons are electrically neutral particles having a mass that is almost identical to that of hyrogen nuclei (Desbrandes, 1985). Neutron logs are porosity logs that measure the hydrogen concentration in a formation and were introduced in the early 1940s (Asquith et al., 2004). The first tools were known as neutron-gamma tools, since the detector measured the gamma rays emitted on capture. Neutron-neutron tools (see Fig. 23), using a thermal neutron detector were introduced in 1950 (Oilfield Glossary, SLB).

Measuring principle and source:

NEUTRON-NEUTRON SONDE

cable

cable head

long

He-decatron

short

length: 3265 mm

screw connection

neutron generator

Ø 52 mm

Fig. 23: Neutron log (modified from LIAG)
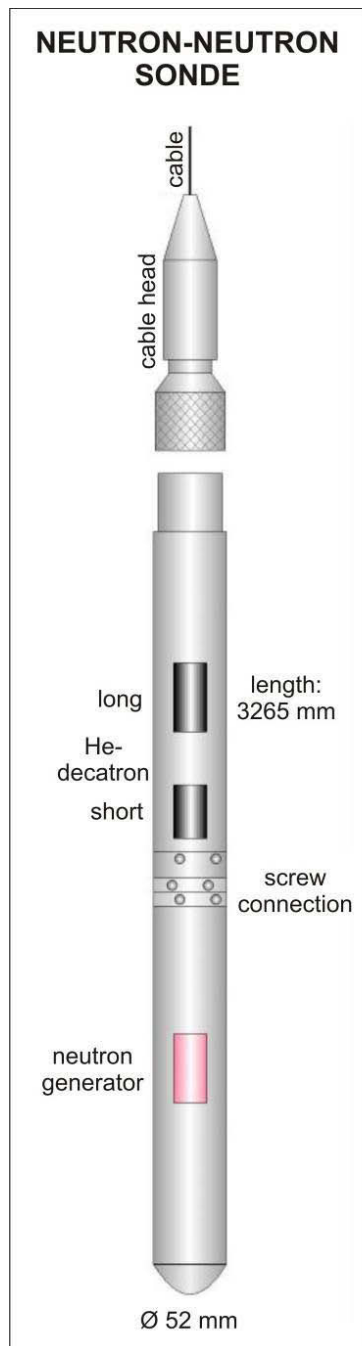
As hydrogen is present in both water and oil, an estimation of its amount in the porous formations will allow the estimation of the amount of liquid-filled porosity. Therefore, an evaluation of the hydrogen index will be directly associated with porosity (Serra, 2004).

Neutrons are created from a chemical radioactive source in the neutron logging tool, which is usually a mixture of americium and beryllium. Both elements are continuously emitting fast neutrons, which typically have high energy. When these fast neutrons collide with the nuclei of the formation, the neutron loses some of its energy, start to scatter elastically and slow down. They decrease progressively in energy to reach the epithermal and finally the thermal energy. With enough collisions, the thermal neutron is absorbed ("captured") by a nucleus and a gamma ray is emitted. As hydrogen is almost equal in mass to the neutron, the energy loss is dominated by the formation's hydrogen concentration. The slowed neutrons, which deflect back to the tool, are counted by detectors. Both epithermal (intermediate with energy between about 0.4 and 10 eV) neutrons and thermal (slow with energy less than 0.4 eV) neutrons can be measured depending on the detector design (Asquith et al., 2004).

Neutron logs are commonly displayed in porosity units referenced to a specific lithology, like usually either limestone or sandstone, depending on the geologic environment expected. Whenever pores are filled with gas rather than oil or water, the reported neutron porosity is less than the actual formation porosity. This is a result of the lower concentration of hydrogen in gas than in oil or water. This lower concentration is not accounted for by the processing software of the logging tool and therefore is interpreted as low porosity. For this reason, a decrease of neutron porosity due to the presence of gas is called "gas effect" (Asquith et al., 2004).

If clay is part of the formation matrix, the reported neutron porosity is greater than the actual formation porosity, because of hydrogen in form of bound water within the structure of clay minerals. This results in an increase of neutron porosity and is called "shale effect" (Asquith et al., 2004)

Compensated Neutron Log (CNL):
The most commonly used neutron log is the Compensated Neutron Log, which has a neutron source and two detectors. It directly displays values of porosity and the advantage is that they are less affected by borehole irregularities. Compensated neutron logs can be recorded in apparent limestone, sandstone or dolomite porosity units. If the formation is sandstone and the neutron log is recorded in apparent sandstone porosity units, apparent porosity is equal to true porosity. However, if the lithology is wrong, apparent porosity must be corrected to true porosity by using the appropriate chart (Asquith et al., 2004).

CNL tools have a vertical resolution of approximately 2 ft (60 cm) and therefore the log mainly reflects trends within the flushed zone. Furthermore, neutron logs are combinable and usually run simultaneously with other services.

Applications:
As mentioned before, a very important application is the determination of porosity. Moreover, neutron logs are used to identify lithology, detect gas horizons and carry out clay analysis (Serra, 2004).

3.6 Density Log (DL)

The density measurement was introduced in 1953. At this time, the sonde included only a single detector, whereas nowadays measurement is improved by the installation of two detectors (see Fig. 24) (Serra, 2004). The density logging tool has a relatively shallow depth of investigation and therefore it is pressed against the borehole wall during logging to maximize its response to the formation (Asquith et al., 2004).
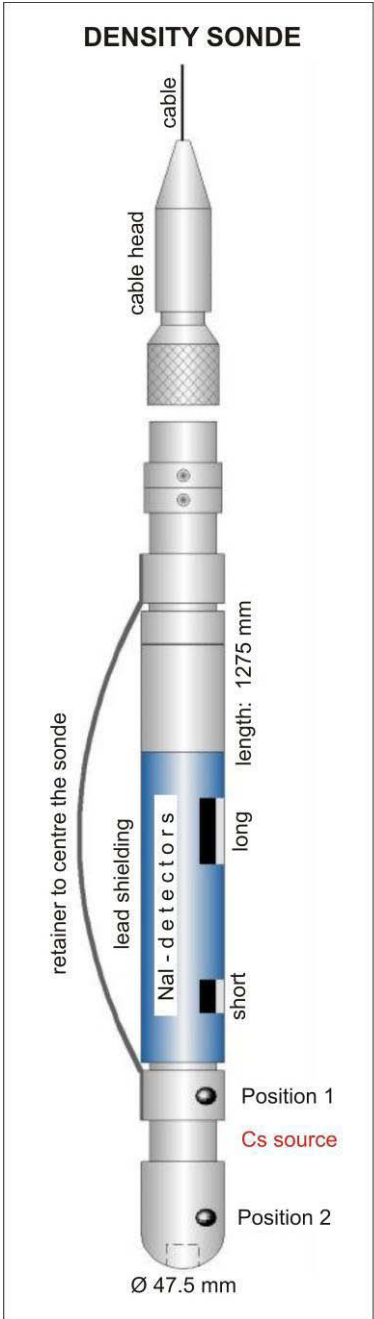
Fig. 24: Density sonde (modified from LIAG)

<u>Measuring principle:</u>
The energy of the incident photons, but also the mass absorption coefficient and type of rock are controlling the density measured. Density measurement uses energy ranging between 0.2 and 2 MeV, which results in attenuation due to Compton scattering.
Compton scattering (see Fig. 25) describes the effect of a collision of gamma ray with an electron. The energy of the gamma ray is partially transferred to the electron, whereas itself is being scattered at a reduced energy in a direction depending on the angle of incidence.
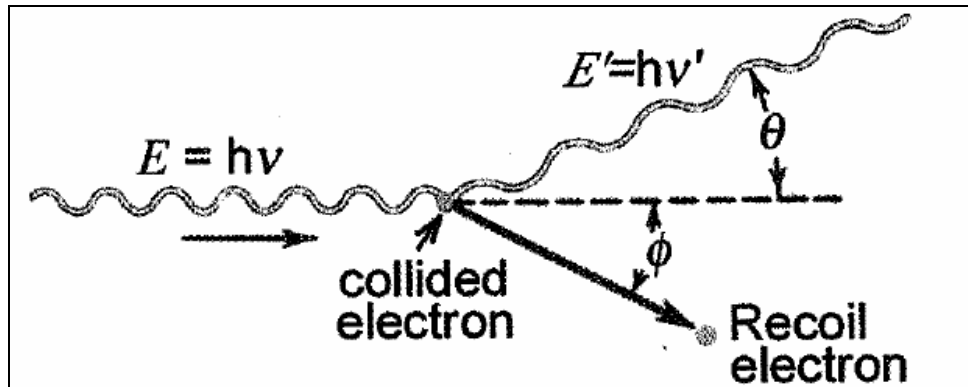
Fig. 25: Effect of Compton scattering
(from Serra, 2004)

Additionally, density measurement requires correction for the photoelectric effect. This effect occurs during the collision of gamma ray with an electron and will be discussed in detail in the course of the next log description ("PEF-Log").
During density logging, the intensity of the scattered gamma rays is measured in some distance from the source. This intensity will be weaker if the number of collisions will be higher, consequently if the number of electrons by unit volume will be higher. Therefore, the number of the electrons by unit volume is proportional to the density of the formation. The higher the density of the formation, the weaker the measured intensity of the scattered gamma rays. For this reason, in formations with high density, photons colliding a great number of electrons do not penetrate very deep into the formation before being absorbed (photoelectric effect). This results in a low part of the initial intensity arriving at the detector. On the contrary, formations with low density show high intensity measured by the detector (Serra, 2004).

Sources of GR mostly used are [137]Cesium and [60]Cobalt. [137]Cesium is preferred, because it emits photons of constant energy of 0.662 MeV and has a half-life of 33 years, whereas [60]Cobalt emits photons of two levels of energy. With NaI scintillometers gamma ray is detected above a certain energy level (Serra, 2004).

Density is measured in grams per cubic centimetre (g/cm³). Two separate density values are used by the density log, the bulk density (RHOB) and the matrix density. The bulk density is the density of the entire formation (solid and fluid parts) as measured by the logging tool, whereas the matrix density refers to the solid framework of the rock assumed to occur (e.g. limestone or sandstone). Based on this data, porosity can be calculated (Asquith et al., 2004).
Since the late 1970s, the density log has also been used for the photoelectric effect measurement (PEFZ) to determine lithology of the formation (Asquith et al., 2004).

Compensated density log:
This describes a density log that has been corrected for the effect of mud and mudcake by using two or more detectors at different spacings from the source. The shorter the spacing, the shallower the depth of investigation and the larger the effect of the mudcake. Thus, a short spaced detector, which is very sensitive to the mudcake, can be used to correct a long-spaced detector, which is only slightly sensitive to it (Oilfield glossary, SLB).
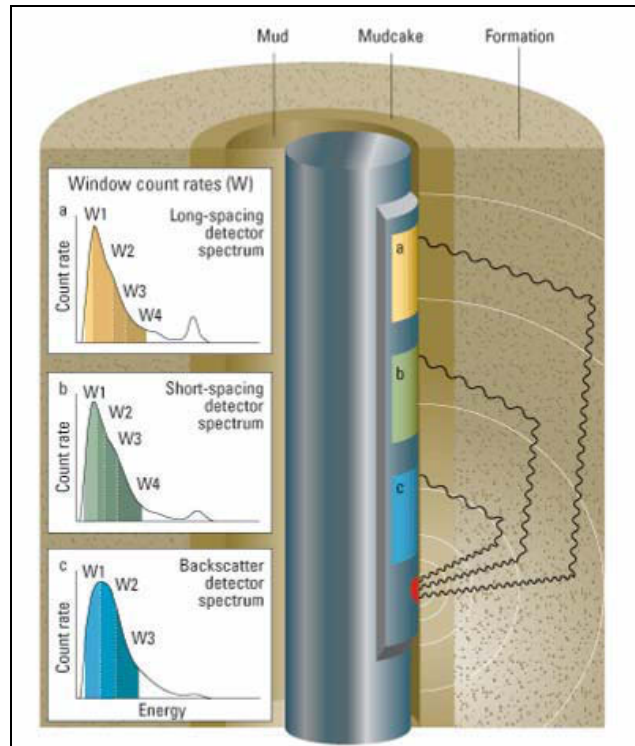
Fig. 26: Three-detector density logging sonde
(from Oilfield glossary, SLB)

Multiple Compton scattering and photoelectric absorption lead to a spectrum of gamma ray photons entering the detector windows from the borehole and formation environment (Oilfield glossary, SLB).

Applications:
There are several applications of the rock density measurement although the determination of lithology, gas-bearing zones and hydrocarbon density may be the most important ones. Additional qualitative information on facies, depositional environment, diagenesis, fractures and possible reservoirs is given (Serra, 2004).

Although porosity logs provide an essential improvement in log interpretation, the significant change was the development of interpretation techniques that combined the measurements from different porosity tools. These combinations of two or three measurements enable the interpretation of lithology and provide better estimation of porosity. The neutron-density combination is the most widely used porosity measurement combination (Asquith et al., 2004).

3.7 Photoelectric Effect Log (PEF)

Measuring and principle:
The PEF-Log is based on the photoelectric effect. The latter occurrs during the collision of gamma ray with an electron, when a photon is able to transfer all its energy to the electron in the form of kinetic energy. If the energy transferred exceeds the binding energy to the atom, the electron will be ejected from its atom (see Fig. 27), whereas the photon disappears and the gamma ray is fully absorbed (Serra, 2004).
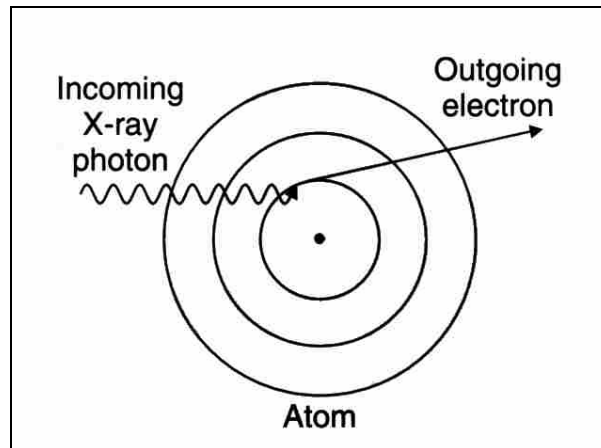
Fig. 27: Principle of the Photoelectric effect
(modified from Serra, 2004)

Normally, the ejected electron will be replaced within the material and a characteristic gamma ray will be emitted with energy that is dependent on the atomic number of the material. The highest probability for this effect occurs at low gamma ray energy and within a material of high atomic number (Serra, 2004).

PEF-Logs were introduced in the late 1970s and measure the photoelectric absorption factor (P_e) to identify lithology. P_e is unitless and defined by formula 1, where "Z" is the average atomic number of the formation.

$$P_e = \left(\frac{Z}{10}\right)^{3.6}$$

Formula 1: Definition of the photoelectric absorption factor P_e

As the photoelectric absorption factor is proportional to the photoelectric cross section per electron, P_e sometimes is given in barns/electron (1 barn $=10^{-24}$ cm²).
Because the photoelectric effect results from interactions with electrons, its intensity will be a function of the number of electrons by unit volume. Therefore, PEF is converted to the volumetric cross section "U" in barns/cm³, by taking the product of PEF and density (Serra, 2004). Table 5 illustrates the photoelectric absorption factor (P_e) and the volumetric cross section (U) for different minerals.

Minerals	P_e	U
Quartz	1.81	4.78
Calcite	5.08	13.77
Dolomite	3.14	9.00
Halite	4.65	9.68
Siderite	14.70	55.90
Pyrite	17.00	82.10
Barite	267.00	1,065.00
Chlorite	6.30	17.58
Illite	3.45	8.69

Table 5: Photoelectric absorption factor (P_e) and the volumetric cross section (U) for different minerals (from Desbrandes, 1985)

Since fluids have very low atomic numbers, they have very little influence, so that P_e is a measure of the rock matrix properties. Low P_e is typical for sandstones, whereas dolomites and limestones, as well as clays, heavy minerals and iron-bearing minerals have high P_e. If there are isolated peaks of the photoelectric absorption factor, this may indicate local deposits of heavy minerals especially containing iron or radioactive placer deposits (uranium and thorium). Igneous or metamorphic rocks generally show high values for the P_e-curve, whereas thin bands of low P_e may indicate coal. The PEF-Log is therefore rather insensitive to differences in the mean atomic number of a formation without being sensitive to changes in the porosity and fluid saturation of that lithology (see Fig. 28). According to that, the log is very useful for determining lithology and is not affected by gas-bearing horizons (Oilfield glossary, SLB).
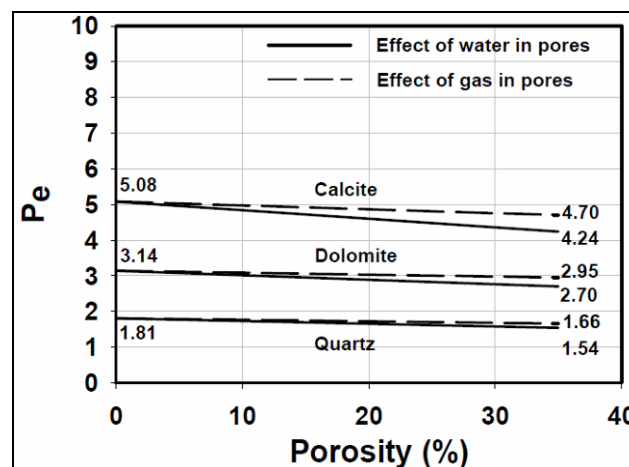
Fig. 28: P_e as a function of porosity and fluid content (from Serra, 2004)

The log is recorded as part of the density measurement and has a depth of investigation of approximately one inch (2.54 cm), which normally represents the flushed zone (Oilfield Glossary, SLB).

Applications:
As already mentioned before, PEF-log is sensitive to the elemental composition of the formations and, consequently, to the lithology and the minerals composing the rocks, which defines its applications (Serra, 2004).

3.8   Resistivity Log (LLD, LLS…)

The measurement of formation resistivity (unit is ohm-m) is essential for the evaluation of hydrocarbon saturation, particularly in the uninvaded zone of the reservoir. Depending on the number of electrodes and the spacing between them, the resistivity can either be measured near (e.g. with LLS) or far (e.g. with LLD) from to the borehole. Resistivity measurements are only possible in boreholes filled with salt water-base mud.

Measuring principle:
There are several techniques used to measure the resistivity. All are variations of a common basic principle, where one or several emitters (electrodes) send a signal in terms of radial electrical current into the formation. One or several receivers (electrodes) measure the response of the formation to this signal at a certain distance from the emitter.
Generally, the bigger the spacing between emitter and receiver, the bigger the depth of investigation with values near to true resistivity of the uninvaded zone. Unfortunately, long spacing affects vertical resolution. As a function of the spacing value, two main categories of tools are existent and named long- and short-spacing devices (Serra, 2004).
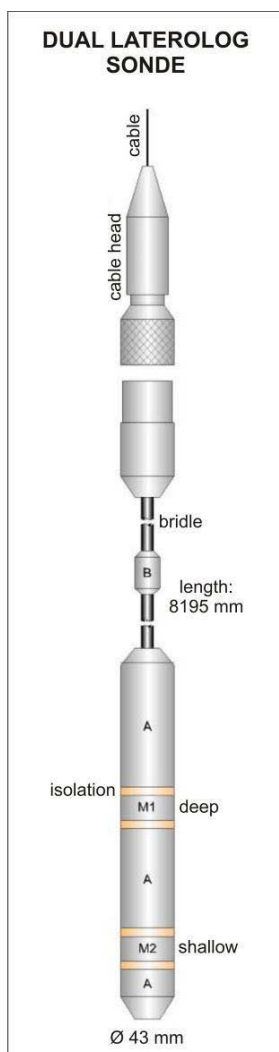
Long-spacing tools:
These tools provide medium to deep readings and include, among others, the laterologs. Laterologs constitute focused devices as they have guard electrodes, which focus the current emitted by the central electrode. Additionally, laterologs are less sensitive to effects of the borehole (Serra, 2004).

The Dual Laterolog (DLL, see Fig. 29) was introduced in the early 1970s and is still in use today. It consists of nine electrodes and provides two resistivity measurements with different depths of investigation: deep (LLD) and shallow (LLS). This simultaneous measurement requires different frequencies used in the LLD and the LLS mode (Serra, 2004).

Fig. 29: Dual Laterolog tool (modified from LIAG)

With the Dual Laterolog, true resistivity of the uninvaded zone can be achieved. Both LLD and LLS systems use the same central electrode A_0 and emit identical current-beam thickness, although they have different focusing to provide their different depths of investigation. Eight symmetrically placed electrodes were connected in pairs, like A_2-A'_2, A_1-A'_1 etc. The LLD system uses remote (surface) returns for the main and bucking currents. Therefore, the current is flowing perpendicular to the tool. The LLS system uses the A_2-A'_2 electrode pair as the return for the bucking current from A_1-A'_1 (see Fig. 30) (Serra, 2004).
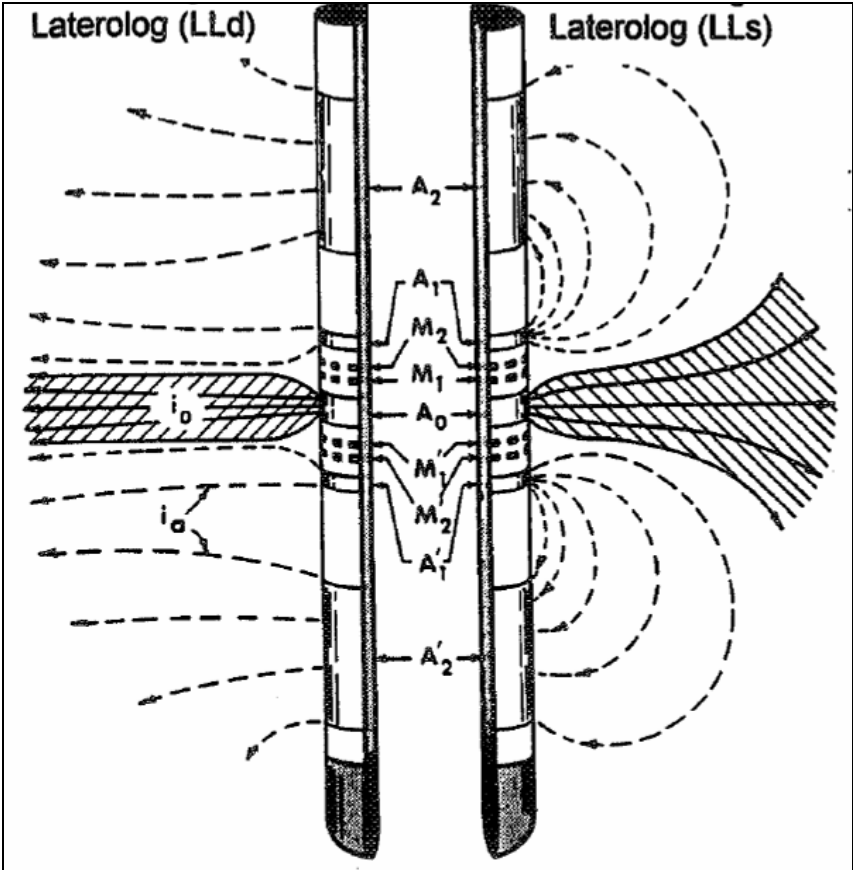
Fig. 30: Principle of the Dual Laterolog (from Serra, 2004)

The Dual Laterolog operates simultaneously at two frequencies, 35 Hz for LLD and 280 Hz for LLS system. The tool is connected to the logging cable by a flexible insulating connector called "bridle".

Short-spacing tools:
All short-spacing tools are mounted on pads applied against the borehole wall by a spring, as they measure resistivity of the shallow, flushed zone (R_{xo}). The logs are hardly affected by borehole fluid, but the mud cake contributes a small signal. There are different types of short-spacing tools, like the Microspherically focused log. The vertical definition obtained with these electrode tools is much finer than with the longer spacings.

The Microspherically focused log (MSFL) is a small-scale spherically focused log array, mounted on a flexible rubber pad.

The log is less sensitive to the mud cake and additionally, it can be combined with other tools. Since the measure current sees mostly the flushed zone and the bucking current sees primarily the mud cake, it is possible to mathematically derive a micro-normal and a micro-inverse curve. However, micro-resistivity measurements must be corrected for mud cake effect (Serra, 2004).

Applications:

The petroleum industry uses resistivity logs especially in formation evaluation to differentiate between non-conductive hydrocarbons and conductive formation water. Clay minerals and a few other minerals, such as pyrite, also conduct electricity and reduce the difference (Oilfield glossary, SLB).

Additionally, resistivity logs are used to indicate permeable zones and determine porosity.

3.9   Formation Micro Imager (FMI)

Borehole images are electronic pictures of the rocks and fluids penetrated by a wellbore, which are created by either electric, acoustic or video devices lowered into the well. Images are oriented, they have high vertical and lateral resolution and provide critical information about geological features, like bedding dip, fractures, faults, unconformities, paleocurrent directions, vuggy and fracture porosity (Serra, 2004).

As coring causes high costs and risk, the use of borehole images has increased in recent years to characterize subsurface sedimentary rocks. Furthermore, the electrical or acoustic contrast between different lithologies may be more significant than the contrast apparent to the human eye (Serra, 2004).

Measuring principle:
As RAG provided borehole images created by electrical devices, these tools will be explained in detail. In general, electrical borehole-imaging devices can be described as sophisticated dipmeters. The big difference to a dipmeter is the complex array of microresistivity electrodes on multiple pads used for borehole imaging.
Tools are first run into the hole with the pads closed. At the start of the log run, depending on the logging device, either four, six or eight pads are pressed against the borehole wall. Electrical current is forced into the rock through the electrodes and remote sensors measure the current after it interacts with the formation. Additionally, caliper log is measured from individual pads.
The sample rate is very high with normally 120 samples per foot (400 samples per metre), which results in huge file size, whereas the depth of investigation is small with less than on inch (2.5 cm). In general, between 40 to 80 % of the borehole wall is imaged and logging rate is 1,600 to 1,800 ft/h (500 to 550 m/h) (Serra, 2004).

The borehole-imaging tool illustrated in Fig. 31 is created by Schlumberger and includes eight pads and 192 electrodes. Special focusing circuitry ensures that the measuring currents are forced into the formation. They adapt in amplitude with the formation conductivities to produce low-frequency signals rich in petrophysical and lithological information and a high-resolution component that provides the microscale information used for imaging and dip interpretation.
The combination of measuring button diameter, pad design and high-speed telemetry system produces a vertical and azimuthal resolution of 0.2 inch (0.51 cm) for the FMI tool. Fine details such as fractures filled with conductive fluids are visible in FMI images (Oilfield glossary, SLB).
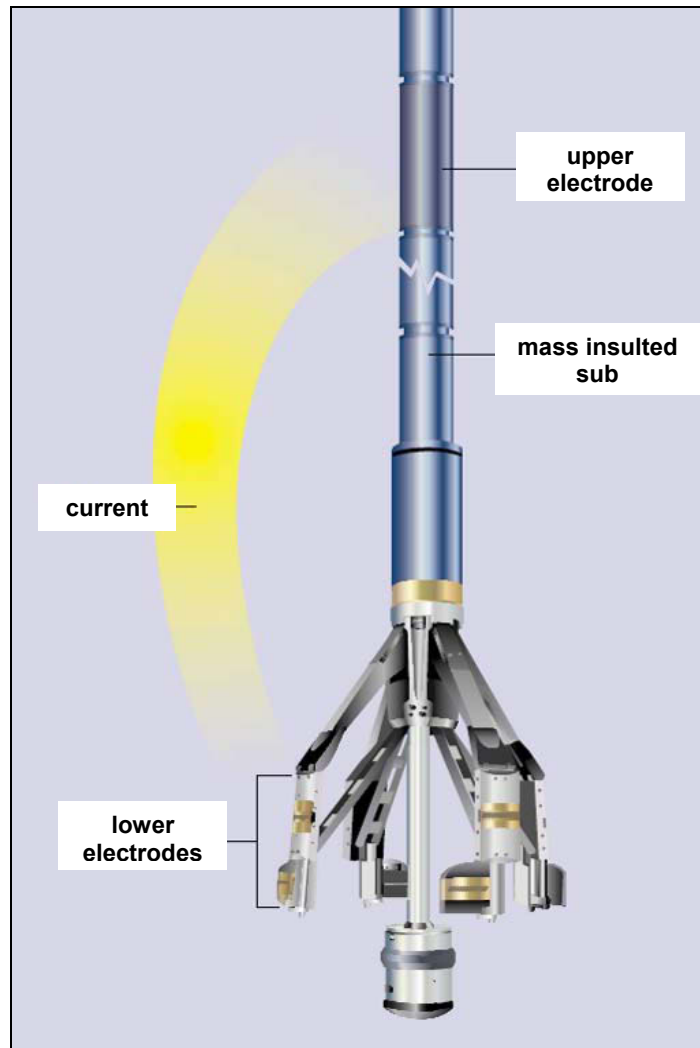
Fig. 31: Formation Micro Imager (FMI)
(modified from Schlumberger, SLB)

The FMI software provides static and dynamic functionality. In static mode, the user can visualize data contained in a digital data file or data stream. Furthermore, it is possible to modify the graphical presentations and customize the displays to improve understanding of the data.

The dynamic mode enhances functionality for borehole images previously processed by Schlumberger. These features include interactive dip picking and classification, plus manual image scaling, which enables the user to fine-tune specific interpretations.

Applications:

The answers provided by the FMI tool help in understanding the reservoir structure, identify and evaluate sedimentary features and fractures, visualize rock texture and complement coring programs. FMI data are increasingly used for geomechanical analysis of the reservoir. Drilling-induced features such as borehole breakouts are identified. In combination with stress field analysis, FMI information is used to control wellbore stability problems by guiding design of the mud program (Oilfield glossary, SLB).

Table 6 is a general summary of logging tools and highlights, which tool is best for which application.

Applications	Qualitatives	Quantitatives	Well logging tools required
Geology	Composition	Percentage of elements Percentage of minerals	Spectrometry tools Litho-density, neutron, sonic, spectrometry tools
	Texture Grain size evolution Sorting	Particle size and shape > 5mm	Image tools, dipmeters
	Sedimentary structure Slumping Bioturbation	Dip angle & azimuth of laminae Paleocurrent direction	Image tools, dipmeters
	Geometry	Apparent & real thickness of laminae, beds, depositional units, facies & sequences	Images tools, dipmeters
	Facies Sequence	Apparent & real sequence thickness	All tools
	Depositional environment Diagenesis Cementation Dissolution Mineralogical transformation Compaction Tectonics Folding, faulting Fractures	Cement nature & percentage Mold & vug percentage Dolomitization Porosity evolution with depth Structural dip Fault angle & azimuth Direction of paleostresses Fracture density and porosity	All tools All tools Porosity & spectrometry tools Porosity and image tools Porosity & spectrometry tools Sonic, density, resistivity Image tools, dipmeters
	Stratigraphy	Relative dating Real dating	All tools Magnetic tool
	Sequence stratigraphy Unconformity Correlations Source rocks		All tools Image tools, dipmeters Radioactivity & resistivity tools Spectrometry tools
Petrophysics	Reservoir evaluation Permeability	Reservoir location & evaluation Porosity, saturation Permeability	All tools Porosity & resistivity tools Nuclear magnetic resonance Testing
Geophysics		Acoustic impedance Reflection coefficient	Density & sonic tools
Others	Coal Uranium Potassium Sulfide ores	Uranium percentage Potassium percentage	All tools Spectrometry tools Radioactivity & spectrometry tools Resistivity, image tools, spectrometry, litho-density, neutron

Table 6: Different domains of applications of the well logging data
(from Serra, 2004)

4. CORE GAMMA RAY MEASUREMENT

From four out of the six wells of interest Core gamma ray (Core-GR) was measured by OMV. For the remaining two wells (KH-003, V-037) these measurements were carried out by MUL.

4.1 Tools

OMV-tool (stationary measurement):
OMV measures Total and Spectral Core-GR with an instrument of the former Norwegian company Reslab, which is now part of Weatherford.

GF Instruments:
Gamma Surveyor (see Fig. 32) is a new group of multi-channel GR-spectrometers and accurate dose rate-meters designed for measurements of natural and artificial isotopes in ground, boreholes and laboratories designed by the company GF Instruments. The Gamma Surveyor is able to measure both, spectrum (and concentrations of K, U, Th) and total gamma (dose rate). The control unit works with all kinds of probes.

The Gamma Surveyor Compact includes a handheld probe, but the control unit and a probe are in one compact casing. The spectrometric probe was available with a BGO detector.
The measuring system supports point, profile and continuous measurements as well as the use of external GPS data. The factory calibration is done on high-volume standards.
The Gamma Surveyor data memory size is 32 MBit, which equals 100,000 measured points in search/dose rate continuous mode, 58,000 measured points in dose rate mode, 1,800 measured points in spectrum and assay mode.

Measuring modes:

Spectra & Assay
• in situ spectral measurements with determination of K, eU, eTh concentrations
• spectrum view, energy & 24 nuclide identification
• adjustable integration time

Dose rate
• precise radiometric measurements
• histogram of previous 64 readings
• adjustable integration time

Search
• quick and selective search for GR sources
  (0.5 s response time)

Determination of concentrations of natural radioactive elements (K, eU, eTh), artificial radiation sources identification, dose rate measurement, radiation monitoring and mapping, geological and raw material survey (uranium ore), laboratory assays and health care are the main applications of the Gamma Surveyor Compact.

Fig. 32: Measurement of Core-GR,
Gamma Surveyor Compact/GF Instruments

Canberra:

The InSpector™ 1000 digital multichannel analyzer (see Fig. 33) is a high-performance, hand-held NaI spectrometer for simple, real time isotope identification and classification.

InSpector™ 1000 has been designed for easy operation. The user interface provides the ultimate flexibility in field operations. It can be used in any field measurement application requiring nuclide identification, activity measurements, dose/count rate measurements or spectrum acquisition and analysis.

The InSpector™ 1000 has a decontaminable, portable, ruggedized and spill-proof design and provides simple, real time isotope identification with activity and dose by isotope calculation.
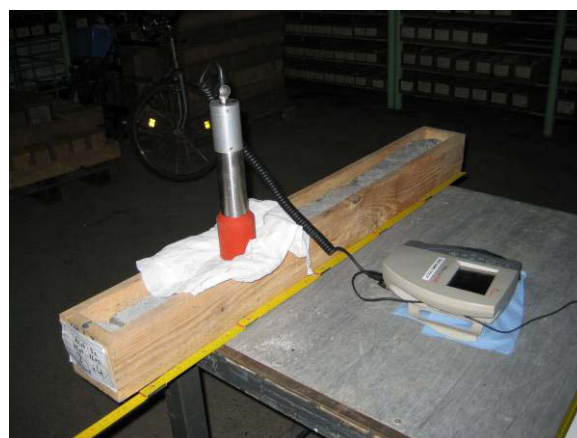
Fig. 33: InSpector™ 1000 Digital hand-held multichannel
analyzer/Canberra

4.2   Advantages and disadvantages of the tools

The main advantage of the Gamma Surveyor Compact of the company GF Instruments is easy handling. Once one initiates the measurement, the instrument does not require any further handling. In comparison, the InSpector^{TM} 1000 of Canberra needs to be hold and stabilized during the measurement. Furthermore, it is recommended to use a special lead shielding during the measurement.

Another positive factor of the Gamma Surveyor Compact is the easy way to transfer the measured data (recorded as Excel file) from the instrument to the computer. Additionally, the measurement accuracy of the Gamma Surveyor Compact is very high and shows a very good fit with the results of the OMV Core-GR measurements.

However, due to the design of InSpector^{TM} 1000 it is possible to measure also relatively small objects, like small-diameter cores packed in narrow core boxes. In this case, the Gamma Surveyor Compact can only measure if the core is unpacked from the box (or at a certain distance from the core in the box).

4.3   Comparison & analysis of the Core-GR results

OMV measures Core-GR in a continuous mode before the core is cut. In contrast, MUL Core-GR measurements have been performed as point measurements (typically one measurement per approximately 33 cm) on cut core surfaces. Because of core handling (cutting, re-packing), shifts in depth between OMV and MUL measurements are expected and have to be considered.
Additionally, the hand-held instruments used by MUL are calibrated for half-spaces (and not for half-cylinders with small diameters), e.g. at an outcrop. Therefore they do not provide absolute concentrations. Thus only trends are meaningful, when comparing OMV and MUL results.

Well BH-N-002 was used for calibrating the Core-GR-tools used by OMV and MUL. As described above, MUL tested two different Core-GR-tools, the GF Instruments' Gamma Surveyor and the InSpector™ 1000 digital multichannel analyzer from the company Canberra.

Total measurement:
Total Core-GR-measurements with MUL-tools of GF Instruments and Canberra show trends similar to OMV. In order to obtain a fit between both measurements, the logs of GF Instruments and Canberra have to be corrected (shifted and squeezed) first to provide a valid comparison with the OMV-log.

The Canberra Core-GR has to be shifted by approximately 30 cm (see Fig. 34), whereas the GF Instruments Core-GR has a shift of approximately 20 cm (see Fig. 35). As the measuring points (= mid point of the instrument) are identical, this may be the result of different positions of the detector within the devices. The detector of the GF Instruments' Gamma Surveyor Compact is situated near the top of the tool. Both logs have to be squeezed by 6.1 % to show the trend of the OMV-log. This shows a core expansion of 6.6 % (!) as a result of core handling (e.g. cutting).
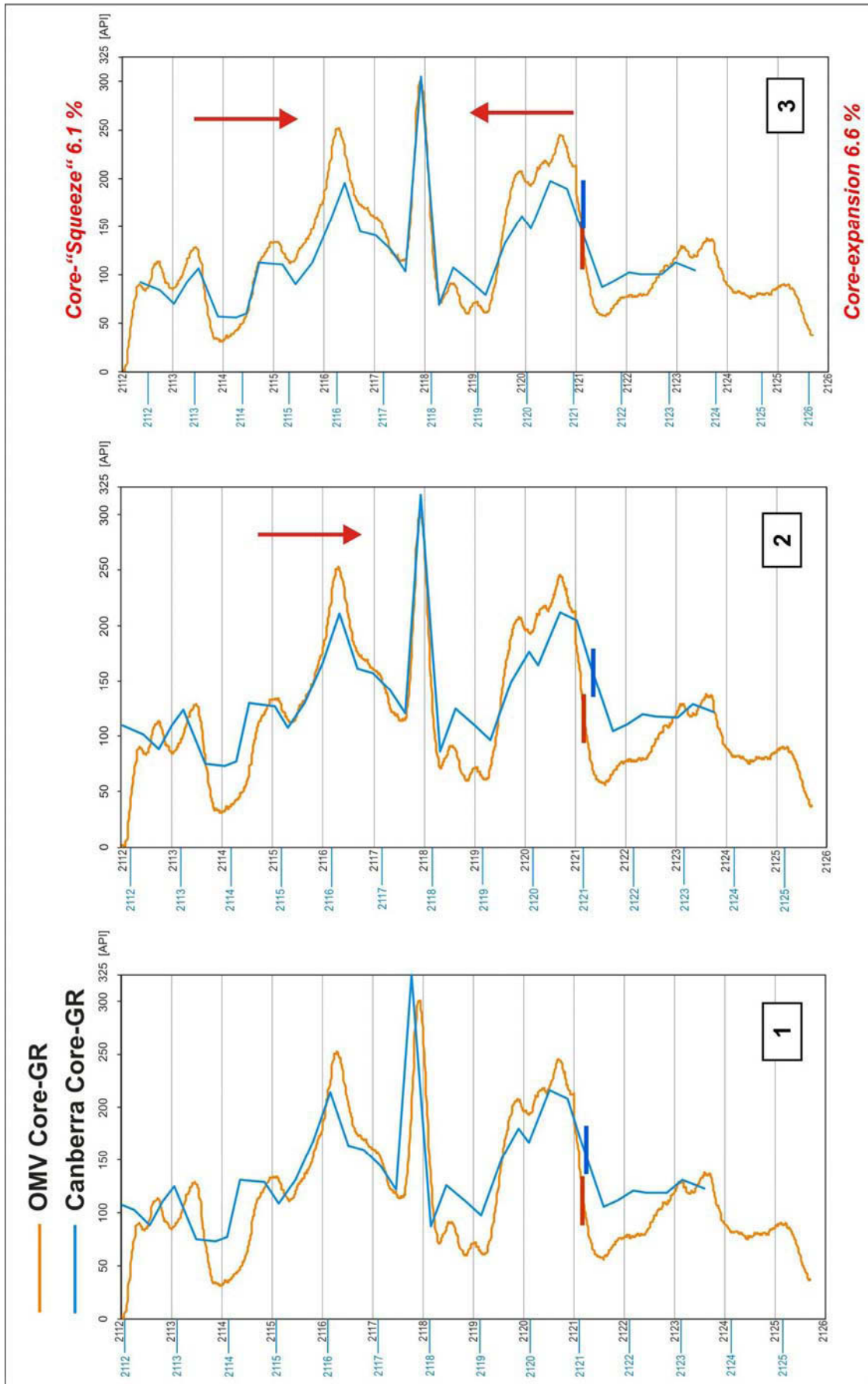
Fig. 34: Comparison of OMV and Canberra Core-GR measurement explaining the correction-process (example BH-N-002)
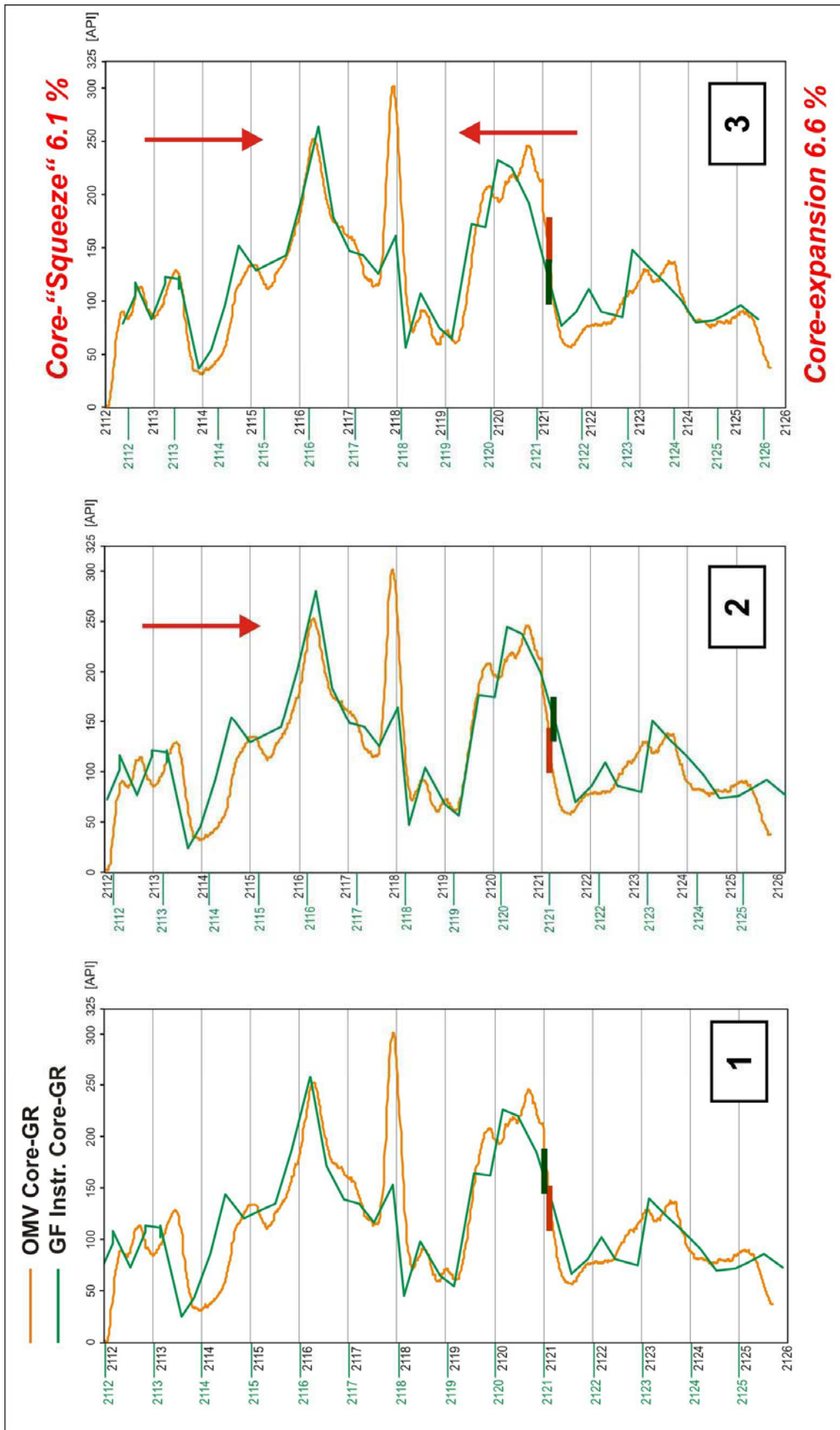
Fig. 35: Comparison of OMV and GF Instruments Core-GR measurement explaining the correction-process (example BH-N-002)
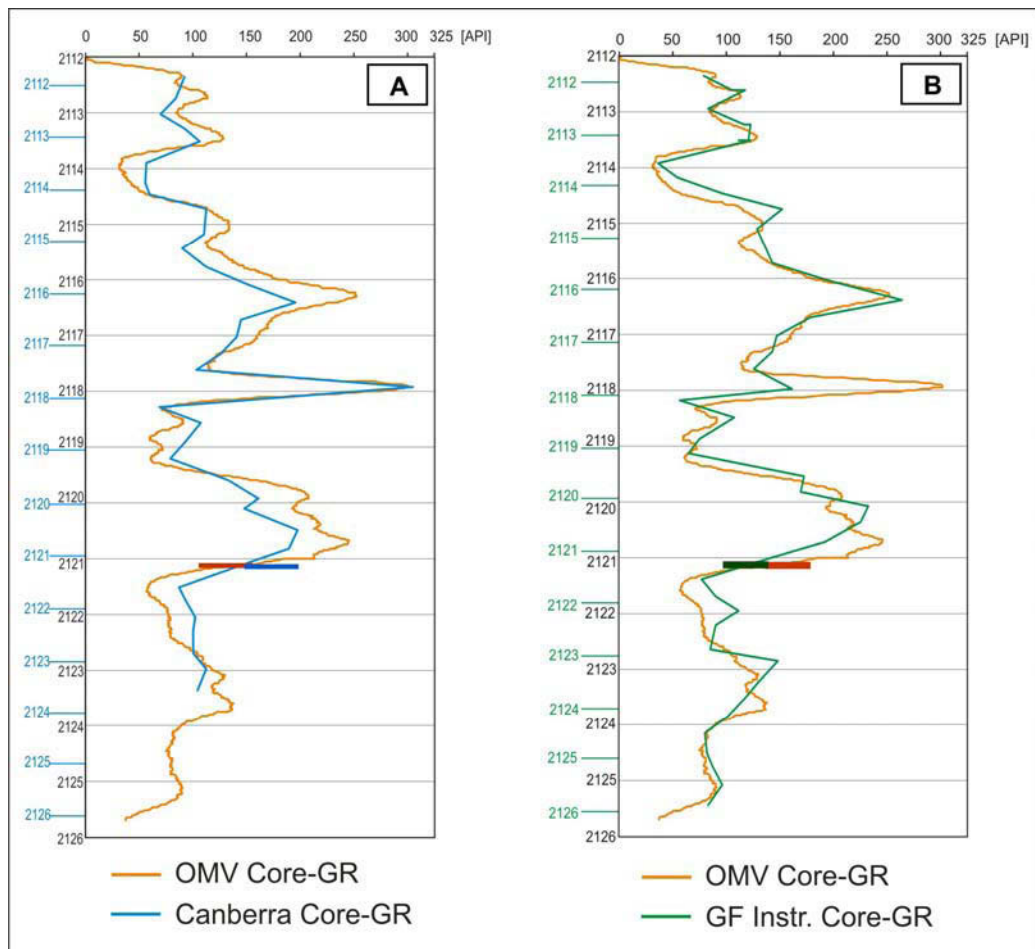
**Fig. 36: Comparison of OMV and MUL Core-GR (example BH-N-002),
A= OMV and Canberra Core-GR, B= OMV and GF Instruments Core-GR**

As displayed in Fig. 36, the Core-GR tool of GF instruments generally shows a better fit, except for a depth of approximately 2,118 m. This may indicate that the high GR reading results from a thin layer missed by the GF instruments Core-GR measurement.

Spectral measurement:
Fig. 37 shows the comparison of Spectral Core-GR measurements of the Canberra tools with the OMV Spectral Core-GR. Especially the content of uranium displays great variance without a clear trend. Again, the tool of GF Instruments provides the better fit (see Fig. 38). The resulting logs of potassium, thorium and uranium had to be corrected similar to the Total Core-GR before, but both tools (those of OMV and GF Instruments) show similar trends.

The Gamma Surveyor Compact of GF Instruments shows the better Core-GR results in comparison with OMV Core-GR measurement. Additionally, the tool of GF Instruments requires more simple data handling.
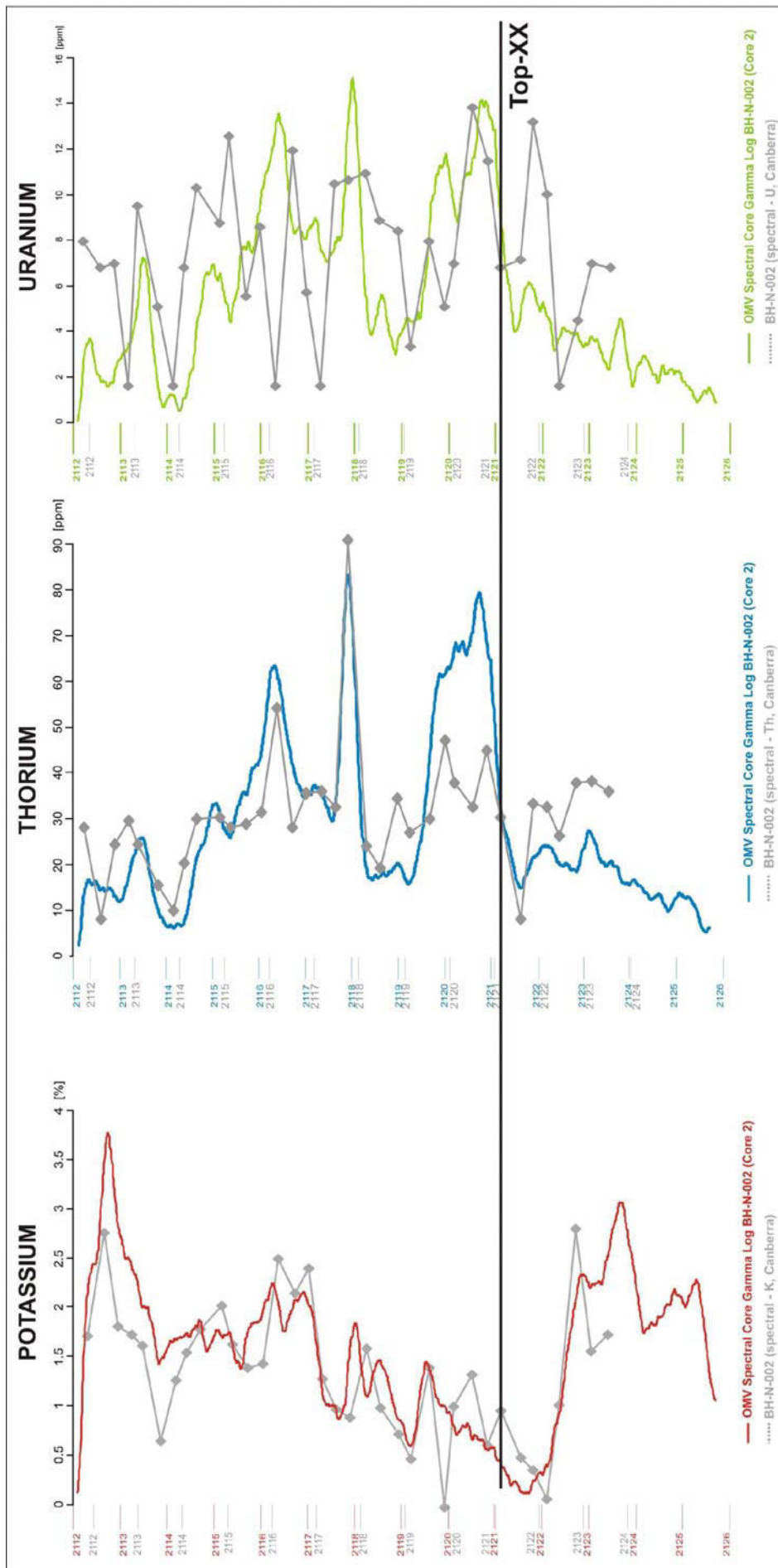
Fig. 37: Comparison of OMV and Canberra Core-GR (example BH-N-002)
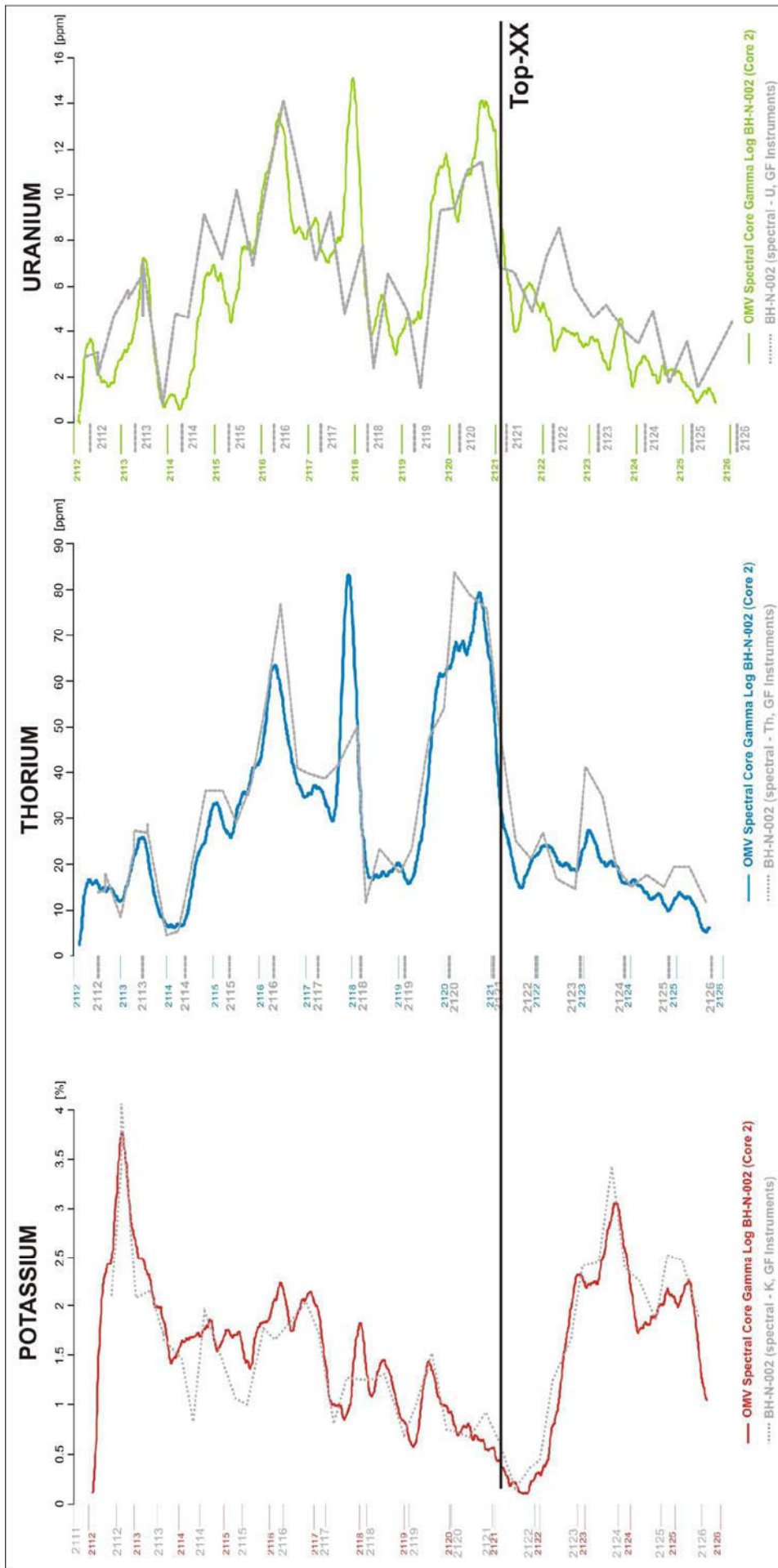
Fig. 38: Comparison of OMV and GF Instruments Core-GR (example BH-N-002)

5. WELL ANALYSIS

The order of the following well analysis is chosen according to the clearness of their results. First, wells with crystalline basement overlain by Cenomanian sediments will be described, starting with the calibration well BH-N-002 and proceeding with BH-N-001. HIER-002A and MLRT-003C with Eocene sediments above Top-XX will follow and the wells KH-003 and V-037 with Jurassic sediments on top of the crystalline basement will be analyzed at the end of this chapter.

5.1 Wells   with Cenomanian sediments overlying Top-XX

BH-N-002

Core analysis:

Total core interval of core 2 from the well BH-N-002 ranges from 2,112 to 2,126 m. Core diameter is 10 cm. Core recovery was 14 m indicating that there was no core loss. Fig. 39 shows the core data sheet from the core interval including Top-XX (core no. 2, box no. 5, from 2,121 to 2,122 m depth). Core data sheets of remaining boxes are attached.

Fig. 39: Core data sheet from top of the crystalline basement in well BH-N-002

Although core recovery is 14 m, the present-day length of the core is slightly higher (resulting in 15 core boxes). This is a result of core expansion due to cutting, core break etc. (see chapter 4).
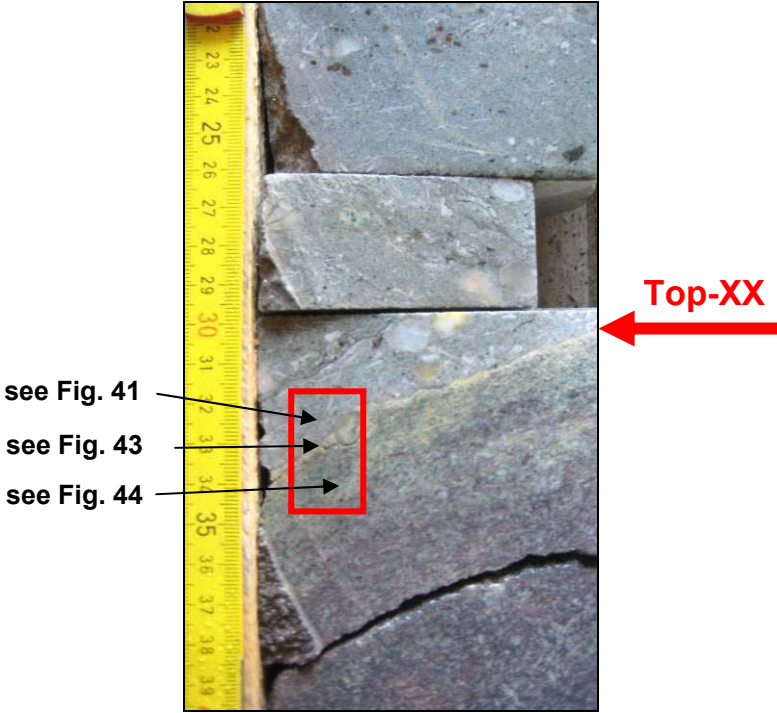
Fig. 40: Core photo of the top of the crystalline basement in BH-N-002.
The position of a thin section at a core depth of 2,121.33 m is indicated.

Top-XX is macroscopically identifiable by a sharp boundary (see Fig. 40) at a core depth of approx. 2,121.30 m.
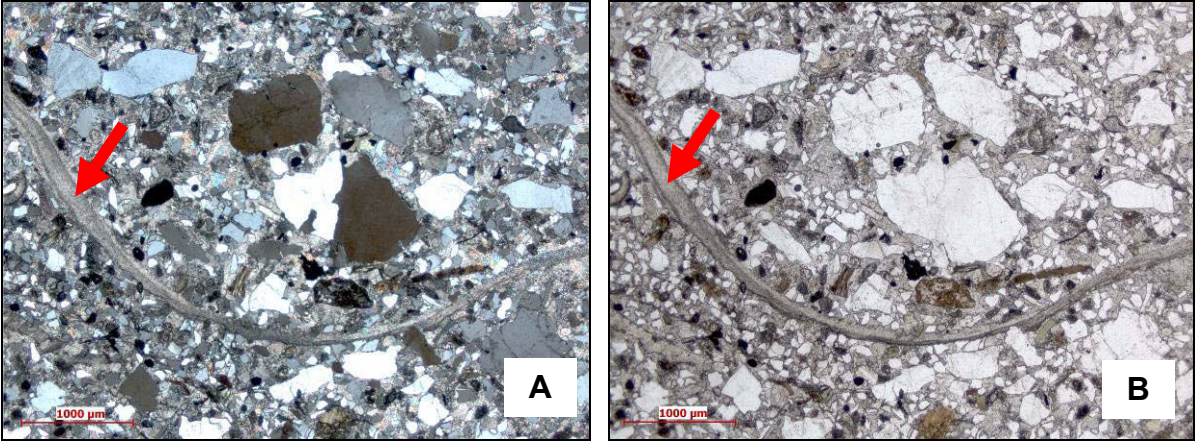
Fig. 41: Microphoto of BH-N-002: Cenomanian sandstone
with relict of shell indicated by the red arrows;
(A= cross-polarizer image, B= plane-polarizer image)

Cenomanian sandstone of BH-N-002 consists mainly of quartz and mica (mainly biotite) and has a carbonatic matrix. Feldspars are predominantly potassium feldspars with partly weathered plagioclase.

Additionally, numerous heavy minerals (see Fig. 42), like zircon, turmaline, garnet and epidote are present. Furthermore, fossils (shells, ?pellets, ?algae...) and small calcitic veins can be found.
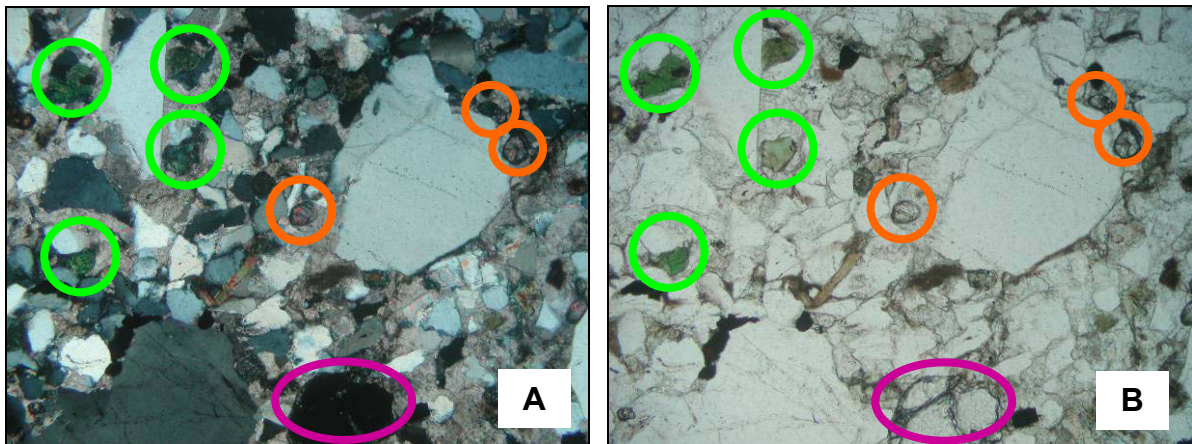
Fig. 42: Microphoto of BH-N-002: Cenomanian sandstone with heavy minerals, green= turmaline, orange= zircon, magenta= garnet (A= cross-polarizer image, B= plane-polarizer image)

The red line in Fig. 43 marks the boundary between crystalline rocks and Cenomanian sandstone, as macroscopically identified above.
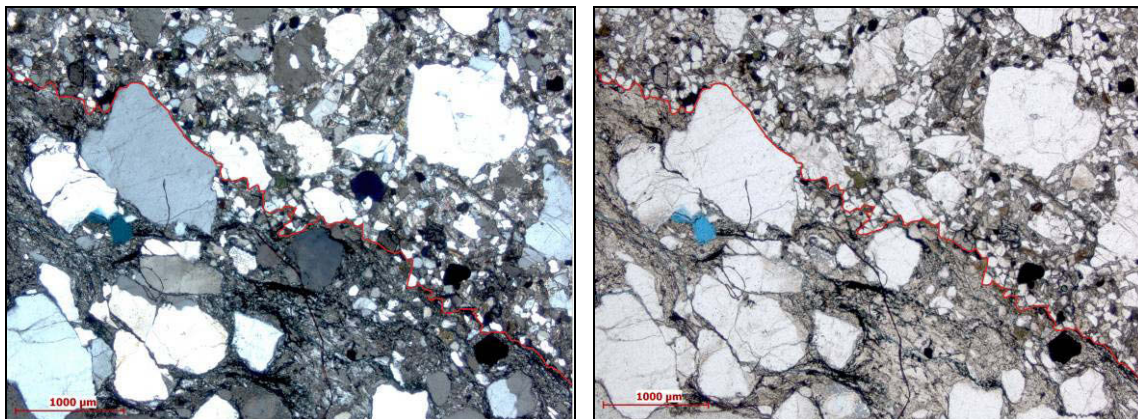
Fig. 43: Microphoto of BH-N-002: Top of the crystalline basement = red boundary; The blue phase represents the resin used for thin section preparation and highlights pore space. (A= cross-polarizer image, B= plane-polarizer image)

Fig. 44 shows weathered crystalline basement, which appears like a kind of mylonitic horizon. The main components are quartz and alterated feldspar embedded in a chloritic-sericitic matrix. Quartz grains are partly broken.
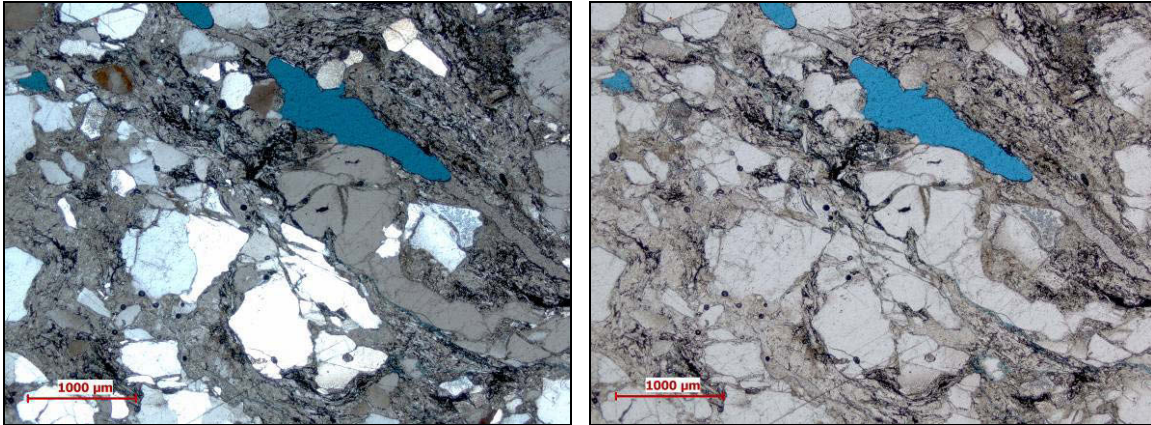
Fig. 44: Microphoto of BH-N-002: Crystalline basement (granodiorite-diorite)
(A= cross-polarizer image, B= plane-polarizer image)

Log analysis:

According to the OMV core log, Top-XX is at a depth of 2,121.10 m (see Fig. 45).
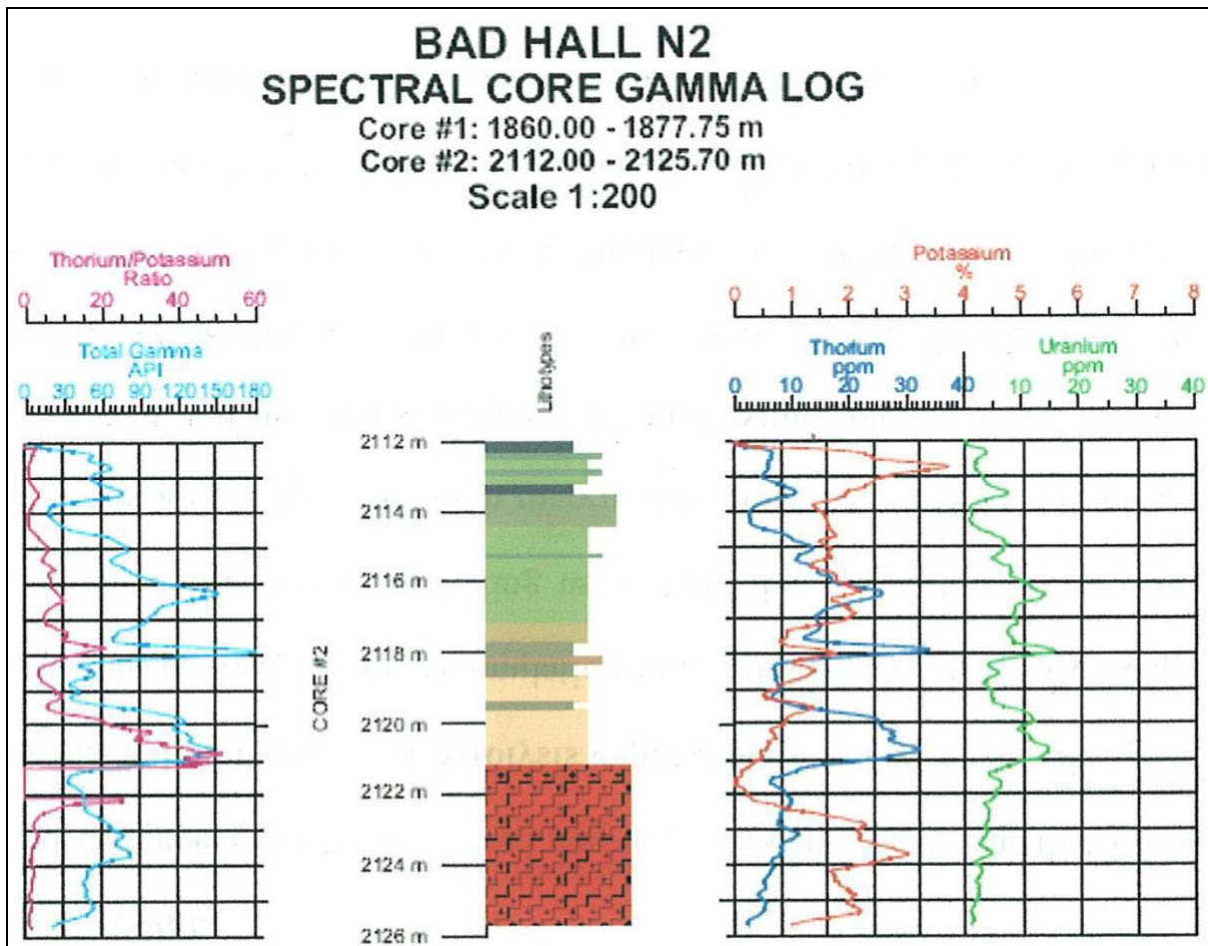
Fig. 45: OMV Spectral Core-GR of well BH-N-002

Spectral Core-GR of OMV illustrated in Fig. 45 and 46 indicate an increase of GR at the base of the Cenomanian sandstone, which is controlled by high contents of thorium and uranium. At Top-XX, Core-GR decreases significantly from approximately 230 to 50 API. Potassium content is low at Top-XX, followed by a continuous increase downwards. Compared to relatively high and fluctuating values within the Cenomanian sandstone, the crystalline basement has quite low GR values.
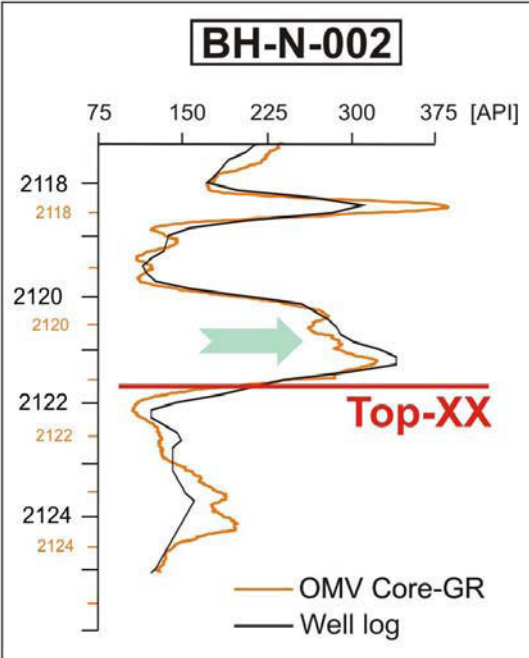
Fig. 46: Comparison OMV Core-GR and well log GR of BH-N-002

After considering a core-to-log shift of 0.70 m, a very good fit exists between the GR-curves of OMV and the well log GR of BH-N-002 (see Fig. 46). Thus, the depth of Top-XX is at 2,121.10 m according to OMV Core depth and at 2,121.80 m, representing log depth.

Based on core analysis (performed in the Pettenbach core store), Top-XX can be identified at 2,121.32 m (see "Pettenbach" Core in Table 7). The difference to the OMV core is a result of core "expansion" due to core handling (see above).

Table 7 summarizes all depths of Top-XX:

	Depth of Top-XX [m]
"OMV" Core	2,121.10
"Pettenbach" Core	2,121.32
Log Depth	2,121.80

Table 7: Depths of top of the crystalline basement of BH-N-002

Fig. 47 shows all logs available for BH-N-002. The dashed blue line indicates Top-XX, whereas the red arrows highlight trends of the curves.

Obviously, the SP log does not show any useful trend at Top-XX. Perhaps it is affected by drilling mud. In any case, it cannot be used as reliable information to define the top of the crystalline basement. Besides SP log, also sonic (DT) and density log (RHOZ) do not indicate a clear boundary and are of little use for the present purpose.

On the other side, GR, CAL, NPHI, PEFZ and resistivity logs are essential to identify Top-XX as they show significant changes. As discussed before, GR and PEFZ decrease significantly, whereas CAL, NPHI and the resistivity logs indicate a downward increase at Top-XX.
Weathering, subsurface alteration and resedimentation often result in an uptake of highly mobile potassium. The Total GR log may therefore be used as an indicator for such processes (Bartetzko et al., 2005).

High contents of thorium and uranium displayed in the Spectral Core-GR may be caused by heavy minerals. Zircon, turmaline, garnet and epidote are present in thin sections. Although these heavy minerals are not typically radioactive, zircon is able to integrate uranium. Potassium may have been removed as a result of weathering, which explains very low contents below Top-XX. Downwards, the potassium content increases significantly. On the one side, this may be the result of the presence of unweathered crystalline basement with a great amount of potassium feldspars suggested. Additionally, this effect could also be based on changing basement lithology.

The green line in the caliper log column indicates the bit size (8.5 inch). Using this information, it is obvious, that a borehole breakout exists near the top of the crystalline basement.
At Top-XX, the neutron porosity (NPHI) shows a significant increase from approximately 11 to 31 %. This can be a result of weathering, which causes alteration and dissolution and therefore creates additional pore space. Unweathered crystalline provides extremely low porosity of approximately 2 %.
PEFZ values are decreasing at Top-XX and increasing downwards within unweathered crystalline. Generally high values of PEFZ represent a typical trend for igneous rocks.

All resistivity logs (flushed zone, shallow, deep) are influenced by change of lithology and decrease at Top-XX. This may be an effect of oxide-rich layers, resulting in values of electrical resistivity lower than 100 ohm-m (Einaudi et al., 2005).
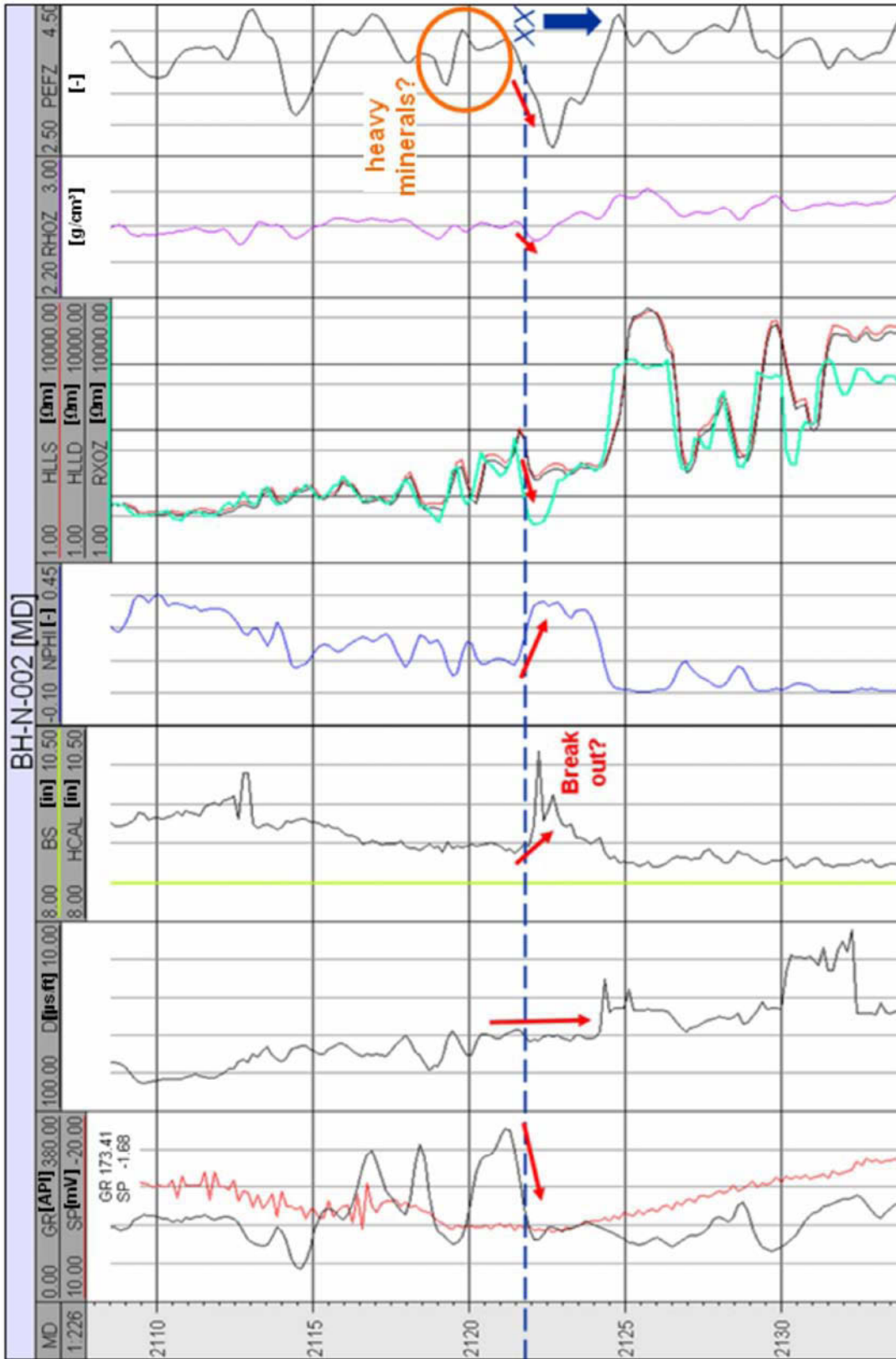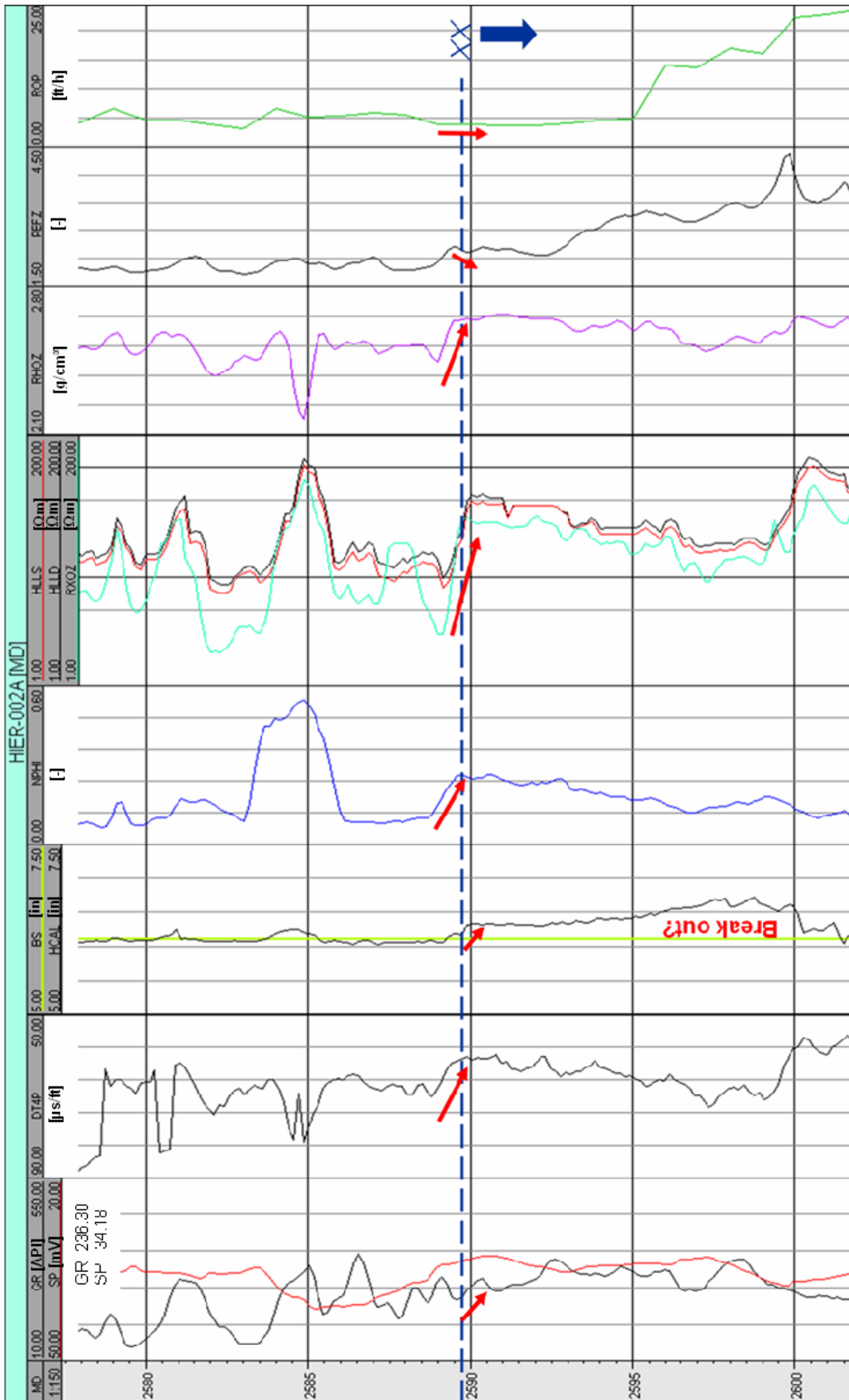
Fig. 47: Correlation of well logs of BH-N-002; the dashed blue line indicates top of the crystalline basement; The values of GR and SP at Top-XX are displayed on top of the logs.
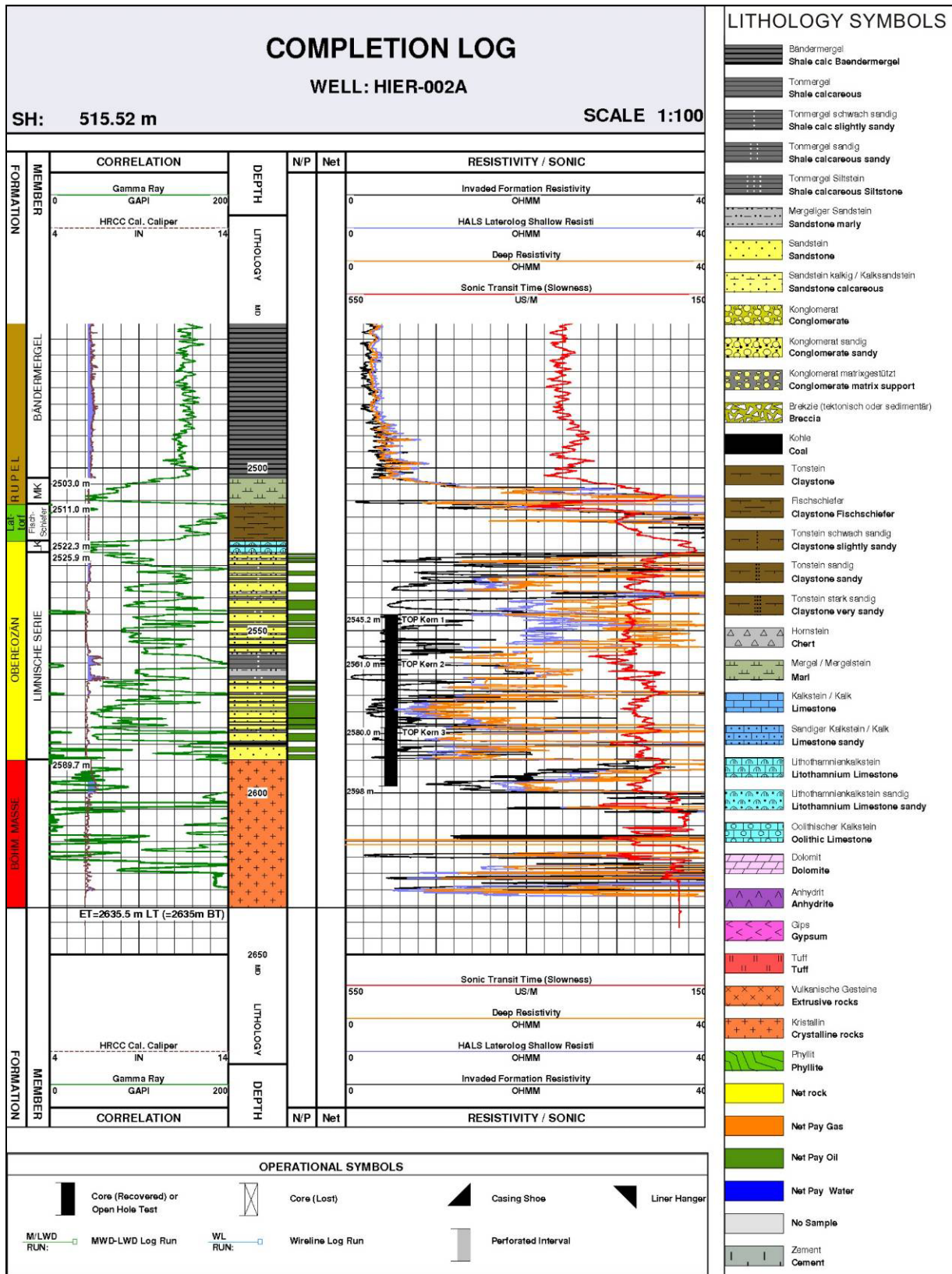
According to the completion log (Fig. 48), Top-XX is defined at a depth of 2,121.40 m and therefore shows a slight difference to the depths defined by OMV core report and well log analysis. However, because of the scale (1:1000), the completion log is difficult to interpret and the reasons for the depth assignment remain unclear.
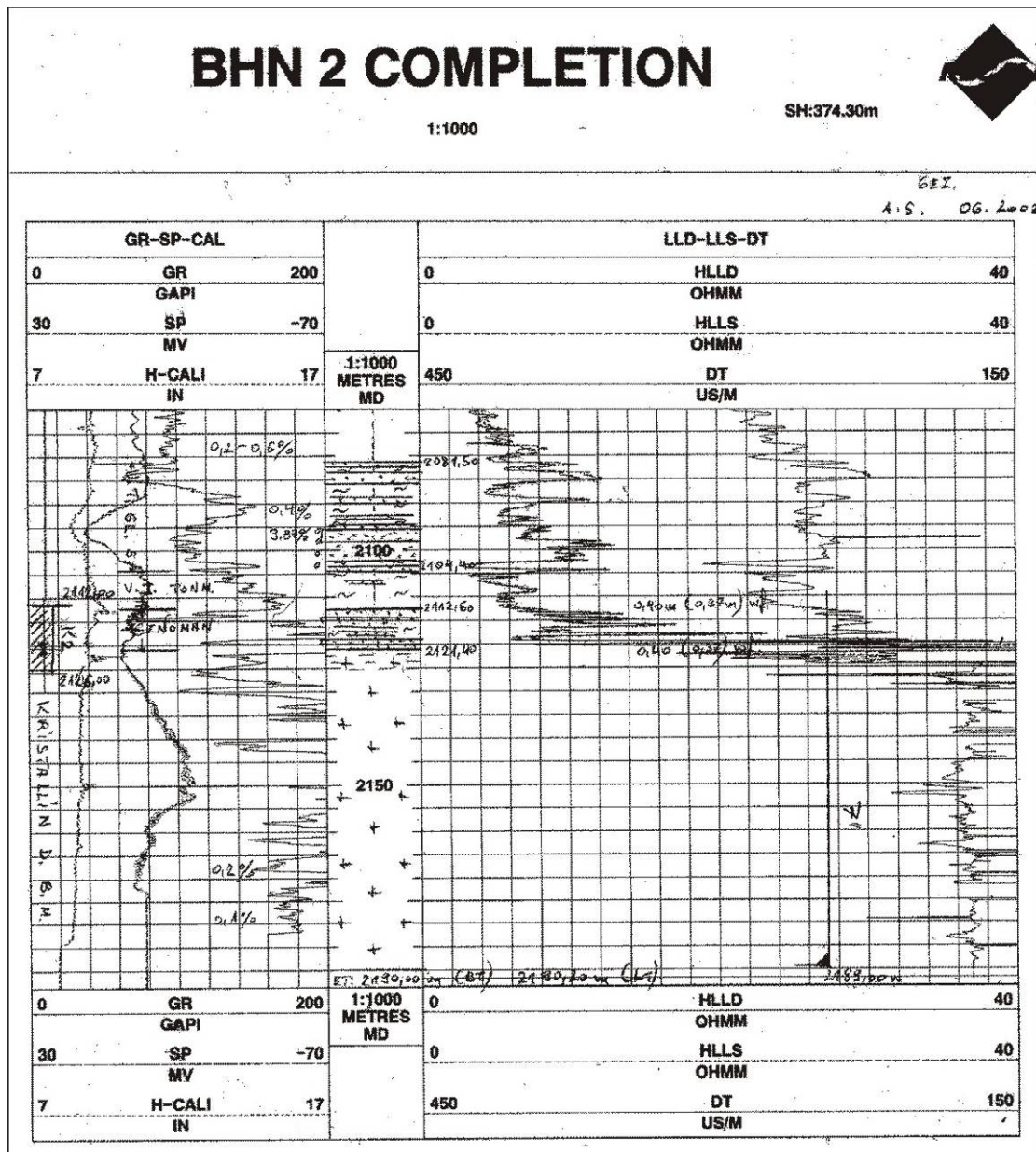
Fig. 48: Completion log of well BH-N-002

BH-N-001

Core analysis:

The top of the crystalline basement in the well BH-N-001 has been recovered by core no. 3 (2,036 - 2,046 m; core diameter: 6.5 cm, core recovery: 7.20 m). Actually, there was a significant core loss, which must be considered for the following analysis. Fig. 49 shows the core data sheet from the core interval including Top-XX (core no. 3, box no. 4, from 2,042 to 2,043 m depth).

Fig. 49: Core data sheet from top of the crystalline basement in well BH-N-001

As Top-XX is just on top of box no. 4 at a depth of 2,042.03 m (see Fig. 49), a core photo of the lower part of box no. 5 containing Cenomanian sandstone is displayed in Fig. 50 to verify the definition of the top of the crystalline basement.

Fig. 50: Core photo of Cenomanian sandstone (BH-N-001)
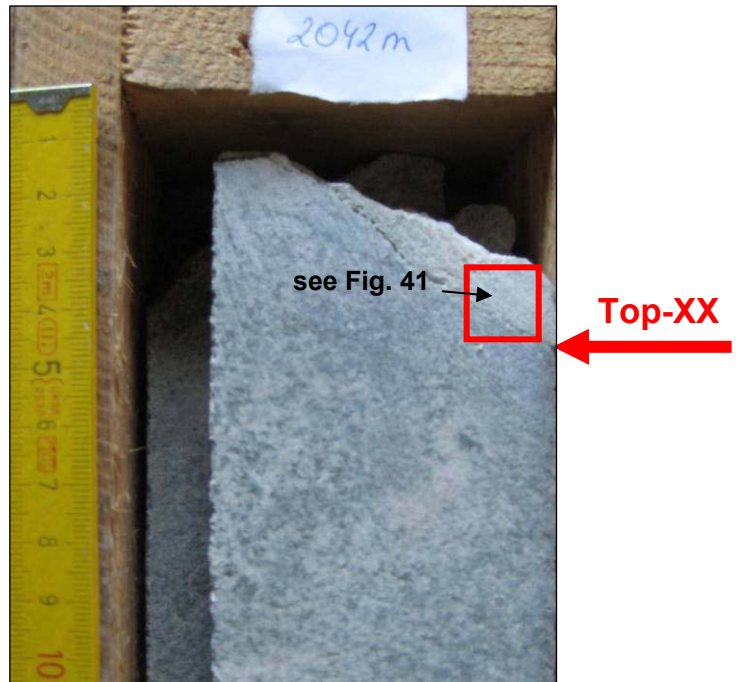
Fig. 51: Core photo of the top of the crystalline basement of BH-N-001

Microphotos of the Cenomanian sandstone are displayed in Fig. 52 and Fig. 53. The main components are quartz grains, which are partly broken. Additionally, muscovite is present, whereas feldspar is apparently missing. The components are surrounded by a phyllosilicatic matrix. Unfilled pore space is highlighted by a blue-coloured resin used for thin section preparation.
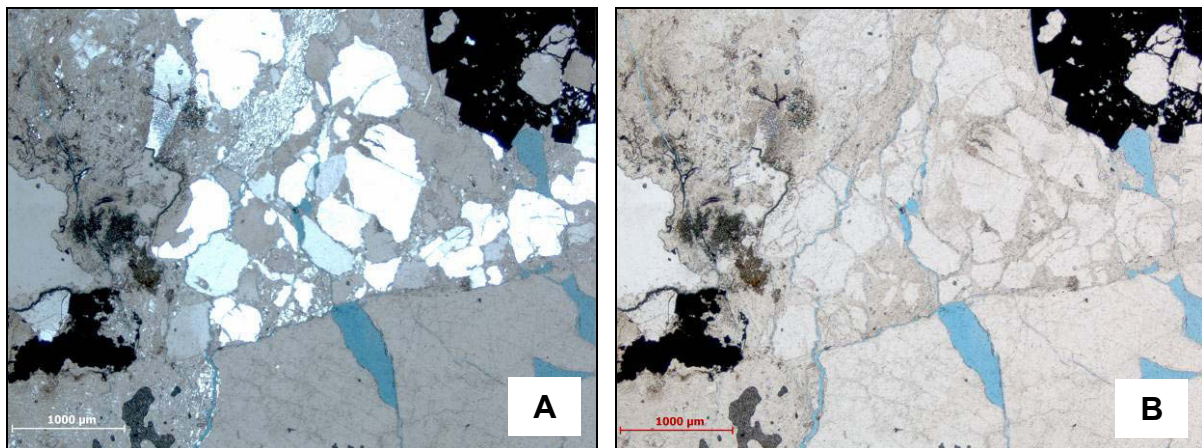
Fig. 52: Cenomanian sandstone of BH-N-001
(A= cross-polarizer image, B= plane-polarizer image)
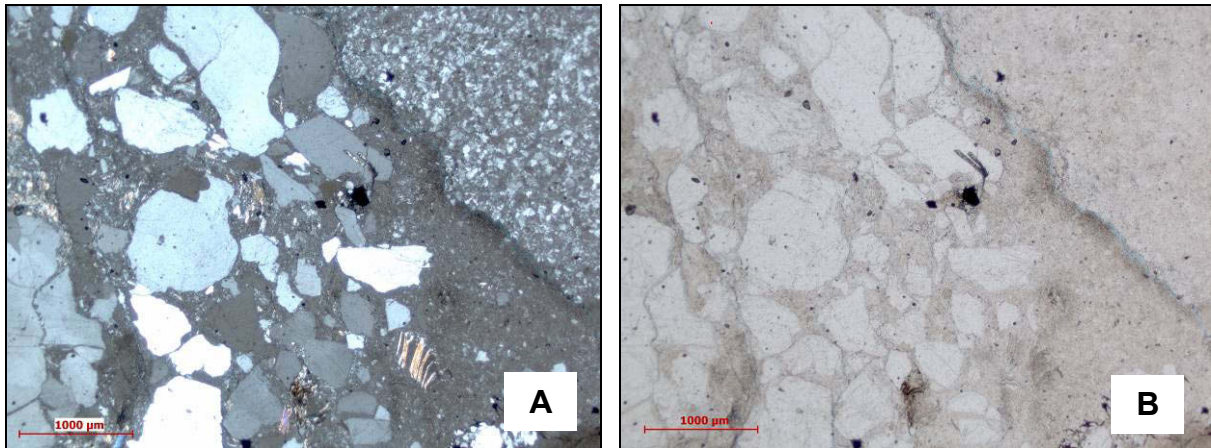
Fig. 53: Cenomanian sandstone of BH-N-001
(A= cross-polarizer image, B= plane-polarizer image)

Unfortunately, there is no microphoto of crystalline rock from this thin section, because of problems during thin sectin preparation.

Log analysis:

Fig. 54 illustrates spectral Core-GR log measured by OMV. Top-XX is defined according to the OMV core report at a depth of 2,039.07 m.
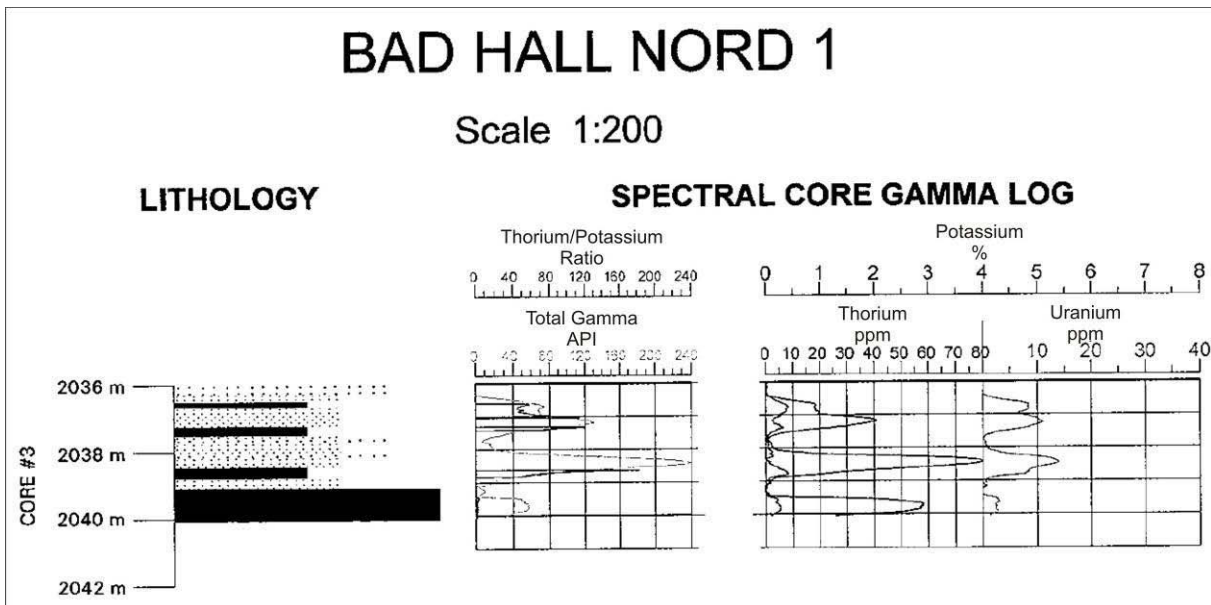
Fig. 54: OMV Spectral Core-GR of well BH-N-001

As seen in well BH-N-002, also well BH-N-001 shows high GR values at the base of the Cenomanian sandstone (see Fig. 54 and 55).
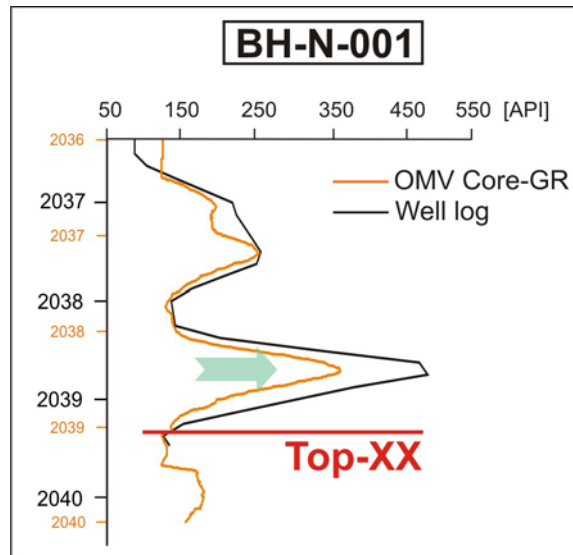
Fig. 55: Comparison OMV Core-GR and well log of BH-N-001

The comparison of the OMV Core-GR of the Cenomanian section and well log GR (Fig. 55) indicates a core-to-log shift of 0.35 m and an excellent fit between both curves. This suggests that the significant core loss (10.0 – 7.2 = 2.8 m) did not occur within the section of Cenomanian rocks, but within the section of crystalline rocks.

According to OMV core report and consideration of the core-to-log shift, Top-XX of the OMV Core-GR is located at a depth of 2,039.07 m, whereas well log shows Top-XX at 2,039.42 m.
Because of the significant core loss and because the depth of the lowermost box no. 1 was equated with the base of the core (= 2,046 m), Top-XX identified during core analysis in the Pettenbach core store is defined at a depth of 2,042.03 m (see Table 8).

	Depth of Top-XX [m]
"OMV" Core	2,039.07
"Pettenbach" Core	2,042.03
Log Depth (~ Completion Log)	2,039.42

Table 8: Depth of top of the crystalline basement (Top-XX) of BH-N-001

Fig. 56 illustrates OMV Spectral Core-GR with Top-XX at a depth of 2,039.07 m. Within the Cenomanian section, thorium and uranium contents are strongly varying. The base of the Cenomanian has high contents in thorium and uranium, but relatively low contents in potassium. Similar to well BH-N-002, this indicates the presence of heavy minerals. A comparison of Total and Spectral Core-GR values show that the high amounts of thorium and uranium control the (total) well log GR. Potassium content is very low at Top-XX as a result of weathering, which may cause its removal. In agreement with this interpretation, potassium contents increase downwards to unweathered crystalline basement with a great amount of potassium feldspars suggested.
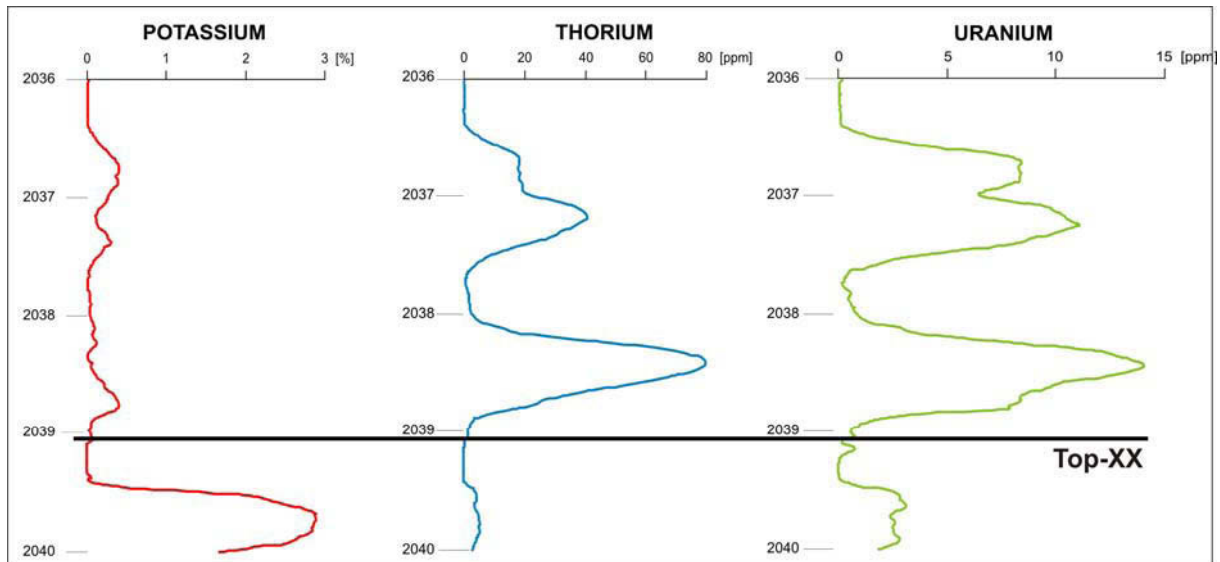
Fig. 56: OMV Spectral Core-GR of well BH-N-001

Different well logs of BH-N-001 are displayed in Fig. 57 with Top-XX at a log depth of 2,039.42 m represented by the dashed blue line. Red arrows indicate trends of the logs.

SP, caliper, porosity and density log do not show clear trends at Top-XX and are therefore not useful for the definition of Top-XX. As in BH-N-002, the SP log may be affected by drilling mud. The caliper log shows a more or less perfect borehole with a bit size (BS) of 6.25 inch. At Top-XX, porosity (NPHI) is about 15 % and the average density is approximately 2.45 g/cm³.

Similar to the observations in BH-N-002, the GR log has strong variations within the Cenomanian section, decreases significantly at Top-XX and exhibits low values within the crystalline basement. Sonic transit time (DT) and PEFZ values decrease in the area of Top-XX.

Resistivity logs measured are RXOZ (flushed zone), HLLS (shallow) and HLLD (deep). The resistivity of the flushed zone decreases strongly at Top-XX, whereas HLLS and HLLD only show a weak decrease followed by a moderate downward increase in resistivity.

Fig. 57: Correlation of well logs of BH-N-001; the dashed blue line indicates top of the crystalline basement (Top-XX); The values for GR and SP at Top-XX are displayed on top of the logs (130.13 API, -81.56 mV).

Fig. 58 illustrates the completion log of well BH-N-001 with Top-XX at 2,039.40 m. This represents a very good fit with Top-XX at 2,039.42 m according to log depth. Core loss within the crystalline basement is also noted (V).
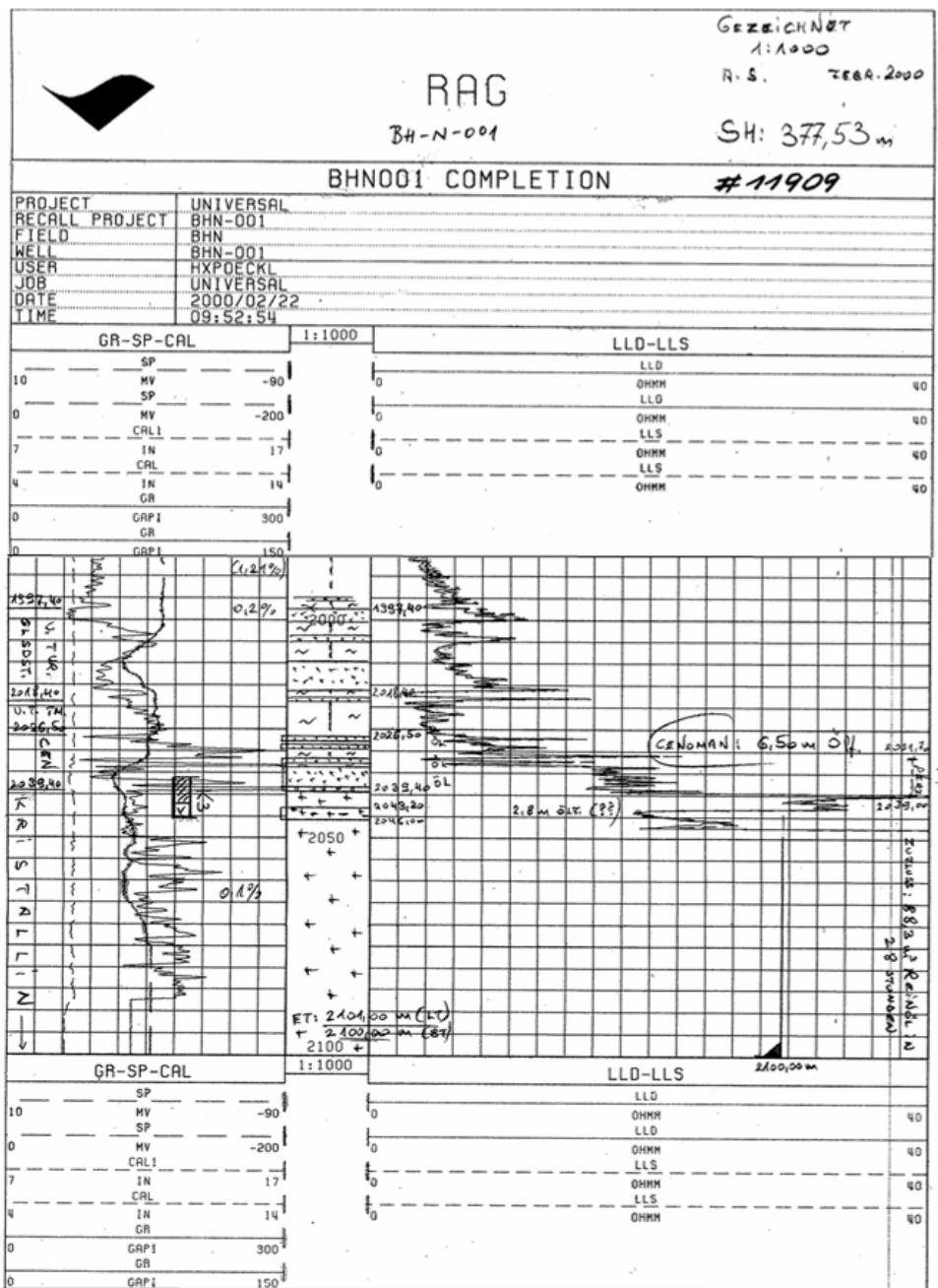
Fig. 58: Completion log of well BH-N-001

INTERPRETATION

Before evaluating the following results it must be considered, that the crystalline basement of both wells (BH-N-001 and BH-N-002) consists of magmatic rocks. BH-N-001 shows granite, whereas the crystalline of well BH-N-002 is composed of granodiorite or diorite.

	BH-N-001	*BH-N-002*
GR (log)	⬇	
CGR	⬇	
HLLS/HLLD	⬇ (weak, below: increase)	⬇
HCAL	⬆	
DT	⬇	⬆ (weak)
NPHI	⬇ (weak)	⬆ (strong!)
RHOZ	⬇ (below: increase)	---
PEFZ	= (below: decrease)	⬇ (strong!)

Table 9: Comparison of log trends of wells BH-N-001 and BH-N-002; Logs, which show similar trends in both boreholes are highlighted by coloured arrows (red= values decrease, green= values increase).

Table 9 represents a comparison of log trends for both wells. Only GR and Core-GR show similar trends for wells BH-N-001 and BH-N-002 and are therefore the best tools for the definition of Top-XX.

GR and obviously also Core-GR logs show high GR values at the base of Cenomanian rocks and a decrease in radiation at Top-XX (see Fig. 59). As mentioned before, these high GR values are due to the presence of heavy minerals, which contain high amounts of uranium and thorium. The radiation from these elements controls the total GR log.
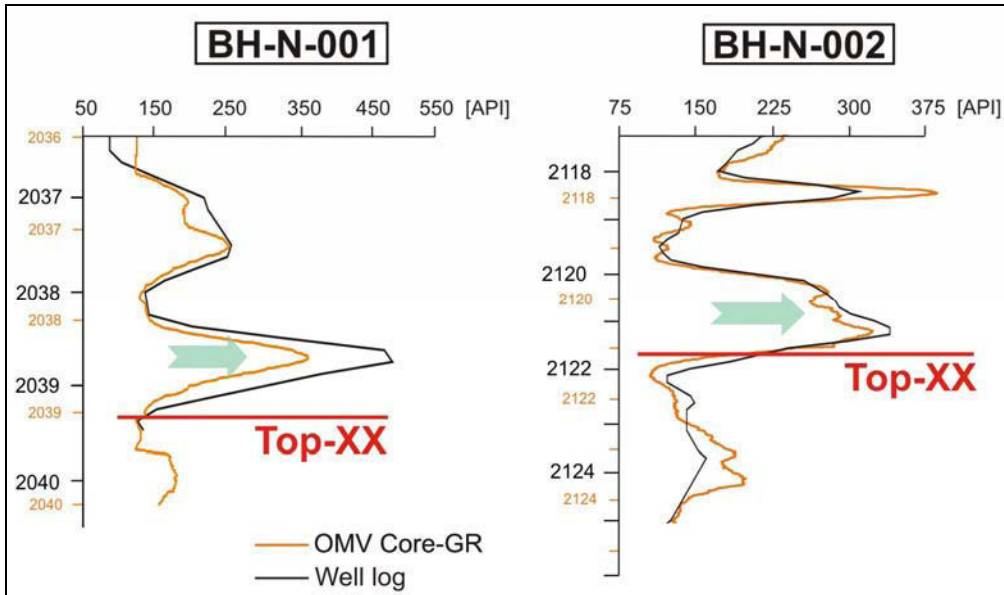
Fig. 59: High GR at base of Cenomanian sandstone

The resistivity logs shallow (HLLS) and deep (HLLD) also show similar, but minor changes. Unfortunately, density log is only available for BH-N-001 and therefore it cannot be used for indicating trends. All other logs (NPOR, NPHI, PEFZ) either show very weak or opposite trends.

5.2 Wells with Eocene sediments overlying Top-XX

HIER-002A

Core analysis:

Core no. 3 (2,577 to 2,595 m; core diameter: 6.5 cm; core recovery: 18 m) has recovered Top-XX. There was no core loss and an additional box is (partially) filled because of core "growth". The top of the crystalline basement is located at a depth of 2,586.10 m (see Fig. 61). Fig. 60 illustrates the core data sheet from the core interval including Top-XX (core no. 3, box no. 9, from 2,586 to 2,587 m depth).

Fig. 60: Core data sheet from the top of the crystalline basement in well HIER-002A

Fig. 61: Core photo of Top-XX of HIER-002A

Fig. 62 shows moderate to well sorted and moderately rounded Eocene sandstone. Components are mainly quartz, feldspars and mica (predominantely muscovite). The matrix is phyllosilicatic/chloritic-sericitic.
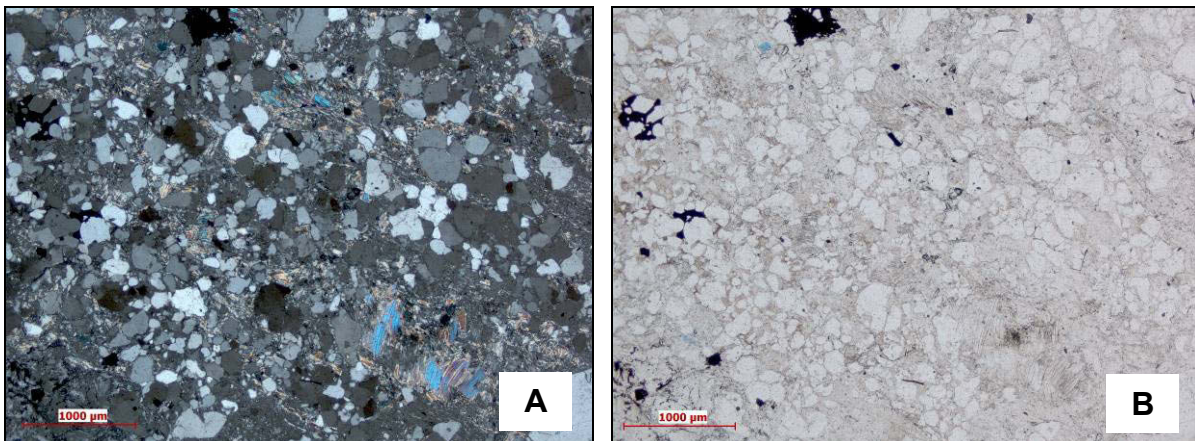
Fig. 62: Microphoto of HIER-002A: Eocene sandstone
(A= cross-polarizer image, B= plane-polarizer image)

Photomicrographs in Fig. 63 illustrate Top-XX of HIER-002A as a sharp boundary, indicated by a red line. Especially, the cross-polarizer image shows a difference between Eocene sandstone and crystalline basement.
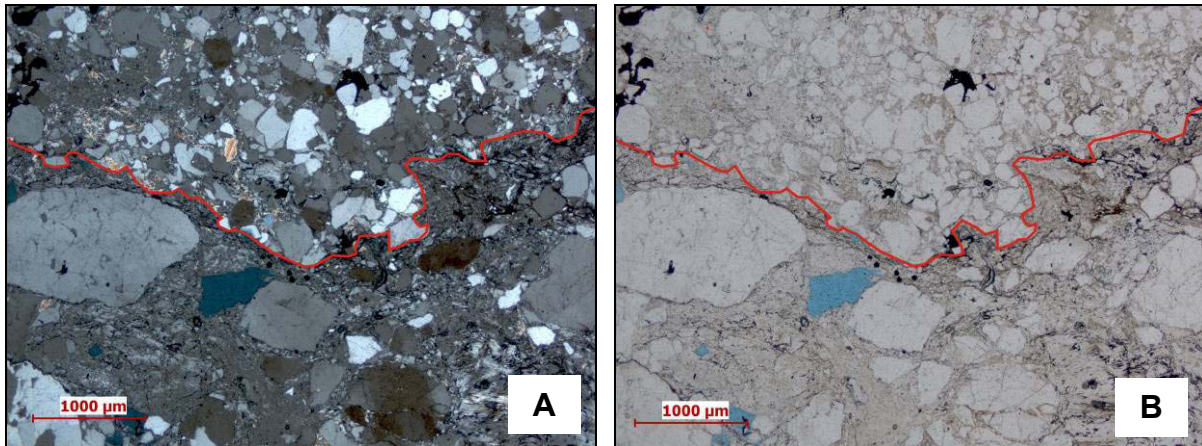
**Fig. 63: Microphoto of HIER-002A: Top of the crystalline basement = red boundary;
Blue phases indicate pore space highlighted by blue-coloured resin used for
thin section preparation. (A= cross-polarizer image, B= plane-polarizer image)**

The crystalline basement of HIER-002A is formed by coarse, weathered granite (see Fig. 64). Feldspars are completely altered and/or transformed to chlorite. The main components are angular and partly broken quartz grains. Additionally, mica (muscovite) and opaque minerals (pyrite) can be identified.
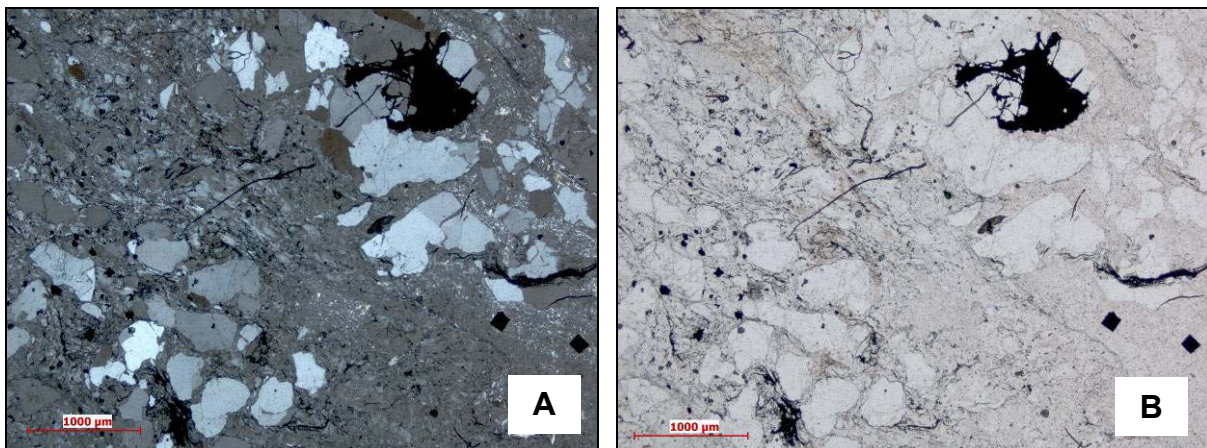
**Fig. 64: Microphoto of HIER-002A: Crystalline basement (granite)
(A= cross-polarizer image, B= plane-polarizer image)**

Log analysis:

Fig. 65 shows OMV Spectral Core-GR Log of well HIER-002A with Top-XX at a depth of 2,586.50 m. Crystalline basement is present within core no. 3.
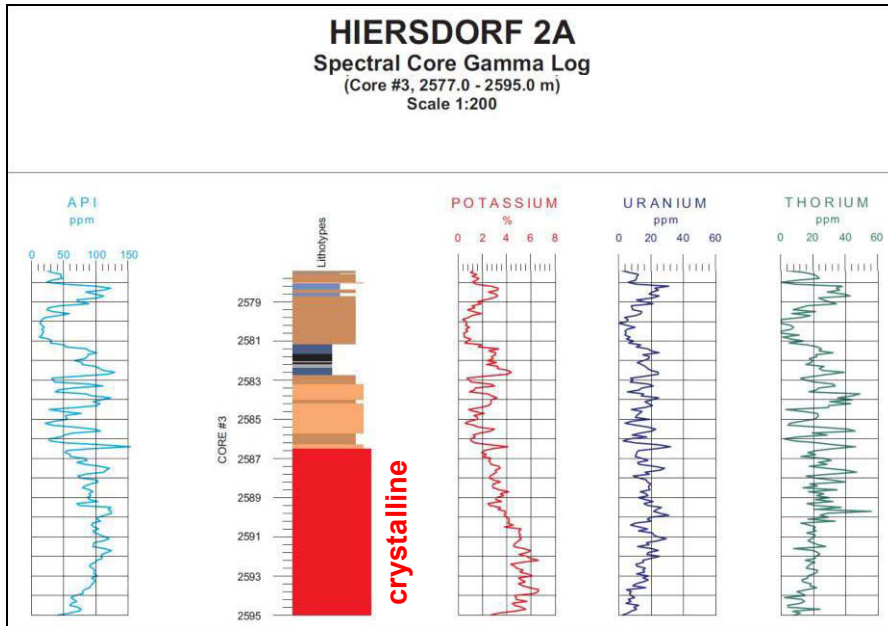
Fig. 65: OMV Core-GR of core no. 3 from well HIER-002A

A comparison of OMV Core-GR and well log GR of HIER-002A is illustrated in Fig. 66. Additionally, GR is significantly fluctuating within the Eocene succession.

The comparison of both curves identifies a core-to-log shift of 3.2 m. Considering the OMV core report and core-to-log shift, Top-XX according to OMV Core-GR is defined at 2,586.50 m, whereas according to log depth and completion log it is located at a depth of 2,589.70 m.
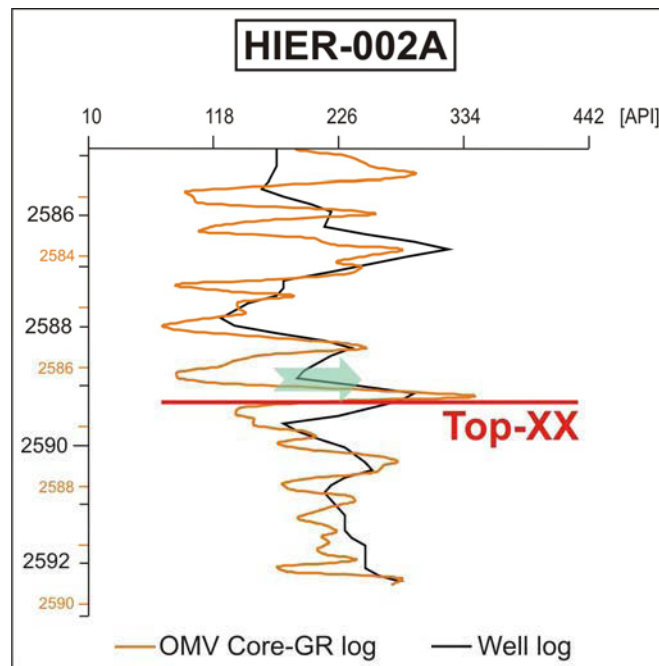
Fig. 66: Comparison of OMV Core-GR and well log of HIER-002A

Table 10 summarizes all depths of Top-XX and highlights again the shift between OMV core and well log.

	Depth of Top-XX [m]
"OMV" Core	2,586.50
"Pettenbach" Core	2,586.10
Log Depth (= Completion Log)	2,589.70

Table 10: Depth of top of the crystalline basement of HIER-002A

The Spectral Core-GR measured by OMV is represented by Fig. 67. Especially the contents of thorium and uranium show great variations. Hardly any trend can be identified within the Eocene rocks, compared to the base of the Eocene with a minor peak of potassium content.

Within the uppermost 8 m of the granitic section, trends are visible for all three elements measured. The uppermost 4 m of granite represent high, but strongly varying contents of thorium and uranium. Below, uranium and thorium contents decrease downwards. In contrast, potassium contents increase downwards.
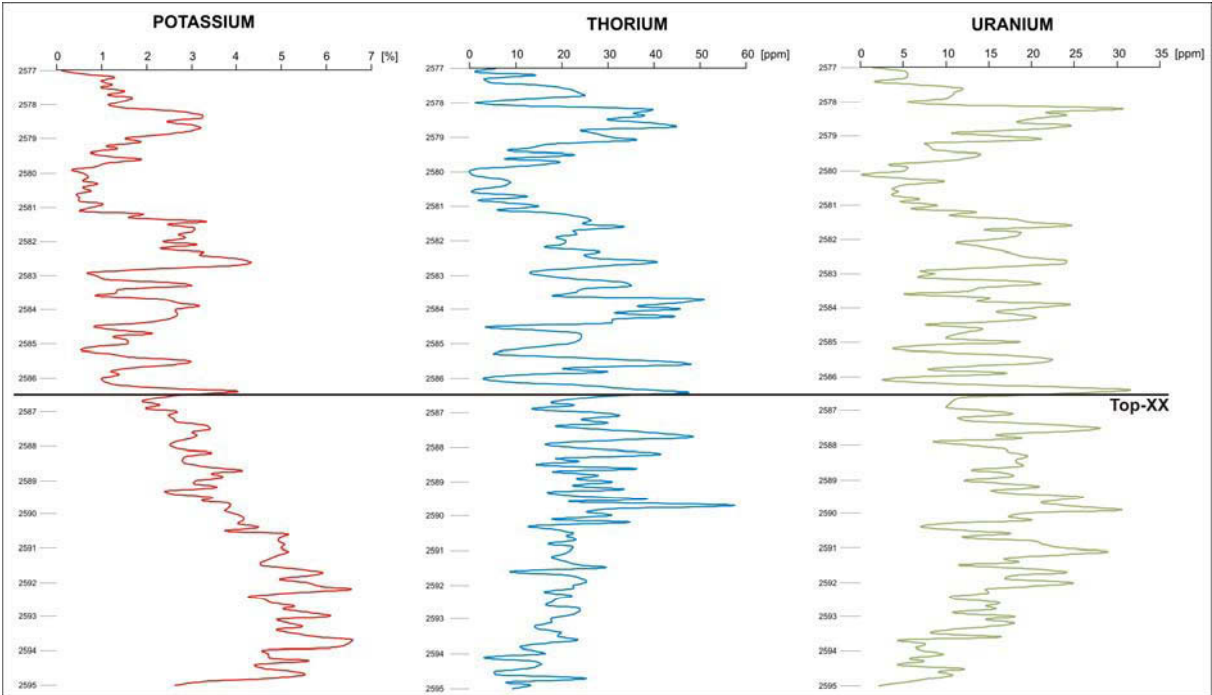
Fig. 67: OMV Spectral Core-GR of core no. 3 from well HIER-002A

The correlation of all well logs available for well HIER-002A with Top-XX at 2,589.7 m is displayed in Fig. 68.

The SP log is probably again affected by drilling mud and not useful for defining Top-XX. The GR values show a subtle downward increase across Top-XX, whereas values of transit time (DT) from the sonic log are decreasing or, in other words, velocity is increasing.

Bit size (BS) is 6.125 inch and thus the caliper log indicates some minor borehole breakouts within the crystalline basement. At base Eocene porosity is increasing and within the uppermost crystalline it shows high, constant values of about 25 %.

All resistivity logs (RXOZ, HLLS, HLLD) indicate strong increase in resistivity up to approximately 100 Ωm at Top-XX. In this case, they are the most reliable tools for the definition of Top-XX.

According to RHOZ log, the density is also increasing at Top-XX, whereas PEFZ log decreases slightly. Within the uppermost 5 m of the crystalline section the rate of penetration (ROP) shows constant values of approximately 4 ft/h.

Fig. 69 represents the completion log of well HIER-002A with Top-XX at 2,589.7 m, which agrees with Top-XX defined by core inspection.

Fig. 68: Correlation of well logs of HIER-002A; dashed blue line indicates top of the crystalline basement (Top-XX); The values for GR (236.30 API) and SP (34.18 mV) at Top-XX are displayed on top of the logs.

Fig. 69: Completion log of well HIER-002A

MLRT-003C

Core analysis:

In well MLRT-003C, Top-XX has been recovered by core no. 4 (3,604 to 3,622 m; core diameter: 6.5 cm; core recovery: 16 m). According to the core recovery, a core loss of 2 m is indicated. Top-XX is illustrated in the core data sheet of Fig. 70 (core no. 4, box no. 7, from 3,615 to 3,616 m depth).

Fig. 70: Core data sheet of the top of the crystalline basement in MLRT-003C

Fig. 71 shows a photo of Top-XX within the core of MLRT-003C. A sharp boundary between Eocene sandstone and crystalline basement at 3,615.40 m can be identified. In general, crystalline rocks present in well MLRT-003C consist of coarse gneiss, although they show migmatitic structures near the top.
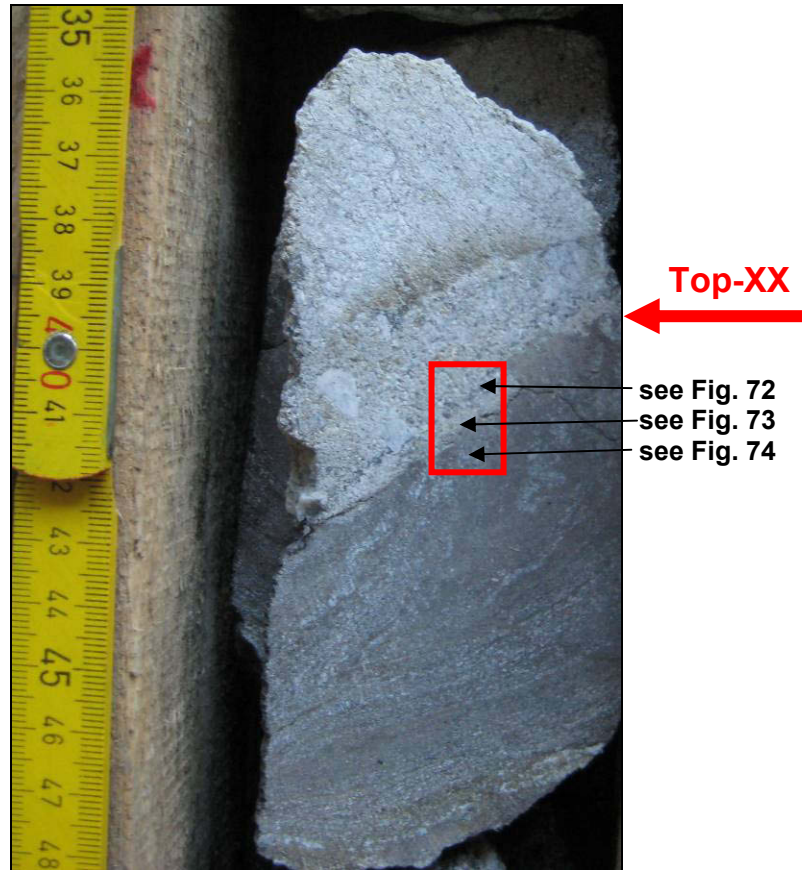
Fig. 71: Core photo of the top of the crystalline basement of MLRT-003C

Eocene of MLRT-003C consists of quartzitic sandstones with strongly elongated polycrystalline quartz grains. Furthermore, mica is present (e.g. muscovite/sericite and biotite), see Fig. 72.
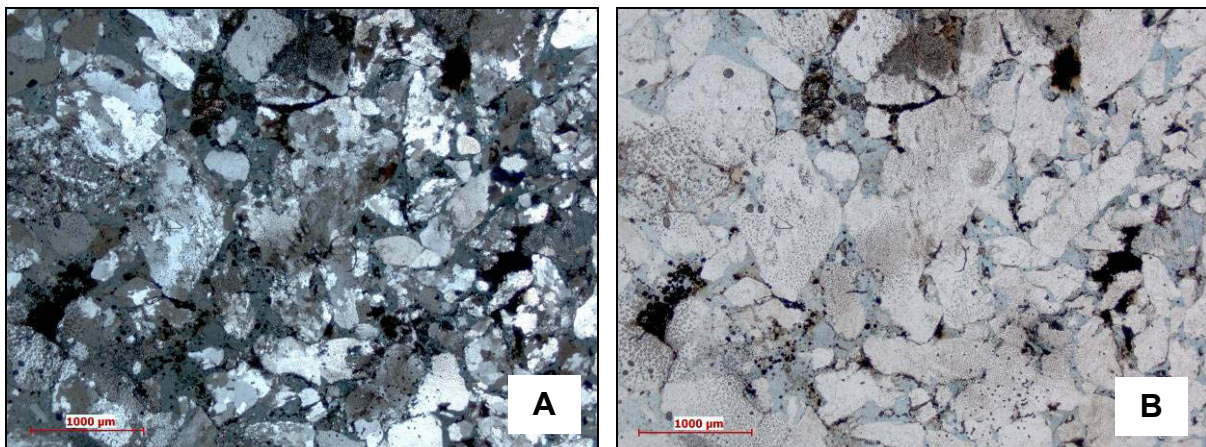
Fig. 72: Microphoto of MLRT-003C: Eocene sandstone;
Porosity is highlighted by blue-coloured resin used for thin section preparation.
(A= cross-polarizer image, B= cross-polarizer image)

Fig. 73 illustrates the sharp boundary (red line) between Eocene sandstones and the crystalline basement.
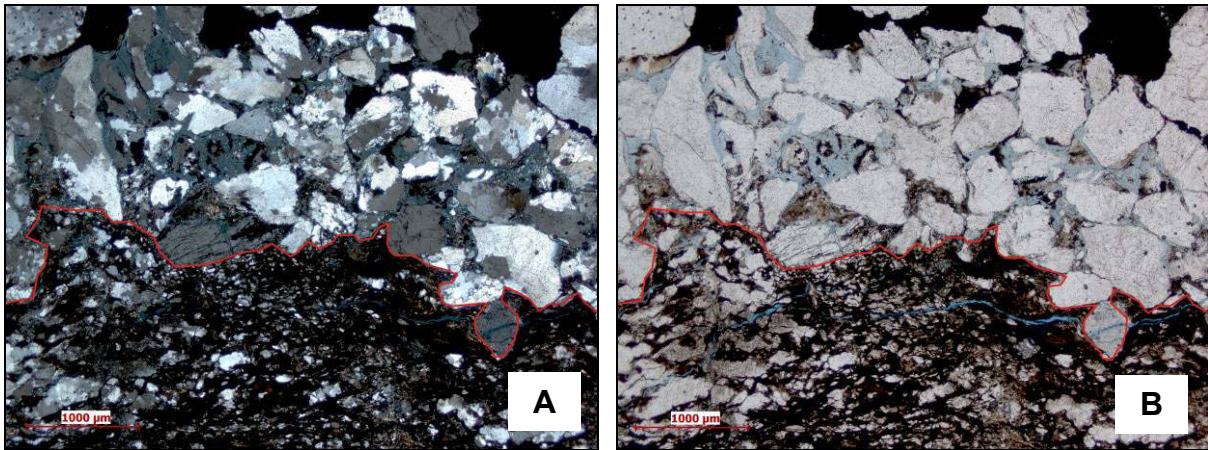
Fig. 73: Microphoto of MLRT-003C: Top of the crystalline basement = red boundary
(A= cross-polarizer image, B= plane-polarizer image)

The crystalline basement of MLRT-003C is formed by weathered gneiss with migmatitic structures (Fig. 74), which predominantely appear at the top of the formation. Small quartz grains are present. In contrast, feldspar is missing, probably due to dissolution.
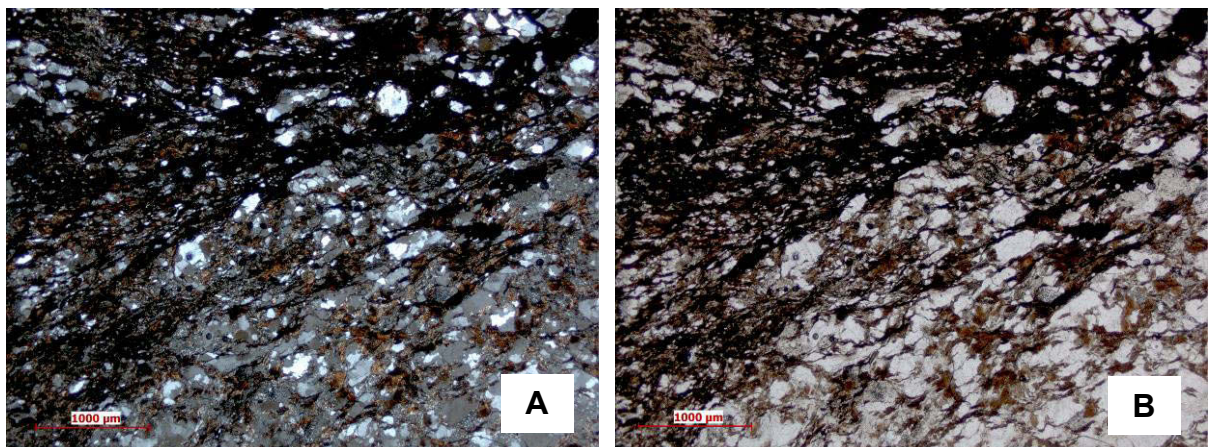
Fig. 74: Microphoto of MLRT-003C: Crystalline basement (gneiss with migmatitic structures)
(A= cross-polarizer image, B= plane-polarizer image)

Log analysis:

According to OMV core report Top-XX is defined at a depth of 3,613.38 m (see Fig. 75).
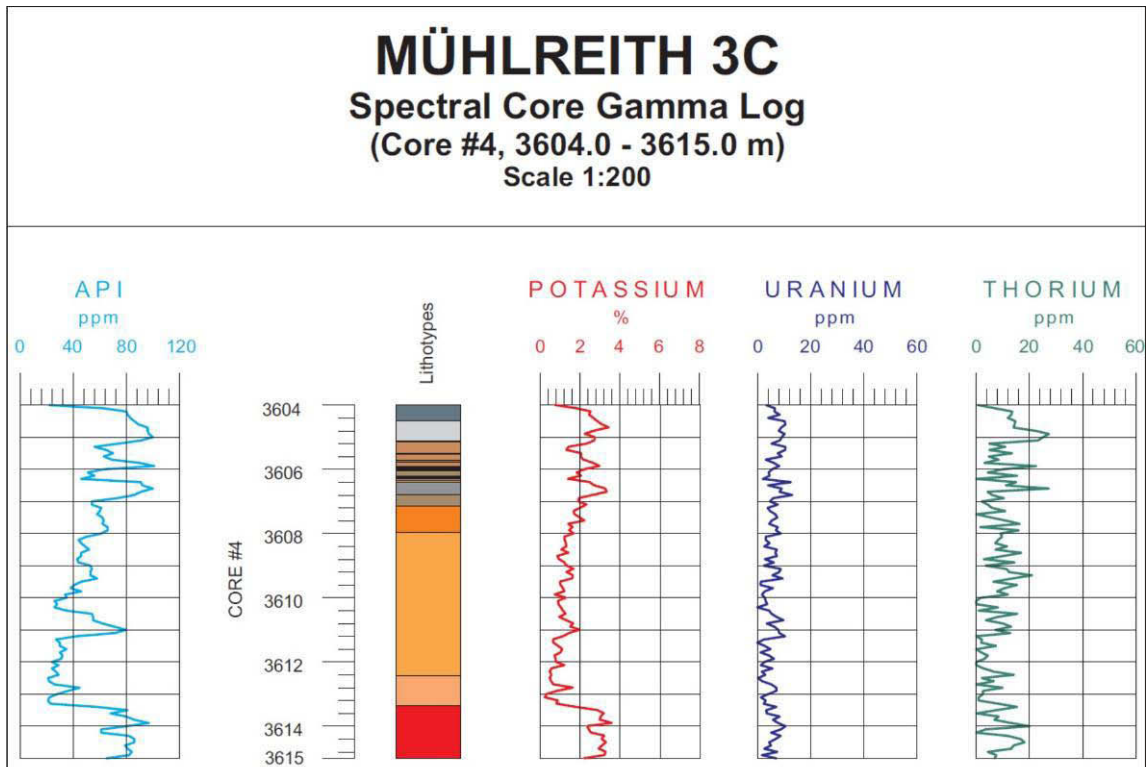
Fig. 75: OMV Core-GR log of well MLRT-003C;
The red block represents the crystalline basement in core no. 4.

Fig. 76 shows the comparison of OMV Core-GR and well log GR of MLRT-003C. Both curves show a good fit indicating that there is no core-to-log shift for the top of the crystalline basement. However, the fit is poor in the uppermost part of the core. This indicates that part of the core loss (< 1 m) occurred near the top of the core in the Eocene succession. Considering that the total core loss is about 2 m, it is evident that core loss also occurred in the crystalline basement.

Because of the latter (and because the depth of the lowermost box no. 1 was equated with the base of the core at 3,622 m), the top of the crystalline basement identified during core analysis in the Pettenbach core store ("Pettenbach" Core: 3,615.40 m) is significantly deeper than the well log depth (Table 11).
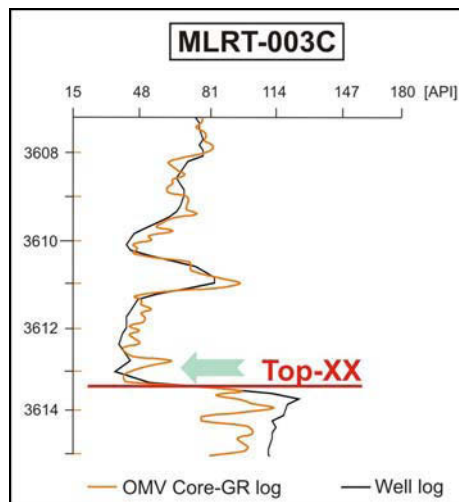
Fig. 76: Comparison of OMV Core-GR and well log GR of MLRT-003C

Table 11 provides a summary of depths of Top-XX and marks the difference between "Pettenbach" Core and "OMV" core or log depth visible. As explained before, this may be the result of core loss within Eocene and to some extent also within crystalline basement. Furthermore, starting to log from the bottom of the core upwards also affects the depth of Top-XX.

	Depth of Top-XX [m]
"OMV" Core	3,613.38
"Pettenbach" Core	3,615.40
Log Depth (= Completion Log)	3,613.38

Table 11: Depth of top of the crystalline basement (Top-XX) of MLRT-003C

The OMV Spectral Core-GR log of well MLRT-003C is represented in Fig. 77. The concentrations of potassium, thorium and uranium show that total GR is mainly controlled by variations in the potassium content. In contrast, thorium contents do not show a significant trend and also uranium contents only displays weak trends.

Potassium content is decreasing within Eocene and indicates a strong increase at Top-XX (3,613.38 m). Within crystalline basement the content of potassium is relatively high compared to the Eocene section.
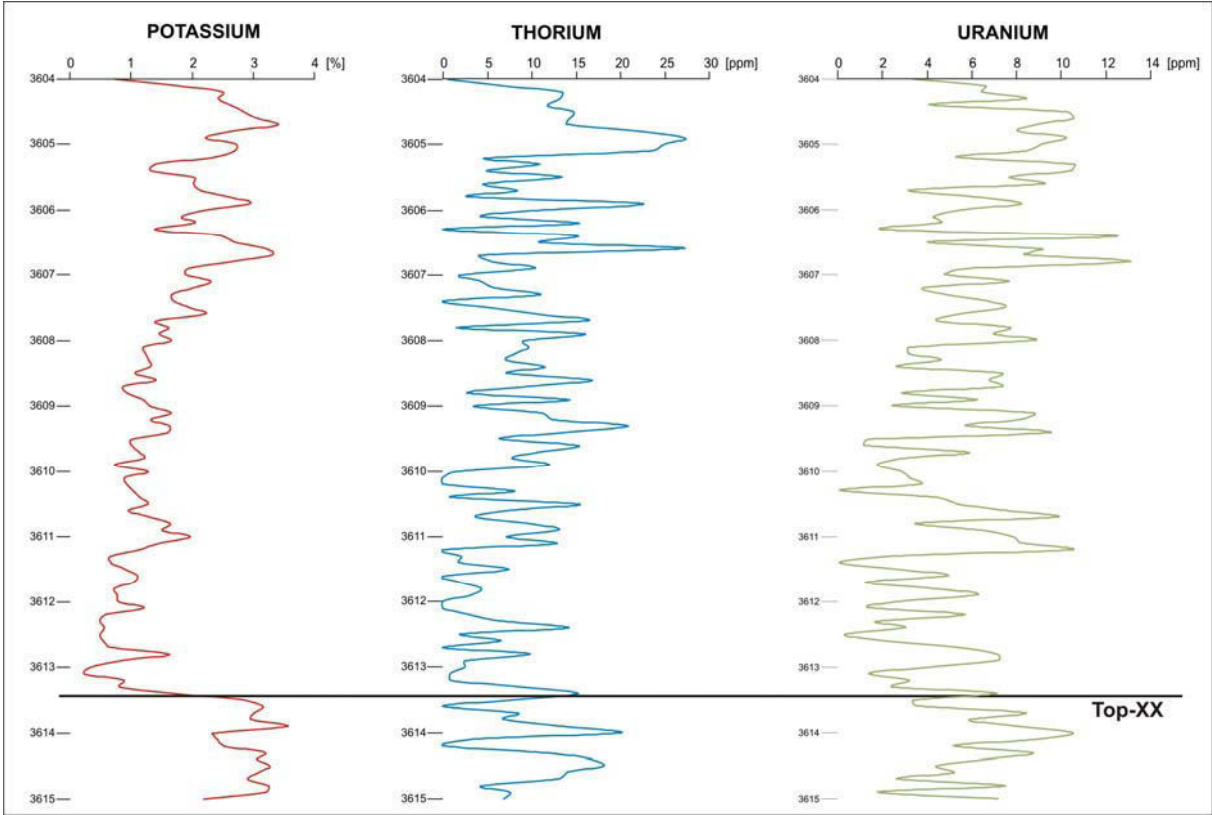
Fig. 77: OMV Spectral Core-GR of well MLRT-003C

Well logs available from MLRT-003C are displayed in Fig. 78. Only GR and (with limitations) the resistivity logs can be used to define Top-XX at a depth of 3,613.38 m. In this case, also SP log trends show a break at Top-XX and behave similar to the GR log. At Top-XX, GR is 74.67 API (compared to about 85 API within the crystalline), whereas SP shows 105.37 mV, which is displayed on top of the logs.

The caliper log displays a nearly perfect borehole with a bit size of 6.125 inch, which does not show any trend at Top-XX. NPOR exhibits a slight increase at Top-XX, but this trend is too weak for a reliable definition of Top-XX.

All resistivity logs show an increase in resistivity near the base Eocene and a nearly steady trend across Top-XX. Density and PEFZ logs are both increasing within the area of Top-XX, but are not useful for a identifying the boundary between Eocene and crystalline basement.

In contrast to the other wells, a FMI log has been measured for well MLRT-003C. According to the interpretation of Schlumberger (2008), the FMI log shows more or less horizontal layering within Eocene sediments. Furthermore, highly resistive, but also extremely fractured gneiss represents the crystalline basement.
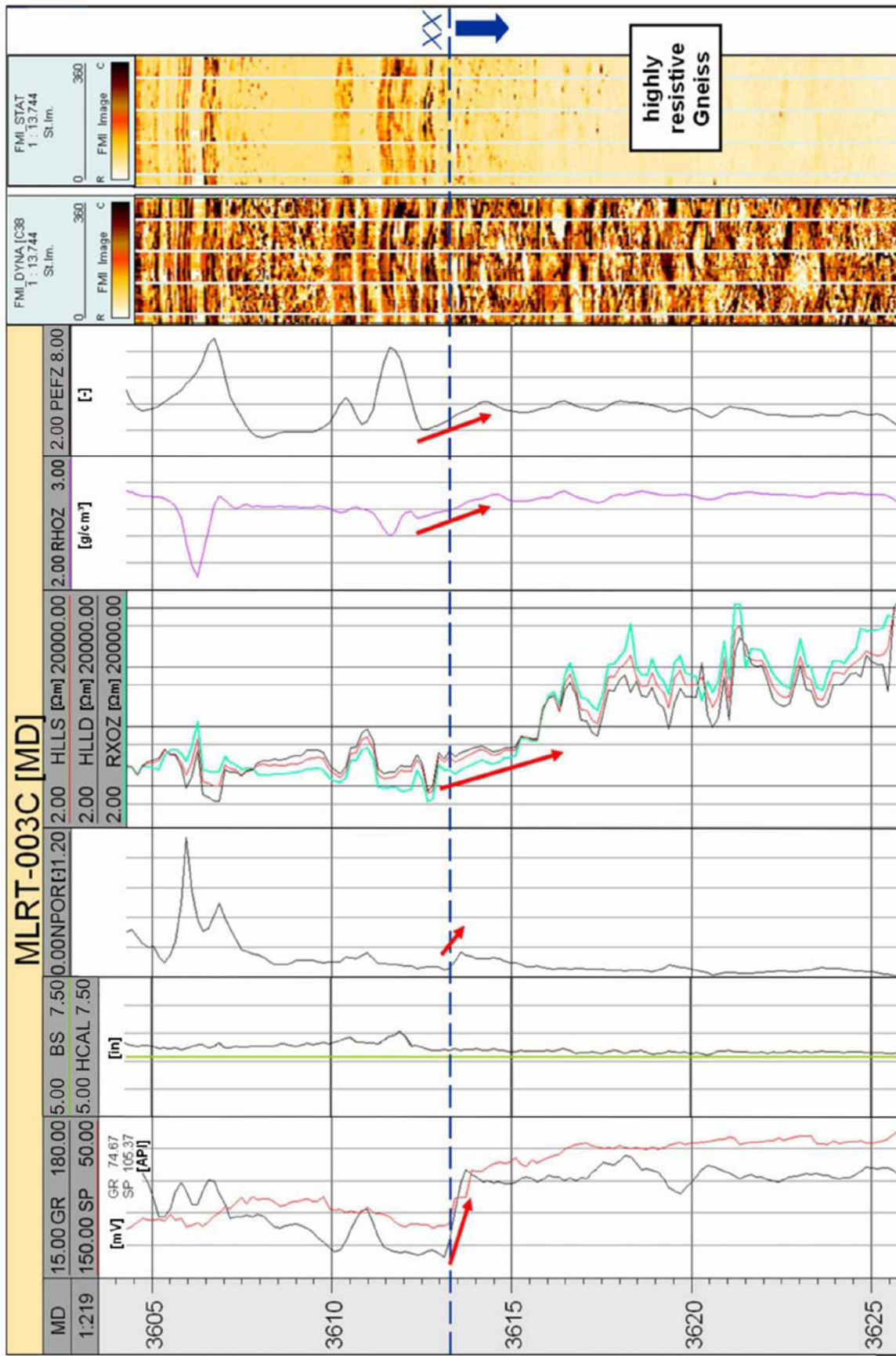
Fig. 78: Correlation of well logs of MLRT-003C; dashed blue line indicates Top-XX;

According to the FMI interpretation of Schlumberger, Top-XX is defined at a depth of 3,616 m. However, regarding the results of core inspection, this is clearly too deep.

Whereas, the value of the FMI log to define the top of the crystalline basement is clearly limited, FMI borehole images can be used for structural analysis.

According to Fig. 79, conductive fractures (displayed in blue) are present within the crystalline basement. They are related to syn-sedimentary faults, show low (few degree) to very high dip angles (90°) and two major strike directions:
- NNE-SSW
- E-W
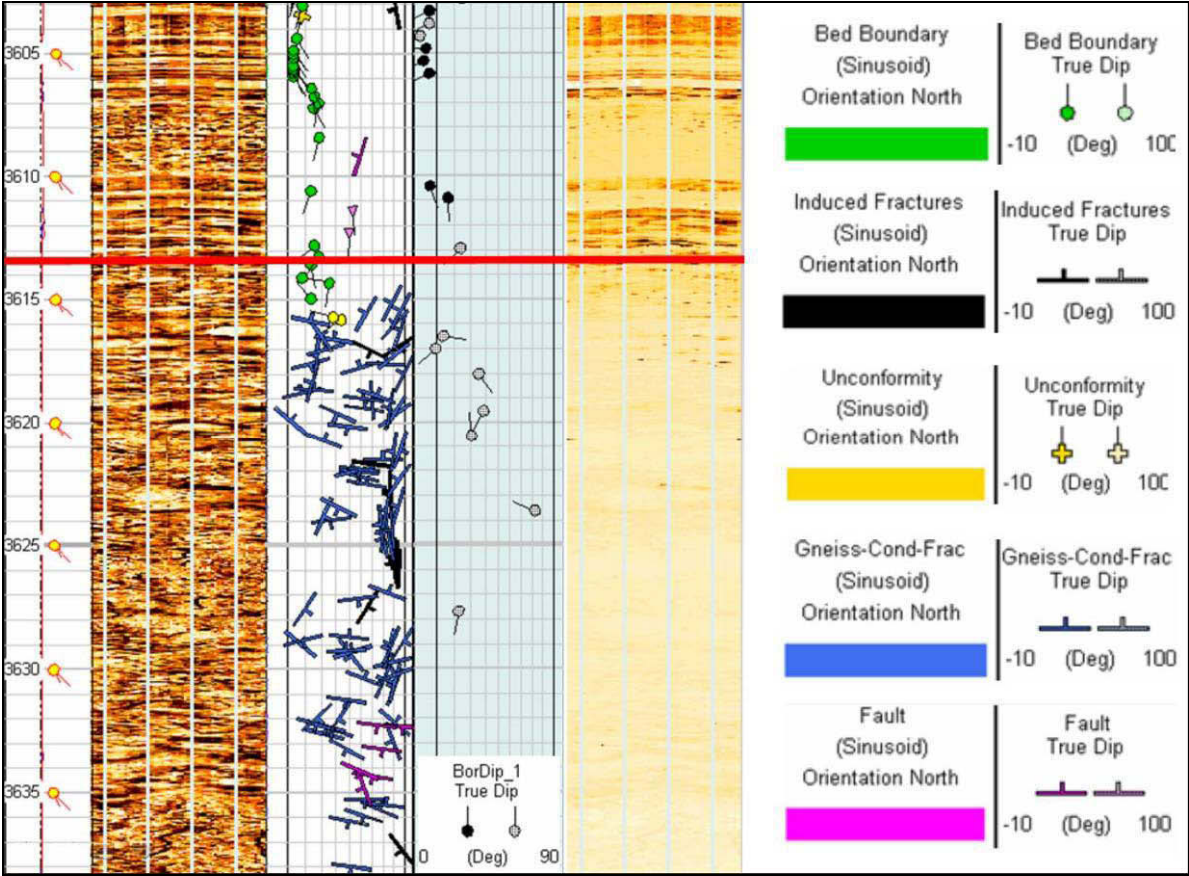
Fig. 79: FMI log interpretation of well MLRT-003C

Fig. 80 shows FMI log interpretations concerning stress analysis and fractures. The crystalline basement is highly fractured, including drilling-induced fractures (black arrows). From the orientation of drilling-induced fractures it can be concluded that the maximal horizontal stress is NNW-SSE directed. Additionally, fractures forming a "petal" shape are visible.
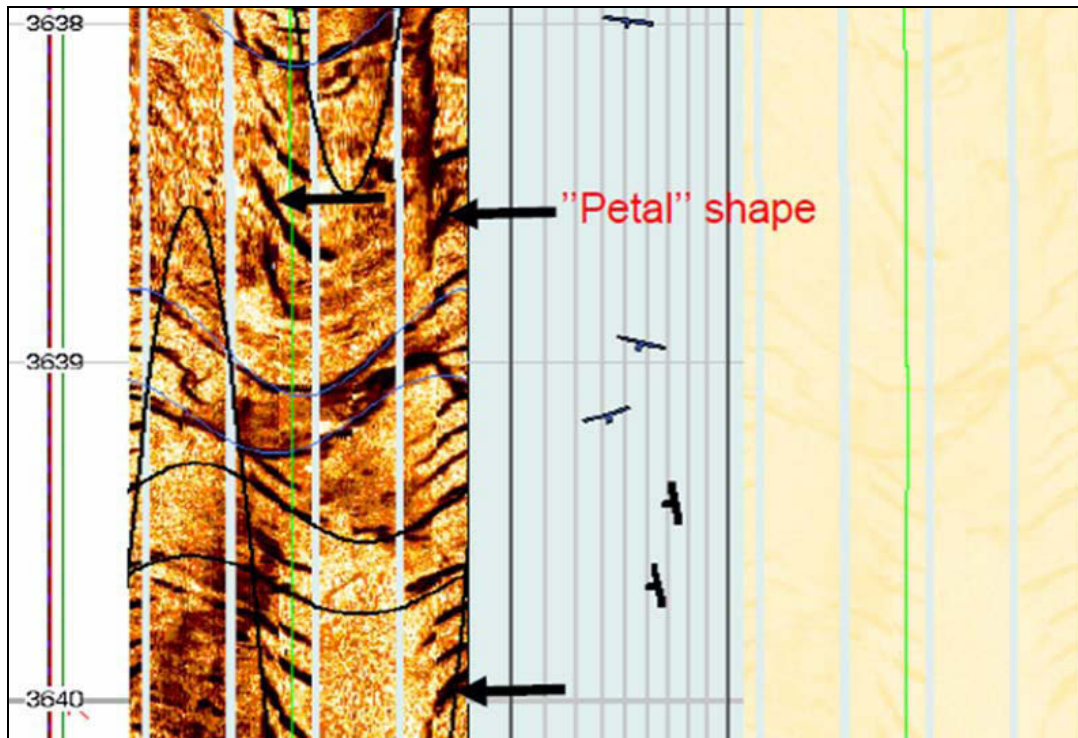
Fig. 80: Fractures within crystalline basement of well MLRT-003C

The completion log of well MLRT-003C is displayed by Fig. 81. Top-XX is defined at 3,613.40 m, which agrees fairly well with Top-XX according to core inspection and core to well log correlation (3,613.38 m depth).
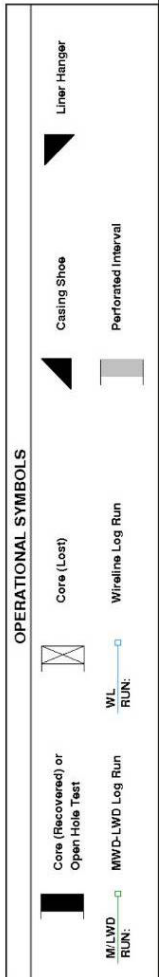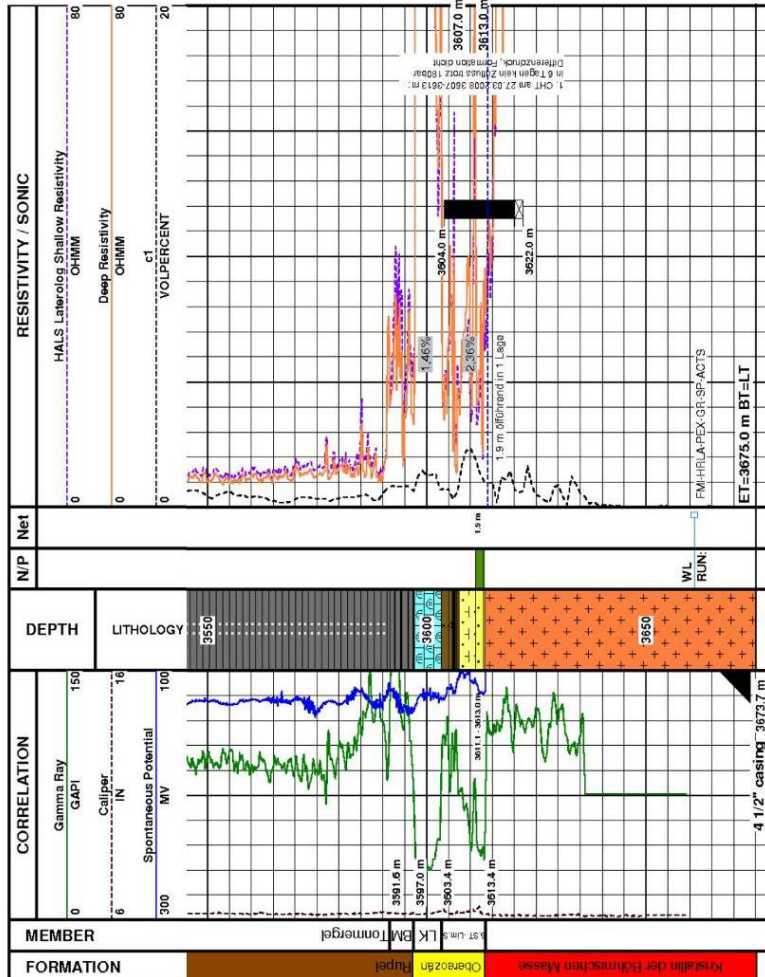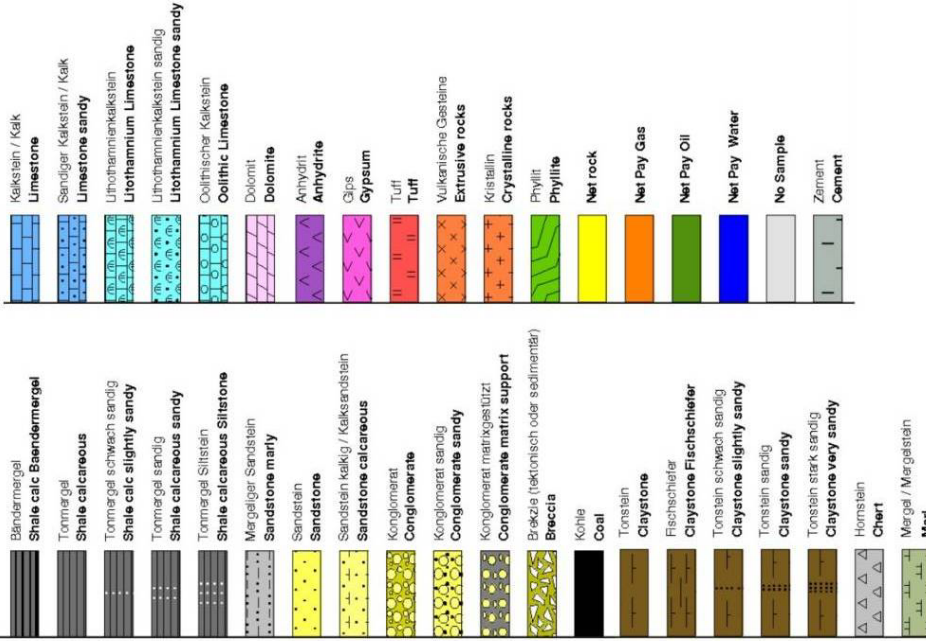
Fig. 81: Completion log of well MLRT-003C

INTERPRETATION

The crystalline basement in well HIER-002A consists of coarse granite, whereas it consists of gneiss with migmatitic structures in well MLRT-003C. The difference in basement lithology strongly influences the log patterns. Therefore, different log trends occur across the top of the crystalline basement depending on whether the Eocene sediments are underlain by magmatic or metamorphic rocks (Table 12).

Obviously there are only few logs, which show similar, but weak trends. Therefore they are not useful for a reliable interpretation of Top-XX. However, porosity, density and PEFZ log of both wells are increasing at Top-XX. Sonic log indicates a decrease within well HIER-002A, but as this measurement is missing for MLRT-003C, no meaningful conclusion can be drawn.

	HIER-002A	*MLRT-003C*
GR (log)	⬇	⬆
CGR	⬇	⬆
HLLS/HLLD	⬇ (weak, below: increase)	⬆
HCAL	⬆	=
DT	🔻	---
NPHI	🔼	NPOR: 🔼 (weak)
RHOZ	🔼	🔼 (weak)
PEFZ	🔼 (weak)	🔼 (weak)

Table 12: Comparison of log trends of wells HIER-002A and MLRT-003C; Logs, which show similar trends in both boreholes are highlighted by coloured arrows (red= values decrease, green= values increase).

All other logs do not have similar trends for both wells and are therefore not useful. Even GR log shows opposite trends, as highlighted in Fig. 82. The graph on the left illustrates GR log of HIER-002A, which decreases.

In difference to other wells studied, the GR values in well MLRT-003C (right graph) decrease downwards within the lowermost 8 m of the sedimentary succession and increase sharply at the top of the crystalline basement. Within the gneiss, GR values remain constantly high with approximately 80 API. Obviously, this is an effect of the different types of crystalline rocks within the wells.
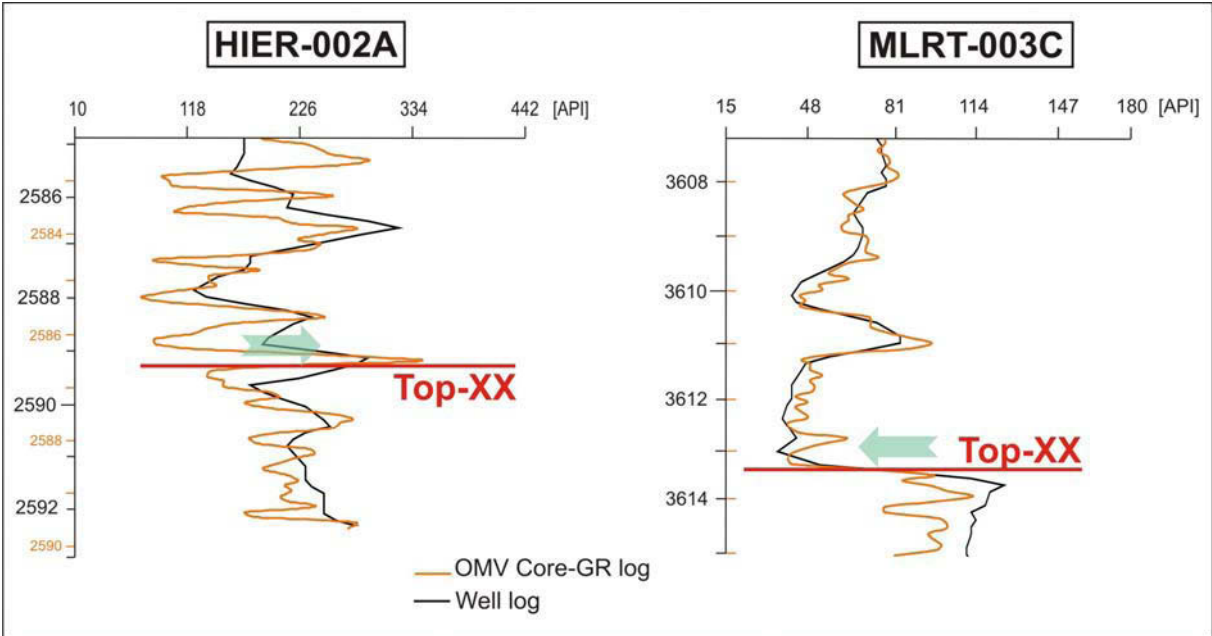
Fig. 82: Different trends of GR log at top of the crystalline basement

5.3 Wells with Jurassic sediments overlying Top-XX

KH-003

Core analysis:

Top-XX has been recovered by core no. 4 (3,127.85 to 3,144 m based on core inspections; core diameter: 10 cm; core recovery: 15 m). According to the core recovery, a significant core loss is indicated. Top-XX is illustrated in the core data sheet of Fig. 83 (core no. 4, box no. 1, from 3,143 to 3,144 m depth).

Fig. 83: Core data sheet with top of the crystalline basement of KH-003

Fig. 84 represents part of the RAG core report of 1983 with Top-XX defined at a depth of 3,142.90 m, showing a slight difference to the results of core analysis above (Fig. 83) and log data.
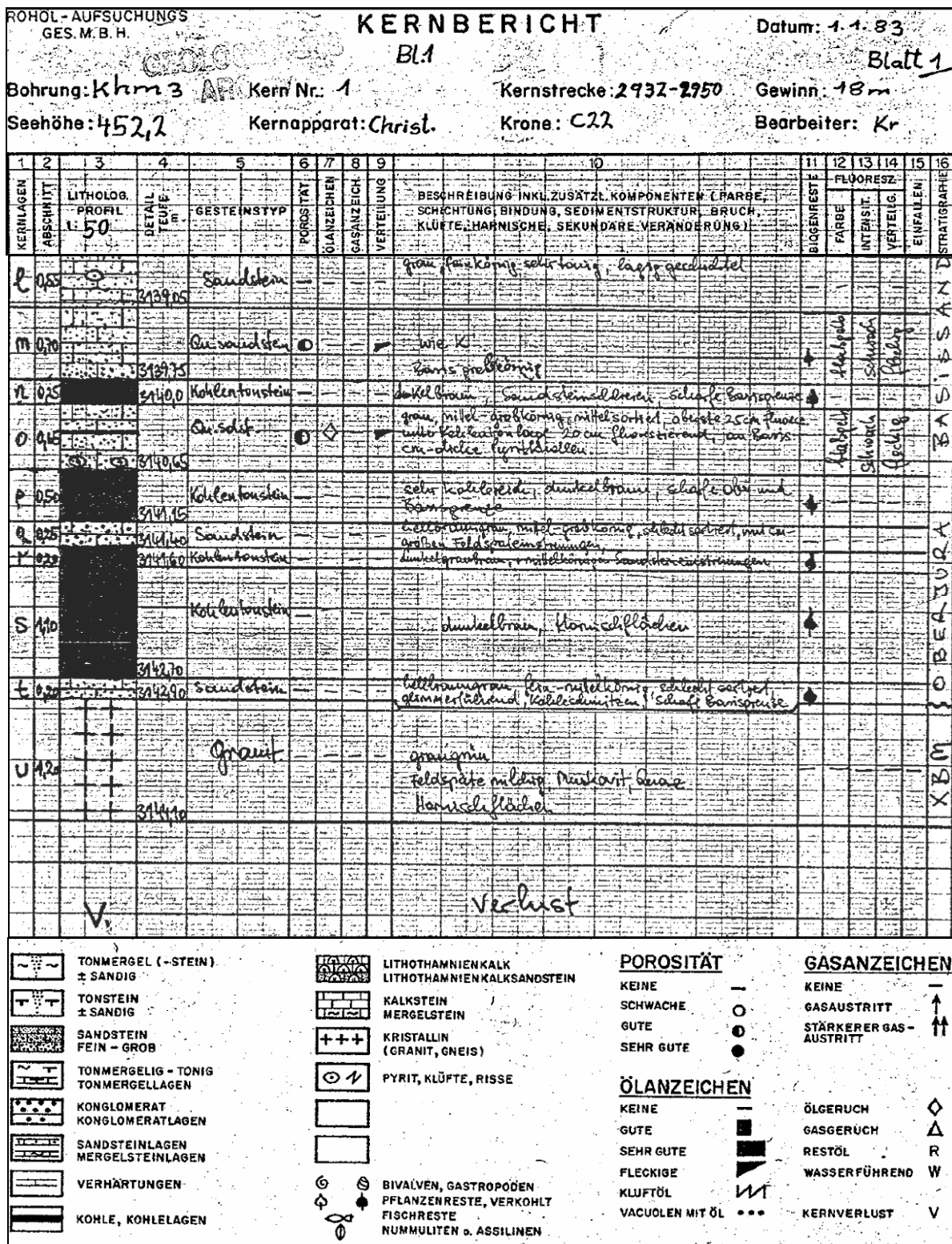

Fig. 84: RAG core report (1983) of well KH-003

Top-XX in well KH-003 is neither easily recognizable at the core data sheet, nor at the core photo (Fig. 85). However, thin sections are a good method to fix the boundary between Jurassic sandstone and underlying crystalline basement at a depth of 3,143.10 m. Unfortunately the crystalline rocks in well KH-003 are not represented by a long core section, which causes unuseful trends within the crystalline basement.

Fig. 85: Core photo of top of the crystalline basement of KH-003

Fig. 86 displays the poorly sorted Jurassic sandstone of well KH-003. As a result of weathering lithology appears as "greywacke-like" sandstone. The main components are quartz grains with some mica (predominantely muscovite). A combination of phyllosilicates and a fine-grained quartz-feldspar mass forms the matrix. Blue-coloured resin used for thin section preparation facilitates identifying open pore space.
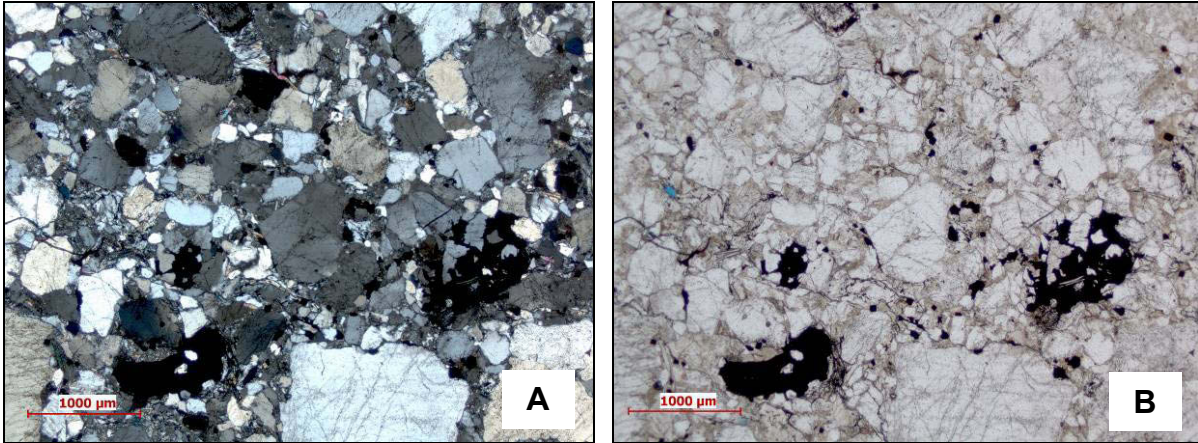
Fig. 86: Microphoto of KH-003: Jurassic sandstone
(A= cross-polarizer image, B= plane-polarizer image)

Top-XX can be identified based on Fig. 87 and is graphically displayed as a red line. As in thin sections of the wells before, also in this case the change in lithology is clearly visible.
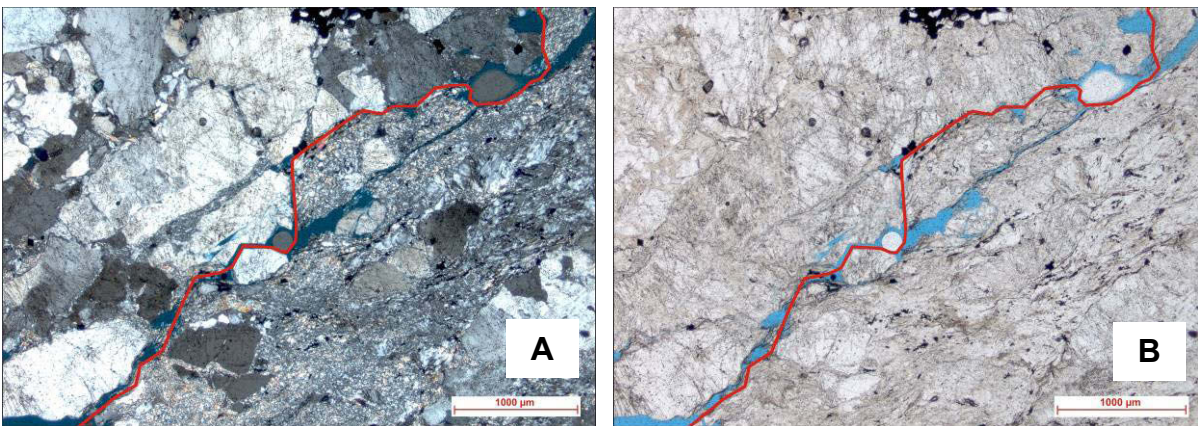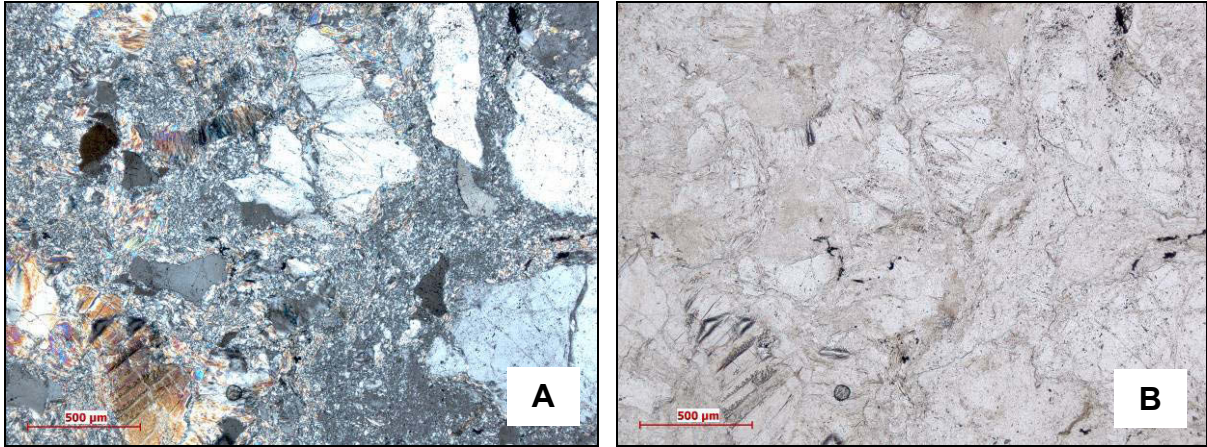

Fig. 87: Microphoto of KH-003: Top of the crystalline basement = red boundary;
Blue-coloured phases represent the resin used for thin section preparation.
(A= cross-polarizer image, B= plane-polarizer image)

According to the core report of OMV, the crystalline basement of well KH-003 can be characterized as extremely weathered granite (Fig. 88). Feldspars are totally dissolved and may appear in relics as chlorite and sericite. Quartz grains are partly broken and embedded in a phyllosilicatic-chloritic matrix.

Fig. 88: Microphoto of KH-003: Crystalline basement (granite)
(A= cross-polarizer image, B= plane-polarizer image)

Log analysis:

Fig. 89 illustrates the comparison of well log and Core-GR log measured with GF Instruments Gamma Surveyor with Top-XX at a depth of 3,143.10 m. The crystalline basement of well KH-003 consists of granite and GR log shows a peak at base Jurassic. This trend also occurres in wells with magmatic rocks as crystalline basement, for example BH-N-001, BH-N-002 and HIER-002A.

However, both GR measurements show a very good fit and actually there is no core-to-log shift. The GR scale is derived from the well log.
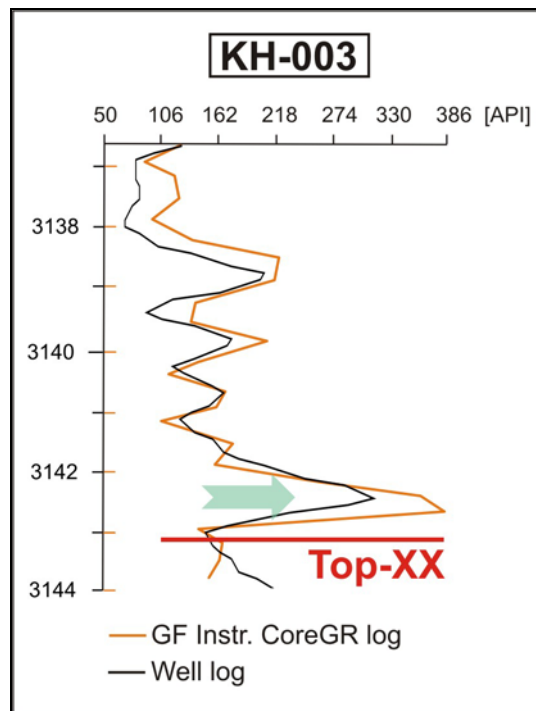

Fig. 89: Comparison KH-003 well log and Core-GR
measured with GF Instruments Gamma Surveyor

As there is no core-to-log shift and Core-GR was measured directly with the tool of GF Instruments, Top-XX is defined at 3,143.10 m.

	Depth of Top-XX [m]
GF Instr. CoreGR	3,143.10
"Pettenbach" Core	3,143.10
Log Depth	3,143.10

Table 13: Summary of depth of top of the crystalline basement for well KH-003

The Spectral Core-GR measured by GF Instruments Gamma Surveyor with Top-XX at 3,143.10 m is illustrated by Fig. 90. Dots on the measured curves are representing measuring points. High contents of uranium and thorium at base Jurassic may be related to the presence of heavy minerals and are dominating total GR. The slight increase of potassium content at Top-XX is immediately followed by a decrease and therefore does not show a clear trend.
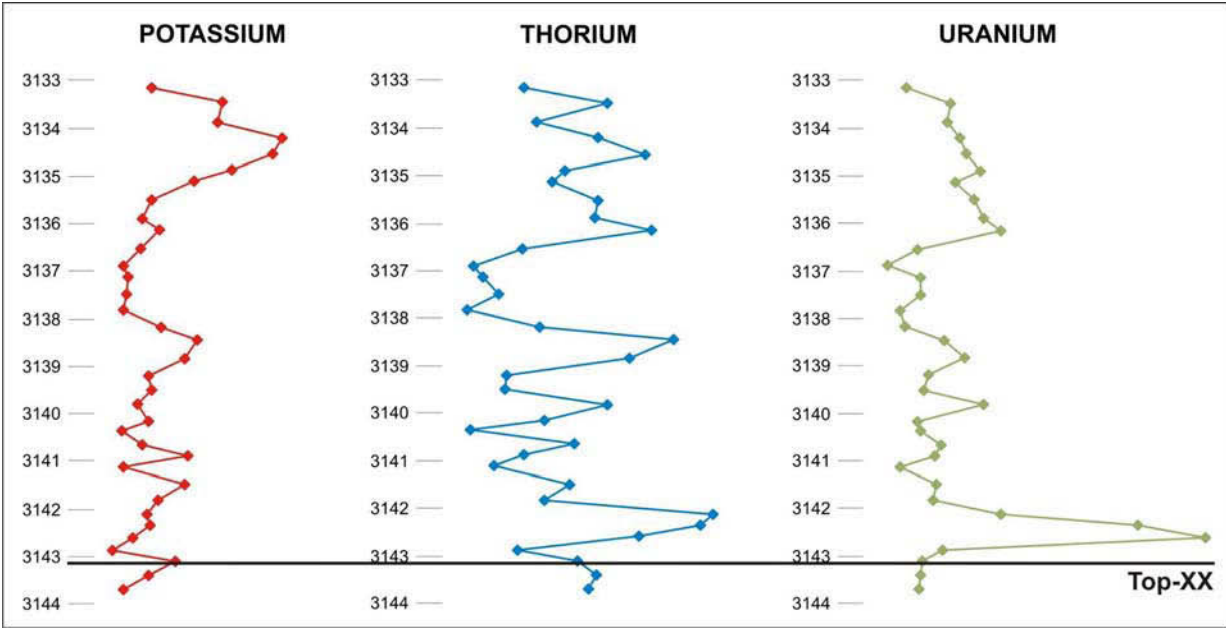

Fig. 90: Spectral Core-GR of well KH-003 measured with GF Instruments Gamma Surveyor

The logs available of well KH-003 are displayed by Fig. 91 with Top-XX at 3,143.10 m. All logs show changes at Top-XX, although GR log illustrates the most significant trend with high GR at the lowermost part of Jurassic followed by a strong decrease downwards to Top-XX. As mentioned, total GR log is dominated by high contents of thorium and uranium. At Top-XX, GR has a value of 194.92 API, whereas SP is 30.40 mV, which is displayed on top of the logs.

SP log is no reliable tool for the definition of Top-XX. This may be again affected by drilling mud and does not show a significant trend.

The bit size (BS) of 8.5 inch is illustrated as green line and makes it easier to interpret the caliper log. At base Jurassic, caliper log indicates a possible breakout, whereas apart from that it seems that some mud cake accumulated.

Sonic log is decreasing downwards to Top-XX and shows steady values of approximately 60 µs/ft within the crystalline basement. Low values of transit time correspond to high velocity, which is typical for hard material, as it is represented by granite of KH-003.

Within the uppermost section of the crystalline, resistivity logs shallow (LLS) and deep (LLD) indicate increasing values. The Microspherically Focused Log (MSFL) shows a significant increase of resistivity at Top-XX with unchanging high values within the crystalline.
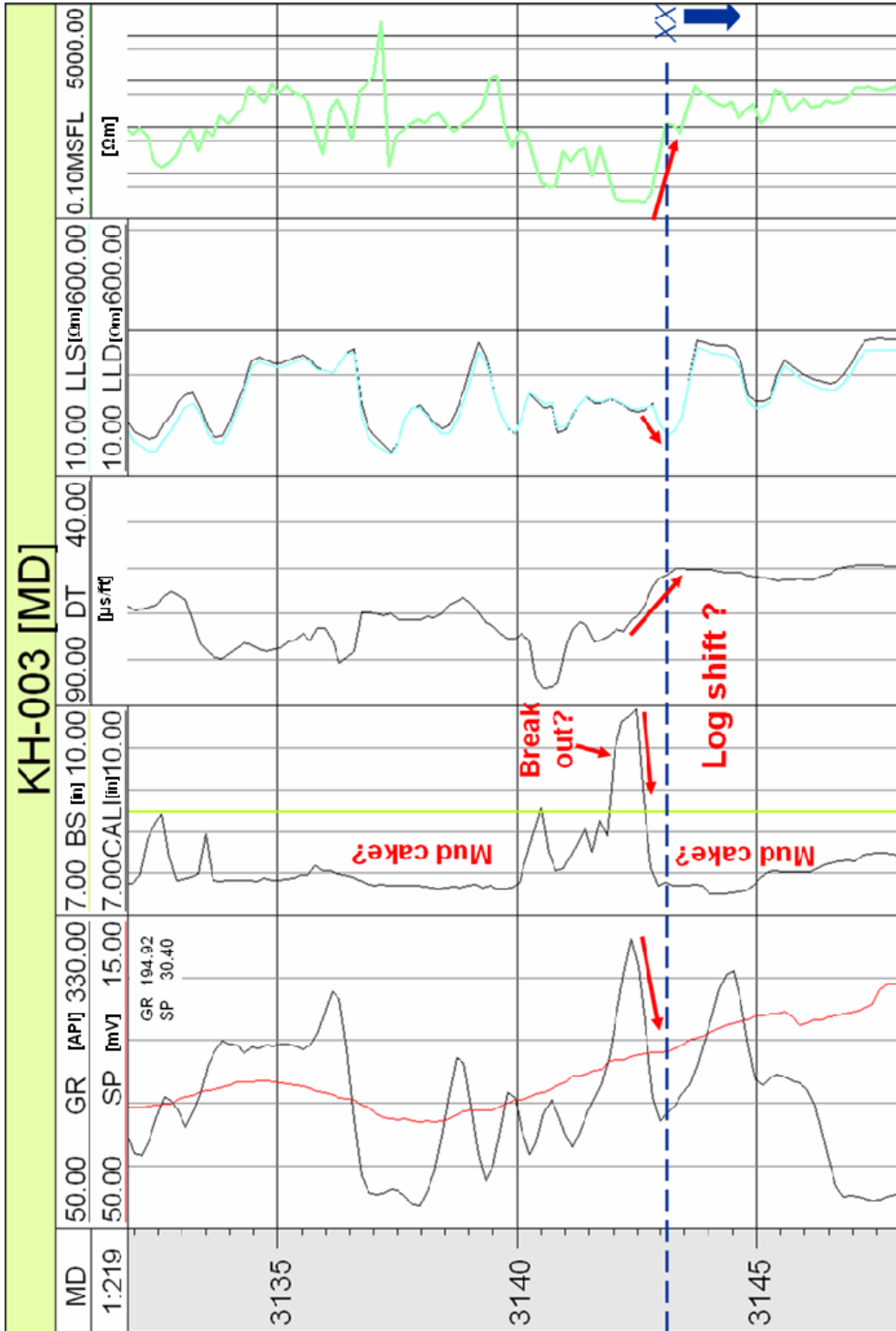
Fig. 91: Well logs of well KH-003 with top of the crystalline basement (Top-XX = dashed blue line); The values of GR and SP at Top-XX are displayed at the top of the logs (194.92 API, 30.40 mV).

The completion log of well KH-003 is illustrated below (Fig. 92). It shows a slightly different depth of Top-XX (3,143.40 m).
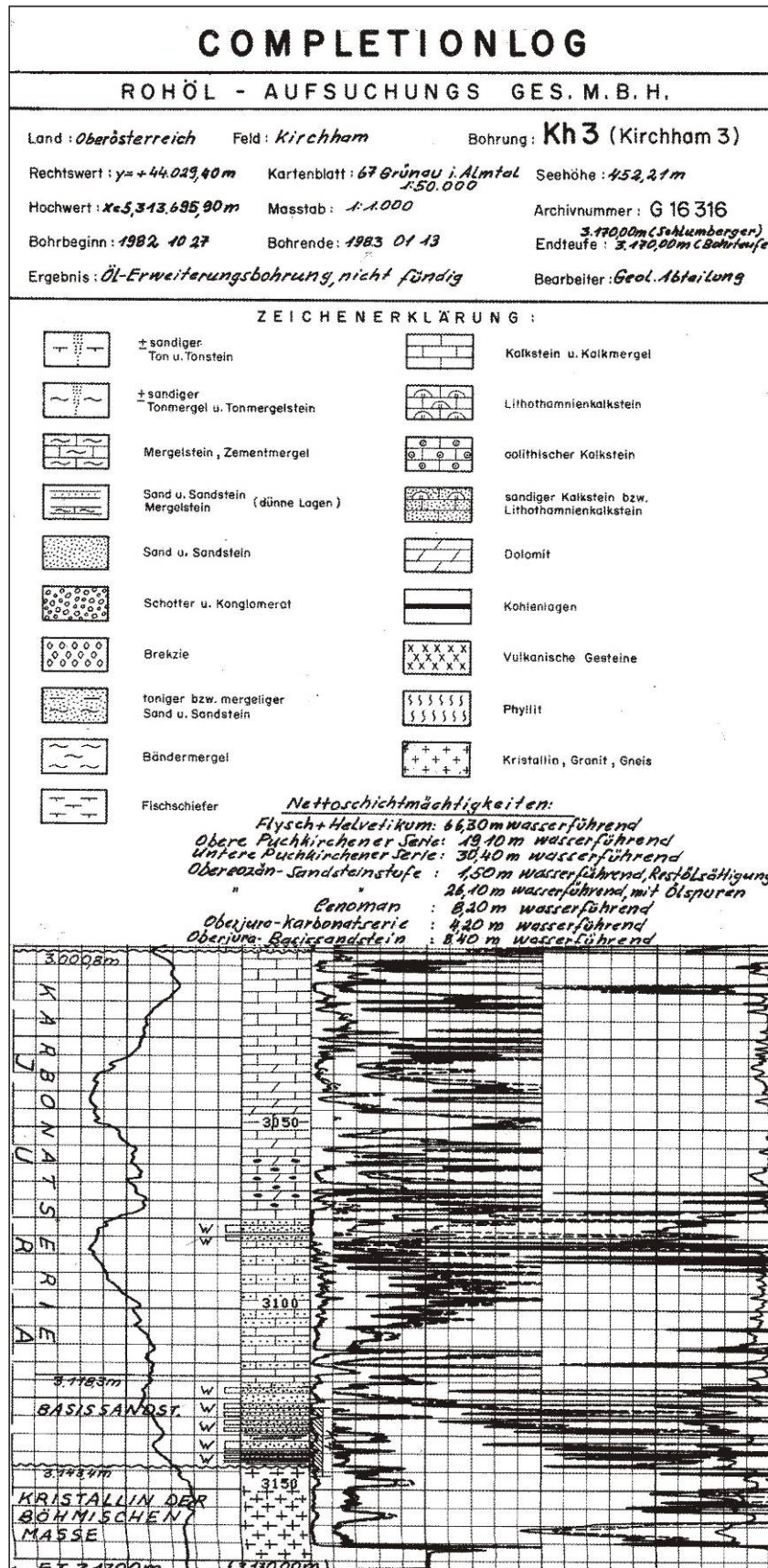

Fig. 92: Completion log of well KH-003

V-037

Core analysis:

According to core reports of RAG, Top-XX of well V-037 should be at a depth of 2,182.5 m. However, this is questionable. Based on the effects of partial recrystallisation and intensive weathering RAG personnel assumes that the grains within a migmatitic gneiss need not show any orientation.

However, the following results suggest, that the crystalline basement is not existent in cores of well V-037.

According to RAG core reports, Top-XX has been recovered by core no. 4 (2,170.5 to 2,187.5 m; core diameter: 10 cm; core recovery: 17 m). RAG defined Top-XX at 2,182.5 m, which is illustrated in the core data sheet of Fig. 93 (core no. 4, box no. 5, from 2,182.5 to 2,183.5 m depth).

Fig. 93: Core data sheet of well V-037 ranging from 2,182.5 to 2,183.5 m (box no. 5)

Part of the RAG core report of 1981 with Top-XX defined at a depth of 2,182.50 m, is represented by Fig. 94.
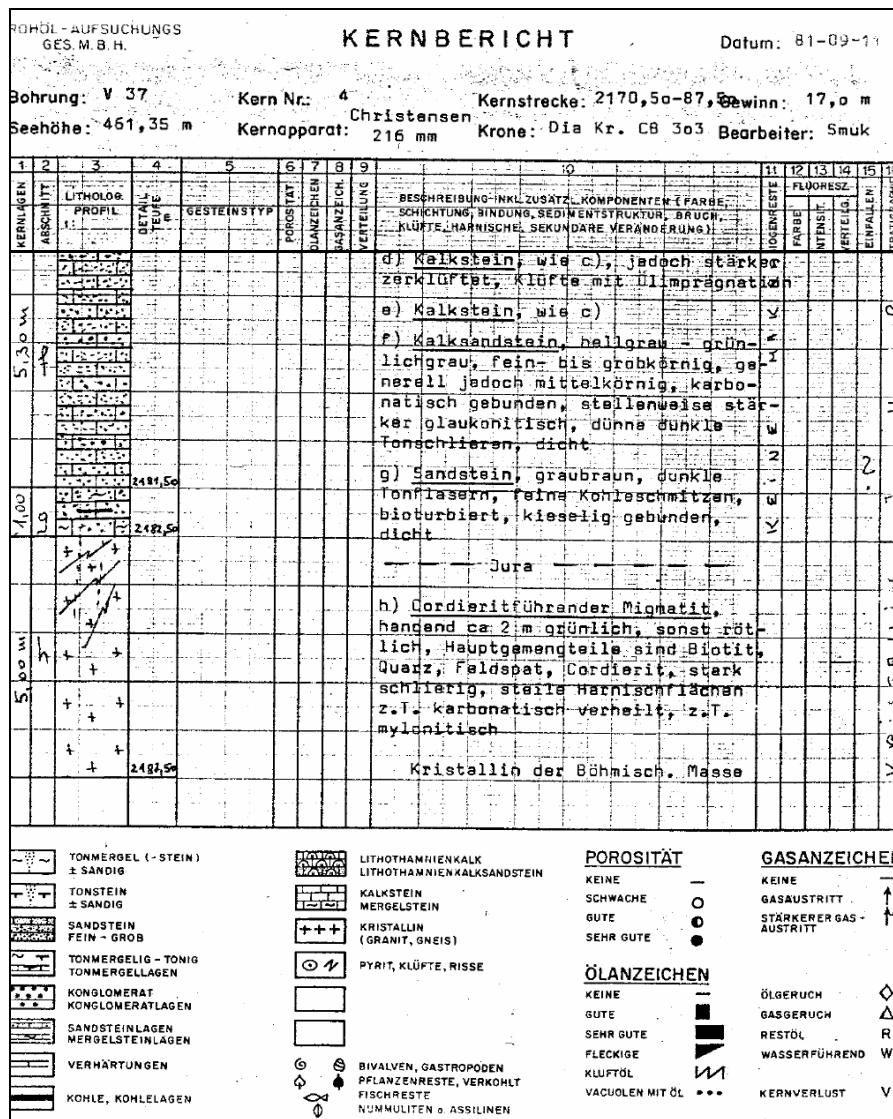
Fig. 94: Part of RAG core report of well V-037

Fig. 95 illustrates the interval of core no. 4 of well V-037 between 2,181.5 and 2,187.5 m depth. It shows the positions of the five thin sections preparated. The core is extremely fractured and affected by weathering. Between 2,181.5 and 2.182.5 m, the core is swelling. This could be the effect of weathered coaly layers.

Lithology changes along the 6 m long interval and shows greenish-grey and dark red colours in the lowermost part. Additionally, grain size increases downwards.

Fig. 95: Photo of core of well V-037 ranging from 2,181.5 to 2,187.5 m;
The blue line (2,182.5 m) represents Top-XX defined by RAG core report,
whereas the green line (2,183.8 m) shows Top-XX according to completion log.

Except thin section no. 4, all thin sections of well V-037 have been prepared with blue-coloured resin to highlight open pore space or rather visualize porosity. Additionally, thin sections no. 1 to 3 were prepared with ethylene glycol, as the core samples interacted with water.

Thin section no. 1 (Fig. 96) represents a core sample at a depth of 2,182.63 m. The very fine-grained and homogeneous mass visible possibly consists of chlorite and shows dark colours. Uniform distribution additionally enforces the assumption of a mudstone being displayed. Furthermore, opaque phases are present, which could

represent coaly remains. Unfortunately, because of the very small grain size a definite microscopic identification is impossible. In the RAG core report, this section is described as weathered cordierite-bearing migmatitic gneiss.
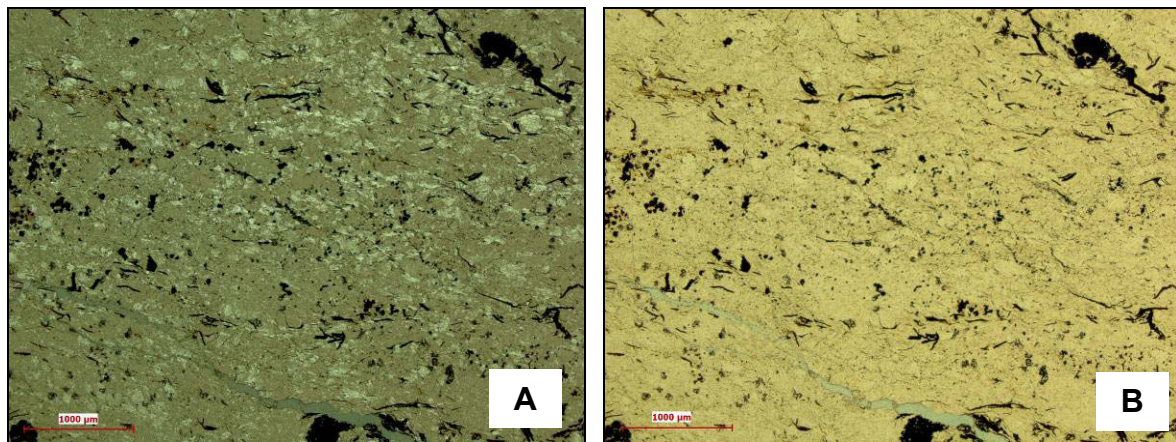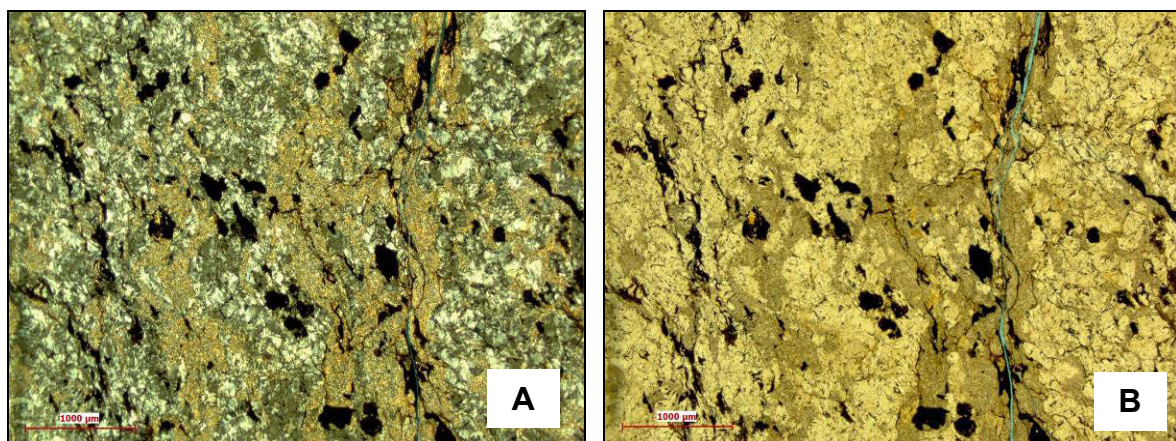

Fig. 96: Microphoto of V-037 (TS 1): ?Crystalline basement (cordierit-bearing migmatite) at a core depth of 2,182.63 m (A= cross-polarizer image, B= plane-polarizer image)

Fig. 97 shows again very fine-grained material of a depth of 2,183.27 m, consisting of phyllosilicates (?chlorite) and coaly opaque phases. Additionally, based on grain size and colour, 2 phases can be distinguished. The cross-polarizer image exhibits the more fine-grained, brown coloured phase, which seems to appear predominantely along fissures or fractures. This may be the evidence of fluids penetrating into the rock and resulting in alteration. The other phase appears to be not that fine-grained and has white to grey colours illustrated by cross-polarizer image. Each of the two phases described appears to be relatively homogeneous and may represent relicts or recrystallisation of muscovite, sericite or even illite.

Fig. 97: Microphoto of V-037 (TS 2): ?Crystalline basement (cordierit-bearing migmatite) at a core depth of 2,183.27 m (A= cross-polarizer image, B= plane-polarizer image)

As in thin section no. 2, also in thin section no. 3 (Fig. 98), the illustrations seem to show a kind of mudstone with sericite from a depth of 2,183.87 m. However, a definite identification based on microscopic analysis is not possible.

Again, influence of fluids along fractures is probable and therefore, two different phases appear. One phase is extremely fine-grained (upper part of thin section) compared to the other, but both are homogeneous. Additionally, opaque phases are visible. In general, there are no indications for deformation and based on all these facts, it is questionable, if the thin section represents crystalline basement.
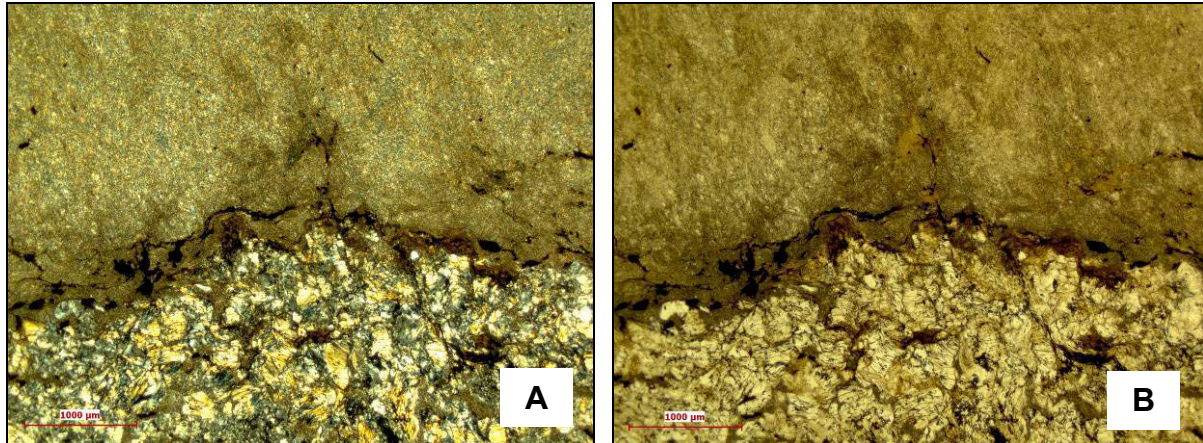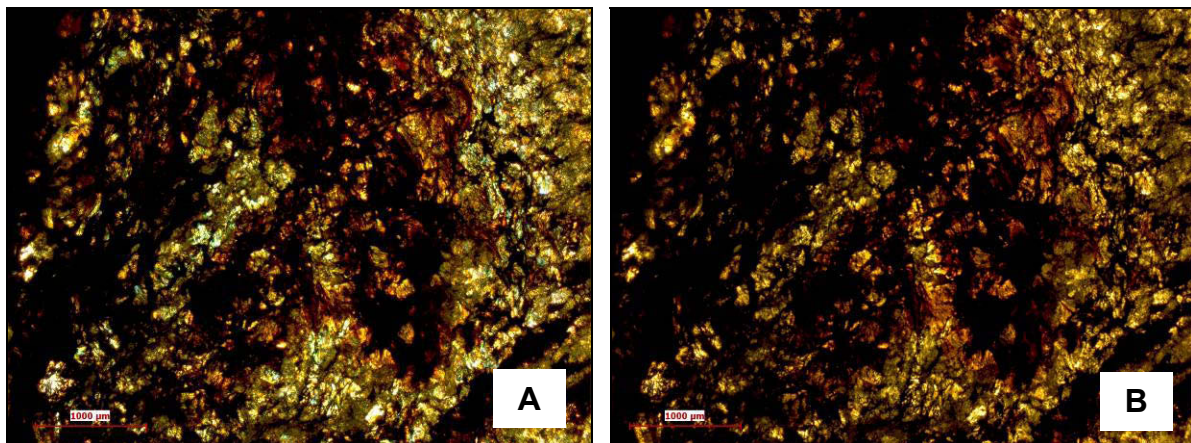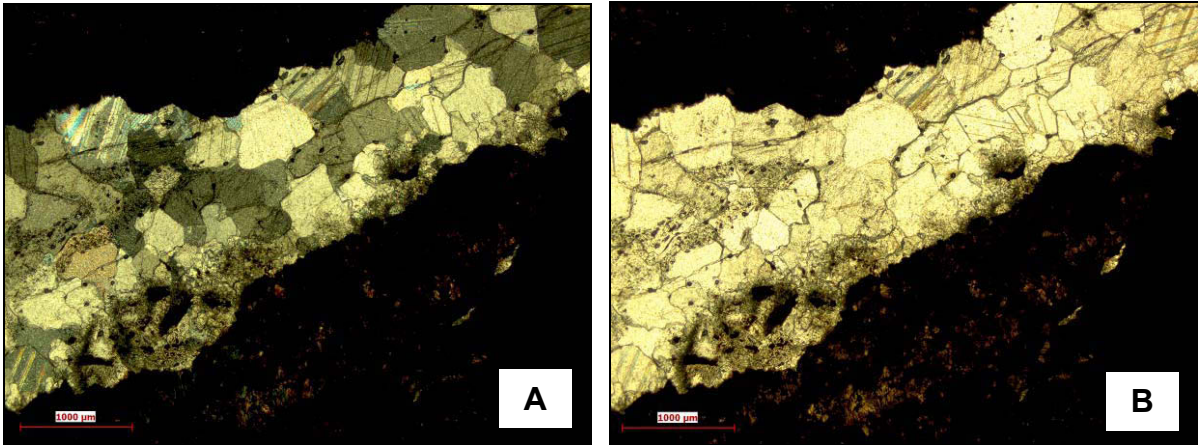

Fig. 98: Microphoto of V-037 (TS 3): ?Crystalline basement (cordierit-bearing migmatite) at a core depth of 2,183.87 m (A= cross-polarizer image, B= plane-polarizer image)

Based on good condition of the core sample, thin section no. 4 of a depth of 2,184.48 m has been prepared without synthetic resin. Fig. 99 shows dark brown material, which seems to be strongly influenced by weathering. Again, based on microscopic analysis a finite statement concerning the type of lithology present is not possible. It could be a kind of transition horizon with some chloritic phases.

Fig. 99: Microphoto of V-037 (TS 4): ?Crystalline basement (cordierit-bearing migmatite) at a core depth of 2,184.48 m (A= cross-polarizer image, B= plane-polarizer image)

Additionally, calcitic veins are existent within thin section no. 4 (Fig. 100). They can be easily identified by the angle of grain boundary, which typically is 120° for calcite. Furthermore, effects of calcitic twinning (lamellas) are visible in the cross-polarizer image (Fig. 100A).

Fig. 100: Microphoto of V-037 (TS 4): ?Crystalline basement (cordierit-bearing migmatite) with cc-vein at a core depth of 2,184.48 m (A= cross-polarizer image, B= plane-polarizer image)

Thin section no. 6 was prepared from a core sample of well V-037, located at a depth of 2,186.95 m. A clear difference to the other thin sections of well V-037 can be identified. Fig. 101 and Fig. 102 show a large amount of angular and broken quartz grains embedded in a clayey-sericitic matrix. The angularity of the grains indicates, that they were hardly transported and the hinterland is not far away. Additionally, feldspars are weathered. This section appears like a reworked horizon with components of the underlying crystalline basement.
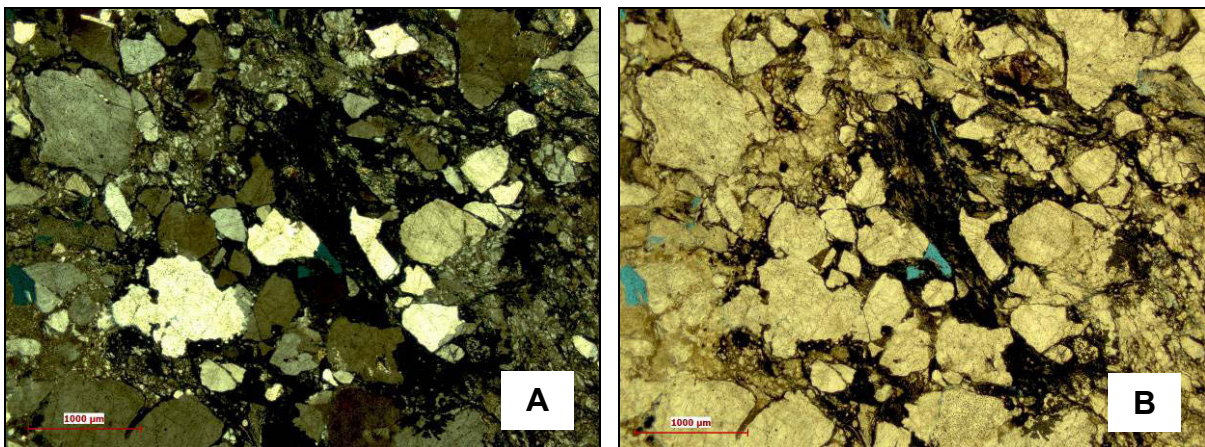
Fig. 101: Microphoto of V-037 (TS 6): ?Crystalline basement (cordierit-bearing migmatite) at a core depth of 2,186.95 m; Blue phases indicate the blue-coloured resin used for thin section preparation and highlight open pore space. (A= cross-polarizer image, B= plane-polarizer image)

In comparison to the other thin sections of well V-037, the porosity of thin section no. 6 seems to be higher.
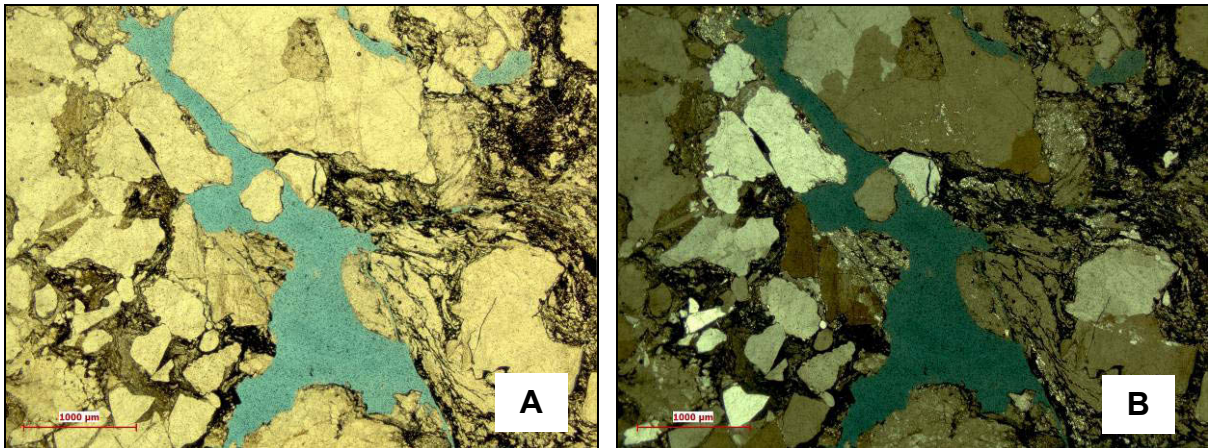
Fig. 102: Microphoto of V-037 (TS 6): ?Crystalline basement (cordierit-bearing migmatite) at a core depth of 2,186.95 m; Blue phases indicate the blue-coloured resin used for thin section preparation and highlight open pore space. (A= cross-polarizer image, B= plane-polarizer image)

Log analysis:

According to RAG core report, Top-XX is defined at a depth of 2,182.50 m. The comparison of well log and Core-GR log measured with GF Instruments Gamma Surveyor (Fig. 103) is illustrated below. The core-to-log shift is one metre, but both curves show a very good fit. The GR scale is derived from GR well log.
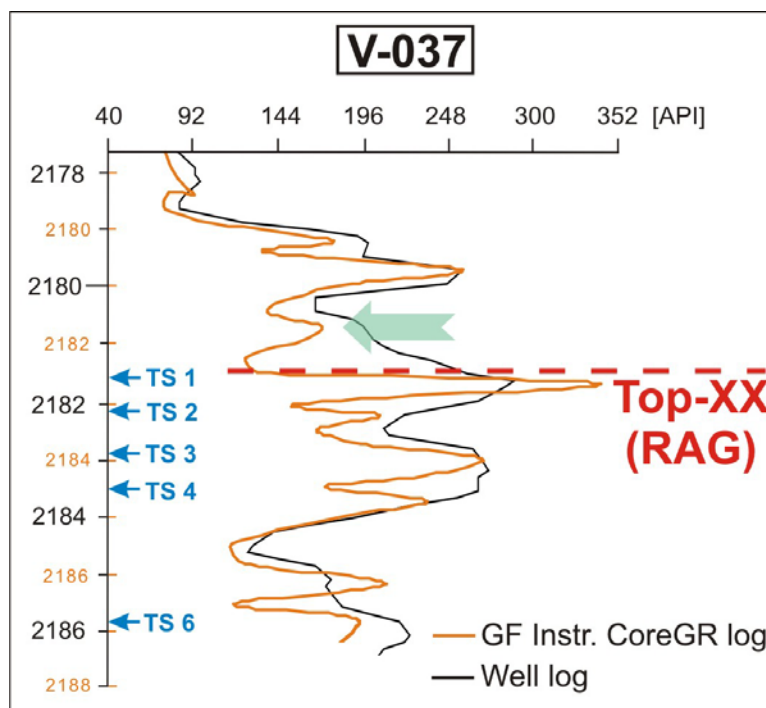
Fig. 103: Comparison V-037 well log and Core-GR measured with GF Instruments Gamma Surveyor (TS= position of thin sections)

As there is a core-to-log shift, Top-XX (RAG) according to well log is defined at a depth of 2,181.50 m (Table 14).

	Depth of ?Top-XX [m]
"Pettenbach" Core (= RAG core report)	2,182.50
Log depth	2,181.50

Table 14: Summary of depths of ?top of the crystalline basement (according to RAG core report)

Fig. 104 shows Spectral Core-GR measured with GF Instruments' Gamma Surveyor Compact. Potassium content shows a relatively steady curve with the only peak at approximately 2,180.50 m (see core photo of Fig. 105).
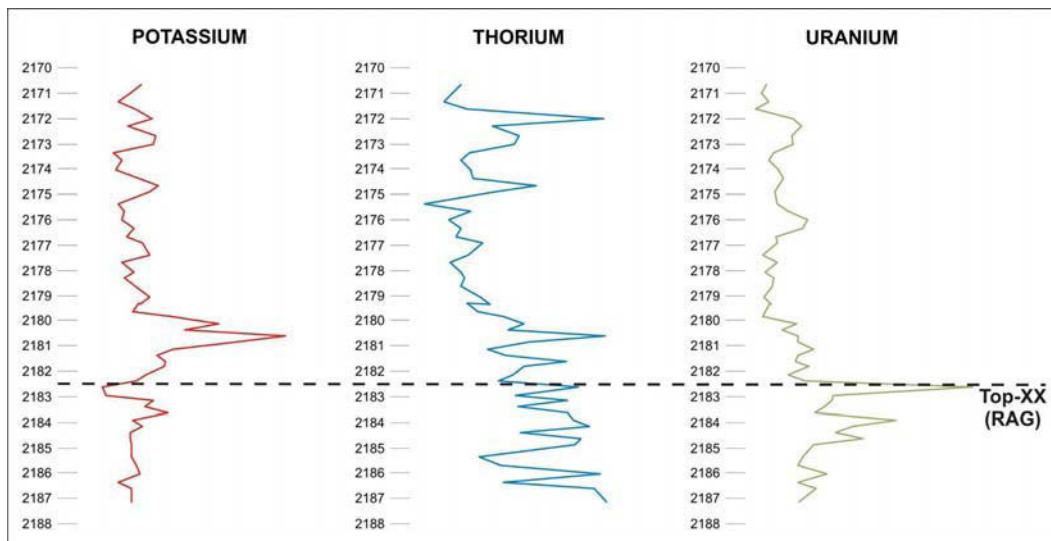
Fig. 104: Spectral Core-GR of well V-037 measured with GF Instruments Gamma Surveyor

Thorium curve is quite similar to the potassium curve, but has peaks at approximately 2172 m and high, but changing contents from base Jurassic downwards into crystalline basin. At the depth of Top-XX defined by RAG (2,182.5 m), the content of uranium exhibits a significant peak. This may result from roots visible within the core (see core photo of Fig. 106). Apart from that, uranium has low contents within Jurassic and slightly elevated values within the crystalline basement.

Fig. 105: Core photo of well V-037 at a core depth of approx. 2,180.50 m
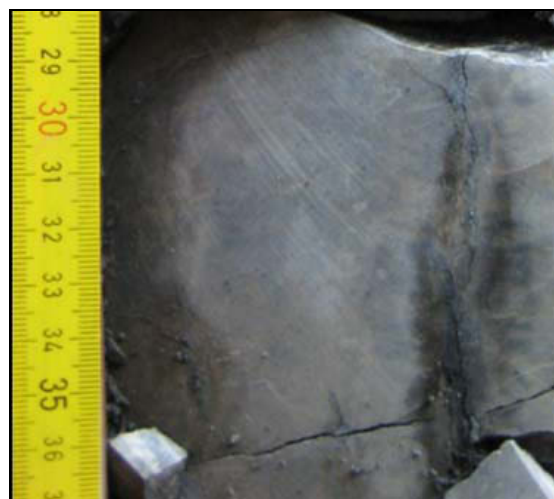
Fig. 106: Core photo of well V-037 at a core depth of approx. 2,182.80 m

Well logs available of well V-037 are displayed in Fig. 107. Top-XX interpretated by RAG (core report) is illustrated as green dashed line at a log depth of 2,181.5 m, whereas completion log shows Top-XX at 2,183.8 m (see blue dashed line). Additionally, log shifts are possible and must be considered.

Considering the logs, the definition of ?Top-XX by completion log (see green line in Fig. 95) seems to be the better solution, as there are more significant trends visible. The boundary is defined between thin section no. 2 and no. 3.

GR log generally shows elevated values at base Jurassic, which decrease in the uppermost part of the ?crystalline basement, considering Top-XX defined by completion log. At Top-XX of RAG, GR is increasing.

Again, the SP log may be affected by drilling mud and therefore a clear trend cannot be identified. Just below, Top-XX defined by completion log, caliper log indicates a possible breakout, whereas at Top-XX of RAG no changes are visible. The bit size is 8.5 inch, as displayed by the green line (BS).

Sonic log decreases at Top-XX of RAG, but does not show any significant trend below 2,182 m. At this depth, all resistivity logs (LLS, LLD and MSFL) are decreasing, compared to Top-XX defined by completion log, where MSFL also exhibits a strong decrease, but LLS and LLD are significantly increasing.

Fig. 107: Well logs of well V-037 with interpreted top of the crystalline basement (dashed lines)

The completion log of well V-037 is displayed below (Fig. 108) and defines Top-XX at a depth of 2,183.8 m.
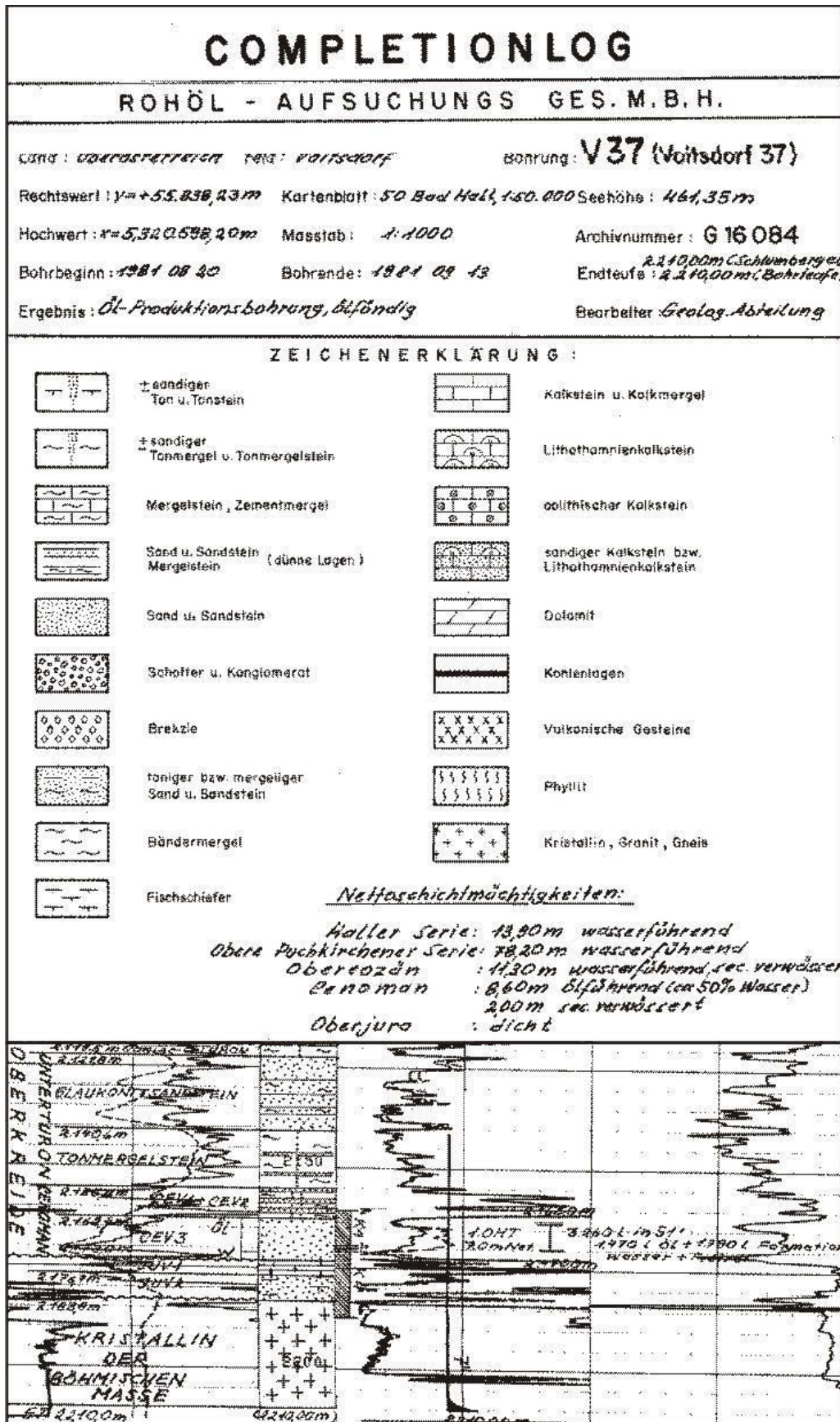
Fig. 108: Completion log of well V-037

INTERPRETATION

The crystalline basement of well KH-003 consists of granite, whereas at well V-037 it is described as corierit-bearing gneiss with migmatitic structures, according to RAG core report of 1981.

	KH-003	*V-037*
GR (log)	⬇ (above)	
CGR	⬇	
HLLS/HLLD	⬇	
MSFL	⬆	**?**
HCAL	⬇	
DT	⬇	

Table 15: Comparison of log trends of wells KH-003 and V-037

According to the results of core inspection including thin section analysis, it is questionable, if well V-037 has cored Top-XX (although RAG defined Top-XX at a core depth of 2,182.5 m). Based on the assumption, that crystalline basement has not been cored in well V-037, a comparison of log trends with well KH-003 is impossible.

KH-003 shows high GR values at the base of Jurassic sediments, whereas V-037 has low GR content above Top-XX of RAG (see Fig. 109). Heavy minerals may trigger high GR at base Jurassic of well KH-003 and illustrate similar trends as visible in wells with magmatic crystalline rocks.
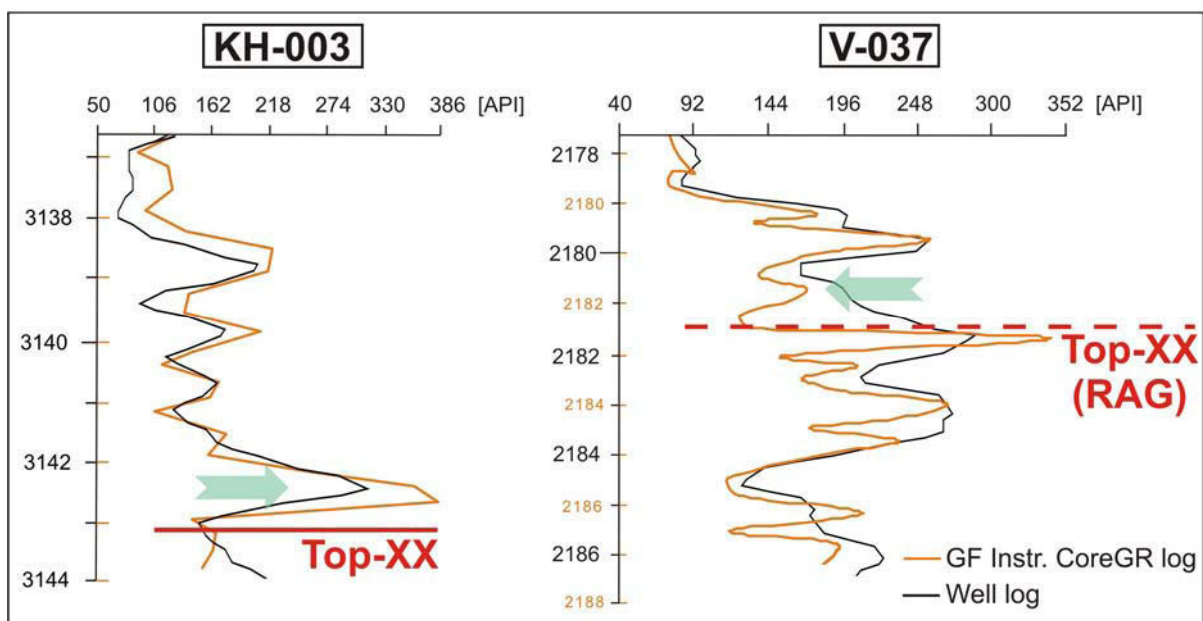
Fig. 109: Different trends of GR log at top of the crystalline basement
(left picture= KH-003, right picture= V-037)

CONCLUSION

The following interpretation highlights different log trends depending on the age of the overlying sediments (Jurassic, Cenomanian, Eocene) and the lithology of crystalline rocks present.

I. Wells with XX overlain by Mesozoic rocks

The wells BH-N-001, BH-N-002 (Cenomanian overlying XX), KH-003 and V-037 (Jurassic overlying XX) are overlain by Mesozoic sediments. Apart from well V-037, all show crystalline basement composed of plutonic rocks, like granite (BH-N-001 and KH-003) or (grano)diorite (BH-N-002). According to RAG core report, core no. 4 of well V-037 recovered crystalline basement consisting of cordierite-bearing gneiss.

Spectral Core-GR log patterns of wells with crystalline basement consisting of plutonic rocks are illustrated in Fig. 110. High GR values at the base of the Mesozoic sandstones are caused by heavy minerals (high contents of uranium and thorium), whereas low GR contents result from weathering of the crystalline basement (removal of K). Potassium content is low in the area of the top of the crystalline basement and increases downwards to unweathered crystalline basement, where potassium feldspars are expected.
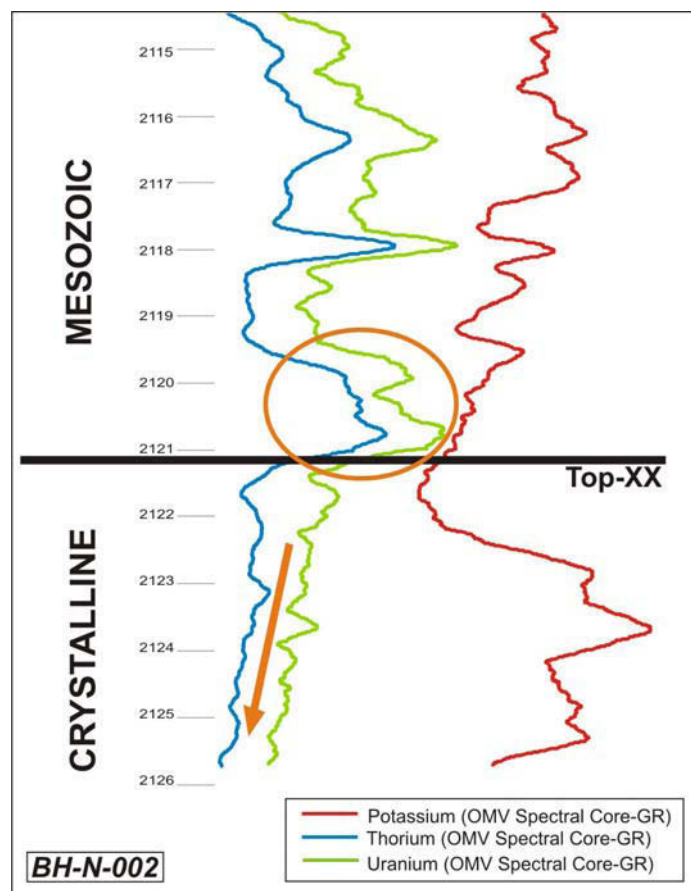
Fig. 110: Characteristic log trends for wells with Mesozoic sediments overlying crystalline basement, example of well BH-N-002

Fig. 111 displays Total GR log patterns of wells BH-N-001, BH-N-002 and KH-003 including the top of the crystalline basement represented by the red boundary.
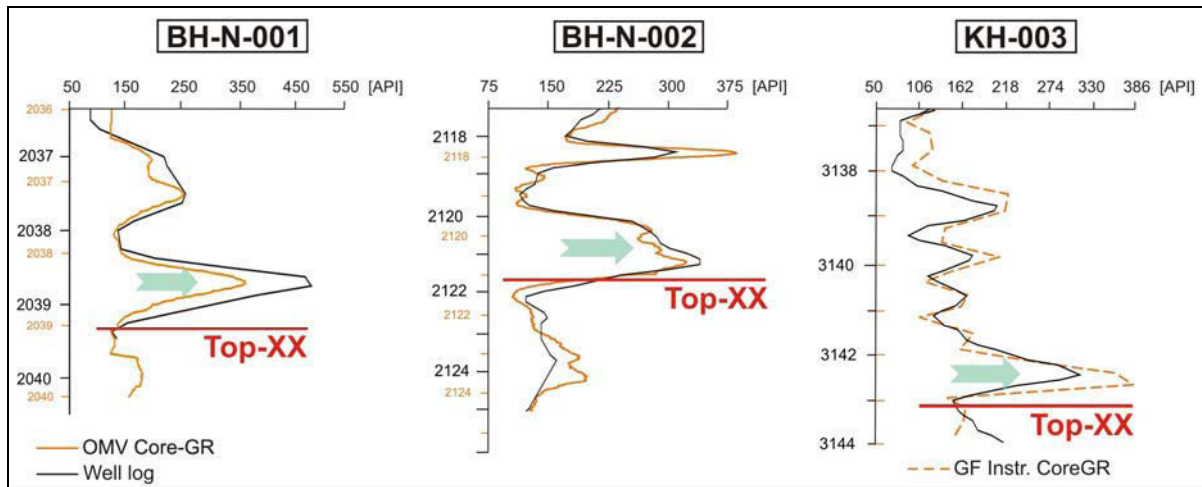
Fig. 111: High GR at the base of Mesozoic sediments

On closer inspection it can be identified, that all wells including Mesozoic sandstones overlying plutonic rocks (BH-N-001, BH-N-002 and KH-003) illustrate high contents of total GR (dominated by high values of uranium and thorium) at the base of the sandstones and significantly low values of total GR within the uppermost part of the crystalline basement.

As mentioned in chapter "Well Analysis", core no. 4 of well V-037 probably did not encounter crystalline basement. However, according to RAG, well V-037 reached cordierite-bearing gneiss with migmatitic structures at a depth of 2,182.5 m. If the RAG report is correct, the basement lithology is different compared to the plutonic rocks drilled in wells BH-N-001, BH-N-002 and KH-003.

Fig. 112 displays Total GR log of V-037 with Top-XX interpreted by RAG. If the definition of Top-XX is correct, the totally different log pattern may reflect the different basement lithology.
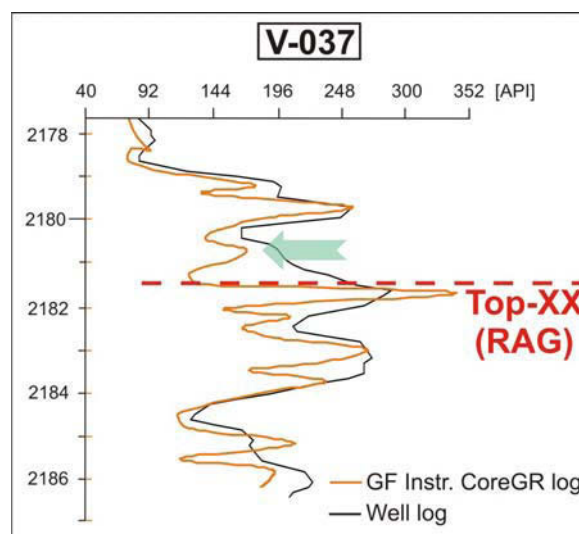
Fig. 112: Low GR at the base (?) of Mesozoic sediments (Jurassic)

As mentioned, RAG staff uses mainly resistivity logs for the definition of the top of the crystalline basement. According to Fig. 113 it is obvious, that resistivity logs (predominantly LLS, LLD) do not show equal significant trends for the wells with Mesozoic sediments overlying the plutonic crystalline basement. The wells BH-N-002 and KH-003 indicate contrary changes at Top-XX, whereas BH-N-001 does not show a significant trend. As these logs display contradictory results, they may not be the best tools for an accurate definition of Top-XX.
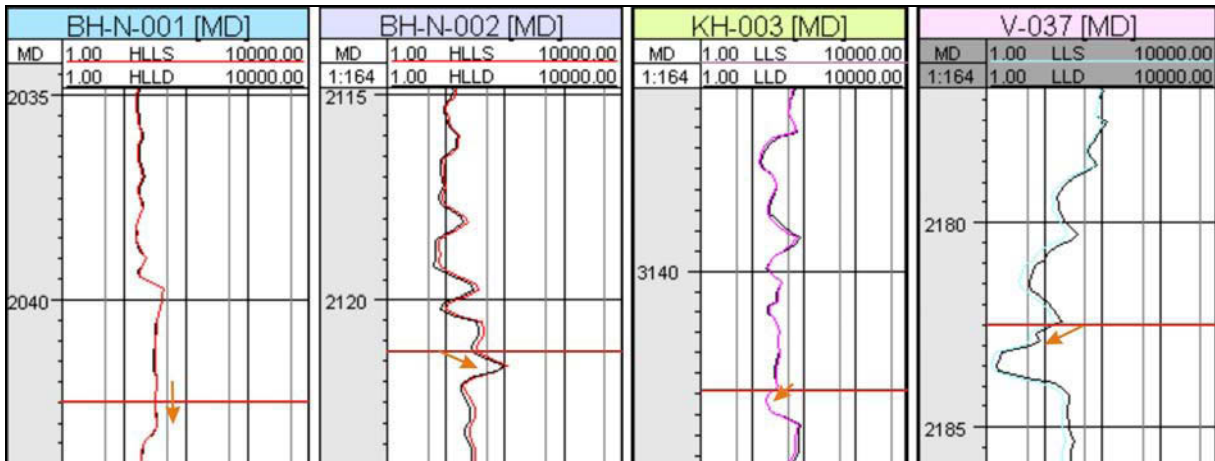
Fig. 113: Resistivity logs with varying trends at the top of the crystalline basement (red lines)

Well V-037 with Mesozoic rocks overlying metamorphic crystalline basement exhibits decreasing resistivity at Top-XX.

Table 16 summarizes core and log data of crystalline rocks overlain by Mesozoic sediments. Data of the uppermost (weathered) parts of the crystalline basement are displayed. Additionally, information on the unweathered crystalline below is given in brackets. Question marks in brackets indicate limited core length within the crystalline.

The definition of Top-XX in well V-037 is based on RAG core reports. Core-GR data of the wells KH-003 and V-037 are missing, as the measuring tool Gamma Surveyor Compact of GF Instruments does not provide absolute measurement, but identification of trends.

Well	Lithology	Total GR [API]	Total C-GR [API]	Spectral C-GR K [%]	Spectral C-GR Th [ppm]	Spectral C-GR U [ppm]	LLS, LLD [Ωm]	Φ [-]	DT [µs/ft]	PEFZ [-]	CAL [in]	RHOZ [g/cm³]
BH-N-001	granite	145 (170)	8 (60)	0.1 (3)	1 (5)	1 (3)	40 (700)	0.15 (0.05)	32 (50)	1.34 (4.23)	6.35 (6.4)	2.56 (2.76)
BH-N-002	(grano)diorite	150 (243)	100 (70)	0.2 (3)	10 (5)	5 (2)	20 (3000)	0.36 (0.05)	65 (52)	3.25 (3.8)	9.4 (8.7)	2.6 (2.7)
KH-003	granite	270 (225)	-	-	-	-	57 (28)	-	60 (62)	-	7.4 (7.85)	-
V-037	?migmatite	270 (228)	-	-	-	-	12 (36)	-	66 (62)	-	8.4 (8.77)	-

Table 16: Summary of log data of the crystalline rocks overlain by Mesozoic rocks (orange= plutonic crystalline rocks, green= metamorphic crystalline rocks)

II. Wells with XX overlain by Eocene rocks

Also log patterns of wells with Eocene rocks overlying crystalline basement are affected by basement lithology. Well HIER-002A drilled plutonic crystalline rocks (granite), whereas the basement of well MLRT-003C consists of metamorphic rocks (gneiss with migmatitic structures).

As illustrated in Fig. 114, total GR log shows opposite trends for both wells. Well HIER-002A exhibits a peak at base Eocene, whereas well MLRT-003C indicates low GR values at the same position.
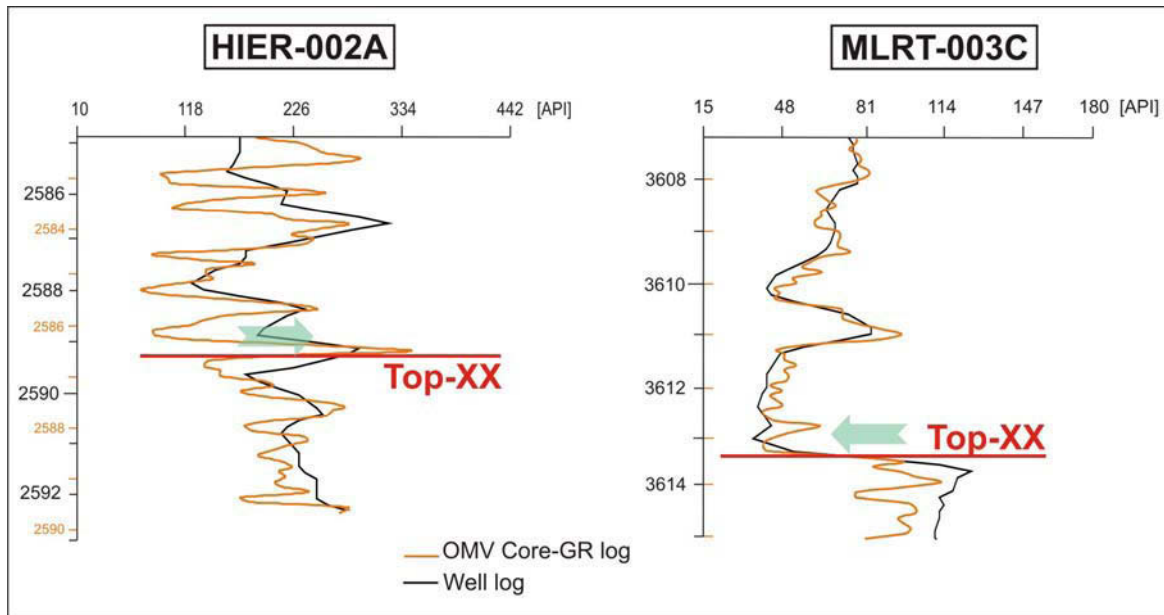
Fig. 114: Different trends of GR log at top of the crystalline basement

In contrast to Mesozoic sandstones, Eocene sandstones provide a positive correlation of total GR values and the content of potassium. In this case, heavy minerals are not dominating GR values. According to the lithology of the crystalline basement, GR values are either increasing (metamorphic basement) or do not show significant changes (plutonitic rocks).

The wells HIER-002A and MLRT-003C exhibit different resistivity trends at the top of the crystalline basement. The latter shows a weak decrease, with an increase downwards. Resistivity of well HIER-002A increases slightly at Top-XX.
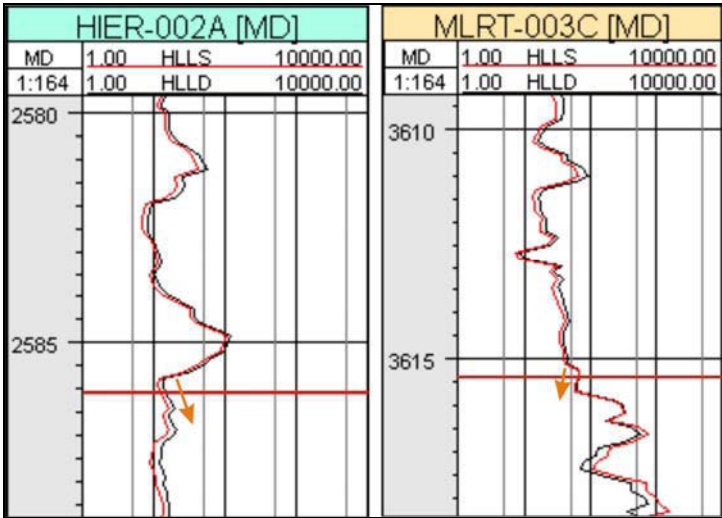
Fig. 115: Resistivity logs with contrary trends at the top of the crystalline basement (red lines)

A summary of core and log data of wells with crystalline rocks overlain by Eocene rocks is provided by Table 17. Data of Top-XX and the uppermost (weathered) parts of the crystalline basement are displayed in comparison to information on the unweathered crystalline (in brackets). Again, question marks in brackets indicate limited core length within the crystalline basement.

Well	Lithology	Total GR [API]	Total C-GR [API]	Spectral C-GR K [%]	Spectral C-GR Th [ppm]	Spectral C-GR U [ppm]	LLS, LLD [Ωm]	Φ [-]	DT [µs/ft]	PEFZ [-]	CAL [in]	RHOZ [g/cm³]
HIER-002A	granite	250 (238)	80 (100)	3 (6)	30 (20)	15 (20)	51 (170)	0.3 (0.05)	61 (51)	2.3 (3.6)	6.3 (6.2)	2.64 (2.68)
MLRT-003C	gneiss	112 (125)	80 (?)	3 (?)	10 (?)	8 (?)	41 (3100)	0.15 (0.04)	-	4.28 (5.7)	6.22 (6.16)	2.67 (2.7)

Table 17: Summary of log data of the crystalline rocks overlain by Eocene rocks (orange= plutonic crystalline rocks, green= metamorphic crystalline rocks)

The result of this study demonstrates that the well logging signal is influenced by several factors. These are, among others, the lithology, as well as heavy minerals at the base of the overlying formation, but also the degree of weathering and the lithology of the crystalline basement (magmatic versus metamorphic). Therefore, a general log pattern within the area of Top-XX of the investigated wells cannot be observed.

However, GR log seems to be a good tool to define Top-XX in most cases, although log patterns change depending on the lithology of basement rocks. Therefore, investigations of further wells are necessary to demonstrate, if a general trend exists to provide a reliable definition of the top of the crystalline basement.

LIST OF REFERENCES

Asquith, G., Krygowski, D. (2004): Basic Well Log Analysis; AAPG Methods in Exploration Series, No. 16

Bartetzko, A., Delius, H., Pechnig, R. (2005): Effect of compositional and structural variations on log responses of igneous and metamorphic rocks. I: mafic rocks; Geological Society, London, Special Publications 2005, Vol. 240, 255-278

De Ruig, M.J. (2003): Deep Marine Sedimentation and Gas Reservoir Distribution in Upper Austria; OIL GAS European Magazine – 2

Desbrandes, R. (1985): Encyclopedia of Well Logging; Institut francais du pétrole publications

Einaudi, F., Pezard, P. A.,Ildefonse, B., Glover, P. (2005): Electrical properties of slow-spreading ridge gabbros from ODP Hole 1105A, SW Indian Ridge; Geological Society, London, Special Publications 2005, Vol. 240, 179-193

Fuchs, R., Wessely, G. (1996): The autochthonous Cretaceous at the southern edge of the Bohemian Massif (Austria); EAGE Special Publication No. 5, 249-253

Genser, J., Cloetingh, S.A.P.L., Neubauer, F. (2007): Late orogenic rebound and oblique Alpine convergence: New constraints from subsidence analysis of the Austrian Molasse basin; Science Direct, Vol. 58, 214-223

Goldbrunner, J. E. (2000): Hydrogeology of deep groundwaters in Austria; Mitteilungen der Österreichischen Geologischen Gesellschaft, 92 (1999), 281-294

Hubbard, S. M., De Ruig, M. J., Graham, S. A. (2005): Utilizing outcrop analogs to improve subsurface mapping of natural gas-bearing strata in the Puchkirchen Formation, Molasse Basin, Upper Austria; Austrian Journal of Earth Sciences, Vol. 98, 52-66

Janoschek, R. (1961): Über den Stand der Aufschlussarbeiten in der Molassezone Oberösterreichs; Erdöl-Zeitschrift, 77. Jg., 161-175

Kollmann, K. (1977): Die Öl- und Gasexploration der Molassezone Oberösterreichs und Salzburgs aus regional-geologischer Sicht; Erdöl-Erdgas-Zeitschrift, 93. Jg., Sonderausgabe 1977

Kollmann, K., Wagner, L., Zimmer, W. (1987): Geologisches Profil durch den westlichen Teil der österreichischen Molassezone; Beilage 6 in F. Brix & O. Schultz (Herausg.): Erdöl und Erdgas in Österreich, Verlag: Naturhistorisches Museum Wien und F. Berger, Horn

Kuhlemann, J., Kempf, O. (2002): Post-Eocene evolution of the North Alpine Foreland Basin and its response to Alpine tectonics; Sedimentary Geology, Vol. 152, 45-78

Malzer, O., Rögl, F., Seifert, P., Wagner, L., Wessely, G., Brix, F. (1993): Die Molassezone und deren Untergrund; in F. Brix & O. Schultz (Herausg.): Erdöl und Erdgas in Österreich, Verlag: Naturhistorisches Museum Wien und F. Berger, Horn

Nachtmann, W. (1989): Lagerstättengeologisches Modell des Obereozäns im Raum Sattledt (Oberösterreichische Molasse); Geol. Paläont. Mitt. Innsbruck 16, 213-227

Nachtmann, W. (1995a): Das Cenoman im Untergrund der oberösterreichischen Molasse – eine lagerstättengeologische Betrachtung; Zbl. Geol. Paläont. Teil I (1994)

Nachtmann, W. (1995b): Bruchstrukturen und ihre Bedeutung für die Bildung von Kohlenwasserstoff-Fallen in der Oberösterreichischen Molasse; Geol. Paläont. Mitt. Innsbruck, 20, 221-230

Nachtmann, W., Wagner, L. (1986): Mesozoic and Early Tertiary evolution of the Alpine foreland in Upper Austria and Salzburg, Austria; Tectonophysics, 137 (1987), 61-76

Rasser, M. W., Piller, W. E. (2004): Crustose algal frameworks from the Eocene Alpine foreland; PALAEO – Palaeogeography, Palaeoclimatology, Palaeoecology 206, 21-39

Sachsenhofer, R. F., Gratzer, R., Tschelaut, W., Bechtel, A. (2006): Characterisation of non-producible oil in Eocene reservoir sandstones (Bad Hall Nord field, Alpine Foreland Basin, Austria); Marine and Petroleum Geology, 23, 1-15

Sachsenhofer, R. F., Schultz, H.-M. (2006): Architecture of Lower Oligocene source rocks in the Alpine Foreland Basin: a model for syn- and post-depositional source-rock features in the Paratethyan realm; Petroleum Geoscience, Vol. 12, 363-377

Schlumberger Logelco Inc.(RO), Data & Consulting Services Division (2008): Processing and Structural Interpretation of a Fullbore Formation MicroImager (FMI*) image log of MLRT-003C; Romania

Schön, J., Fricke, S. (1999): Praktische Bohrlochgeophysik; Enke im Georg Thieme Verlag, Stuttgart

Serra, O., Serra, L. (2004): Well logging – Data Acquisition and Applications; Editions Serralog

Sissingh, W. (1997): Tectonostratigraphy of the North Alpine Foreland Basin: correlation of Tertiary depositional cycles and orogenic phases; Tectonophysics, Vol. 282, 223-256

Wagner, L. R. (1998): Tectono-stratigraphy and hydrocarbons in the Molasse Foredeep of Salzburg, Upper and Lower Austria; Geological Society Special Publications, Vol. 134, 339-369

Wagner, L. R. (1996): Stratigraphy and hydrocarbons in the Upper Austrian Molasse Foredeep (active margin); EAGE Special Publication, No. 5, 217-235

Wagner, L. (1980): Geologische Charakteristik der wichtigsten Erdöl- und Erdgasträger der oberösterreichischen Molasse, Teil I: Die Sandsteine des Obereozän; Erdöl-Erdgas-Zeitschrift, 96. Jg.

Wieseneder, H., Freilinger, G., Kittler, G., Tsambourakis, G. (1976): Der kristalline Untergrund der Nordalpen in Österreich; Geologische Rundschau, Volume 65, Issue 1, 512-525

Ziegler, P. A., Cloetingh, S., Van Wees, J.-D. (1995): Dynamics of intra-plate compressional deformation: the Alpine foreland and other examples; Tectonophysics, 252 (1995), 7-59

Core reports:

Smuk, A. (1981): RAG Kernbericht V-037, Kern 1-4

Zimmer, W. (1983): RAG Kernbericht KH-003, Kern 1-4

Sauer, R., Kuffner, T. (2000): OMV Bad-Hall N1 Core – documentation 1:10 and 1:200 and routine core analysis, cores #1-3; OMV Laboratory for Exploration and Production

Sauer, R., Schreiber, O, Kacirek, J., Geiter, L. Mekonnen, E. (2000): Bad Hall N 2 – Ergebnisse der mineralogisch-petrologischen Analysen von ausgewählten Bohrkernproben, Kerne #1 und #2; OMV Laboratory for Exploration and Production

Sauer, R., Hujer, W., Mekonnen, E., Pfeiler, W., Huber, L., Reichl, J. (2008): Hiersdorf 2A – Core documentation 1:10 and 1:200 and routine core analyses, cores #1, #2 & #3; OMV Laboratory for Exploration and Production

Sauer, R., Hujer, W., Kacirek, J., Mekonnen, E., Geiter, L., Huber, L. (2008): Hiersdorf 2A – Ergebnisse der mineralogisch-petrologischen Analysen von ausgewählten Bohrkernproben, Kerne #1, #2 & #3; OMV Laboratory for Exploration and Production

Sauer, R., Hujer, W., Mekonnen, E., Kacirek, J., Geiter, L., Reichl, J., Pfeiler, W., Huber, L. (2009): Mühlreith 3C – Core documentation, sedimentological and petrographical analyses core #4; OMV Laboratory for Exploration and Production

───────────────────────────────────

LIAG – Leibnitz-Institut für Angewandte Geowissenschaften:
http://www.liag-hannover.de/methodenforschung-sektionen/gesteinsphysik-bohrlochgeophysik/ausstattung/bohrlochsonden-bis-1300m.html

Schlumberger Oilfield Glossary:
http://www.glossary.oilfield.slb.com

LIST OF FIGURES

LIST OF TABLES

ATTACHMENT

Well: BH-N-002

Core No. [Total interval]:   2 [2,112 - 2,126 m]
Core Recovery: 14 m
Core Diameter: 10 cm
Date of Coring: May 2002

Displayed Box [interval]:   15 [2,111.38 - 2,112 m]
Date of Core Inspection: 06.10.2009

Photo Depth Top: 2,111.38	Lithology & Grain size							Sedimentary Structures	Sorting	Rounding	Core Description
	Clay (C)	Silt (U)	f-Sand (fS)	m-Sand (mS)	c-Sand (cS)	Granule (g)	Pebble (p)				
									medium	angular	dark grey matrix consisting of silt and fine-grained sand with qtz/fsp-grains of approx. 1 mm in size, small fractures are partly filled with calcite (HCl !)

Depth Bottom: 2,112 m

DEFINITION OF TOP-CRYSTALLINE BASEMENT
IN THE AUSTRIAN MOLASSE BASIN

Gloria Thürschmid

Well: BH-N-002

Core No. [Total interval]: 2 [2,112 - 2,126 m]
Core Recovery: 14 m
Core Diameter: 10 cm
Date of Coring: May 2002

Displayed Box [interval]: 14 [2,112 - 2,113 m]
Date of Core Inspection: 06.10.2009

Photo Depth Top: 2,112 m	Lithology & Grain size							Sedimentary Structures	Sorting	Rounding	Core Description
	Clay (C)	Silt (U)	f-Sand (fS)	m-Sand (mS)	c-Sand (cS)	Granule (g)	Pebble (p)				
								part with many qtz/cc-grains	medium	angular	dark grey matrix consisting of silt and fine-grained sand with numerous qtz/fsp- and cc-grains (strong reaction with HCl !)
								part with many cc-grains / part with many cc-grains	medium	angular	dark grey matrix consisting of silt and fine-grained sand, almost no components (?dispersed organic matter; coal included) / gradual increase of amount of qtz/cc-grains ! / part with numerous cc-grains / part with numerous cc-grains / nearly no components in dark grey matrix

Depth Bottom: 2,113 m

DEFINITION OF TOP-CRYSTALLINE BASEMENT
IN THE AUSTRIAN MOLASSE BASIN

Gloria Thürschmid

Well: BH-N-002

Core No. [Total interval]: 2 [2,112 - 2,126 m]
Core Recovery: 14 m
Core Diameter: 10 cm
Date of Coring: May 2002
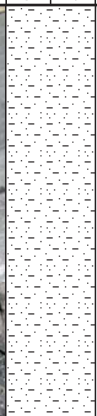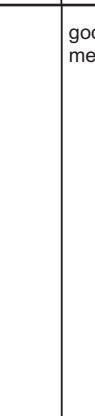
Displayed Box [interval]: 13 [2,113 - 2,114 m]
Date of Core Inspection: 06.10.2009

Photo Depth Top: 2,113 m	Lithology & Grain size							Sedimentary Structures	Sorting	Rounding	Core Description
	Clay (C)	Silt (U)	f-Sand (fS)	m-Sand (mS)	c-Sand (cS)	Granule (g)	Pebble (p)				
									good to medium	angular	dark brown matrix consisting of silt and fine-grained sand with qtz/fsp and ?cc-grains of approx. 1 mm size, number of grains increases downwards
									very good	angular	coarse-grained sandstone (max. ~3 mm grain size), greenish matrix, components are partly cc (HCl), very homogeneous, no internal structures visible

Depth Bottom: 2,114 m

Well: **BH-N-002**

Core No. [Total interval]: 2 [2,112 - 2,126 m]
Core Recovery: 14 m
Core Diameter: 10 cm
Date of Coring: May 2002

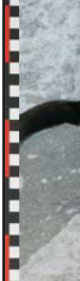Displayed Box [interval]: 12 [2,114 - 2,115 m]
Date of Core Inspection: 06.10.2009

Photo Depth Top: 2,114 m	Lithology & Grain size							Sedimentary Structures	Sorting	Rounding	Core Description
	Clay (C)	Silt (U)	f-Sand (fS)	m-Sand (mS)	c-Sand (cS)	Granule (g)	Pebble (p)				
									good	angular	coarse-grained sandstone with coloured (white, yellow, orange-brown...) components (max. ~5 mm grain size), greenish matrix and partly white cement, homogeneous and no structures visible
									good	sub-rounded	fine-grained sandstone, greenish to dark grey (?organic matter/coal), white calcitic components with sizes from 1 to 4 mm, laminations within organic matter/coal
									good	sub-rounded	fine-grained sandstone with greenish phases, nearly no extraordinary components, laminations!

Depth Bottom: 2,115 m

DEFINITION OF TOP-CRYSTALLINE BASEMENT
IN THE AUSTRIAN MOLASSE BASIN

Gloria Thürschmid

Well: **BH-N-002**

Core No. [Total interval]:   2 [2,112 - 2,126 m]
Core Recovery: 14 m
Core Diameter: 10 cm
Date of Coring: May 2002

Displayed Box [interval]:   11 [2,115 - 2,116 m]
Date of Core Inspection: 06.10.2009

Photo Depth Top: 2,115 m	Lithology & Grain size							Sedimentary Structures	Sorting	Rounding	Core Description
	Clay (C)	Silt (U)	f-Sand (fS)	m-Sand (mS)	c-Sand (cS)	Granule (g)	Pebble (p)				
									good	sub-rounded	fine-grained sandstone, laminated, olive-green to brownish, components of cc up to ~1 mm grain size (number of cc components increase with depth) fracture / fault
									good	sub-rounded	fine-grained sandstone, laminated, dark green/grey, nearly no white calcitic components (grain size ~1 mm)

Depth Bottom: 2,116 m

Well: BH-N-002

Core No. [Total interval]: 2 [2,112 - 2,126 m]
Core Recovery: 14 m
Core Diameter: 10 cm
Date of Coring: May 2002

Displayed Box [interval]: 10 [2,116 - 2,117 m]
Date of Core Inspection: 06.10.2009

Photo Depth Top: 2,116 m	Lithology & Grain size							Sedimentary Structures	Sorting	Rounding	Core Description
	Clay (C)	Silt (U)	f-Sand (fS)	m-Sand (mS)	c-Sand (cS)	Granule (g)	Pebble (p)		medium	sub-angular	sandstone (fS-mS), greenish-grey with shells (HCl reaction !) and calcitic components; small amount of non-calcitic (?fsp) components
											non-calcitic components with max. size of 6 mm!

Depth Bottom: 2,117 m

Well: BH-N-002

Core No. [Total interval]:   2 [2,112 - 2,126 m]
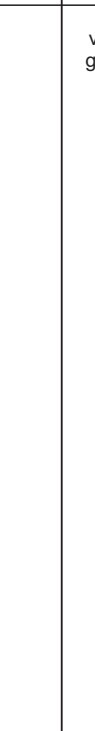Core Recovery: 14 m
Core Diameter: 10 cm
Date of Coring: May 2002

Displayed Box [interval]:   9 [2,117 - 2,118 m]
Date of Core Inspection: 06.10.2009

Photo Depth Top: 2,117 m	Lithology & Grain size							Sedimentary Structures	Sorting	Rounding	Core Description
	Clay (C)	Silt (U)	f-Sand (fS)	m-Sand (mS)	c-Sand (cS)	Granule (g)	Pebble (p)				
									medium	angular	sandstone (fS-mS), greenish-grey with shells and calcitic components, also fsp
									medium-good	sub-angular	bright (beige-grey) sandstone, bioturbation (trace fossils of digging, drilling...), strong reaction of HCl due to considerable amount of cc
											change of dip ! (?due to cut)
									medium-good	sub-angular	dark grey, sandstone (fS-mS) with silt and organic material (?coal), calcitic rests, bioturbation (!) and ?small slides
											change of dip

Depth Bottom: 2,118 m

Well: BH-N-002

Core No. [Total interval]:   2 [2,112 - 2,126 m]
Core Recovery: 14 m
Core Diameter: 10 cm
Date of Coring: May 2002

Displayed Box [interval]:   8 [2,118 - 2,119 m]
Date of Core Inspection: 06.10.2009

Photo Depth Top: 2,118 m	Lithology & Grain size							Sedimentary Structures	Sorting	Rounding	Core Description
	Clay (C)	Silt (U)	f-Sand (fS)	m-Sand (mS)	c-Sand (cS)	Granule (g)	Pebble (p)				
									medium-good	sub-angular	dark grey, organic material (?coal) within sandstone (fS-U), cc. components, bioturbation !
									good	angular	sandstone (cS-mS), light grey, transition zone with dark, thin layers
											partly calcitic cementation, qtz-grains with max. size of 2 mm, homogeneous, no internal structure
									medium	angular	interbedding of sandstone and organic material (?coal), some clasts are existent, partly fine laminations, ?bioturbation
									medium-good	sub-angular	reddish-beige qtz-sandstone (fS-mS), nearly no reaction of HCl, some calcitic phases between grains and as filling material for fractures, only few fossil rests (shells)
									medium-good	sub-angular	greenish-grey qtz-sandstone (fS-mS) with strong HCl-reaction, amount of shells increase with depth

Depth Bottom: 2,119 m

DEFINITION OF TOP-CRYSTALLINE BASEMENT
IN THE AUSTRIAN MOLASSE BASIN

Gloria Thürschmid

Well: BH-N-002

Core No. [Total interval]:   2 [2,112 - 2,126 m]
Core Recovery: 14 m
Core Diameter: 10 cm
Date of Coring: May 2002

Displayed Box [interval]:   7 [2,119 - 2,120 m]
Date of Core Inspection: 06.10.2009

Photo Depth Top: 2,119 m	Lithology & Grain size							Sedimentary Structures	Sorting	Rounding	Core Description
	Clay (C)	Silt (U)	f-Sand (fS)	m-Sand (mS)	c-Sand (cS)	Granule (g)	Pebble (p)				
									medium	angular	greenish-grey qtz-sandstone (fS-mS), strong reaction with HCl due to numerous shells (cc.) and calcitic phases
									medium	angular	interbedding of sandstone and organic material (?coal), few shells left
									good- very good	sub- rounded	greenish-grey qtz-sandstone with numerous small fossil rests, few bigger shells, strong HCl-reaction !

Depth Bottom: 2,120 m

Well: BH-N-002

Core No. [Total interval]:   2 [2,112 - 2,126 m]
Core Recovery: 14 m
Core Diameter: 10 cm
Date of Coring: May 2002

Displayed Box [interval]:   6 [2,120 - 2,121 m]
Date of Core Inspection: 06.10.2009

Photo Depth Top: 2,120 m	Lithology & Grain size							Sedimentary Structures	Sorting	Rounding	Core Description
	Clay (C)	Silt (U)	f-Sand (fS)	m-Sand (mS)	c-Sand (cS)	Granule (g)	Pebble (p)				
									good-very good	sub-rounded	greenish-grey sandstone (fS-mS), small cc. phases (HCl), laminations
									good	sub-angular	light beige sandstone (fS), stronger HCl-reaction, shells, little lamination, mostly homogeneous
									good	sub-angular	interbedding of light and dark sandstone, shells (HCl)
									good-very good	sub-rounded	light beige sandstone with strong HCl-reaction (fS), homogeneous, only at the bottom some laminations

Depth Bottom: 2,121 m

DEFINITION OF TOP-CRYSTALLINE BASEMENT
IN THE AUSTRIAN MOLASSE BASIN

Core No. [Total interval]:   2 [2,112 - 2,126 m]
Core Recovery: 14 m
Core Diameter: 10 cm
Date of Coring: May 2002

Displayed Box [interval]:   5 [2,121 - 2,122 m]
Date of Core Inspection: 06.10.2009

Photo Depth Top: 2,121 m	Grain size	(Sedimentary) Structures	(Sorting)	(Rounding)	Core Description
			medium	sub-angular	light grey qtz-sandstone (fS-mS), some laminations on top, fossil shells and ?fsp-grains on the bottom, red-brown weathered grains with a size of 1-2 mm (?mica/biotite)
		TS			sharp boundary to XX !
		fine-grained phase			crystalline / ?granodiorite, weathered with reddish-violet colour (fine-grained matrix?) and very angular qtz-grains with max. size of 9 mm
					crystalline / ?granodiorite, light grey-beige, some ?fine-grained parts included, qtz-grains with 1-2 mm in size, partly qtz-veins (thickness approx. 2 mm), darker phases cover qtz-grains, some scattered pyrite crystals

Depth Bottom: 2,122 m

TS .... **Thin section**

DEFINITION OF TOP-CRYSTALLINE BASEMENT
IN THE AUSTRIAN MOLASSE BASIN

Gloria Thürschmid

Well: BH-N-002

Core No. [Total interval]:   2 [2,112 - 2,126 m]
Core Recovery: 14 m
Core Diameter: 10 cm
Date of Coring: May 2002

Displayed Box [interval]:   4 [2,122 - 2,123 m]
Date of Core Inspection: 06.10.2009

Photo Depth Top: 2,122 m	fine-grained / medium-grained / coarse-grained	Structures	Core Description
			crystalline / ?granodiorite, light grey-beige, some ?fine-grained phases, qtz-grains with sizes of 2-3 mm, some scattered elongated qtz-grains, dark grey phases, some scattered pyrite crystals, very angular grains!
			coarser qtz-grains (size up to 4 mm), angular, light grey
		fine-grained phase / biotite	?shaly phases, numerous biotite, qtz-grains get coarser with depth (max. size 6 mm) transition zone to unweathered, fresh XX ! fracture with numerous biotite !

Depth Bottom: 2,123 m

Well: BH-N-002

Core No. [Total interval]:   2 [2,112 - 2,126 m]
Core Recovery: 14 m
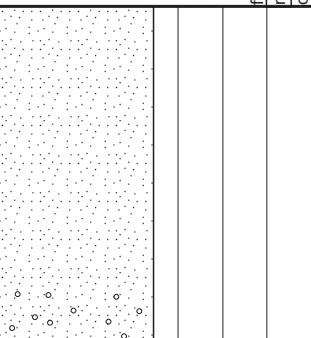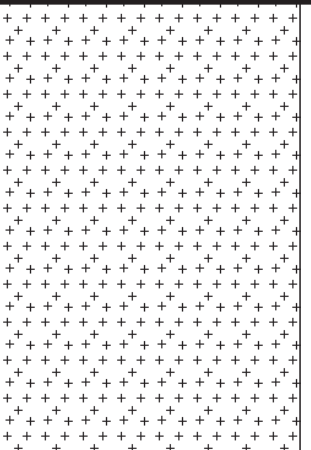Core Diameter: 10 cm
Date of Coring: May 2002

Displayed Box [interval]:   3 [2,123 - 2,124 m]
Date of Core Inspection: 06.10.2009

Photo Depth Top: 2,123 m		fine-grained	medium-grained	coarse-grained	Structures	Core Description
						crystalline / ?granodiorite, coarse grains, numerous biotite, white and pink fsp (plagioclase, kali-fsp) and qtz, not homogenous distributed ("phases"), no HCl-reaction
					biotite qtz	
					biotite	
					vein	
						fracture with approx. 1 mm thickness, filled with qtz and white fsp., covered with pink fsp.
					biotite	

Depth Bottom:
2,124 m

Well: **BH-N-002**
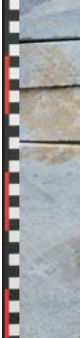
Core No. [Total interval]: 2 [2,112 - 2,126 m]
Core Recovery: 14 m
Core Diameter: 10 cm
Date of Coring: May 2002

Displayed Box [interval]: 2 [2,124 - 2,125 m]
Date of Core Inspection: 06.10.2009

Photo Depth Top: 2,124 m		fine-grained / medium-grained / coarse-grained	Structures	Core Description
				crystalline / ?granodiorite, fresh and unweathered, pink vein with aplite (thickness of approx. 3-5 cm) at the top, qtz-grains with size up to 9 mm, coarse grains, numerous biotite
			vein of aplite	
			vein of qtz	spherically shaped inclusion (greenish phases covered with qtz-grains, next to mica/biotite, fsp.)
				flowing texture, fold (?migmatitic)

Depth Bottom: 2,125 m

DEFINITION OF TOP-CRYSTALLINE BASEMENT
IN THE AUSTRIAN MOLASSE BASIN

Gloria Thürschmid

Core No. [Total interval]:   2 [2,112 - 2,126 m]
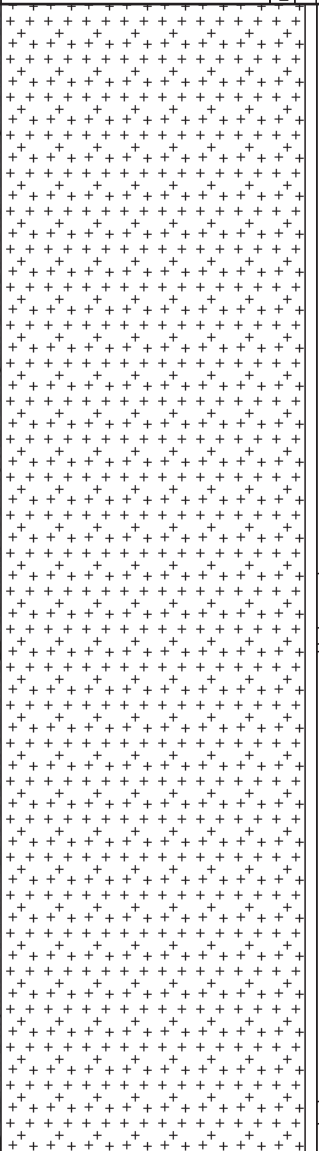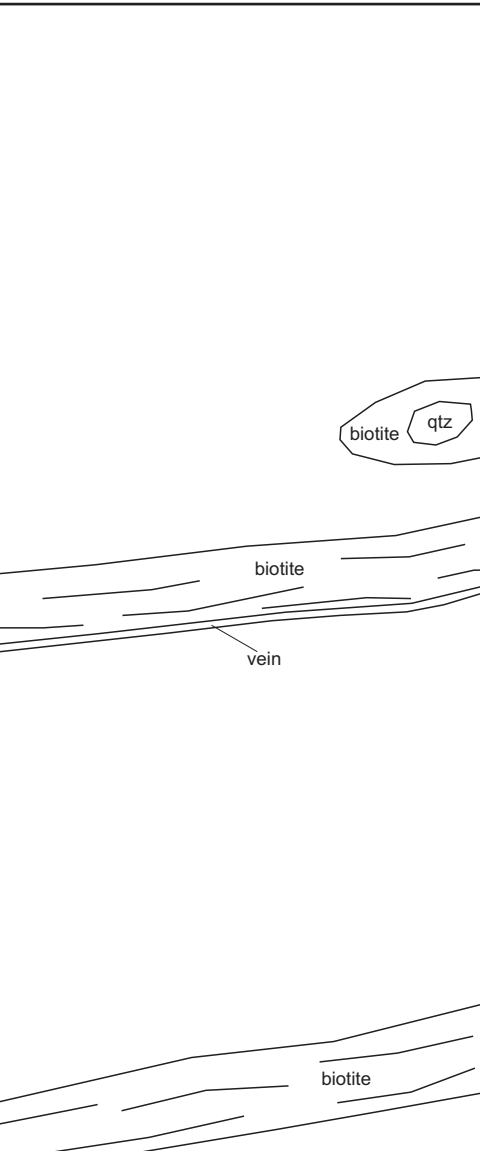Core Recovery: 14 m
Core Diameter: 10 cm
Date of Coring: May 2002

Displayed Box [interval]:   1 [2,125 - 2,126 m]
Date of Core Inspection: 06.10.2009

Photo Depth Top: 2,125 m		fine-grained	medium-grained	coarse-grained	Structures	Core Description
						crystalline / ?granodiorite, fresh and unweathered, qtz-grains up to ~2 cm in size, layers with numerous biotite, coarse grains, angular in shape, mica: biotite and ?phlogopite
						upper part of the half-cylindric core is missing !
					biotite fracture	dark grey, opalescent XX-components with approx. 5 mm in size, between biotite

Depth Bottom: 2,126 m

DEFINITION OF TOP-CRYSTALLINE BASEMENT
IN THE AUSTRIAN MOLASSE BASIN

Gloria Thürschmid

Well: BH-N-001

Core No. [Total interval]: 3 [2,036 - 2,046 m]
Core Recovery: 7.20 m
Core Diameter: 6.5 cm
Date of Coring: Feb. 2000

Displayed Box [interval]: 8 [2,038.87 - 2,039 m]
Date of Core Inspection: 07.10.2009

Photo Depth Top: 2,038.87	Lithology & Grain size							Sedimentary Structures	Sorting	Rounding	Core Description
	Clay (C)	Silt (U)	f-Sand (fS)	m-Sand (mS)	c-Sand (cS)	Granule (g)	Pebble (p)				
									good	angular	sandstone (qtz!), homogeneous + muscovite No HCl-reaction!

Depth Bottom: 2,039 m

DEFINITION OF TOP-CRYSTALLINE BASEMENT
IN THE AUSTRIAN MOLASSE BASIN

Gloria Thürschmid

Well: BH-N-001

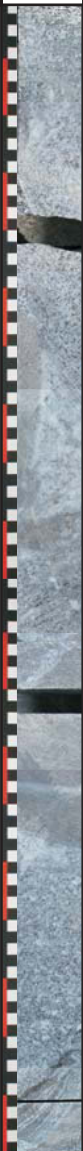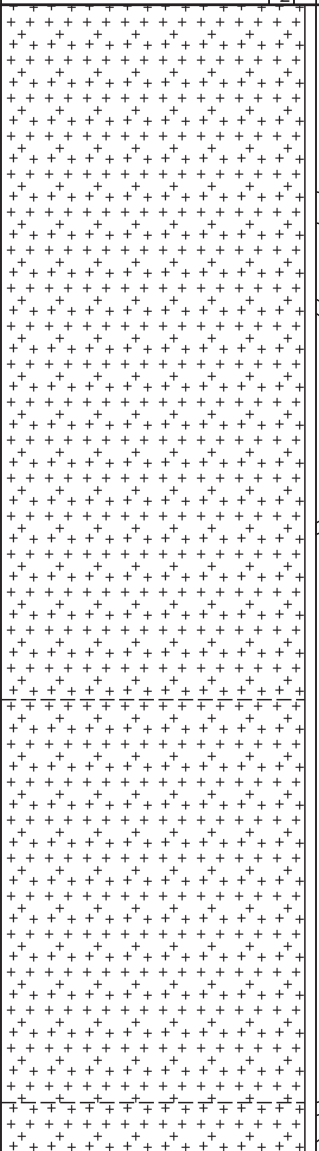Core No. [Total interval]:   3 [2,036 - 2,046 m]
Core Recovery: 7.20 m
Core Diameter: 6.5 cm
Date of Coring: Feb. 2000

Displayed Box [interval]:   7 [2,039 - 2,040 m]
Date of Core Inspection: 07.10.2009

Photo	Lithology & Grain size							Sedimentary Structures	Sorting	Rounding	Core Description
Depth Top: 2,039 m	Clay (C)	Silt (U)	f-Sand (fS)	m-Sand (mS)	c-Sand (cS)	Granule (g)	Pebble (p)				
									good	angular	sandstone (qtz!), homogeneous + muscovite No HCl-reaction!
									good	angular	sandstone (qtz!), laminated + muscovite No HCl-reaction!

Depth Bottom: 2,040 m

DEFINITION OF TOP-CRYSTALLINE BASEMENT
IN THE AUSTRIAN MOLASSE BASIN

Gloria Thürschmid

Well: BH-N-001

Core No. [Total interval]:   3 [2,036 - 2,046 m]
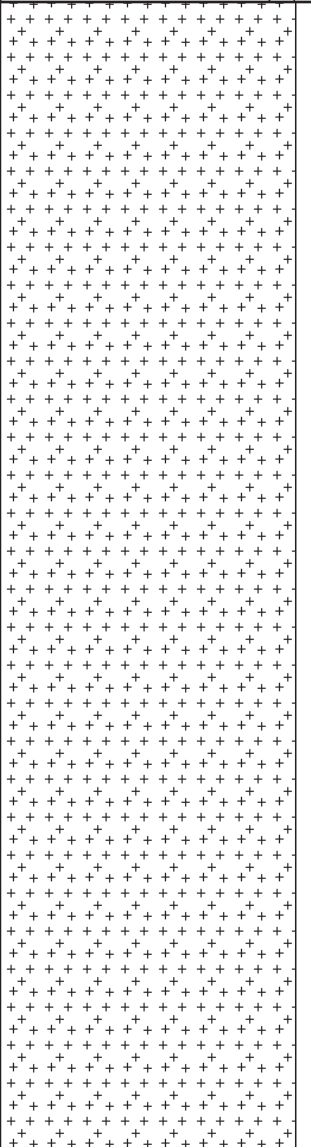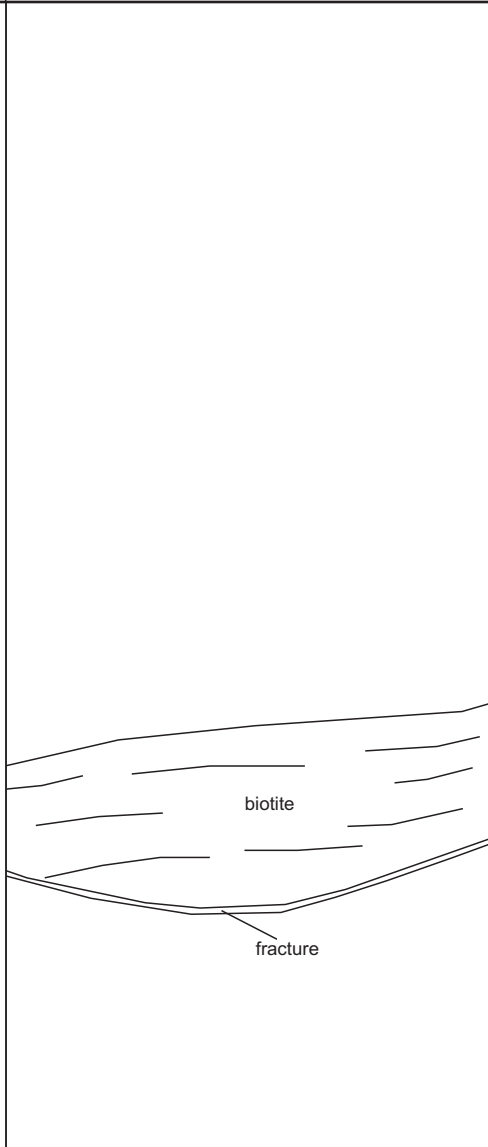Core Recovery: 7.20 m
Core Diameter: 6.5 cm
Date of Coring: Feb. 2000

Displayed Box [interval]:   6 [2,040 - 2,041 m]
Date of Core Inspection: 07.10.2009

Photo Depth Top: 2,040 m	Lithology & Grain size							Sedimentary Structures	Sorting	Rounding	Core Description
	Clay (C)	Silt (U)	f-Sand (fS)	m-Sand (mS)	c-Sand (cS)	Granule (g)	Pebble (p)				
									good	angular	sandstone (qtz!), mostly homogeneous, some scattered granules / pebbles, partly laminated + muscovite No HCl-reaction!

Depth Bottom: 2,041 m

DEFINITION OF TOP-CRYSTALLINE BASEMENT
IN THE AUSTRIAN MOLASSE BASIN

Gloria Thürschmid

Well: BH-N-001

Core No. [Total interval]:   3 [2,036 - 2,046 m]
Core Recovery: 7.20 m
Core Diameter: 6.5 cm
Date of Coring: Feb. 2000

Displayed Box [interval]:   5 [2,041 - 2,042 m]
Date of Core Inspection: 07.10.2009

Photo Depth Top: 2,041 m	Lithology & Grain size							Sedimentary Structures	Sorting	Rounding	Core Description
	Clay (C)	Silt (U)	f-Sand (fS)	m-Sand (mS)	c-Sand (cS)	Granule (g)	Pebble (p)				
									good	angular	sandstone (qtz!), layers of scattered granules / pebbles (> 3 cm), + muscovite No HCl-reaction!
									medium		
									good		
									medium		
									medium		
									good		fracture

Depth Bottom: 2,042 m

DEFINITION OF TOP-CRYSTALLINE BASEMENT
IN THE AUSTRIAN MOLASSE BASIN

Gloria Thürschmid

Well: BH-N-001

Core No. [Total interval]:   3 [2,036 - 2,046 m]
Core Recovery: 7.20 m
Core Diameter: 6.5 cm
Date of Coring: Feb. 2000

Displayed Box [interval]:   4 [2,042 - 2,043 m]
Date of Core Inspection: 07.10.2009

Photo Depth Top: 2,042 m	C	U	fS	mS	cS	g	p	(Sedimentary) Structures	(Sorting)	(Rounding)	Core Description
						fine	medium coarse		medium	angular	qtz-sandstone, some scattered granules / pebbles (> 3 cm), + muscovite No HCl-reaction!
								TS			crystalline - ?granite, medium to coarse-grained (maximum crystal size of ~5 mm), bright grey, partly fractures with striation (with chlorite), mostly homogeneous
											general trend: crystal size decreases with depth

Depth Bottom: 2,043 m

TS **.... Thin section**

DEFINITION OF TOP-CRYSTALLINE BASEMENT
IN THE AUSTRIAN MOLASSE BASIN

Gloria Thürschmid

Well: **BH-N-001**

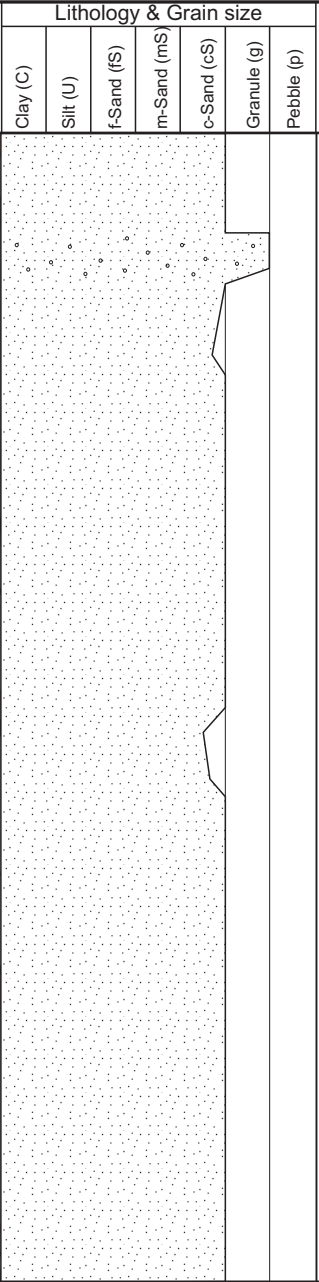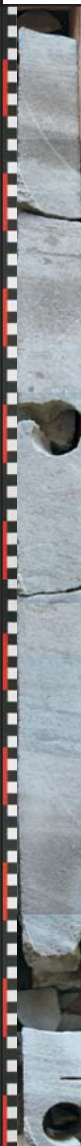Core No. [Total interval]: 3 [2,036 - 2,046 m]
Core Recovery: 7.20 m
Core Diameter: 6.5 cm
Date of Coring: Feb. 2000

Displayed Box [interval]: 3 [2,043 - 2,044 m]
Date of Core Inspection: 07.10.2009

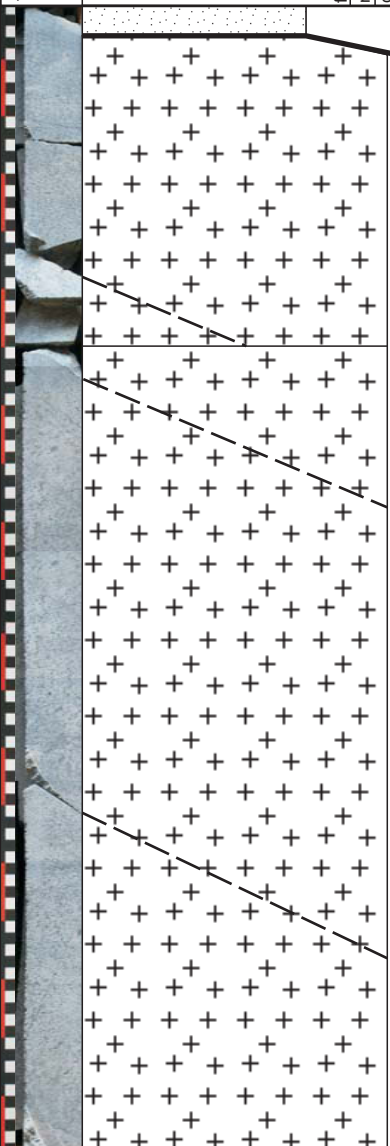| Photo Depth Top: 2,043 m	fine-grained / medium-grained / coarse-grained	Structures	Core Description
			crystalline - ?granite (feldspar, quartz, mica), unweathered, homogeneous, fine to medium-grained (max. crystal size ~5 mm)
			crystalline - ?granite (feldspar, quartz, mica), unweathered, coarse-grained (max. feldspar-crystal size ~2,5 cm)
			crystalline - ?granite (feldspar, quartz, mica!), great amount of biotite, unweathered, homogeneous, fine grained
			crystalline - ?granite (feldspar, quartz, mica), unweathered, coarse-grained (max. feldspar-crystal size ~2 cm)
			crystalline - ?granite (feldspar, quartz, mica), unweathered, homogeneous, fine to medium-grained (max. feldspar-crystal size ~4 mm)

Depth Bottom: 2,044 m

DEFINITION OF TOP-CRYSTALLINE BASEMENT
IN THE AUSTRIAN MOLASSE BASIN

Gloria Thürschmid

Well: BH-N-001

Core No. [Total interval]:   3 [2,036 - 2,046 m]
Core Recovery: 7.20 m
Core Diameter: 6.5 cm
Date of Coring: Feb. 2000

Displayed Box [interval]:   2 [2,044 - 2,045 m]
Date of Core Inspection: 07.10.2009

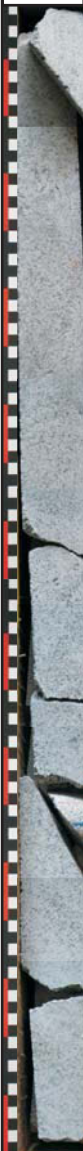| Photo Depth Top: 2,044 m		fine-grained / medium-grained / coarse-grained	Structures	Core Description
				crystalline - ?granite (feldspar, quartz, mica), unweathered, more/less homogeneous, medium-grained, bright colour
				fracture with slickenside and reddish-brown coating

Depth Bottom: 2,045 m

DEFINITION OF TOP-CRYSTALLINE BASEMENT
IN THE AUSTRIAN MOLASSE BASIN

Gloria Thürschmid

Well: BH-N-001

Core No. [Total interval]: 3 [2,036 - 2,046 m]
Core Recovery: 7.20 m
Core Diameter: 6.5 cm
Date of Coring: Feb. 2000

Displayed Box [interval]: 1 [2,045 - 2,046 m]
Date of Core Inspection: 07.10.2009

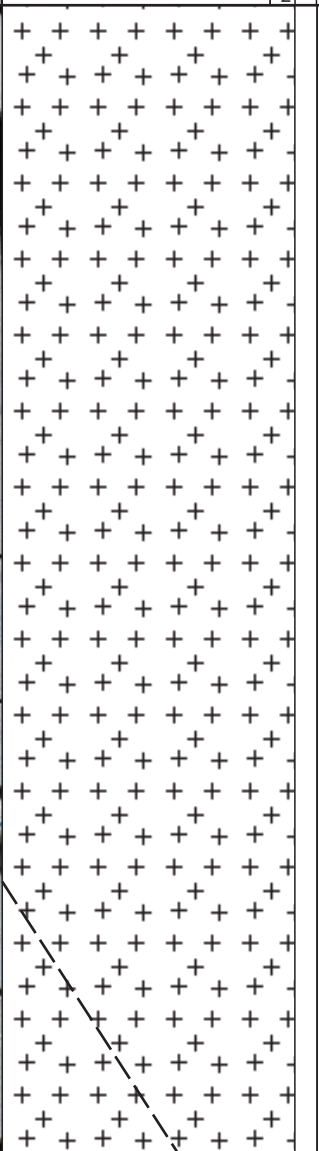| Photo Depth Top: 2,045 m	fine-grained medium-grained coarse-grained	Structures	Core Description
			crystalline - ?granite (feldspar, quartz, mica), unweathered, more/less homogeneous, medium-grained (max. crystal size ~2 mm), bright colour, partly accumulation of feldspar-minerals
			fractures with slickenside and chlorite-coating

Depth Bottom: 2,046 m

DEFINITION OF TOP-CRYSTALLINE BASEMENT
IN THE AUSTRIAN MOLASSE BASIN

Gloria Thürschmid

Well: HIER-002A

Core No. [Total interval]: 3 [2,577 - 2,595 m]
Core Recovery: 18 m
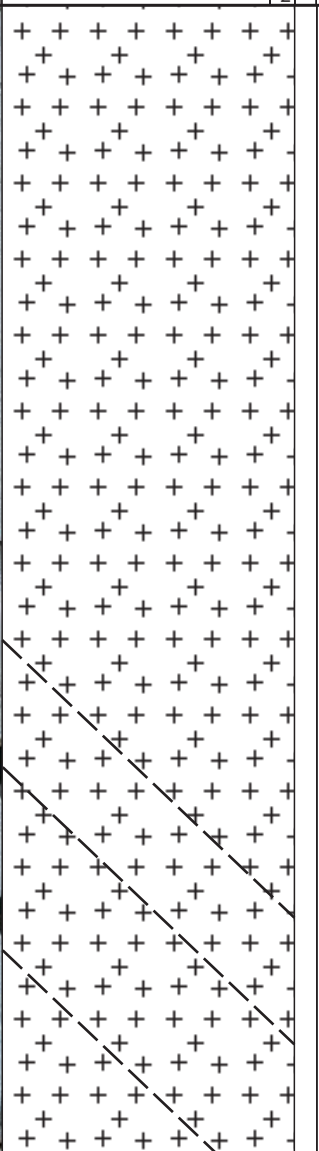Core Diameter: 6.5 cm
Date of Coring: Feb. 2007

Displayed Box [interval]: 19 [2,576.33 - 2,577 m]
Date of Core Inspection: 07.10.2009

Photo Depth Top: 2,576.33	Lithology & Grain size							Sedimentary Structures	Sorting	Rounding	Core Description
	Clay (C)	Silt (U)	f-Sand (fS)	m-Sand (mS)	c-Sand (cS)	Granule (g)	Pebble (p)				
									good	angular	qtz-sandstone (medium-grained), laminated, contains muscovite, no reaction to HCl, beige/grey colour, partly dark areas of slickenside
									good		sandy mudstone, dark grey, fractured!

Depth Bottom: 2,577 m

Well: HIER-002A

Core No. [Total interval]: 3 [2,577 - 2,595 m]
Core Recovery: 18 m
Core Diameter: 6.5 cm
Date of Coring: Feb. 2007

Displayed Box [interval]: 18 [2,577 - 2,578 m]
Date of Core Inspection: 07.10.2009

Photo	Lithology & Grain size							Sedimentary Structures	Sorting	Rounding	Core Description
Depth Top: 2,577 m	Clay (C)	Silt (U)	f-Sand (fS)	m-Sand (mS)	c-Sand (cS)	Granule (g)	Pebble (p)				
									good-normal	angular	qtz-sandstone (medium-grained), laminated, contains muscovite, no reaction to HCl, beige/grey colour, partly some coarser components (?qtz-grains) at the top and near the bottom of this lithology section (see also fracture at the top)
											grain size increases (coarse-grained)!
											coarser components!
									good		sandy mudstone, dark grey, massive
											transition zone
									good	angular	qtz-sandstone (medium-grained), laminated, contains muscovite, no reaction to HCl, beige/grey colour

Depth Bottom: 2,578 m

Well: HIER-002A

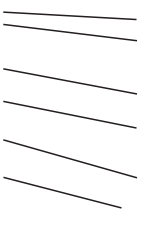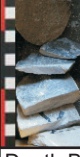Core No. [Total interval]:   3 [2,577 - 2,595 m]
Core Recovery: 18 m
Core Diameter: 6.5 cm
Date of Coring: Feb. 2007
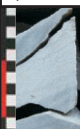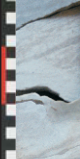
Displayed Box [interval]:   17 [2,578 - 2,579 m]
Date of Core Inspection: 07.10.2009

| Photo Depth Top: 2,578 m | Lithology & Grain size | | | | | | | Sedimentary Structures | Sorting | Rounding | Core Description |
	Clay (C)	Silt (U)	f-Sand (fS)	m-Sand (mS)	c-Sand (cS)	Granule (g)	Pebble (p)				
									good		sandy mudstone, dark grey, fractured, slight laminations
									good-normal	angular	qtz-sandstone (fine-grained at the top, coarse-grained at the bottom), laminated, contains muscovite, no reaction to HCl, beige/grey colour grain size increases with depth!

Depth Bottom: 2,579 m

Well: **HIER-002A**

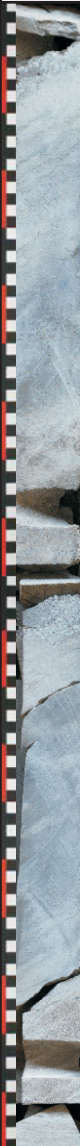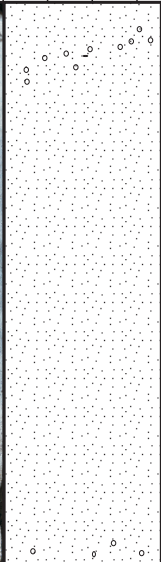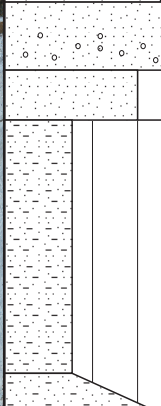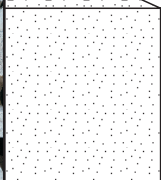Core No. [Total interval]: 3 [2,577 - 2,595 m]
Core Recovery: 18 m
Core Diameter: 6.5 cm
Date of Coring: Feb. 2007

Displayed Box [interval]: 16 [2,579 - 2,580 m]
Date of Core Inspection: 07.10.2009

Photo Depth Top: 2,579 m	Lithology & Grain size							Sedimentary Structures	Sorting	Rounding	Core Description
	Clay (C)	Silt (U)	f-Sand (fS)	m-Sand (mS)	c-Sand (cS)	Granule (g)	Pebble (p)				
									good	angular	qtz-sandstone (varying grain size), partly laminated, contains muscovite, no reaction to HCl, beige/grey colour
											fracture!

Depth Bottom: 2,580 m

Well: HIER-002A

Core No. [Total interval]: 3 [2,577 - 2,595 m]
Core Recovery: 18 m
Core Diameter: 6.5 cm
Date of Coring: Feb. 2007

Displayed Box [interval]: 15 [2,580 - 2,581 m]
Date of Core Inspection: 07.10.2009

Photo Depth Top: 2,580 m	Lithology & Grain size							Sedimentary Structures	Sorting	Rounding	Core Description
	Clay (C)	Silt (U)	f-Sand (fS)	m-Sand (mS)	c-Sand (cS)	Granule (g)	Pebble (p)				
									good	angular	qtz-sandstone (coarse-grained), partly laminated, contains muscovite, no reaction to HCl, beige/grey colour
											fine-grained qtz-sandstone
									good		mudstone, fractured, more/less homogeneous, dark grey colour
Depth Bottom: 2,581m											

DEFINITION OF TOP-CRYSTALLINE BASEMENT
IN THE AUSTRIAN MOLASSE BASIN

Gloria Thürschmid
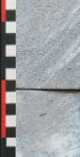
Well: HIER-002A

Core No. [Total interval]:   3 [2,577 - 2,595 m]
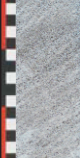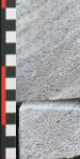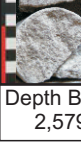Core Recovery: 18 m
Core Diameter: 6.5 cm
Date of Coring: Feb. 2007

Displayed Box [interval]:   14 [2,581 - 2,582 m]
Date of Core Inspection: 07.10.2009

Photo Depth Top: 2,581 m	Lithology & Grain size							Sedimentary Structures	Sorting	Rounding	Core Description
	Clay (C)	Silt (U)	f-Sand (fS)	m-Sand (mS)	c-Sand (cS)	Granule (g)	Pebble (p)				
									good		mudstone, fractured, more/less homogeneous, dark grey colour
											coaly material, partly laminated, weak, fractured
									good		shaly/coaly section, laminated
											coaly material, partly laminated, weak, fractured
									good		shaly/coaly section, laminated, fractured

Depth Bottom: 2,582 m

DEFINITION OF TOP-CRYSTALLINE BASEMENT
IN THE AUSTRIAN MOLASSE BASIN

Gloria Thürschmid

Well: HIER-002A

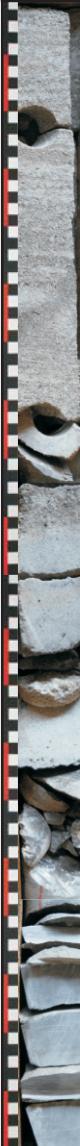Core No. [Total interval]: 3 [2,577 - 2,595 m]
Core Recovery: 18 m
Core Diameter: 6.5 cm
Date of Coring: Feb. 2007
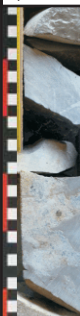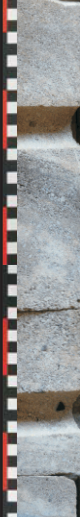
Displayed Box [interval]: 13 [2,582 - 2,583 m]
Date of Core Inspection: 07.10.2009

Photo Depth Top: 2,582 m	Lithology & Grain size							Sedimentary Structures	Sorting	Rounding	Core Description
	Clay (C)	Silt (U)	f-Sand (fS)	m-Sand (mS)	c-Sand (cS)	Granule (g)	Pebble (p)				
									good		mudstone, fractured, more/less homogeneous, dark grey colour
									good-normal	angular	sandstone (medium to coarse-grained), beige/grey colour, more/less homogeneous, slight laminations visible, few ?pyrite components
									good-normal		sandy/shaly phase
									normal	sub-angular	sandstone (very coarse-grained) or well cemented qtz-conglomerate, beige/grey colour, very coarse components (qtz) with size of approx. 8 mm

Depth Bottom: 2,583 m

DEFINITION OF TOP-CRYSTALLINE BASEMENT
IN THE AUSTRIAN MOLASSE BASIN

Gloria Thürschmid

Well: HIER-002A

Core No. [Total interval]:   3 [2,577 - 2,595 m]
Core Recovery: 18 m
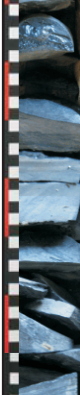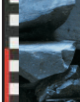Core Diameter: 6.5 cm
Date of Coring: Feb. 2007

Displayed Box [interval]:   12 [2,583 - 2,584 m]
Date of Core Inspection: 07.10.2009

Photo Depth Top: 2,583 m	Lithology & Grain size							Sedimentary Structures	Sorting	Rounding	Core Description
	Clay (C)	Silt (U)	f-Sand (fS)	m-Sand (mS)	c-Sand (cS)	Granule (g)	Pebble (p)				
									normal	sub-angular	sandstone (very coarse-grained) or well cemented qtz-conglomerate, beige/grey colour, very coarse qtz-grains (approx. 8 mm), more/less homogeneous
											change of orientation of lamination!
											component of ?crystalline (fine-grained)
											grain size decreases to medium-grained sandstone, laminations visible
											coarse-grained sandstone

Depth Bottom: 2,584 m

DEFINITION OF TOP-CRYSTALLINE BASEMENT
IN THE AUSTRIAN MOLASSE BASIN

Gloria Thürschmid

Well: **HIER-002A**

Core No. [Total interval]:   3 [2,577 - 2,595 m]
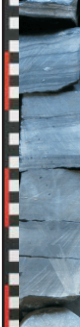Core Recovery: 18 m
Core Diameter: 6.5 cm
Date of Coring: Feb. 2007

Displayed Box [interval]:   11 [2,584 - 2,585 m]
Date of Core Inspection: 07.10.2009

Photo Depth Top: 2,584 m	Lithology & Grain size							Sedimentary Structures	Sorting	Rounding	Core Description
	Clay (C)	Silt (U)	f-Sand (fS)	m-Sand (mS)	c-Sand (cS)	Granule (g)	Pebble (p)				
									normal	sub-angular	sandstone (medium to coarse-grained), beige/grey colour, more/less homogeneous, slight laminations visible, but mainly massive
											fracture
											fracture

Depth Bottom: 2,585 m

Well: HIER-002A
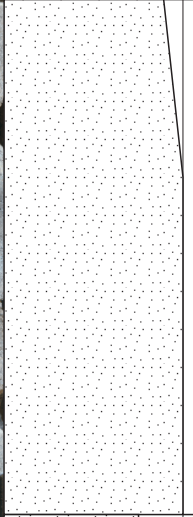
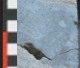Core No. [Total interval]:   3 [2,577 - 2,595 m]
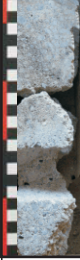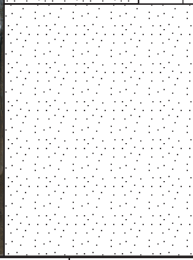Core Recovery: 18 m
Core Diameter: 6.5 cm
Date of Coring: Feb. 2007

Displayed Box [interval]:   10 [2,585 - 2,586 m]
Date of Core Inspection: 07.10.2009

Photo Depth Top: 2,585 m	Lithology & Grain size							Sedimentary Structures	Sorting	Rounding	Core Description
	Clay (C)	Silt (U)	f-Sand (fS)	m-Sand (mS)	c-Sand (cS)	Granule (g)	Pebble (p)				
									normal	sub-angular	sandstone (medium to coarse-grained), beige/grey colour, more/less homogeneous, slight laminations visible, but mainly massive
											fine-grained phase (?shale)
											fracture
											change of colour from beige-grey to light grey (coarse-grained), variation in orientation of laminations

Depth Bottom: 2,586 m

DEFINITION OF TOP-CRYSTALLINE BASEMENT
IN THE AUSTRIAN MOLASSE BASIN

Gloria Thürschmid

Well: HIER-002A

Core No. [Total interval]:   3 [2,577 - 2,595 m]
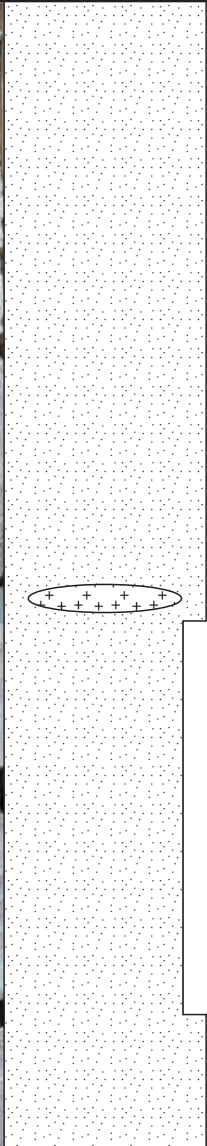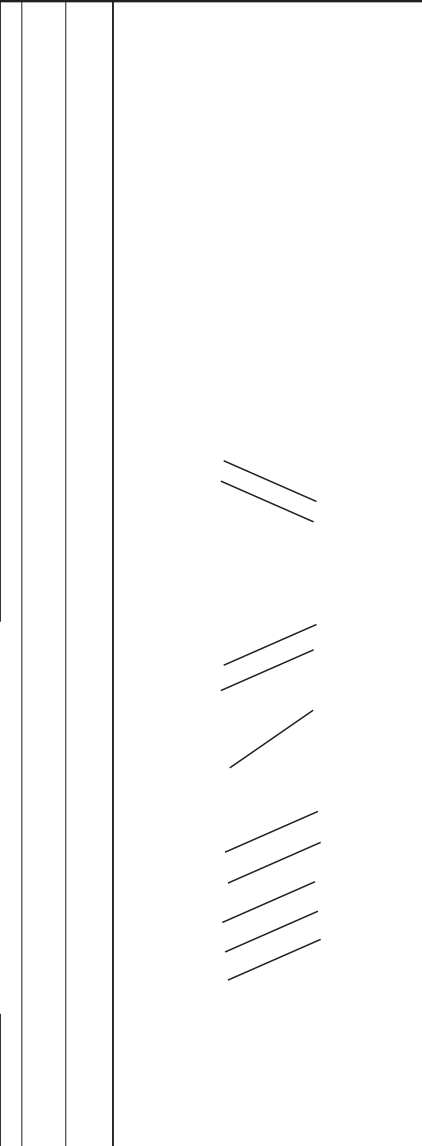Core Recovery: 18 m
Core Diameter: 6.5 cm
Date of Coring: Feb. 2007

Displayed Box [interval]:   9 [2,586 - 2,587 m]
Date of Core Inspection: 07.10.2009

Photo Depth Top: 2,586 m	C U fS mS cS g p (fine medium coarse)	(Sedimentary) Structures	(Sorting)	(Rounding)	Core Description
			good	sub-angular	sandstone (fine to medium-grained), beige/grey colour, more/less homogeneous, mainly massive
		TS			crystalline/granite (sharp boundary, although difficult to see), fine to medium-grained, grey colour, larger ?qtz-grains included, main grain size of approx. 3 mm; fsp, mu grains; green phases (?chlorite), more/less homogeneous, partly fractured

Depth Bottom: 2,587 m

TS .... **Thin section**

DEFINITION OF TOP-CRYSTALLINE BASEMENT
IN THE AUSTRIAN MOLASSE BASIN

Gloria Thürschmid

Well: HIER-002A

Core No. [Total interval]: 3 [2,577 - 2,595 m]
Core Recovery: 18 m
Core Diameter: 6.5 cm
Date of Coring: Feb. 2007

Displayed Box [interval]: 8 [2,587 - 2,588 m]
Date of Core Inspection: 07.10.2009

Photo Depth Top: 2,587 m		fine-grained	medium-grained	coarse-grained	Structures	Core Description
						crystalline (?granite), fine to medium-grained, grey colour, larger components included, main grain size of approx. 3 mm; fsp, mu grains; green phases, more/less homogeneous, partly fractured

Depth Bottom: 2,588 m

DEFINITION OF TOP-CRYSTALLINE BASEMENT
IN THE AUSTRIAN MOLASSE BASIN

Gloria Thürschmid

Well: HIER-002A

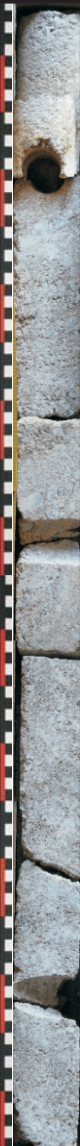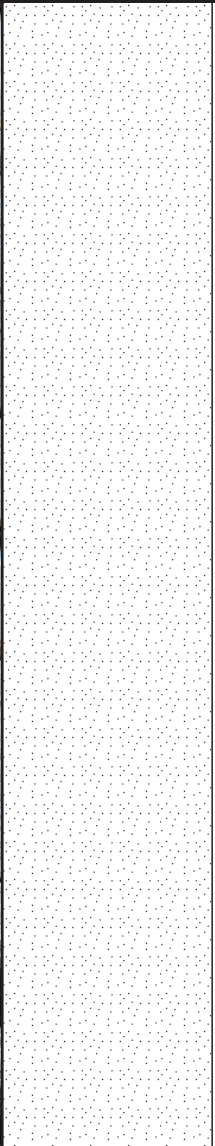Core No. [Total interval]: 3 [2,577 - 2,595 m]
Core Recovery: 18 m
Core Diameter: 6.5 cm
Date of Coring: Feb. 2007

Displayed Box [interval]: 7 [2,588 - 2,589 m]
Date of Core Inspection: 07.10.2009

Photo Depth Top: 2,589 m	fine-grained	medium-grained	coarse-grained	Structures	Core Description
					crystalline (?granite), fine to medium-grained, grey colour, main grain size of approx. 3 mm; fsp, mu grains; green phases, more/less homogeneous, strongly fractured, slickenside

Depth Bottom: 2,589 m

DEFINITION OF TOP-CRYSTALLINE BASEMENT
IN THE AUSTRIAN MOLASSE BASIN

Gloria Thürschmid

Well: HIER-002A

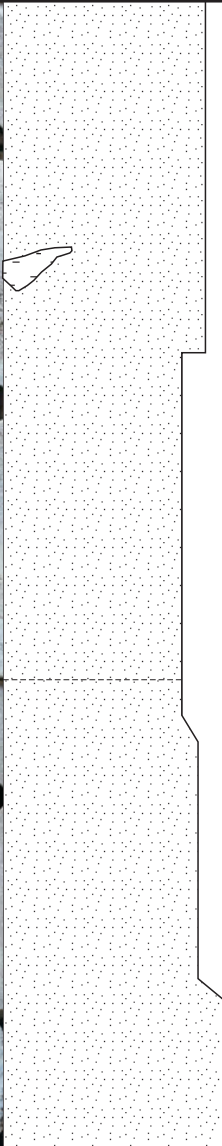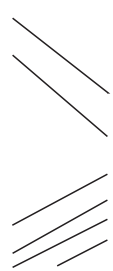Core No. [Total interval]: 3 [2,577 - 2,595 m]
Core Recovery: 18 m
Core Diameter: 6.5 cm
Date of Coring: Feb. 2007

Displayed Box [interval]: 6 [2,589 - 2,590 m]
Date of Core Inspection: 07.10.2009

Photo Depth Top: 2,589 m	fine-grained	medium-grained	coarse-grained	Structures	Core Description
?					crystalline (?granite), fine to medium-grained, grey colour, larger components included, main grain size of approx. 3 mm; fsp, mu grains; green phases, more/less homogeneous, partly fractured
					?pyrite component

Depth Bottom: 2,590 m

DEFINITION OF TOP-CRYSTALLINE BASEMENT
IN THE AUSTRIAN MOLASSE BASIN

Gloria Thürschmid

Well: **HIER-002A**

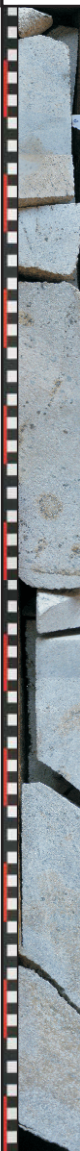Core No. [Total interval]: 3 [2,577 - 2,595 m]
Core Recovery: 18 m
Core Diameter: 6.5 cm
Date of Coring: Feb. 2007

Displayed Box [interval]: 5 [2,590 - 2,591 m]
Date of Core Inspection: 07.10.2009

Photo Depth Top: 2,590 m		fine-grained	medium-grained	coarse-grained	Structures	Core Description
						crystalline (?granite), coarse-grained (up to approx. 8 mm), larger ?qtz grains included; fsp, mu grains; green phases, ?pyrite, more/less homogeneous, fractured

Depth Bottom: 2,591 m

DEFINITION OF TOP-CRYSTALLINE BASEMENT
IN THE AUSTRIAN MOLASSE BASIN

Gloria Thürschmid

Well: HIER-002A

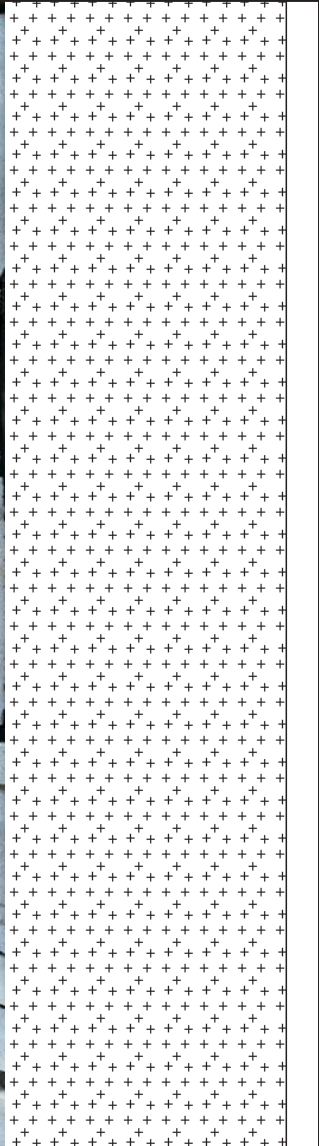Core No. [Total interval]: 3 [2,577 - 2,595 m]
Core Recovery: 18 m
Core Diameter: 6.5 cm
Date of Coring: Feb. 2007

Displayed Box [interval]: 4 [2,591 - 2,592 m]
Date of Core Inspection: 07.10.2009

Photo Depth Top: 2,591 m		fine-grained	medium-grained	coarse-grained	Structures	Core Description
						crystalline (?granite), coarse-grained; fsp, mu grains; green phases, more/less homogeneous, fractured
						fine-grained crystalline (size below 1 mm)

Depth Bottom: 2,592 m

Well: HIER-002A

Core No. [Total interval]:   3 [2,577 - 2,595 m]
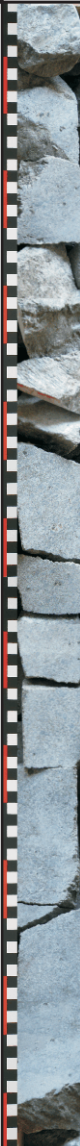Core Recovery: 18 m
Core Diameter: 6.5 cm
Date of Coring: Feb. 2007

Displayed Box [interval]:   3 [2,592 - 2,593 m]
Date of Core Inspection: 07.10.2009

Photo Depth Top: 2,592 m		fine-grained	medium-grained	coarse-grained	Structures	Core Description
						crystalline (?granite), coarse-grained, larger components included; fsp, mu grains; green phases, more/less homogeneous
						fractures!

Depth Bottom: 2,593 m

Well: HIER-002A

Core No. [Total interval]:   3 [2,577 - 2,595 m]
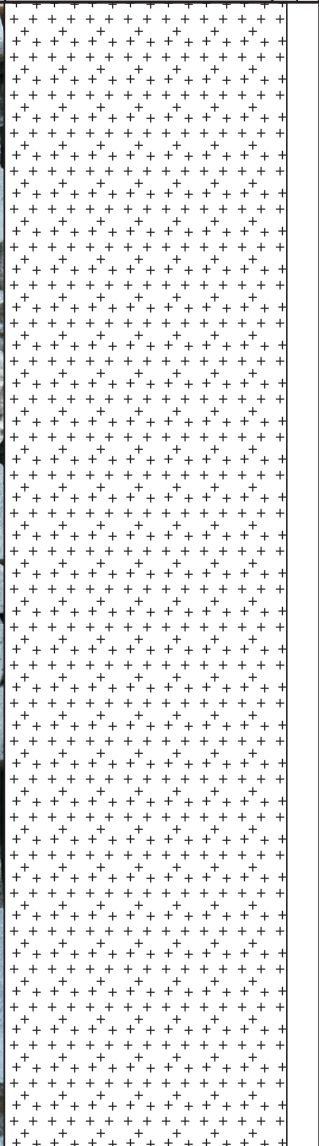Core Recovery: 18 m
Core Diameter: 6.5 cm
Date of Coring: Feb. 2007

Displayed Box [interval]:   2 [2,593 - 2,594 m]
Date of Core Inspection: 07.10.2009

Photo Depth Top: 2,593 m	fine-grained / medium-grained / coarse-grained	Structures	Core Description
			crystalline (?granite), coarse-grained, larger components included; fsp, mu grains; green phases, more/less homogeneous, fractured
			large components (fine-grained)
			change to fine-grained crystalline (size below 1 mm)
			fracture zone

Depth Bottom: 2,594 m

DEFINITION OF TOP-CRYSTALLINE BASEMENT
IN THE AUSTRIAN MOLASSE BASIN

Gloria Thürschmid

Well: HIER-002A

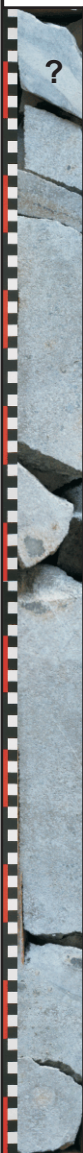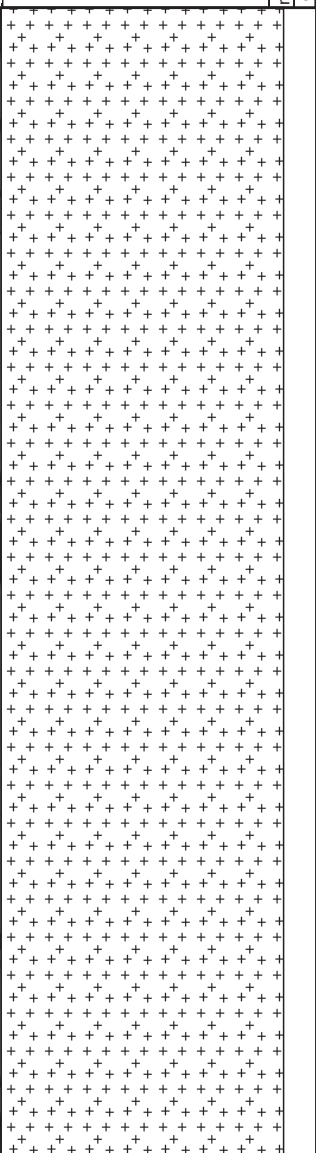Core No. [Total interval]:   3 [2,577 - 2,595 m]
Core Recovery: 18 m
Core Diameter: 6.5 cm
Date of Coring: Feb. 2007

Displayed Box [interval]:   1 [2,594 - 2,595 m]
Date of Core Inspection: 07.10.2009

Photo Depth Top: 2,594 m		fine-grained / medium-grained / coarse-grained	Structures	Core Description
				crystalline (?granite), fine-grained; fsp, mu grains; green phases, more/less homogeneous, partly fractured

Depth Bottom: 2,595 m

Well: MLRT-003C

Core No. [Total interval]:   4 [3,604 - 3,622 m]
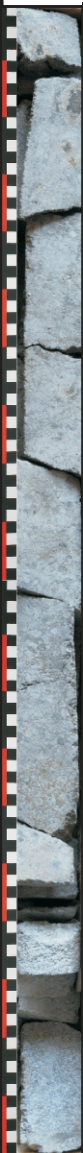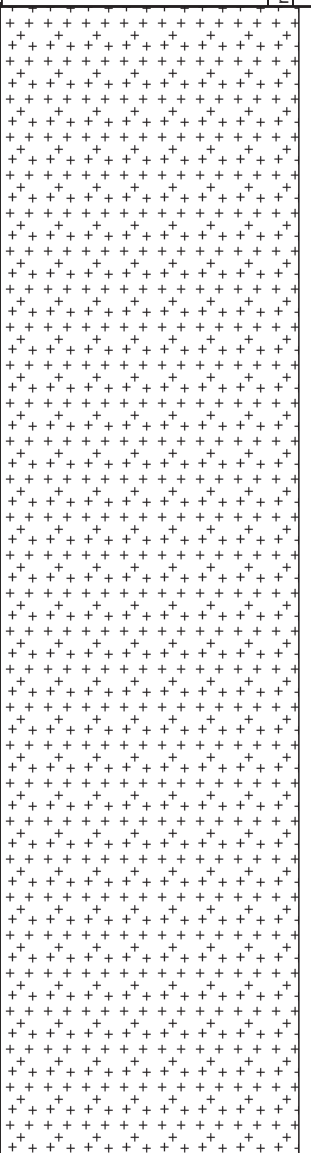Core Recovery: 16 m
Core Diameter: 6.5 cm
Date of Coring: 2008

Displayed Box [interval]:   17 [3,605 - 3,606 m]
Date of Core Inspection: 16.10.2009

Photo Depth Top: 3,605 m	Lithology & Grain size							Sedimentary Structures	Sorting	Rounding	Core Description
	Clay (C)	Silt (U)	f-Sand (fS)	m-Sand (mS)	c-Sand (cS)	Granule (g)	Pebble (p)				
									good-normal		mudstone, dark brown/grey, some shell remnants visible (HCl reaction!), mostly homogeneous

Depth Bottom: 3,606 m

Well: MLRT-003C

Core No. [Total interval]:   4 [3,604 - 3,622 m]
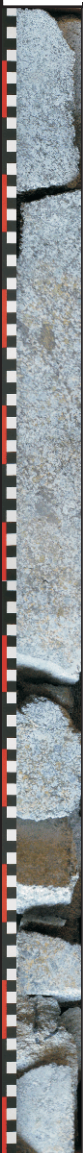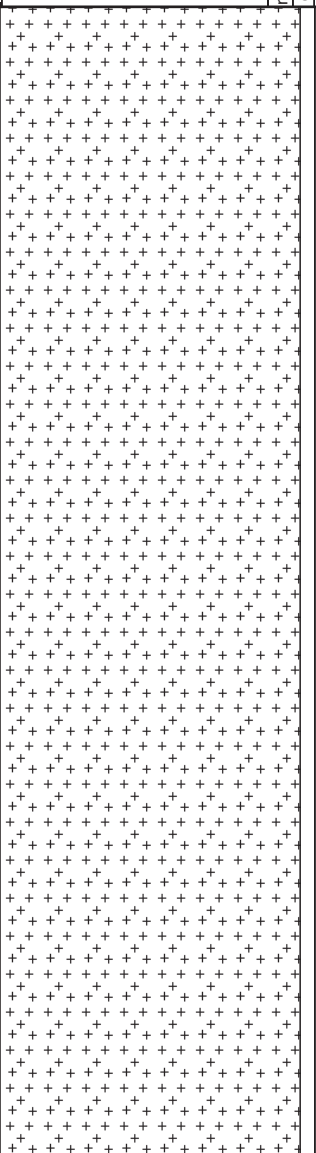Core Recovery: 16 m
Core Diameter: 6.5 cm
Date of Coring: 2008

Displayed Box [interval]:   16 [3,606 - 3,607 m]
Date of Core Inspection: 16.10.2009

Photo Depth Top: 3,606 m	Lithology & Grain size							Sedimentary Structures	Sorting	Rounding	Core Description
	Clay (C)	Silt (U)	f-Sand (fS)	m-Sand (mS)	c-Sand (cS)	Granule (g)	Pebble (p)				
									good-normal		mudstone, dark brown/grey, partly laminated, some shell remnants visible (HCl reaction!), mostly homogeneous
											extremely fractured !

Depth Bottom: 3,607 m

Well: MLRT-003C

Core No. [Total interval]:   4 [3,604 - 3,622 m]
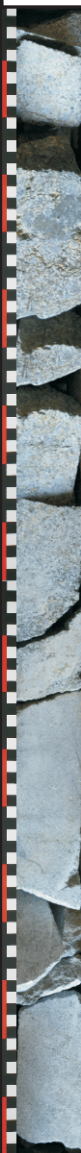Core Recovery: 16 m
Core Diameter: 6.5 cm
Date of Coring: 2008

Displayed Box [interval]:   15 [3,607 - 3,608 m]
Date of Core Inspection: 16.10.2009

Photo Depth Top: 3,607 m	Lithology & Grain size							Sedimentary Structures	Sorting	Rounding	Core Description
	Clay (C)	Silt (U)	f-Sand (fS)	m-Sand (mS)	c-Sand (cS)	Granule (g)	Pebble (p)				
									good-normal		mudstone, dark brown/grey, ?coaly, some shell remnants visible (HCl reaction!), mostly homogeneous, very weak (can be scratched with fingernail)
											numerous shells !
											extremely fractured ! (white phases of less than 1 mm in size)

Depth Bottom: 3,608 m

DEFINITION OF TOP-CRYSTALLINE BASEMENT
IN THE AUSTRIAN MOLASSE BASIN

Gloria Thürschmid

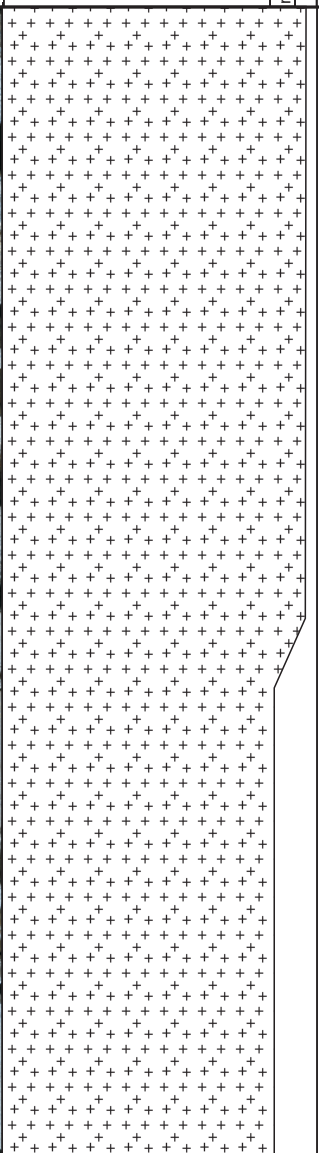# Well: MLRT-003C

Core No. [Total interval]:   4 [3,604 - 3,622 m]
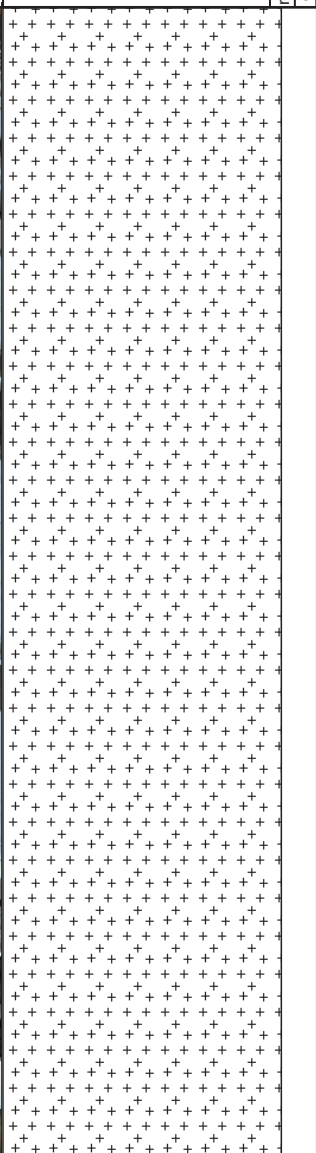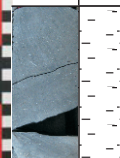Core Recovery: 16 m
Core Diameter: 6.5 cm
Date of Coring: 2008

Displayed Box [interval]:   14 [3,608 - 3,609 m]
Date of Core Inspection: 16.10.2009

Photo Depth Top: 3,608 m	Lithology & Grain size							Sedimentary Structures	Sorting	Rounding	Core Description
	Clay (C)	Silt (U)	f-Sand (fS)	m-Sand (mS)	c-Sand (cS)	Granule (g)	Pebble (p)				
									good-normal		mudstone, dark brown/grey, partly laminated, mostly homogeneous, some effects of weathering of thin coal layers visible extremely fractured !

Depth Bottom: 3,609 m

Well: MLRT-003C

Core No. [Total interval]:   4 [3,604 - 3,622 m]
Core Recovery: 16 m
Core Diameter: 6.5 cm
Date of Coring: 2008

Displayed Box [interval]:   13 [3,609 - 3,610 m]
Date of Core Inspection: 16.10.2009

Photo Depth Top: 3,609 m	Lithology & Grain size							Sedimentary Structures	Sorting	Rounding	Core Description
	Clay (C)	Silt (U)	f-Sand (fS)	m-Sand (mS)	c-Sand (cS)	Granule (g)	Pebble (p)				
									good-normal		mudstone, dark brown/grey, some shell remnants visible (HCl reaction!), mostly homogeneous
									good		transition zone (no sharp boundary!): mudstone - sandstone, fine-grained
									good		sandstone (fine-grained), light grey colour

Depth Bottom: 3,610 m

Well: MLRT-003C

Core No. [Total interval]:   4 [3,604 - 3,622 m]
Core Recovery: 16 m
Core Diameter: 6.5 cm
Date of Coring: 2008

Displayed Box [interval]:   12 [3,610 - 3,611 m]
Date of Core Inspection: 16.10.2009

Photo Depth Top: 3,610 m	Lithology & Grain size							Sedimentary Structures	Sorting	Rounding	Core Description
	Clay (C)	Silt (U)	f-Sand (fS)	m-Sand (mS)	c-Sand (cS)	Granule (g)	Pebble (p)				
									good	angular	sandstone (medium to coarse-grained), light grey colour, homogeneous

Depth Bottom: 3,611 m

DEFINITION OF TOP-CRYSTALLINE BASEMENT
IN THE AUSTRIAN MOLASSE BASIN

Gloria Thürschmid

Well: MLRT-003C
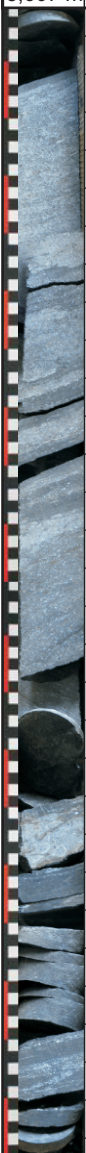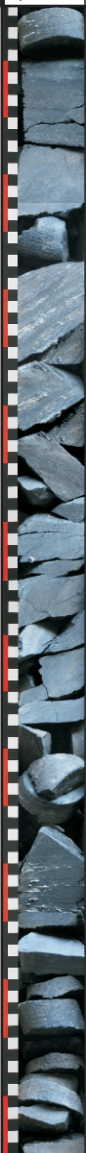
Core No. [Total interval]: 4 [3,604 - 3,622 m]
Core Recovery: 16 m
Core Diameter: 6.5 cm
Date of Coring: 2008

Displayed Box [interval]: 11 [3,611 - 3,612 m]
Date of Core Inspection: 16.10.2009

Photo Depth Top: 3,611 m	Lithology & Grain size							Sedimentary Structures	Sorting	Rounding	Core Description
	Clay (C)	Silt (U)	f-Sand (fS)	m-Sand (mS)	c-Sand (cS)	Granule (g)	Pebble (p)				
									good	sub-angular	sandstone (fine to medium-grained), light grey colour
									good	sub-angular	sandstone (medium to coarse-grained), light grey colour

Depth Bottom: 3,612 m

Well: **MLRT-003C**

Core No. [Total interval]: 4 [3,604 - 3,622 m]
Core Recovery: 16 m
Core Diameter: 6.5 cm
Date of Coring: 2008

Displayed Box [interval]: 10 [3,612 - 3,613 m]
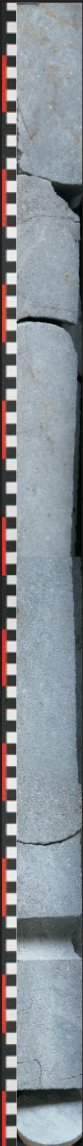Date of Core Inspection: 16.10.2009

Photo / Depth Top: 3,612 m	Lithology & Grain size							Sedimentary Structures	Sorting	Rounding	Core Description
	Clay (C)	Silt (U)	f-Sand (fS)	m-Sand (mS)	c-Sand (cS)	Granule (g)	Pebble (p)				
									good	sub-angular	sandstone (medium to coarse-grained), light grey colour, max. size of qtz-grains is approx. 1.3 cm
									good	sub-angular	sandstone (fine-grained), light grey

Depth Bottom: 3,613 m

DEFINITION OF TOP-CRYSTALLINE BASEMENT
IN THE AUSTRIAN MOLASSE BASIN

Gloria Thürschmid

Well: MLRT-003C

Core No. [Total interval]: 4 [3,604 - 3,622 m]
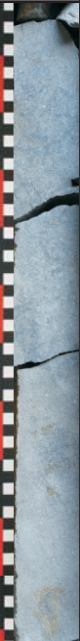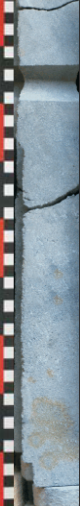Core Recovery: 16 m
Core Diameter: 6.5 cm
Date of Coring: 2008

Displayed Box [interval]: 9 [3,613 - 3,614 m]
Date of Core Inspection: 16.10.2009

Photo Depth Top: 3,613 m	Lithology & Grain size							Sedimentary Structures	Sorting	Rounding	Core Description
	Clay (C)	Silt (U)	f-Sand (fS)	m-Sand (mS)	c-Sand (cS)	Granule (g)	Pebble (p)				
									good	sub-angular	sandstone (fine-grained), grey colour
									good	sub-angular	sandstone (medium to coarse-grained), light grey/beige colour, porous (!), homogeneous, partly coarse qtz-grains in the area of fractures (max. size of approx 2 cm)
									good	sub-angular	sandstone (medium-grained), light grey/beige colour, more/less homogeneous

Depth Bottom: 3,614 m

Well: MLRT-003C

Core No. [Total interval]:   4 [3,604 - 3,622 m]
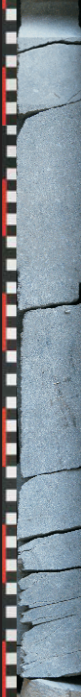Core Recovery: 16 m
Core Diameter: 6.5 cm
Date of Coring: 2008

Displayed Box [interval]:   8 [3,614 - 3,615 m]
Date of Core Inspection: 16.10.2009

Photo / Depth Top: 3,614 m	Lithology & Grain size — Clay (C)	Silt (U)	f-Sand (fS)	m-Sand (mS)	c-Sand (cS)	Granule (g)	Pebble (p)	Sedimentary Structures	Sorting	Rounding	Core Description
									normal -bad	angular	sandstone (medium-grained), light grey/beige colour, partly coarser qtz-grains, ?thin coal layers
									bad	angular	sandstone (medium-grained), grey colour, sharp boundary; number of angular grains increases with depth (qtz, ?fsp, not calcitic!)
											vein filled with breccious material
											transition to breccious sandstone

Depth Bottom: 3,615 m

Well: MLRT-003C

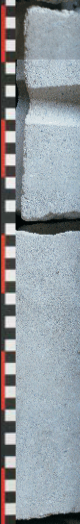Core No. [Total interval]: 4 [3,604 - 3,622 m]
Core Recovery: 16 m
Core Diameter: 6.5 cm
Date of Coring: 2008
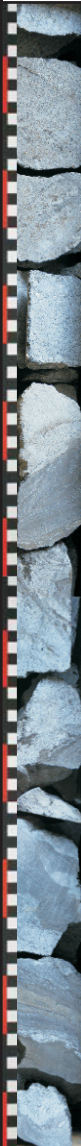
Displayed Box [interval]: 7 [3,615 - 3,616 m]
Date of Core Inspection: 16.10.2009

Photo Depth Top: 3,615 m	C U fS mS cS g p (fine medium coarse)	(Sedimentary) Structures	(Sorting)	(Rounding)	Core Description
			normal-bad	angular	breccious sandstone, grey colour, components with max. size of approx. 1.3 cm
		TS			crystalline (?migmatite, ?gneiss), fine-grained, reddish crystals - sharp boundary!
					crystalline (?migmatite, ?gneiss), coarse-grained, reddish-grey crystals
					crystalline (?migmatite, ?gneiss), alternatively fine and coarse-grained

Depth Bottom: 3,616 m

TS .... Thin section

DEFINITION OF TOP-CRYSTALLINE BASEMENT
IN THE AUSTRIAN MOLASSE BASIN

Gloria Thürschmid

Well: **MLRT-003C**

Core No. [Total interval]:   4 [3,604 - 3,622 m]
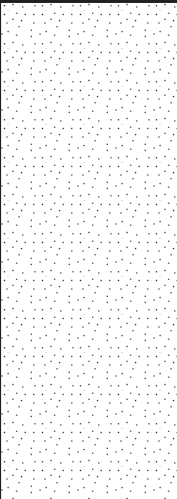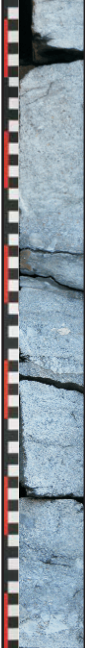Core Recovery: 16 m
Core Diameter: 6.5 cm
Date of Coring: 2008

Displayed Box [interval]:   6 [3,616 - 3,617 m]
Date of Core Inspection: 16.10.2009

Photo Depth Top: 3,616 m		fine-grained	medium-grained	coarse-grained	Structures	Core Description
						crystalline (?migmatite), alternatively coarse and fine-grained, grey/reddish-brown colour
						?„flowing structure"

Depth Bottom: 3,617 m

Well: MLRT-003C

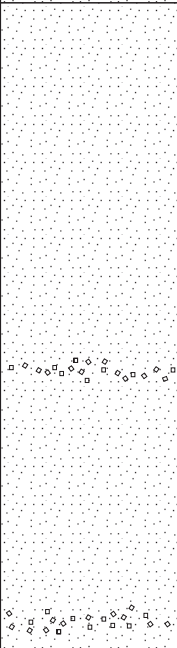Core No. [Total interval]:   4 [3,604 - 3,622 m]
Core Recovery: 16 m
Core Diameter: 6.5 cm
Date of Coring: 2008

Displayed Box [interval]:   5 [3,617 - 3,618 m]
Date of Core Inspection: 16.10.2009

Photo Depth Top: 3,617 m	fine-grained / medium-grained / coarse-grained	Structures	Core Description
			crystalline (?migmatite/granite), fresh and unweathered, coarse-grained, reddish-grey colour, massive and homogeneous; qtz-grains with sitze up to approx. 1.5 cm
			healed fracture

Depth Bottom: 3,618 m

DEFINITION OF TOP-CRYSTALLINE BASEMENT
IN THE AUSTRIAN MOLASSE BASIN

Gloria Thürschmid

Well: **MLRT-003C**
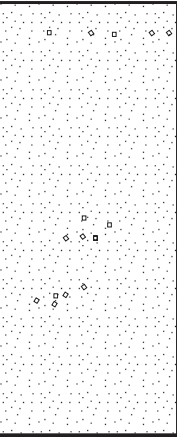
Core No. [Total interval]: 4 [3,604 - 3,622 m]
Core Recovery: 16 m
Core Diameter: 6.5 cm
Date of Coring: 2008

Displayed Box [interval]: 4 [3,618 - 3,619 m]
Date of Core Inspection: 16.10.2009

Photo Depth Top: 3,618 m		fine-grained	medium-grained	coarse-grained	Structures	Core Description
						crystalline (?migmatite/granite), fresh and unweathered, mostly coarse-grained, reddish-grey colour, massive and homogeneous; qtz-grains with sitze up to approx. 1.5 cm
						alternatively coarse and fine grained crystalline

Depth Bottom: 3,619 m

DEFINITION OF TOP-CRYSTALLINE BASEMENT
IN THE AUSTRIAN MOLASSE BASIN

Gloria Thürschmid
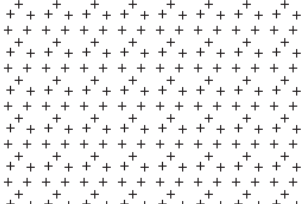
Well: MLRT-003C
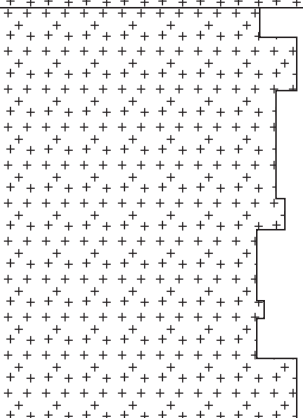
Core No. [Total interval]: 4 [3,604 - 3,622 m]
Core Recovery: 16 m
Core Diameter: 6.5 cm
Date of Coring: 2008

Displayed Box [interval]: 3 [3,619 - 3,620 m]
Date of Core Inspection: 16.10.2009

Photo Depth Top: 3,619 m		fine-grained	medium-grained	coarse-grained	Structures	Core Description
						crystalline (?migmatite/granite), fresh and unweathered, coarse-grained, reddish-grey colour, massive and homogeneous; qtz-grains with sitze up to approx. 1.5 cm

Depth Bottom:
3,620 m

DEFINITION OF TOP-CRYSTALLINE BASEMENT
IN THE AUSTRIAN MOLASSE BASIN

Gloria Thürschmid

Well: **MLRT-003C**

Core No. [Total interval]:   4 [3,604 - 3,622 m]
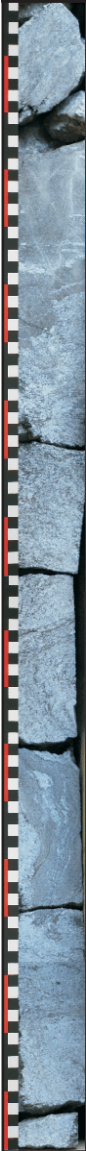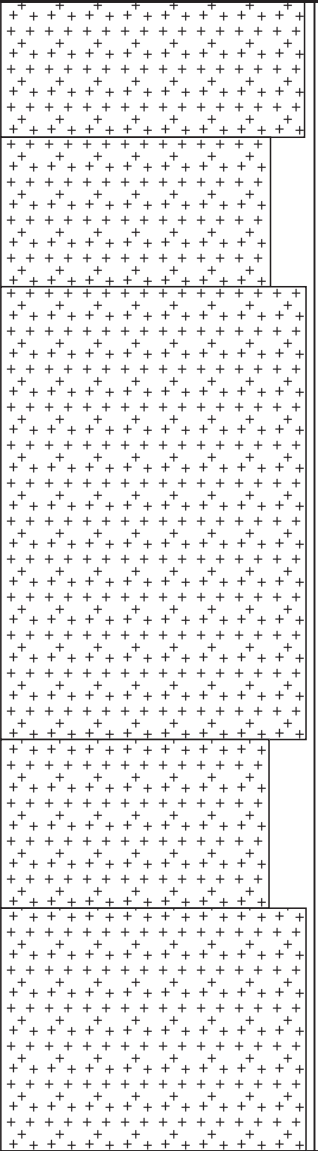Core Recovery: 16 m
Core Diameter: 6.5 cm
Date of Coring: 2008

Displayed Box [interval]:   2 [3,620 - 3,621 m]
Date of Core Inspection: 16.10.2009

Photo Depth Top: 3,620 m	fine-grained	medium-grained	coarse-grained	Structures	Core Description
					crystalline (?migmatite/granite), fresh and unweathered, coarse-grained, light grey colour, massive and homogeneous; qtz-grains with sitze up to approx. 1.5 cm

Depth Bottom: 3,621 m

DEFINITION OF TOP-CRYSTALLINE BASEMENT
IN THE AUSTRIAN MOLASSE BASIN

Gloria Thürschmid

Well: **MLRT-003C**

Core No. [Total interval]:   4 [3,604 - 3,622 m]
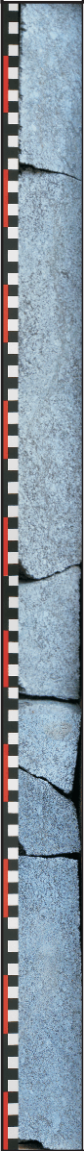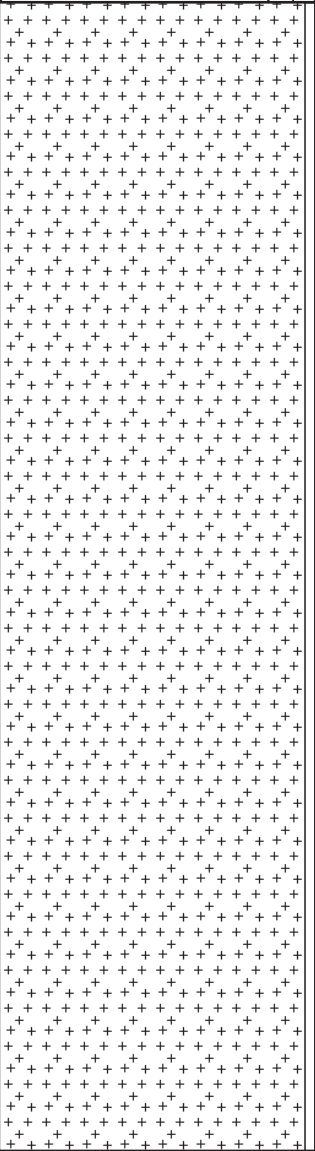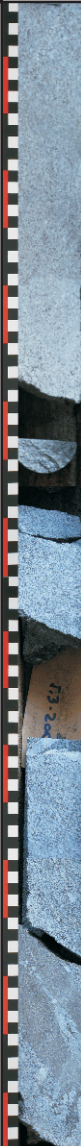Core Recovery: 16 m
Core Diameter: 6.5 cm
Date of Coring: 2008

Displayed Box [interval]:   1 [3,621 - 3,622 m]
Date of Core Inspection: 16.10.2009

Photo Depth Top: 3,621 m	fine-grained / medium-grained / coarse-grained	Structures	Core Description
			crystalline (?migmatite), alternatively coarse (grey) and fine-grained (reddish-brown) qtz-veins ! healed fracture (red)

Depth Bottom:
3,622 m

DEFINITION OF TOP-CRYSTALLINE BASEMENT
IN THE AUSTRIAN MOLASSE BASIN

Gloria Thürschmid

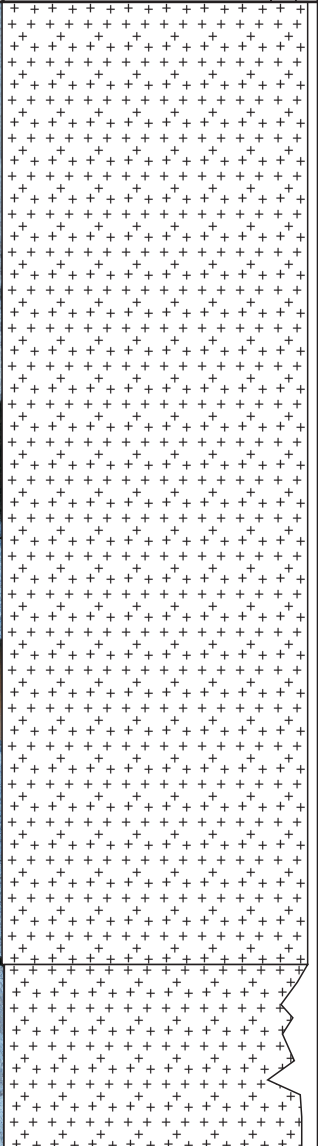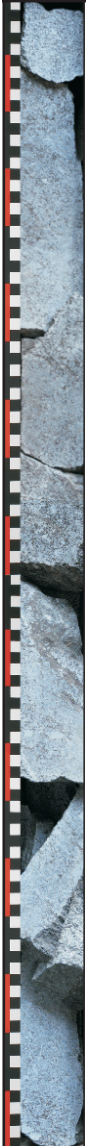# Well: KH-003

Core No. [Total interval]: 4 [3,128 - 3,146 m]
Core Recovery: 15 m
Core Diameter: 10 cm
Date of Coring: Jan. 1983

Displayed Box [interval]: 17 [3,127.85 - 3,128 m]
Date of Core Inspection: 15.10.2009

| Photo Depth Top: 3,127.85 | Lithology & Grain size | | | | | | | Sedimentary Structures | Sorting | Rounding | Core Description |
	Clay (C)	Silt (U)	f-Sand (fS)	m-Sand (mS)	c-Sand (cS)	Granule (g)	Pebble (p)				
									good	sub-angular	glauconitic sandstone (fine to medium-grained), incl. muscovite, quartz (crystal size up to approx. 3 mm), more/less homogeneous, partly „Flaserstruktur", colour: light beige-green, partly darker grey-green phases

Depth Bottom: 3,128 m

Well: KH-003

Core No. [Total interval]:   4 [3,128 - 3,146 m]
Core Recovery: 15 m
Core Diameter: 10 cm
Date of Coring: Jan. 1983

Displayed Box [interval]:   16 [3,128 - 3,129 m]
Date of Core Inspection: 15.10.2009

Photo Depth Top: 3,128 m	Lithology & Grain size							Sedimentary Structures	Sorting	Rounding	Core Description
	Clay (C)	Silt (U)	f-Sand (fS)	m-Sand (mS)	c-Sand (cS)	Granule (g)	Pebble (p)				
									good	sub-angular	glauconitic sandstone (fine to medium-grained),qtz crystals with size up to approx. 3 mm), more/less homogeneous, partly bigger components, colour: light beige-green
											transition zone
									very good		dark grey/brown mudstone, partly components of fine-grained sand and muscovite, slight laminations and membrane of coal

Depth Bottom: 3,129 m

DEFINITION OF TOP-CRYSTALLINE BASEMENT
IN THE AUSTRIAN MOLASSE BASIN

Gloria Thürschmid

Well: KH-003

Core No. [Total interval]: 4 [3,128 - 3,146 m]
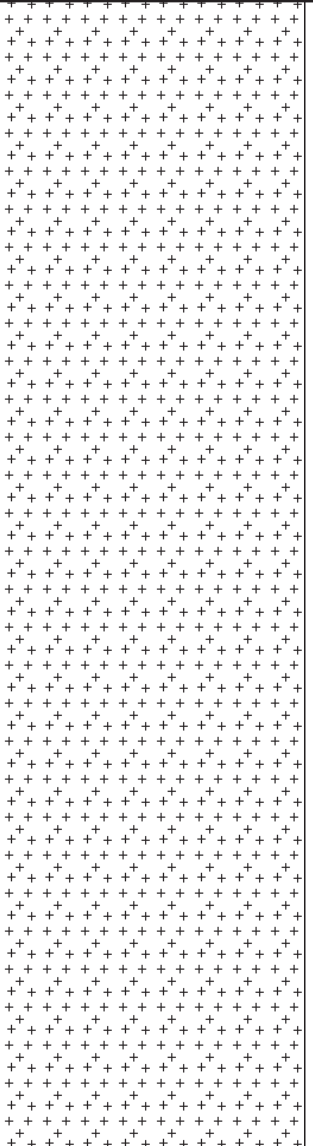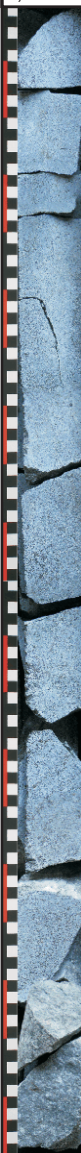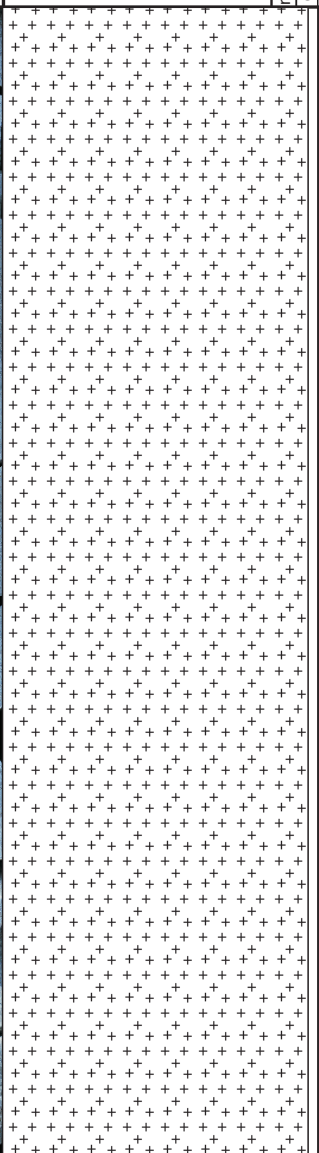Core Recovery: 15 m
Core Diameter: 10 cm
Date of Coring: Jan. 1983

Displayed Box [interval]: 15 [3,129 - 3,130 m]
Date of Core Inspection: 15.10.2009

Photo Depth Top: 3,129 m	Lithology & Grain size							Sedimentary Structures	Sorting	Rounding	Core Description
	Clay (C)	Silt (U)	f-Sand (fS)	m-Sand (mS)	c-Sand (cS)	Granule (g)	Pebble (p)				
									very good		dark grey/greenish mudstone, slight „Flaserstruktur" visible
									good	good	glauconitic sandstone (fine to medium-grained), bright colour, partly with membranes of coal (horizontally layered), more/less homogeneous, qtz crystals size up to approx. 4 mm

Depth Bottom: 3,130 m

DEFINITION OF TOP-CRYSTALLINE BASEMENT
IN THE AUSTRIAN MOLASSE BASIN

Gloria Thürschmid

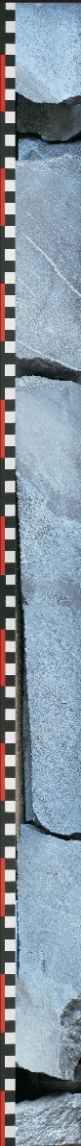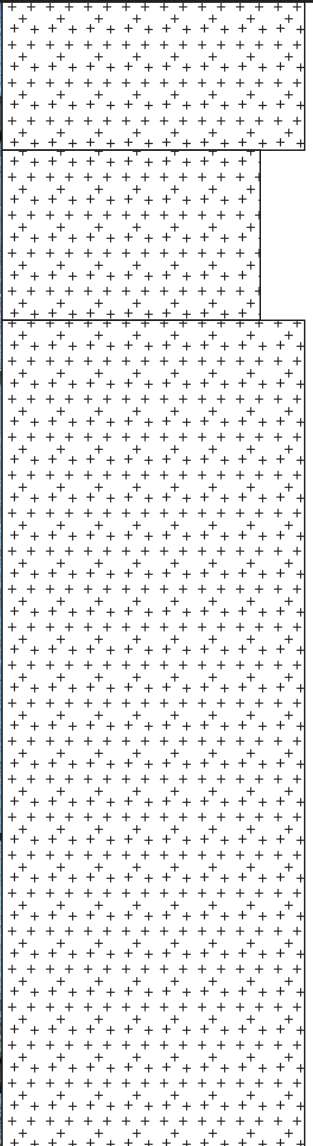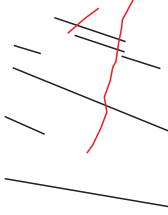# Well: KH-003

Core No. [Total interval]: 4 [3,128 - 3,146 m]
Core Recovery: 15 m
Core Diameter: 10 cm
Date of Coring: Jan. 1983

Displayed Box [interval]: 14 [3,130 - 3,131 m]
Date of Core Inspection: 15.10.2009

Photo Depth Top: 3,130 m	Lithology & Grain size							Sedimentary Structures	Sorting	Rounding	Core Description
	Clay (C)	Silt (U)	f-Sand (fS)	m-Sand (mS)	c-Sand (cS)	Granule (g)	Pebble (p)				
									good	angular	glauconitic sandstone (fine to medium-grained), components of qtz with crystal size up to 3 mm, beige-grey-greenish colour, more/less homogeneous, some bioturbation
									good		mudstone, ?coaly, incl. muscovite, dark grey/brown colour, mostly homogeneous, some light phases/layers on the bottom (due to ?bioturbation)
									good	angular	sandstone (medium-grained), light grey colour, numerous small fractures (partly filled with foliated minerals - ?coal/swelling clay), high porosity!, change in colour due to weathering (yellow) fracture; below: change of colour to greenish!
									good	angular	homogeneous sandstone (fine to medium-grained), beige-grey colour, partly weathered inclusions (size approx. 2 mm)
									good	angular	sandstone with small fractures, incl. coal and muscovite, bioturbation!

Depth Bottom: 3,131 m

Well: KH-003

Core No. [Total interval]: 4 [3,128 - 3,146 m]
Core Recovery: 15 m
Core Diameter: 10 cm
Date of Coring: Jan. 1983

Displayed Box [interval]: 13 [3,131 - 3,132 m]
Date of Core Inspection: 15.10.2009

Photo Depth Top: 3,131 m	Lithology & Grain size							Sedimentary Structures	Sorting	Rounding	Core Description
	Clay (C)	Silt (U)	f-Sand (fS)	m-Sand (mS)	c-Sand (cS)	Granule (g)	Pebble (p)				
									good	angular	sandstone with small fractures (partly filled with ?coal/swelling clay), components of muscovite, light beige/grey-greenish colour
											fracture (dark coating due to ?coal)
											homogeneity increases with depth!
											starting from now: no small fractures anymore, but membranes of coal

Depth Bottom: 3,132 m

Well: KH-003

Core No. [Total interval]: 4 [3,128 - 3,146 m]
Core Recovery: 15 m
Core Diameter: 10 cm
Date of Coring: Jan. 1983

Displayed Box [interval]: 12 [3,132 - 3,133 m]
Date of Core Inspection: 15.10.2009

Photo Depth Top: 3,132 m	Lithology & Grain size							Sedimentary Structures	Sorting	Rounding	Core Description
	Clay (C)	Silt (U)	f-Sand (fS)	m-Sand (mS)	c-Sand (cS)	Granule (g)	Pebble (p)				
									good	angular	sandstone (medium-grained), qtz-grains with size of approx. 2 mm, bigger (weathered) components of sandstone
											fractures! (due to ?swelling)
											thin layer of ?clay; membranes of coal (between laminations), grain size decreases with depth
									good		swelling of clay (mudstone), dark brown/greenish, with „Flasergefüge" and ?bioturbation, more lamination with depth

Depth Bottom: 3,133 m

Well: KH-003

Core No. [Total interval]:   4 [3,128 - 3,146 m]
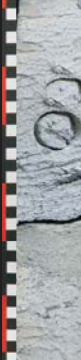Core Recovery: 15 m
Core Diameter: 10 cm
Date of Coring: Jan. 1983
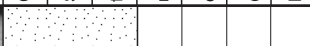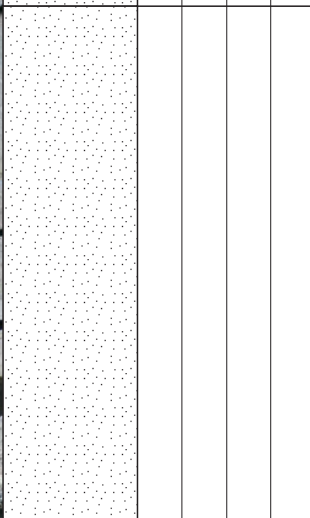
Displayed Box [interval]:   11 [3,133 - 3,134 m]
Date of Core Inspection: 15.10.2009

Photo / Depth Top: 3,133 m	Lithology & Grain size							Sedimentary Structures	Sorting	Rounding	Core Description
	Clay (C)	Silt (U)	f-Sand (fS)	m-Sand (mS)	c-Sand (cS)	Granule (g)	Pebble (p)				
									good	angular	sandstone (fine to medium-grained), muscovite existent, thin dark membranes of ?coal
									poor	angular	sandstone, more/less homogeneous, components of qtz-grains up to 1 cm, some small („swelling") fractures
												small fractures!
												swelling of ?clay (filling of small fractures)
									good		mudstone (?coaly), slight laminations, dark brown to black colour, partly inclusions (olive-green, max. size of approx. 1 cm), components of pyrite
												swelling layers in between (?clay minerals smectite, montmorillonite)
												partly fracture planes with slickenside (smooth with striae)

Depth Bottom: 3,134 m

DEFINITION OF TOP-CRYSTALLINE BASEMENT
IN THE AUSTRIAN MOLASSE BASIN

Gloria Thürschmid

Well: **KH-003**

Core No. [Total interval]:   4 [3,128 - 3,146 m]
Core Recovery: 15 m
Core Diameter: 10 cm
Date of Coring: Jan. 1983

Displayed Box [interval]:   10 [3,134 - 3,135 m]
Date of Core Inspection: 15.10.2009

Photo Depth Top: 3,134 m	Lithology & Grain size							Sedimentary Structures	Sorting	Rounding	Core Description
	Clay (C)	Silt (U)	f-Sand (fS)	m-Sand (mS)	c-Sand (cS)	Granule (g)	Pebble (p)				
									very good		mudstone, dark brown/grey colour, partly light layers in between, some olive-green inclusions

Depth Bottom: 3,135 m

Well: KH-003

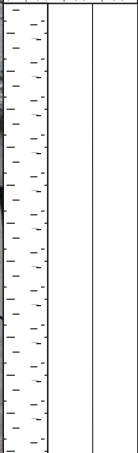Core No. [Total interval]: 4 [3,128 - 3,146 m]
Core Recovery: 15 m
Core Diameter: 10 cm
Date of Coring: Jan. 1983

Displayed Box [interval]: 9 [3,135 - 3,136 m]
Date of Core Inspection: 15.10.2009

Photo Depth Top: 3,135 m	Lithology & Grain size							Sedimentary Structures	Sorting	Rounding	Core Description
	Clay (C)	Silt (U)	f-Sand (fS)	m-Sand (mS)	c-Sand (cS)	Granule (g)	Pebble (p)				
									very good		mudstone, dark grey colour
											swelling of ?clay minerals
											swelling of ?clay minerals
											bright fracture planes with slickenside!
											bright fracture planes with slickenside!

Depth Bottom: 3,136 m

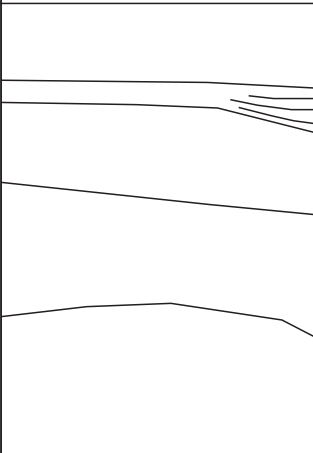# Well: KH-003

Core No. [Total interval]: 4 [3,128 - 3,146 m]
Core Recovery: 15 m
Core Diameter: 10 cm
Date of Coring: Jan. 1983

Displayed Box [interval]: 8 [3,136 - 3,137 m]
Date of Core Inspection: 16.10.2009

Photo Depth Top: 3,136 m	Lithology & Grain size							Sedimentary Structures	Sorting	Rounding	Core Description
	Clay (C)	Silt (U)	f-Sand (fS)	m-Sand (mS)	c-Sand (cS)	Granule (g)	Pebble (p)				
									very good		mudstone, laminated, partly membranes of ?coal
									normal	angular	swelling of ?clay minerals (filling of fractures) sandstone (medium-grained), beige/grey colour, more/less homogenegous, no internal structure visible, muscovite existent

Depth Bottom: 3,137 m

Well: KH-003

Core No. [Total interval]: 4 [3,128 - 3,146 m]
Core Recovery: 15 m
Core Diameter: 10 cm
Date of Coring: Jan. 1983

Displayed Box [interval]: 7 [3,137 - 3,138 m]
Date of Core Inspection: 16.10.2009

Photo Depth Top: 3,137 m	Lithology & Grain size							Sedimentary Structures	Sorting	Rounding	Core Description
	Clay (C)	Silt (U)	f-Sand (fS)	m-Sand (mS)	c-Sand (cS)	Granule (g)	Pebble (p)				
									good	angular	sandstone (fine to medium-grained), mostly homogeneous, beige/grey colour
									poor	angular	sandstone (coarse-grained), remnants of coal, qtz-components with size of approx. 2 mm, fractures with membranes of coal
									good	angular	sandstone (fine to medium-grained), mostly homogeneous, beige/grey colour
									good		layer of coaly mudstone: very soft, horizontally laminated, components of muscovite
									good	angular	sandstone (fine to medium-grained), mostly homogeneous, beige/grey colour fracture filled with coaly mudstone membranes of coal

Depth Bottom: 3,138 m

DEFINITION OF TOP-CRYSTALLINE BASEMENT
IN THE AUSTRIAN MOLASSE BASIN

Gloria Thürschmid
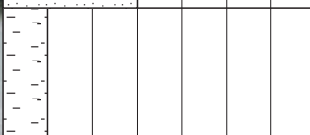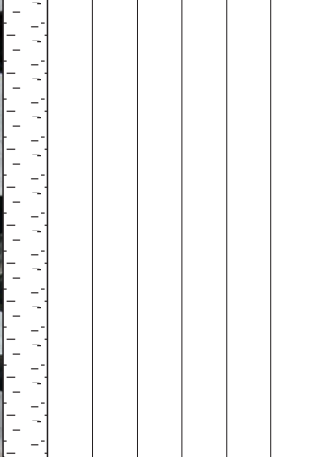
Well: KH-003

Core No. [Total interval]: 4 [3,128 - 3,146 m]
Core Recovery: 15 m
Core Diameter: 10 cm
Date of Coring: Jan. 1983

Displayed Box [interval]: 6 [3,138 - 3,139 m]
Date of Core Inspection: 16.10.2009

Photo Depth Top: 3,138 m	Lithology & Grain size							Sedimentary Structures	Sorting	Rounding	Core Description
	Clay (C)	Silt (U)	f-Sand (fS)	m-Sand (mS)	c-Sand (cS)	Granule (g)	Pebble (p)				
									very good	sub-angular	sandstone (medium-grained), beige/grey colour, lots of muscovite, partly greenish-grey inclusions with yellow coating (due to ?weathering)
											fractures with dark grey filling
											swelling of ?clay minerals (dark grey material, looks like flocks)
									good		silty mudstone, alternately laminated with light/dark layers, bioturbation (traces of digging), muscovite existent

Depth Bottom: 3,139 m

Well: KH-003

Core No. [Total interval]: 4 [3,128 - 3,146 m]
Core Recovery: 15 m
Core Diameter: 10 cm
Date of Coring: Jan. 1983

Displayed Box [interval]: 5 [3,139 - 3,140 m]
Date of Core Inspection: 16.10.2009

Photo Depth Top: 3,139 m	Lithology & Grain size							Sedimentary Structures	Sorting	Rounding	Core Description
	Clay (C)	Silt (U)	f-Sand (fS)	m-Sand (mS)	c-Sand (cS)	Granule (g)	Pebble (p)				
									very good	sub-angular	sandstone (medium-grained), more/less massive, beige/grey colour, also muscovite (increasing amount at fractures!), some membranes of coal visible
									good	angular	sandstone (fine-grained), laminated
									good		mudstone (?coaly), dark grey to black, massive and homogeneous
											increasing grain size of qtz-crystals with depth, lamination
									good	sub-angular	qtz-sandstone (max. grain size of 4 mm), beige/grey colour, membranes of coal within fractures, also muscovite

Depth Bottom: 3,140 m

DEFINITION OF TOP-CRYSTALLINE BASEMENT
IN THE AUSTRIAN MOLASSE BASIN

Gloria Thürschmid

Well: KH-003

Core No. [Total interval]: 4 [3,128 - 3,146 m]
Core Recovery: 15 m
Core Diameter: 10 cm
Date of Coring: Jan. 1983

Displayed Box [interval]: 4 [3,140 - 3,141 m]
Date of Core Inspection: 16.10.2009

Photo Depth Top: 3,140 m	Lithology & Grain size							Sedimentary Structures	Sorting	Rounding	Core Description
	Clay (C)	Silt (U)	f-Sand (fS)	m-Sand (mS)	c-Sand (cS)	Granule (g)	Pebble (p)				
									good	sub-angular	sandstone (coarse-grained), partly massive, membranes of coal in fractures, components of muscovite, qtz-grains with size up to 3 mm, beige/grey colour, partly darker phases
									no evaluation possible		sandstone with high clay content, no reliable description possible due to destruction (swelling!)
									good		coal, mostly crumbled
									good		mudstone (coaly), dark grey with black membranes of coal (more/less vertically orientated!), more/less massive

Depth Bottom: 3,141 m

Well: KH-003

Core No. [Total interval]: 4 [3,128 - 3,146 m]
Core Recovery: 15 m
Core Diameter: 10 cm
Date of Coring: Jan. 1983
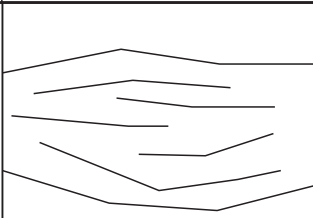
Displayed Box [interval]: 3 [3,141 - 3,142 m]
Date of Core Inspection: 16.10.2009

Photo Depth Top: 3,141 m	Lithology & Grain size							Sedimentary Structures	Sorting	Rounding	Core Description
	Clay (C)	Silt (U)	f-Sand (fS)	m-Sand (mS)	c-Sand (cS)	Granule (g)	Pebble (p)				
									normal	angular	silty stone (mixture between mudstone and extremely fine-grained sandstone), qtz-grains up to approx 1 mm in size swelling of ?clay-minerals!
									good	sub-angular	sandstone (coarse-grained), fractures filled with coaly material, qtz-grains up to approx. 5 mm in size increasing amount of clayey phases with depth (laminations)
									normal		mudstone, dark grey, ?coaly, more/less homogeneous, some inclusions of darker phases fracture planes are smooth and bright, partly with white coating (due to ?drilling mud), which has no reaction with HCl; some parts show effects of ?weathering (yellow colour)

Depth Bottom: 3,142 m

DEFINITION OF TOP-CRYSTALLINE BASEMENT
IN THE AUSTRIAN MOLASSE BASIN

Gloria Thürschmid

Well: KH-003

Core No. [Total interval]:   4 [3,128 - 3,146 m]
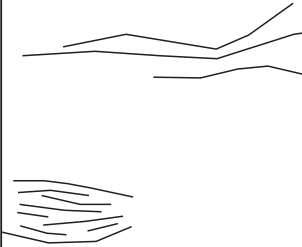Core Recovery: 15 m
Core Diameter: 10 cm
Date of Coring: Jan. 1983

Displayed Box [interval]:   2 [3,142 - 3,143 m]
Date of Core Inspection: 16.10.2009

Photo Depth Top: 3,142 m	Lithology & Grain size							Sedimentary Structures	Sorting	Rounding	Core Description
	Clay (C)	Silt (U)	f-Sand (fS)	m-Sand (mS)	c-Sand (cS)	Granule (g)	Pebble (p)				
									normal		mudstone, dark grey, massive, without internal structure
											transition zone: gradual transition to fine-grained sandstone, brightness of colour increases with depth, qtz-minerals visible
								TS	normal	angular	
									normal	angular	?sandstone light grey-beige-brownish colour, coarse qtz-grains existent (size approx. 10 mm), darker phases existent, also muscovite and biotite

Depth Bottom: 3,143 m

TS .... **Thin section**

DEFINITION OF TOP-CRYSTALLINE BASEMENT
IN THE AUSTRIAN MOLASSE BASIN

Gloria Thürschmid

Well: KH-003

Core No. [Total interval]: 4 [3,128 - 3,146 m]
Core Recovery: 15 m
Core Diameter: 10 cm
Date of Coring: Jan. 1983

Displayed Box [interval]: 1 [3,143 - 3,144 m]
Date of Core Inspection: 16.10.2009

Photo Depth Top: 3,143 m	C	U	fS	mS	cS	g	p fine medium coarse	(Sedimentary) Structures	(Sorting)	(Rounding)	Core Description
									normal	angular	?sandstone light grey-beige-brownish colour, coarse qtz-grains existent (size approx. 10 mm), darker phases existent, also muscovite and biotite
											crystalline (?granite), unweathered, beige-grey-brownish colour
											fractures filled with clayey material
											crystalline (?granite), unweathered, very coarse-grained with qtz-crystals up to 1,5 cm diameter!
											fracture with chlorite-coating!

Depth Bottom: 3,144 m

DEFINITION OF TOP-CRYSTALLINE BASEMENT
IN THE AUSTRIAN MOLASSE BASIN

Gloria Thürschmid

Well: V-037

Core No. [Total interval]: 2 [2,169.5 - 2,170 m]
Core Recovery: 0.30 m
Core Diameter: 10 cm
Date of Coring: Sept. 1981

Displayed Box [interval]: 1 [2,169.5 - 2,170 m]
Date of Core Inspection: 16.10.2009

Photo Depth Top: 2,169.5	Lithology & Grain size							Sedimentary Structures	Sorting	Rounding	Core Description
	Clay (C)	Silt (U)	f-Sand (fS)	m-Sand (mS)	c-Sand (cS)	Granule (g)	Pebble (p)				
									very good	sub-angular	sandstone with qtz (medium-grained), more/less tight and massive, grey/beige colour, partly coaly-clayey filled fractures, ?remnants of oil (water rolls off the core)

Depth Bottom: 2,170 m

DEFINITION OF TOP-CRYSTALLINE BASEMENT
IN THE AUSTRIAN MOLASSE BASIN

Gloria Thürschmid

Well: **V-037**

Core No. [Total interval]:   3 [2,170 - 2,170.5 m]
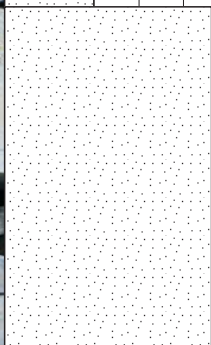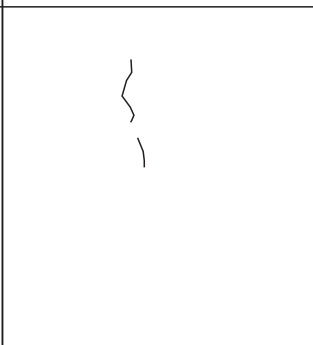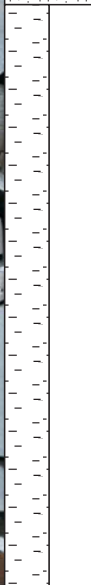Core Recovery: 0.40 m
Core Diameter: 10 cm
Date of Coring: Sept. 1981

Displayed Box [interval]:   1 [2,170 - 2,170.5 m]
Date of Core Inspection: 16.10.2009

Photo Depth Top: 2,170 m	Lithology & Grain size							Sedimentary Structures	Sorting	Rounding	Core Description
	Clay (C)	Silt (U)	f-Sand (fS)	m-Sand (mS)	c-Sand (cS)	Granule (g)	Pebble (p)				
									very good	sub-angular	sandstone with qtz (medium-grained), more/less tight and massive/homogeneous, grey/beige colour, partly bigger qtz-grains up to approx. 4 mm, components of muscovite, dark and clayey coating of fractures, also membranes/small layers of coal, further inclusions: white, slight reaction to HCl

Depth Bottom: 2,170.5 m

Well: V-037

Core No. [Total interval]:	4 [2,170.5 - 2,187.5 m]
Core Recovery:	17 m
Core Diameter:	10 cm
Date of Coring:	Sept. 1981
Displayed Box [interval]:	17 [2,170.5 - 2,171.5 m]
Date of Core Inspection:	16.10.2009

Photo Depth Top: 2,170.5	Lithology & Grain size							Sedimentary Structures	Sorting	Rounding	Core Description
	Clay (C)	Silt (U)	f-Sand (fS)	m-Sand (mS)	c-Sand (cS)	Granule (g)	Pebble (p)				
									very good	angular	sandstone with qtz grains (medium to coarse-grained), more/less tight and massive/ homogeneous, light brown to grey/beige colour, partly darker (clayey/shaly) and brighter (?fsp) phases, ?remnants of oil (water rolls of the core)
											grains (?fsp) with max. size of approx. 3.5 cm

Depth Bottom: 2,171.5 m

Well: V-037

Core No. [Total interval]:   4 [2,170.5 - 2,187.5 m]
Core Recovery: 17 m
Core Diameter: 10 cm
Date of Coring: Sept. 1981

Displayed Box [interval]:   16 [2,171.5 - 2,172.5 m]
Date of Core Inspection: 16.10.2009

Photo / Depth Top: 2,171.5	Lithology & Grain size							Sedimentary Structures	Sorting	Rounding	Core Description
	Clay (C)	Silt (U)	f-Sand (fS)	m-Sand (mS)	c-Sand (cS)	Granule (g)	Pebble (p)				
									good	sub-angular	sandstone (medium-grained), no HCl reaction, partly lighter components (white - ?fsp + qtz), beige/grey colour
											fracture with clayey-?coaly filling, qtz-grains up to approx. 1.8 cm
									good	sub-angular	sandstone (fine-grained), porous, many fissures, qtz with grain size up to approx. 1.5 cm
											sandstone (fine to medium-grained), dark filling of fissures
									good	sub-angular	sandstone (fine to medium-grained), dark filling of fissures

Depth Bottom: 2,172.5 m

DEFINITION OF TOP-CRYSTALLINE BASEMENT
IN THE AUSTRIAN MOLASSE BASIN

Gloria Thürschmid
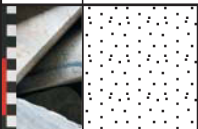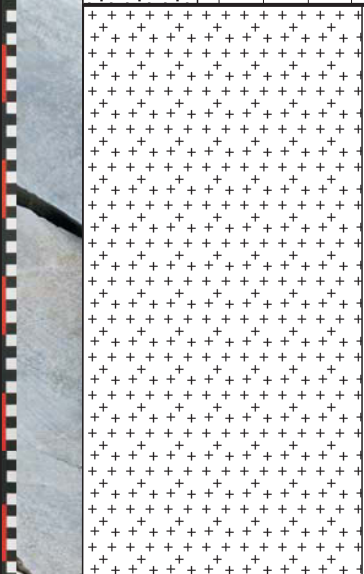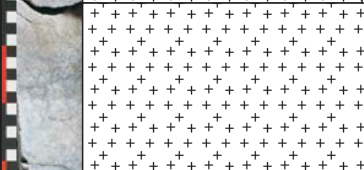
Well: V-037

Core No. [Total interval]:   4 [2,170.5 - 2,187.5 m]
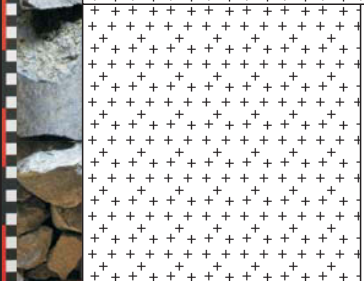Core Recovery: 17 m
Core Diameter: 10 cm
Date of Coring: Sept. 1981

Displayed Box [interval]:   15 [2,172.5 - 2,173.5 m]
Date of Core Inspection: 16.10.2009

Photo Depth Top: 2,172.5	Lithology & Grain size							Sedimentary Structures	Sorting	Rounding	Core Description
	Clay (C)	Silt (U)	f-Sand (fS)	m-Sand (mS)	c-Sand (cS)	Granule (g)	Pebble (p)				
									good	sub-angular	sandstone (fine to medium-grained), greenish-grey colour, fractures filling and coating with clayey-?coaly material, partly bigger qtz/fsp-components
									bad	angular	breccia with fine-grained, greenish-grey calcitic matrix, components: qtz, shaly fragments, ?fsp, big pyrite-crystals (up to 1 cm)
									very good		limestone (HCl!!!), light grey/beige colour, massive and more/less homogeneous, some fissures (?shaly)

Depth Bottom: 2,173.5 m

DEFINITION OF TOP-CRYSTALLINE BASEMENT
IN THE AUSTRIAN MOLASSE BASIN

Gloria Thürschmid

Well: V-037

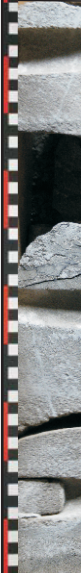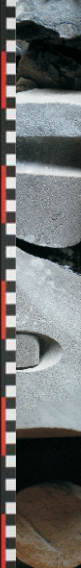Core No. [Total interval]: 4 [2,170.5 - 2,187.5 m]
Core Recovery: 17 m
Core Diameter: 10 cm
Date of Coring: Sept. 1981

Displayed Box [interval]: 14 [2,173.5 - 2,174.5 m]
Date of Core Inspection: 16.10.2009

Photo Depth Top: 2,173.5	Lithology & Grain size							Sedimentary Structures	Sorting	Rounding	Core Description
	Clay (C)	Silt (U)	f-Sand (fS)	m-Sand (mS)	c-Sand (cS)	Granule (g)	Pebble (p)				
									very good		limestone (HCl!!!), light grey/beige colour, massive, partly white components (grain size max. 1 mm), small fractures
											colour changes alternatively (light beige/grey to darker blue-greyish)
											dark coloured vein (?shaly)

Depth Bottom: 2,174.5 m

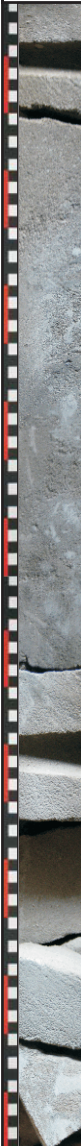Core No. [Total interval]: 4 [2,170.5 - 2,187.5 m]
Core Recovery: 17 m
Core Diameter: 10 cm
Date of Coring: Sept. 1981

Displayed Box [interval]: 13 [2,174.5 - 2,175.5 m]
Date of Core Inspection: 16.10.2009

Photo Depth Top: 2,174.5	Lithology & Grain size							Sedimentary Structures	Sorting	Rounding	Core Description
	Clay (C)	Silt (U)	f-Sand (fS)	m-Sand (mS)	c-Sand (cS)	Granule (g)	Pebble (p)				
									very good		limestone (HCl!!!), light grey colour, massive, partly white components (grain size max. 1 mm), small fractures, no internal structure
									good	angular	sandstone (medium to coarse-grained), hardly any reaction to HCl, bended/deformed structure
									very good		limestone (HCl!!!), light grey colour, massive, partly white components (grain size max. 1 mm), small fractures, no internal structure

Depth Bottom: 2,175.5 m

DEFINITION OF TOP-CRYSTALLINE BASEMENT
IN THE AUSTRIAN MOLASSE BASIN

Gloria Thürschmid

Well: V-037

Core No. [Total interval]:   4 [2,170.5 - 2,187.5 m]
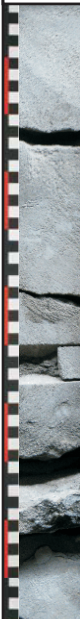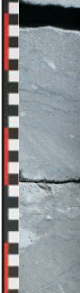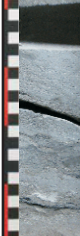Core Recovery: 17 m
Core Diameter: 10 cm
Date of Coring: Sept. 1981

Displayed Box [interval]:   12 [2,175.5 - 2,176.5 m]
Date of Core Inspection: 16.10.2009

Photo Depth Top: 2,175.5	Lithology & Grain size							Sedimentary Structures	Sorting	Rounding	Core Description
	Clay (C)	Silt (U)	f-Sand (fS)	m-Sand (mS)	c-Sand (cS)	Granule (g)	Pebble (p)				
									very good		limestone (HCl!!!), light grey colour, massive, partly white components (grain size max. 1 mm), small fractures, no internal structure
											colour changes to glue-greyish!
											fracture filled with ?shale (dark brown/grey)
									good	angular	calcitic sandstone (fine to medium-grained)

Depth Bottom: 2,176.5 m

DEFINITION OF TOP-CRYSTALLINE BASEMENT
IN THE AUSTRIAN MOLASSE BASIN

Gloria Thürschmid

Well: V-037

Core No. [Total interval]: 4 [2,170.5 - 2,187.5 m]
Core Recovery: 17 m
Core Diameter: 10 cm
Date of Coring: Sept. 1981

Displayed Box [interval]: 11 [2,176.5 - 2,177.5 m]
Date of Core Inspection: 16.10.2009

Photo Depth Top: 2,176.5	Lithology & Grain size							Sedimentary Structures	Sorting	Rounding	Core Description
	Clay (C)	Silt (U)	f-Sand (fS)	m-Sand (mS)	c-Sand (cS)	Granule (g)	Pebble (p)		good	angular	calcitic sandstone (medium to coarse-grained), blue-greyish colour, strongly fractured, porous, length of components up to approx. 2 cm (cc), dark fractures, ?rests of shells

Depth Bottom: 2,177.5 m

DEFINITION OF TOP-CRYSTALLINE BASEMENT
IN THE AUSTRIAN MOLASSE BASIN

Gloria Thürschmid

Well: V-037

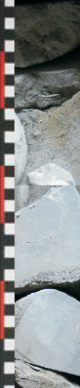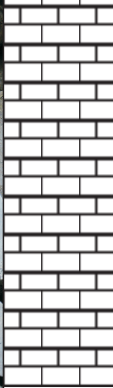Core No. [Total interval]: 4 [2,170.5 - 2,187.5 m]
Core Recovery: 17 m
Core Diameter: 10 cm
Date of Coring: Sept. 1981

Displayed Box [interval]: 10 [2,177.5 - 2,178.5 m]
Date of Core Inspection: 16.10.2009

Photo Depth Top: 2,177.5	Lithology & Grain size							Sedimentary Structures	Sorting	Rounding	Core Description
	Clay (C)	Silt (U)	f-Sand (fS)	m-Sand (mS)	c-Sand (cS)	Granule (g)	Pebble (p)				
									good	angular	calcitic sandstone (medium to coarse-grained), blue-greyish colour, strongly fractured, porous, length of components up to approx. 2 cm (cc), dark fractures, ?rests of shellsnumerous fractures
											numerous fractures!

Depth Bottom: 2,178.5 m

Well: V-037

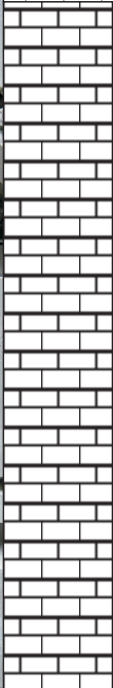Core No. [Total interval]: 4 [2,170.5 - 2,187.5 m]
Core Recovery: 17 m
Core Diameter: 10 cm
Date of Coring: Sept. 1981

Displayed Box [interval]: 9 [2,178.5 - 2,179.5 m]
Date of Core Inspection: 16.10.2009

Photo Depth Top: 2,178.5	Lithology & Grain size							Sedimentary Structures	Sorting	Rounding	Core Description
	Clay (C)	Silt (U)	f-Sand (fS)	m-Sand (mS)	c-Sand (cS)	Granule (g)	Pebble (p)				
									good	angular	calcitic sandstone (medium to coarse-grained), blue-greyish colour, strongly fractured, porous, length of components up to approx. 2 cm (cc), dark fractures, ?rests of shellsnumerous fractures
											numerous fractures!

Depth Bottom: 2,179.5 m

DEFINITION OF TOP-CRYSTALLINE BASEMENT
IN THE AUSTRIAN MOLASSE BASIN

Gloria Thürschmid

Well: V-037
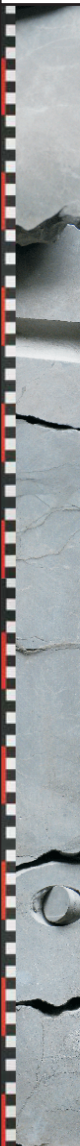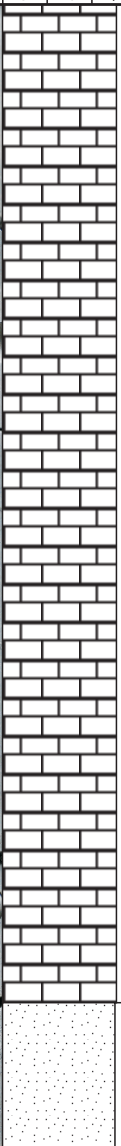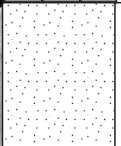
Core No. [Total interval]: 4 [2,170.5 - 2,187.5 m]
Core Recovery: 17 m
Core Diameter: 10 cm
Date of Coring: Sept. 1981

Displayed Box [interval]: 8 [2,179.5 - 2,180.5 m]
Date of Core Inspection: 16.10.2009

Photo Depth Top: 2,179.5	Lithology & Grain size							Sedimentary Structures	Sorting	Rounding	Core Description
	Clay (C)	Silt (U)	f-Sand (fS)	m-Sand (mS)	c-Sand (cS)	Granule (g)	Pebble (p)				
									good	angular	calcitic sandstone (medium to coarse-grained), blue-greyish colour, strongly fractured, porous, length of components up to approx. 2 cm (cc), dark fractures, ?rests of shellsnumerous fractures
											numerous fractures!
									normal-bad		transition zone, sandy mudstone, weathered, very crumbly
									good		mudstone, fresh, dark brown, massive, no HCl reaction

Depth Bottom: 2,180.5 m

DEFINITION OF TOP-CRYSTALLINE BASEMENT
IN THE AUSTRIAN MOLASSE BASIN

Gloria Thürschmid

Well: V-037

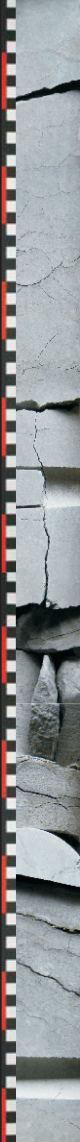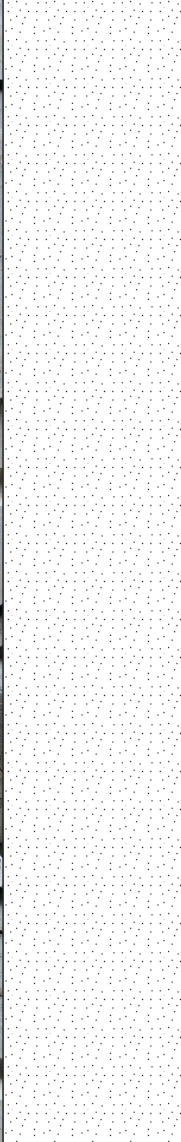Core No. [Total interval]:   4 [2,170.5 - 2,187.5 m]
Core Recovery: 17 m
Core Diameter: 10 cm
Date of Coring: Sept. 1981

Displayed Box [interval]:   7 [2,180.5 - 2,181.5 m]
Date of Core Inspection: 16.10.2009

Photo Depth Top: 2,180.5	Lithology & Grain size							Sedimentary Structures	Sorting	Rounding	Core Description
	Clay (C)	Silt (U)	f-Sand (fS)	m-Sand (mS)	c-Sand (cS)	Granule (g)	Pebble (p)				
									good		mudstone, fresh, dark brown, massive, no HCl reaction
									good		mudstone, weathered, brown, numerous fissures, porous!!!
									good		mudstone, fresh, dark brown, massive, no HCl reaction
									poor	sub-angular	transition zone from mudstone to sandstone (coarse grained), porous!! qtz-grains with max. size of approx. 2 cm, light components, dark matrix

Depth Bottom: 2,181.5 m

Well: V-037

Core No. [Total interval]: 4 [2,170.5 - 2,187.5 m]
Core Recovery: 17 m
Core Diameter: 10 cm
Date of Coring: Sept. 1981

Displayed Box [interval]: 6 [2,181.5 - 2,182.5 m]
Date of Core Inspection: 16.10.2009

Photo Depth Top: 2,181.5	Lithology & Grain size							Sedimentary Structures	Sorting	Rounding	Core Description
	Clay (C)	Silt (U)	f-Sand (fS)	m-Sand (mS)	c-Sand (cS)	Granule (g)	Pebble (p)				
									normal	sub-angular	sandstone (fine-grained), dark brown with light brown phases
											beginning of fracturing
											total destruction due to weathering!! shaly/coaly material swells, decreasing grain size

Depth Bottom: 2,182.5 m

DEFINITION OF TOP-CRYSTALLINE BASEMENT
IN THE AUSTRIAN MOLASSE BASIN

Gloria Thürschmid

Well: V-037

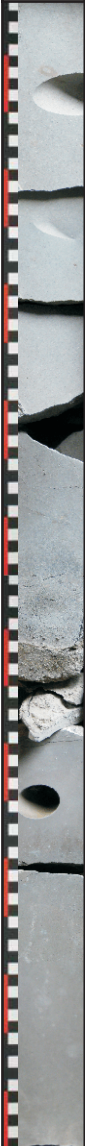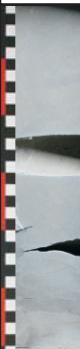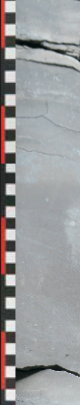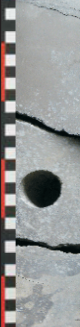Core No. [Total interval]: 4 [2,170.5 - 2,187.5 m]
Core Recovery: 17 m
Core Diameter: 10 cm
Date of Coring: Sept. 1981

Displayed Box [interval]: 5 [2,182.5 - 2,183.5 m]
Date of Core Inspection: 16.10.2009

Photo Depth Top: 2,182.5	Lithology & Grain size							Sedimentary Structures	Sorting	Rounding	Core Description
	Clay (C)	Silt (U)	f-Sand (fS)	m-Sand (mS)	c-Sand (cS)	Granule (g)	Pebble (p)				
								TS	good		mudstone, dark brown/grey, massive, extremely weathered
											mudstone (less weathered)
								TS			

Depth Bottom: 2,183.5 m

TS .... Thin section

DEFINITION OF TOP-CRYSTALLINE BASEMENT
IN THE AUSTRIAN MOLASSE BASIN

Gloria Thürschmid

Well: V-037

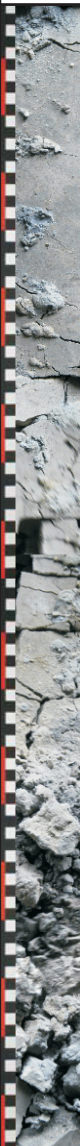Core No. [Total interval]:   4 [2,170.5 - 2,187.5 m]
Core Recovery: 17 m
Core Diameter: 10 cm
Date of Coring: Sept. 1981

Displayed Box [interval]:   4 [2,183.5 - 2,184.5 m]
Date of Core Inspection: 16.10.2009

Photo Depth Top: 2,183.5	Lithology & Grain size							Sedimentary Structures	Sorting	Rounding	Core Description
	Clay (C)	Silt (U)	f-Sand (fS)	m-Sand (mS)	c-Sand (cS)	Granule (g)	Pebble (p)				
								TS	good		mudstone, dark brown/grey-blue (partly reddish), massive, less weathered
								TS			

Depth Bottom: 2,184.5 m

Well: V-037

Core No. [Total interval]:   4 [2,170.5 - 2,187.5 m]
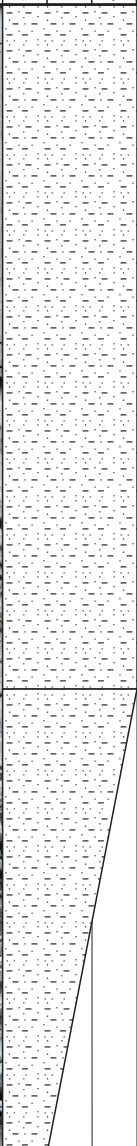Core Recovery: 17 m
Core Diameter: 10 cm
Date of Coring: Sept. 1981

Displayed Box [interval]:   3 [2,184.5 - 2,185.5 m]
Date of Core Inspection: 16.10.2009

Photo Depth Top: 2,184.5	Lithology & Grain size							Sedimentary Structures	Sorting	Rounding	Core Description
	Clay (C)	Silt (U)	f-Sand (fS)	m-Sand (mS)	c-Sand (cS)	Granule (g)	Pebble (p)				
									good		?mudstone, weathered, reddish-greyish colour
									good		?clayey sandstone; reddish-grey; ?qtz/fsp-grains with grain size up to approx. 3 mm

Depth Bottom: 2,185.5 m

DEFINITION OF TOP-CRYSTALLINE BASEMENT
IN THE AUSTRIAN MOLASSE BASIN

Gloria Thürschmid

Well: **V-037**

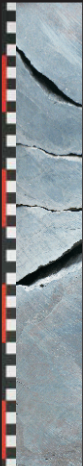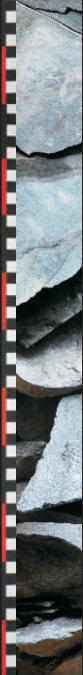Core No. [Total interval]: 4 [2,170.5 - 2,187.5 m]
Core Recovery: 17 m
Core Diameter: 10 cm
Date of Coring: Sept. 1981

Displayed Box [interval]: 2 [2,185.5 - 2,186.5 m]
Date of Core Inspection: 16.10.2009

Photo Depth Top: 2,185.5	Lithology & Grain size							Sedimentary Structures	Sorting	Rounding	Core Description
	Clay (C)	Silt (U)	f-Sand (fS)	m-Sand (mS)	c-Sand (cS)	Granule (g)	Pebble (p)				
									good		?clayey sandstone; reddish-grey; big qtz/fsp-grains, massive
											greenish-grey phase (fine-grained)

Depth Bottom: 2,186.5 m

DEFINITION OF TOP-CRYSTALLINE BASEMENT
IN THE AUSTRIAN MOLASSE BASIN

Gloria Thürschmid

Well: **V-037**

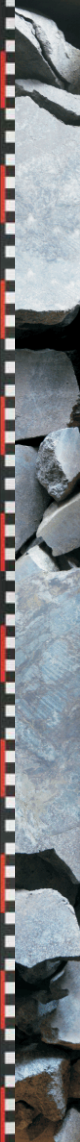Core No. [Total interval]: 4 [2,170.5 - 2,187.5 m]
Core Recovery: 17 m
Core Diameter: 10 cm
Date of Coring: Sept. 1981

Displayed Box [interval]: 1 [2,186.5 - 2,187.5 m]
Date of Core Inspection: 16.10.2009

Photo Depth Top: 2,186.5	Lithology & Grain size							Sedimentary Structures	Sorting	Rounding	Core Description
	Clay (C)	Silt (U)	f-Sand (fS)	m-Sand (mS)	c-Sand (cS)	Granule (g)	Pebble (p)				
									good		?clayey sandstone; reddish-grey; big qtz/fsp-grains, massive
								TS			greenish-grey phase (fine grained)

Depth Bottom: 2,187.5 m

TS .... Thin section